

UNIVERSITÉ DU QUÉBEC À TROIS-RIVIÈRES

EN ASSOCIATION AVEC

UNIVERSITÉ DU QUÉBEC À MONTRÉAL

IMPACTS DES CHANGEMENTS CLIMATIQUES SUR L'HYDROLOGIE  
DES BASSINS VERSANTS DANS L'EST DU CANADA

CLIMATE CHANGE IMPACTS ON CATCHMENT HYDROLOGY  
IN EASTERN CANADA

THÈSE PRÉSENTÉE  
COMME EXIGENCE PARTIELLE  
DU DOCTORAT EN SCIENCES DE L'ENVIRONNEMENT

PAR  
OKAN AYGÜN

JANVIER 2021

Université du Québec à Trois-Rivières

Service de la bibliothèque

Avertissement

L'auteur de ce mémoire ou de cette thèse a autorisé l'Université du Québec à Trois-Rivières à diffuser, à des fins non lucratives, une copie de son mémoire ou de sa thèse.

Cette diffusion n'entraîne pas une renonciation de la part de l'auteur à ses droits de propriété intellectuelle, incluant le droit d'auteur, sur ce mémoire ou cette thèse. Notamment, la reproduction ou la publication de la totalité ou d'une partie importante de ce mémoire ou de cette thèse requiert son autorisation.

UNIVERSITÉ DU QUÉBEC À TROIS-RIVIÈRES

DOCTORAT EN SCIENCES DE L'ENVIRONNEMENT (Ph. D.)

Programme offert par l'Université du Québec à Montréal (UQAM)

en association avec

l'Université du Québec à Chicoutimi (UQAC)

l'Université du Québec à Rimouski (UQAR)

l'Université du Québec en Abitibi-Témiscamingue (UQAT)

et l'Université du Québec à Trois-Rivières (UQTR)

**Cette thèse a été dirigée par :**

Christophe Kinnard, Ph. D. Directeur de recherche, grade	Université du Québec à Trois-Rivières Rattachement institutionnel
Stéphane Campeau, Ph. D. Codirecteur de recherche, grade	Université du Québec à Trois-Rivières Rattachement institutionnel

**Jury d'évaluation de la thèse :**

Christophe Kinnard, Ph. D. Directeur de recherche, grade	Université du Québec à Trois-Rivières Rattachement institutionnel
Stéphane Campeau, Ph. D. Codirecteur de recherche, grade	Université du Québec à Trois-Rivières Rattachement institutionnel
François Anctil, Ph. D. Prénom et nom, grade	Université Laval Rattachement institutionnel
Aubert Michaud, Ph. D. Prénom et nom, grade	Institut de Recherche et de Développement en Agroenvironnement Rattachement institutionnel
Alexandre Roy, Ph. D. Prénom et nom, grade	Université du Québec à Trois-Rivières Rattachement institutionnel

Thèse soutenue le 11 décembre 2020

## ACKNOWLEDGEMENTS

I would like to thank my supervisors Christophe Kinnard and Stéphane Campeau, for giving me the opportunity to pursue my PhD in Canada. Thank you for your guidance, support, advices, and for always being available for my questions. It has been a great pleasure to work with you.

I thank the members of jury, François Anctil, Aubert Michaud and Alexandre Roy, for taking their time to evaluate my dissertation.

A special thanks goes to Catarina Leote F. Pio for her exceptional problem-solving skills and technical support.

I thank my friends from GlacioLab for their technical and moral support and all the beautiful moments we shared together: Lisane Arsenault, Hafsa Bouamri, Ghada Bzeouich, Vasana Dharmadasa, Arthur de Grandpré, Hadi Mohammadzadeh Khani, Olivier Larouche, Matthieu Loyer and Saida Nemri. Zaccaria Kacem and Elizabeth Grater thank you for being awesome flat mates and friends. I want to thank Maxime Defoy and Pumba for always being by my side and supporting me during my ups and downs during this PhD journey.

Finally, I want to thank my family for their endless support and love. Thank you for trying to understand what I do and why I do.

This research was funded by the Natural Sciences and Engineering Council of Canada, grant number RGPIN-2015-03844 (Christophe Kinnard) and RGPIN-2017-06571 (Stéphane Campeau) and the Canada Research Chair program, grant number 231380 (Christophe Kinnard).

## TABLE OF CONTENTS

<b>ACKNOWLEDGEMENTS.....</b>	<b>iii</b>
<b>LIST OF FIGURES .....</b>	<b>vii</b>
<b>LIST OF TABLES .....</b>	<b>xii</b>
<b>RÉSUMÉ.....</b>	<b>xiii</b>
<b>ABSTRACT.....</b>	<b>xvi</b>
<b>INTRODUCTION.....</b>	<b>1</b>
Motivation and Relevance.....	1
Theoretical Background .....	5
Cold Regions Hydrology.....	5
Hydrological Modelling.....	11
Projected Effects of Climate Change on Hydrology and Soil Erosion in Cold Regions .....	13
Research Objectives, Scope and Importance .....	16
Thesis Outline .....	20
<b>CHAPTER I – SHIFTING HYDROLOGICAL PROCESSES IN A CANADIAN AGROFORESTED CATCHMENT DUE TO A WARMER AND WETTER CLIMATE .....</b>	<b>22</b>
Abstract .....	23
1.1 Introduction.....	24
1.2 Materials and Methods .....	27
1.2.1 Study Area and Data .....	27
1.2.2 Hydrological Model Configuration .....	31
1.2.3 Climate Sensitivity Analysis.....	37
1.3 Results .....	38
1.3.1 Historical Simulations.....	38
1.3.2 Climate Sensitivity.....	46

1.4 Discussion.....	59
1.5 Conclusion.....	63
Acknowledgments.....	65
References.....	66
<b>CHAPTER II – CONTRASTED CLIMATE SENSITIVITIES OF TWO COLD-REGION CATCHMENTS IN EASTERN CANADA .....</b>	<b>79</b>
Key Points.....	80
Abstract.....	80
2.1 Introduction.....	82
2.2 Materials and Methods .....	86
2.2.1 Study Area and Data Sources .....	86
2.2.2 Hydrological Modelling and Parameter Estimation .....	89
2.2.3 Climate Sensitivity Analysis.....	96
2.3 Results and Discussion .....	98
2.3.1 Evaluation of the Hydrological Modelling Performance.....	98
2.3.2 Simulation of Water Fluxes.....	102
2.3.3 Comparison of the Hydrological Sensitivity of the Montmorency River Catchment to Climate Change with the Acadie River Catchment.....	107
2.4 Conclusions .....	119
Acknowledgments.....	122
Supporting Information.....	123
References.....	126
<b>CHAPTER III – RESPONSES OF SOIL EROSION TO WARMING AND WETTING IN A COLD CANADIAN AGRICULTURAL CATCHMENT...</b>	<b>138</b>
Highlights.....	139
Abstract.....	139
3.1 Introduction.....	141
3.2 Materials and Methods .....	145
3.3 Results .....	154
3.4 Discussion and Conclusions .....	162

Acknowledgments.....	166
References.....	167
<b>CONCLUSIONS.....</b>	<b>174</b>
Synthesis and Concluding Discussions.....	174
Concluding Remarks.....	179
Outlook.....	182
<b>REFERENCES.....</b>	<b>186</b>

## LIST OF FIGURES

Figure		Page
1	Major cold regions hydrological processes operating in a) open environments and b) forest environments. Adapted from Pomeroy et al. (2007b).....	5
1.1	Acadie River Catchment drainage area, contour lines (every 10 m), land cover, discharge gauge, main meteorological station, snow survey station and soil moisture/temperature sensors .....	28
1.2	Observed and simulated snow water equivalent (SWE) at the Hemmingford snow survey station .....	38
1.3	Comparisons of simulated and observed SWE for (a, c) agriculture and (b, d) deciduous forest for the winters of 2017–2018 and 2018–2019, respectively. Error bars represent the standard deviation of SWE .....	40
1.4	SWE simulations at the (a) catchment and (b) landscape scale. The grey envelope in (a) illustrates the inter-annual variability for the 1996–2019 period .....	41
1.5	Average simulated cumulative snow mass fluxes and daily SWE between the years 1996 and 2019 in (a) agriculture (b) forest .....	42
1.6	Assessment of the CRHM platform performance in simulating streamflow at the outlet of the Acadie River Catchment by comparing (a) daily streamflow, (b) flow duration curve, and (c) cumulative mean daily streamflow. The shades around the average values in panel (c) represent the inter-annual variability .....	44
1.7	Average annual cumulative water fluxes at the catchment scale between the years 1996 and 2019. The shades around the average values represent the inter-annual variability ( $\pm$ standard deviation).....	46
1.8	Sensitivity of snow accumulation to selected climate change scenarios ..	48

1.9	Climate sensitivity of snow metrics. (a) Annual peak SWE; (b) relative change in annual peak SWE; (c) change in annual peak SWE date—negative values represent a shift towards earlier dates; (d) change in snow cover duration (SCD); (e) relative change in the snowmelt rate .....	49
1.10	Peak SWE in response to temperature and precipitation changes in (a) agriculture, (b) forest, and (c) difference between forest and agriculture .....	50
1.11	Changes in mean daily streamflow in response to selected warming and increasing precipitation scenarios. Changes in (a) mean daily streamflow, and (b) exceedance probability of mean daily streamflow ..	53
1.12	Climate sensitivity of streamflow in Acadie River. (a) Changes in annual peak daily discharge; (b) changes in annual peak daily discharge date; (c) changes in annual total discharge in response to temperature and precipitation changes; and (d) projected changes in annual temperature and precipitation for the periods 2041–2070 and 2071–2100 under a moderate emission scenario (RCP 4.5) and a high emission scenario (RCP 8.5) for Montérégie region of Québec (Ouranos 2015) .....	55
2.1	a) Locations of Montmorency and Acadie River catchments, b) Montmorency River Catchment drainage area, contour lines (every 100 m), land cover, discharge gauge, and main meteorological station. The Montmorency River Catchment encloses the BEREV watershed with snow stations and the Lac Laflamme watershed with soil moisture/temperature stations .....	87
2.2	Pre-processing procedure showing the spatial layers used for generating Hydrologic Response Units (HRUs) in the Montmorency River Catchment .....	94
2.3	Projected changes in annual temperature and precipitation for the periods 2041–2070 and 2071–2100 under moderate emission scenario (RCP 4.5) and high emission scenario (RCP 8.5) for a) Capitale-Nationale, and b) Montérégie regions of Québec (Ouranos 2015) .....	97
2.4	Observed and simulated snow water equivalent (SWE) at a) Station I, and b) Station J in the Montmorency River Catchment. The locations of the stations are given in Figure 2.1b .....	99

2.5	Comparisons of the observed and simulated seasonal daily volumetric soil moisture at the coniferous forest in the Lac Laflamme watershed from 2005 to 2018. Note that comparisons are valid only when the observed soil temperature (at 22 cm) is above 0 °C .....	100
2.6	Comparisons of the observed and simulated seasonal daily volumetric soil moisture at the mixed forest in the Lac Laflamme watershed from 2005 to 2010. Note that comparisons are valid only when the observed soil temperature (at 22 cm) is above 0 °C.....	101
2.7	Assessment of the CRHM model performance in simulated streamflow at the outlet of the Montmorency River Catchment by comparing a) daily observed and simulated streamflow, b) flow duration curve of the observed and simulated streamflow, and c) cumulative mean daily observed and simulated streamflow .....	102
2.8	a) Average annual cumulative water fluxes, and b) average winter mass fluxes for the period 2005–2019. The shades around the average values represent the inter-annual variability ( $\pm$ standard deviation).....	103
2.9	Sensitivity of snow accumulation to changing climate in the Montmorency River Catchment. a) Change in annual peak SWE; b) change in annual peak SWE date; c) change in snow cover duration (SCD); d) relative change in snowmelt rate .....	104
2.10	Sensitivity of streamflow to changing climate in the Montmorency River Catchment. Change in a) annual peak streamflow, b) annual peak streamflow timing, and c) total annual streamflow .....	106
2.11	Snow accumulation under selected climate change scenarios in a) Montmorency, and b) Acadie River catchments .....	109
2.12	Sublimation losses under selected climate change scenarios in a) Montmorency River Catchment, and b) Acadie River Catchment. The ratio of sublimation to annual snowfall is given above each bar.....	111
2.13	Changes in mean daily streamflow and exceedance probability of mean daily streamflow to selected warming and increasing precipitation scenarios in (a-b) Montmorency River Catchment and (c-d) Acadie River Catchment .....	113

2.14	The influences of biophysical and climatological characteristics of the catchments on the climate sensitivity of the annual peak snow water equivalent (SWE) and annual peak specific discharge (Q). (a-b-c) The response of peak SWE and (d-e-f) peak specific Q to 3 °C and/or 20% increasing precipitation under permuted baseline climate conditions. The values in parentheses below the sensitivities (panel a and d) present the current (historically averaged) baseline values of the variables under a given regional climate and biophysiography combination.....	115
S2.1	Sensitivity of annual peak runoff to changing climate in: a) biophysical conditions of Acadie under the climate conditions of Acadie, b) biophysical conditions of Montmorency under the climate conditions of Acadie, c) biophysical conditions of Acadie under the climate conditions of Montmorency, and d) biophysical conditions of Montmorency under the climate conditions of Montmorency .....	123
S2.2	Sensitivity of annual mean water flux to changing climate in: a) biophysical conditions of Acadie under the climate conditions of Acadie, b) biophysical conditions of Montmorency under the climate conditions of Acadie, c) biophysical conditions of Acadie under the climate conditions of Montmorency, and d) biophysical conditions of Montmorency under the climate conditions of Montmorency .....	124
S2.3	Sensitivity of annual mean runoff to changing climate in a) biophysical conditions of Acadie under the climate conditions of Acadie, b) biophysical conditions of Montmorency under the climate conditions of Acadie, c) biophysical conditions of Acadie under the climate conditions of Montmorency, and d) biophysical conditions of Montmorency under the climate conditions of Montmorency .....	125
3.1	Acadie River Catchment drainage area, crop type, the location of the discharge gauge and water quality station, and the drainage area of the water quality station .....	146
3.2	MUSLE soil erosion factors. a) Soil erodibility factor (K); b) Slope factor (LS); c) Conventional till crop management factor (C); d) Conservation till crop management factor (C); e) No-till crop management factor (C) .....	149
3.3	Agriculture hydrological response units (HRUs) of the Acadie River Catchment .....	151

3.4	Comparison of observed and simulated monthly average sediment yields for scenario a and b in a) calibration and b) validation periods. While the non-calibrated scenario a considers the surface runoff as the only pathway for sediment transport, scenario b represents a more realistic simulation in which the sediments are carried by surface runoff and subsurface tile drains with an efficiency of 20% in freezing days and 50% in non-freezing days. RMSE and NSE for scenario b are presented for calibration and validation periods. The grey envelope around the mean monthly observation represents the inter-annual variability ( $\pm$ standard deviation) of monthly sediment yields for the calibration period (a) and validation period (b) .....	155
3.5	Average annual sediment yields (1996–2019) from the agricultural fields in the Acadie River Catchment simulated by a) Scenario a and b) Scenario b .....	156
3.6	Change in average annual sediment yields under climate change scenarios for a) Scenario a (surface runoff only), and b) Scenario b (surface runoff plus tile drainage with an efficiency of 20% in freezing days and 50% in non-freezing days). The crosses overlain on the panels represent the mean and spread (90% confidence) of ensemble projected changes in mean annual temperature and precipitation for the periods 2041–2070 and 2071–2100 under a moderate (RCP 4.5) and high (RCP 8.5) emission scenario for the Montérégie region of Québec (Ouranos, 2015) .....	158
3.7	Average annual and seasonal sediment yields under selected climate change scenarios for a) Scenario a (surface runoff) and b) Scenario b (surface runoff + tile drainage) .....	159
3.8	Average annual sediment yields under selected climate change and crop management scenarios for a) Scenario a (surface runoff) and b) Scenario b (surface runoff + tile drainage).....	161

## LIST OF TABLES

Table		Page
1.1	Modules used in the CRHM to simulate the hydrological processes in the Acadie River catchment.....	32
1.2	Sensitivity of snow variables to selected climate change scenarios. The snow onset date (SOD) and the snow disappearance date (SDD) are the first and last days of the water year with snow on the ground (SWE > 0.1 mm), respectively. SCD, snow cover duration .....	47
1.3	Changes in magnitude of annual snow mass fluxes and resulting annual peak SWE in (a) agriculture and (b) forest under selected warming and increasing precipitation scenarios .....	51
1.4	Mean annual catchment scale water fluxes for the selected climate change scenarios. For the reference period, the mean annual temperature is 7.2 °C and mean annual precipitation is 1030 mm .....	57
1.5	Mean annual catchment scale water fluxes (falsified model) for the selected climate change scenarios.....	59
2.1	Meteorological and biophysical conditions of the Montmorency and Acadie River catchments .....	89
2.2	Comparison of climate sensitivity of snow variables in the Montmorency River Catchment with the Acadie River Catchment .....	108
2.3	Comparison of climate sensitivity of water fluxes in the Montmorency River Catchment with the Acadie River Catchment .....	112

## RÉSUMÉ

Les changements climatiques en cours et à venir pourraient modifier significativement le cycle hydrologique régional et les services écosystémiques rendus aux populations. Dans les régions froides comme l'est du Canada, les interactions multiples entre les différents processus hydrologiques, tels que l'accumulation de neige, la redistribution et la fonte des neiges, l'interception des précipitations par la végétation, l'évapotranspiration, l'infiltration et le ruissellement de surface et souterrain pourraient conduire à une réponse hydrologique complexe aux changements du climat. La réponse d'un bassin versant individuel au changement climatique pourrait être tout à fait unique, en fonction des caractéristiques biophysiques dominantes et du climat régional. Il est donc nécessaire de mieux comprendre et de représenter les processus hydrologiques des régions froides afin de mieux anticiper les changements futurs de quantité d'eau et d'érosion du sol à l'échelle des bassins versants. Dans ce contexte, cette étude a pour but d'évaluer la sensibilité climatique de l'hydrologie de deux bassins versants situés au Québec, dans l'est du Canada: celui de la rivière l'Acadie et celui de la rivière Montmorency. Ces bassins représentent deux portraits types de physiographies longeant le fleuve Saint-Laurent : un paysage agroforestier sur les basses terres de la rive sud pour l'un et le Bouclier canadien, principalement recouvert de forêts sur la rive nord, pour l'autre. Cette étude vise également à évaluer la réponse de l'érosion des sols aux changements projetés de température et de précipitations dans le bassin versant de la rivière l'Acadie. Un modèle hydrologique pour chaque bassin a été mis en place à l'aide de la plateforme de modélisation hydrologique des régions froides (Cold Regions Hydrological Modelling platform–CRHM) et une analyse de sensibilité climatique a été réalisée sur la base de séries de températures de l'air et de précipitations perturbées annuellement. Les sorties

de ruissellement du modèle hydrologique, qui est développé et validé pour le bassin versant de la rivière l'Acadie, ont été couplées à l'équation universelle modifiée des pertes de terre (Modified Universal Soil Loss Equation–MUSLE) pour quantifier le volume de sédiments érodés des champs agricoles du bassin versant sous les conditions climatiques actuelles et futures.

Les résultats ont démontré que la sublimation à partir de la neige interceptée est la principale composante de sublimation dans le bassin versant forestier de la rivière Montmorency, tandis que la sublimation du manteau neigeux domine la sublimation totale dans le bassin versant agroforestier de la rivière l'Acadie. L'accroissement des températures cause un déclin du transport de la neige, ce qui entraîne une diminution de la variabilité spatiale de l'équivalent en eau maximale de la neige (EEN) et une fonte plus synchronisée de la couverture de neige dans le bassin versant de la rivière l'Acadie. Le maximum annuel d'EEN (EEN maximal) montre une très forte sensibilité au réchauffement dans le bassin de la rivière l'Acadie en diminuant d'environ 30 % par degré, alors qu'une réduction de 10 % par degré est simulée pour le bassin versant de la rivière Montmorency. Il y aura une transition dans les régimes hydrologiques des deux bassins versants vers un régime davantage dominé par les pluies, mais cette transition se produit plus rapidement dans le bassin de l'Acadie en réponse au réchauffement de seulement 1.5 °C. Ces changements auront des implications importantes pour l'approvisionnement en eau et les stratégies de gestion des risques d'inondation pour les deux bassins versants. Des expériences climatiques de référence permutées ont démontré que la sensibilité climatique de l'EEN maximal dépend du climat actuel et est peu influencée par les conditions biophysiques. En réponse au réchauffement et à l'augmentation des précipitations, l'EEN maximal diminue, mais le débit maximal augmente dans le bassin l'Acadie aux conditions hivernales plus douces. Un climat plus chaud et plus humide entraîne une augmentation des apports en sédiments en hiver dans le bassin versant de la rivière l'Acadie, en raison d'un ruissellement hivernal plus élevé causé par une fonte plus précoce des neiges,

et plus d'épisodes de fonte au milieu de l'hiver et des fractions de pluie plus élevées. Sous un réchauffement de 2 °C et une augmentation des précipitations de 5 %, la charge sédimentaire annuelle peut diminuer de 20 % ou augmenter de 2 %, en fonction de la contribution des drains souterrains à la charge totale en sédiments. Cela met en évidence la nécessité de mieux connaître le rôle des drains souterrains dans l'exportation de sédiments dans un contexte de changements climatiques. Nos résultats suggèrent que l'adoption de pratiques de conservation du sol est une manière efficace d'atténuer les impacts du changement climatique sur l'érosion de sols agricoles. Cette recherche fournit des conseils utiles aux gestionnaires de l'eau, aux décideurs et aux communautés agricoles sur les impacts potentiels du changement climatique sur la disponibilité de l'eau et l'érosion du sol.

**Mots clés :** hydrologie des régions froides, modélisation hydrologique, sensibilité du climat, fonte des neiges, débit des cours d'eau, érosion du sol, le bassin versant du Saint-Laurent

## ABSTRACT

Ongoing and future climate change could significantly impact the regional scale hydrological cycle and associated ecosystem services rendered to populations. In cold regions like eastern Canada, the multiple interactions among different hydrological processes such as snow accumulation, redistribution and snowmelt, interception of precipitation by vegetation, evapotranspiration, infiltration, surface and subsurface runoff could lead to complex hydrological responses. Yet the response of an individual catchment to climate change could be highly unique, depending on the dominant biophysical characteristics and regional climate. There is therefore a need to better understand and represent the cold regions hydrological processes and anticipate future changes in water quantity and soil erosion at the catchment scale. In this context, this thesis aims to evaluate the climate sensitivity of the hydrology of two catchments located in Québec, eastern Canada: the Acadie River Catchment and the Montmorency River Catchment. These river basins represent two major land covers of the St. Lawrence River watershed in Québec, an agroforested landscape in the south shore lowlands and forest dominated catchment on the Canadian Shield of the north shore, respectively. This study also aims to assess the responses of soil erosion to projected changes in temperature and precipitation in the Acadie River Catchment. A hydrological model for each basin was set up using the Cold Regions Hydrological Modelling platform (CRHM) and a climate sensitivity analysis was carried out based on a series of annually perturbed air temperature and precipitation. The runoff outputs of the hydrological model developed and validated for the Acadie River Catchment was coupled with the Modified Universal Soil Loss Equation (MUSLE) to quantify the amount of sediments eroded from the agricultural fields of the catchment under the current and future climate conditions.

Results revealed that sublimation from intercepted snow is the major sublimation component in the forested Montmorency River Catchment, while snowpack sublimation dominates the total sublimation in the agroforested Acadie River Catchment. Warmer temperatures cause a decline in blowing snow transport, which in turn leads to reduced spatial variability in peak snow water equivalent (SWE) and a more synchronized snow cover depletion across the Acadie River Catchment. The annual peak SWE in Acadie shows a very strong sensitivity to warming, declining by about 30% per °C, whereas a 10% per °C reduction is simulated for Montmorency. There will be a transition in the hydrological regimes of both catchments towards a more rainfall-dominated regime, with faster changes projected to occur in Acadie in response to limited warming (1.5 °C). These changes will have important implications for water supply and flood risk management strategies. Permuted baseline climate experiments have demonstrated that the climate sensitivity of peak SWE depends on current climate and is little influenced by biophysical conditions. In response to warming and increasing precipitation, peak SWE declines but peak discharge increases in catchment with mild winter conditions. A warmer and wetter climate causes increased winter sediment yield in the Acadie River Catchment due to higher winter runoff caused by earlier snowmelt, more mid-winter melt events and greater rainfall fractions. Under 2 °C warming and 5% increasing precipitation, the annual average sediment can decline by 20% or increase by 2%, depending on the contribution of tile drainage to total sediment yield. This highlights the need to better understand the role of tile drains in sediment export under a changing climate. Our results suggest that the adoption of soil conservation practices is an efficient way of mitigating the impacts of climate change on erosion of agricultural soils. This research provides useful guidance to water managers, decision makers and farming communities about potential impacts of climate change on water availability and soil erosion.

**Keywords:** cold regions hydrology, hydrological modelling, climate sensitivity, snowmelt, river discharge, soil erosion, St. Lawrence watershed

## INTRODUCTION

### **Motivation and Relevance**

Cold regions are receiving increasing attention from the scientific community, the general public as well as decision-makers due to their noticeably rapid response to ongoing climate change, which raises concerns about the integrity of ecosystems, the sustainability of water resources, and altered hydrological risks under climate change scenarios (Allen et al. 2014, Hu et al. 2017). Formal definitions of cold regions have been previously made based on air temperature, frost penetration depth, snow depth, or ice cover in water bodies. For example, the 0 °C air temperature isotherm for the coldest month of the year has been used to assign the southern boundary of cold regions in the Northern Hemisphere (Bates and Bilello 1966). Also, a subjectively-chosen seasonal frost penetration depth (e.g. 300 mm) occurring once in 10 years is another commonly accepted method to draw the southern boundary of cold regions (Andersland and Ladanyi 2004). From a hydrological point of view, cold regions represent parts of the world where snow and ice are present at least seasonally (Gelfan and Motovilov 2009). In these regions, the cryosphere has a preponderant influence on the hydrology and the complex interactions among cryospheric and hydrologic processes result in unique hydrological responses to climate change, with marked spatial and temporal heterogeneity. Seasonal accumulation of snow and ice and subsequent melting of this storage are the main factors controlling cold region hydrology. Seasonally accumulated water within the snowpack provides a considerable contribution to total streamflow once melting occurs, which in turn constitutes important water resources in many regions of the world (Barnett et al. 2005). Mankin et al. (2015) estimated that approximately 2 billion people across the Northern Hemisphere depend on water supplied from snowmelt runoff.

Another important aspect of cold region hydrology is the seasonally frozen ground which governs infiltration, thereby partitioning the water fluxes between the surface and subsurface (Lundberg et al. 2016).

There are unequivocal evidences that climate system is warming. In terms of changes in precipitation, based on the IPCC Fifth Assessment Report (Allen et al. 2014), there has been an overall increase across the mid-latitude land areas of the Northern Hemisphere since 1950s, however seasonal trends show regional variations. Regardless of this overall increase in precipitation, the ratio of rainfall to total precipitation has been reported to increase over some regions such as contiguous US (Feng and Hu 2007). Cold regions, located in mid- to high-latitudes in the Northern Hemisphere, have been shown to be sensitive to the aforementioned changes in temperature and precipitation (Aygün et al. 2020), with the most acute impacts being on seasonal snow cover and associated runoff processes. In fact, both natural climate variability and historical climate trends have already been observed to impact snow cover key characteristics, such as declines in snow accumulation, shifts of peak snow accumulation towards earlier days and shorter snow cover durations (Allen et al. 2014). Changes that are even more dramatic are projected to occur as the result of future changes in temperature and precipitation due to continued greenhouse gas emissions, which would greatly influence the hydrological regime of cold regions in the future.

In Canada, the impacts of climate change are projected to vary depending on the region and the season. In southern Québec, climate warming is expected to decrease snow accumulation and the duration of snow cover, which should lead to earlier and reduced springtime floods (Boyer et al. 2010, Guay et al. 2015). In summer, models predict increased evapotranspiration and overall reduced precipitation, which should lead to decreased summer flows (Ouranos 2015). However, the response of individual catchment to anthropogenic climate is likely to be highly specific, depending on the unique physiographic settings, ecological processes and human influences on the

catchment (Beven 2000). Even neighbouring catchments may demonstrate different degrees of response to similar climate forcing trends (Teutschbein et al. 2015).

Over the last decades, intensified agricultural activities have become the largest non-point source of surface water pollution in Canada (Rousseau et al. 2013) and in Québec alone, agriculture is addressed to be responsible for more than 70% of the total non-point source pollution (Gollamudi et al. 2007), resulting in adverse effects on rivers and lakes, i.e. accelerating eutrophication and deoxygenating. Land erosion, favoured by agriculture, is the primary source of leaching of nutrients to lakes and rivers, which in turn deteriorates water quality. “How will climate-driven changes in hydrology affect soil erosion, independently of future changes in agricultural practices and land use” is an important question for water managers which has been little explored (Whitehead et al. 2009). In agricultural catchments in eastern Canada, a few studies (e.g. Dayyani et al. 2012, Gombault et al. 2015a) showed that climatic changes would induce greater winter flows and nutrient losses and earlier snowmelt by the end of the century attributable to an increase in rainfall and snowmelt events during winter.

The complex interactions between the different hydrological processes at play makes it difficult to predict future hydrological conditions, and its potential impacts on soil erosion under climate change scenarios. The traditional approach to assess climate change impact on hydrology is a “top-down” approach, whereas one or several hydrological models are forced by climate change scenarios from one or several climate models (Peel and Blöschl 2011). This approach requires accurate and time-consuming downscaling of climate projections to catchments. Given the enduring uncertainties of GCM simulations (Blöschl and Montanari 2010), some have advocated the use of simpler approaches. These approaches have been adopted under different names such as scenario-neutral (Prudhomme et al. 2010), arbitrary/incremental scenarios (Smith and Mendelsohn 2007, Smith and Pitts 1997) and sensitivity analysis (Keller et al. 2005, Krogh et al. 2017, Rasouli et al. 2015). In this approach, uniform annual and/or

seasonal changes are assigned over a region based on existing climate change projections. Historical records of temperature and precipitation are then perturbed based on these incremental climate scenarios and used to perform climate-sensitivity analyses with a hydrological model. Due to its relatively easy application and capability of allowing a wide range of simulations, they have been favored over scenario-based methods by many studies (Harder et al. 2015, Mahmood et al. 2017, Rasouli et al. 2015, Sproles et al. 2013). Simple, scenario-free sensitivity analyses of hydrological models to a wide range of plausible climate conditions can reveal how specific, and socially important hydrological characteristics (e.g. flood amplitude and timing, low flow duration, snow cover duration and distribution, soil moisture, etc.) respond to climate change, independently of the often uncertain projected climate trajectory (Blöschl et al. 2013, Peel and Blöschl 2011). The variable(s) targeted by the model sensitivity analyses can be defined a priori with regards to the hydrological services most valued by the water stakeholders in each catchment (Prudhomme et al. 2010). If a target variable is found to cross some coping threshold for a given combination of climate variables (typically temperature and precipitation), then the likelihood of observing these climate conditions in the future can be checked posteriori against the most up to date climate scenarios; conversely if the climate risk is found to be low there is no need to seek, or produce at great cost, specific climate scenarios for the catchment.

The main objective of this thesis is to assess the potential impacts of climate change on the hydrology of Acadie and Montmorency River catchments in eastern Canada, using a sensitivity-based approach.

The following section presents the theoretical background of this research by describing key hydrological processes encountered in cold regions, followed by a description of hydrological models.

## Theoretical Background

### *Cold Regions Hydrology*

The hydrological cycle of cold regions is shaped by both cryospheric and hydrological processes, which are shown in Figure 1. Precipitation has two components, rainfall and snowfall, whose fraction depends on air temperature. Snowmelt is the main contributor to both surface and subsurface flow, whereas the amount of infiltration is governed by the frequency and depth of soil freezing as well as the amount of ground ice formed. Snowfall is typically intercepted by canopy in forest environments (Figure 1b), while the wind redistributes snow from exposed terrain with bare soil or low vegetation to depressions and vegetated surfaces (Figure 1a) (Pomeroy and Gray 1995). Water is lost to the atmosphere in winter by sublimation from the snowpack, from blowing snow, and from snow stored on the forest canopy, while further water losses occur in summer from evaporation and evapotranspiration of intercepted and soil water, and from open water bodies (Figure 1).

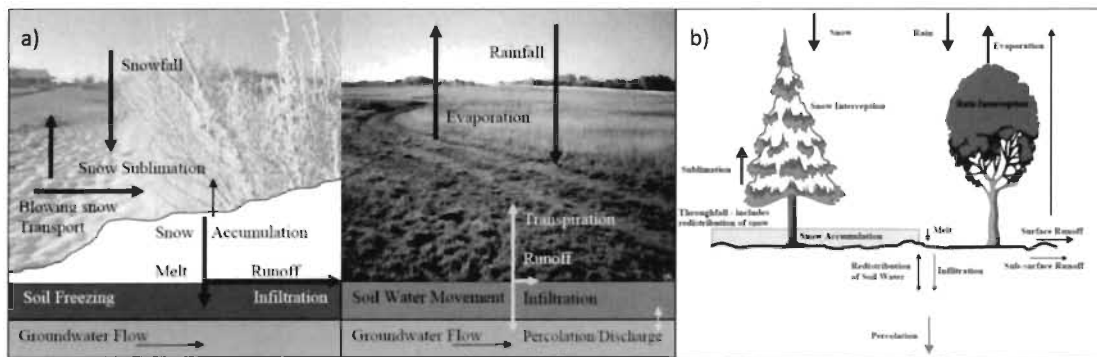


**Figure 1.** Major cold regions hydrological processes operating in **a)** open environments and **b)** forest environments. Adapted from Pomeroy et al. (2007b).

Snow processes consist of snowfall, interception, sublimation losses, blowing snow and snowmelt. Snow accumulation is largely impacted by elevation, land cover and wind characteristics. The depth of seasonal cover generally shows an increase

with rising elevation due to the orographic enhancement of precipitation, adiabatic cooling and resulting increased frequency of snowfall events, along with reduced evaporation/sublimation and melt rates, where other factors such as vegetation and micro-relief do not vary with elevation (Pomeroy and Gray 1995). Interactions between snow and vegetation play a significant role in snow accumulation. Considerable amounts of snowfall can be intercepted by vegetation before snow begins accumulating on the ground, depending upon tree species and the structure of their canopy. Thus, forested and open environments can be subjected to different snow accumulation amounts (Pomeroy et al. 2002). In terms of tree species, deciduous forests generally have greater snow accumulations on the ground compared to coniferous forests due to the lack of leaves in winter (Pomeroy and Gray 1995). Conversely, coniferous trees in the boreal forest can intercept up to 60% of cumulative snowfall in mid-winter (Pomeroy and Schmidt 1993).

Sublimation, the transformation of snow/ice into water vapor without melting into water, leads to water loss to the atmosphere. Besides the direct sublimation of the snowpack on the ground, intercepted snow by vegetation can also sublimate before it unloads to the ground. Sublimation from the canopy can be higher than sublimation on the ground due to the larger absorption of short wave radiation by the canopy, and stronger winds and hence greater exposure to turbulent exchange forces (Lundberg et al. 2004). Sublimation rates from the canopy highly depend on the tree species and density. Sublimation losses of intercepted snow in boreal forests can reach more than 30% of annual snowfall (Pomeroy and Schmidt 1993).

A considerable amount of snow redistribution by wind can occur over open and wind-exposed environments. Snow accumulation due to blowing snow varies spatially in association with the type and spatial distribution of vegetation and topography, such that snow is typically transported from sparsely vegetated and exposed terrains to densely vegetated areas and to topographic depressions (Essery and Pomeroy 2004,

Liston et al. 2007). Larger blowing snow rates are expected to be recorded with increased amounts of snowfall, higher wind speeds and relatively cold temperatures that slow down snow metamorphism and snowmelt (Pomeroy and Brun 2001). Compared to static snowpack surfaces, blowing snow has a larger surface exposed to atmospheric turbulence, thus increasing the potential for sublimation. For instance, Essery et al. (1999) report that the ratio of blowing snow sublimation to annual snowfall can be as much as 47% over northern Canada.

Snowmelt is governed by any surplus of energy resulting from the energy exchanges between the snowpack and the atmosphere. The fluxes involved in the energy exchanges are the shortwave radiation, longwave radiation, turbulent heat (sensible and latent heat) fluxes and heat (sensible and latent heat) flux input by precipitation and ground heat flux. The relative importance of each flux and energy transfer mechanisms on melting varies depending on climate, vegetation and topography (Gray and Landine 1988). For instance, melt rates observed in open areas are typically higher than in forests, since more shortwave radiation can reach the ground (Gelfan et al. 2004, Winkler et al. 2005). The response of the snow cover to rising temperature and varying precipitation can be different, depending on the energy partitioning between the snow and the atmosphere. For instance, at high latitudes where solar elevation is low, longwave radiation can supply greater amounts of energy for melting than shortwave radiation (Sicart et al. 2006). During snow accumulation in winter, ground heat conduction can supply some amount of energy for melt (Armstrong and Brun 2008). For example, in the Pacific Northwest of the US where the ground temperature remains above freezing throughout the winter due to warm air temperatures, a considerable fraction of energy (up to 29%) used for melting is supplied by the ground (Mazurkiewicz et al. 2008).

The substantially low thermal conductivity of snow makes it a perfect insulation material between the ground surface and the atmosphere. For instance, the thermal

conductivity of dry snow ( $0.045 \text{ W m}^{-1} \text{ k}^{-1}$ ) is much lower than that of mineral soil (for example thermal conductivity is  $1.8 \text{ W m}^{-1} \text{ k}^{-1}$  for clay and on average  $1.3 \text{ W m}^{-1} \text{ k}^{-1}$  for limestone), thus snow is assumed to have an insulation capacity much greater than that of an equivalent soil depth (Pomeroy and Brun 2001). Due to the snow insulative properties, the ground surface temperature in cold regions can be significantly warmer than the air temperature when snow is present on the ground and as such could impede the formation of deep soil frost. As a result, meltwater could infiltrate more efficiently during snowmelt period. The snow depth, snow cover duration along with onset and offset dates of snow cover play an important role on the soil thermal regime (Zhang 2005). The most favorable condition for higher soil temperatures is a combination of early snow accumulation in autumn (before the temperature falls below the freezing point), and early snowmelt in spring (when solar elevation increases). It is often said that a thin layer of snow has a great influence on soil temperature, but above a critical snow depth (30–40 cm) further influence is limited (Sutinen et al. 2008, Zhang 2005).

Seasonally frozen soils are exposed to freeze-thaw cycles due to fluctuations of soil surface temperature around the freezing point, which are governed by air temperature and snow cover depth. For instance, reduced snow cover and thus decreased thermal insulation can cause more freeze-thaw cycles to occur since the ground temperature can follow more closely the changes in air temperature (Groffman et al. 2001, Henry 2008). Successive freeze-thaw cycles alter the soil structure, including soil hydraulic properties. An increase in freeze-thaw cycle frequency has been shown to enhance the soil saturated hydraulic conductivity (Asare et al. 1999, Benson et al. 1995, Meiers et al. 2011), while soil permeability can also increase as the soil becomes fissured due to repeated freeze-thaw cycles (Fouli et al. 2013). In addition, soil freeze-thaw cycles reduce the aggregate stability of soils and can thus increase the soil erosion potential in early spring (Ferrick and Gatto 2005, Hayhoe et al. 1992, Xie et al. 2015, Zuzel and Pikul 1987). Seasonally frozen soils are not necessarily impermeable. Having reviewed field studies from Canada and the former Soviet Union (USSR), Gray and Granger

(1987) grouped the frozen soils into three categories according to their infiltration potential: (i) restricted: infiltration is restrained by ice lenses on or near the soil surface, such that infiltration amount is negligible, and all snowmelt water goes to direct runoff and evaporation; (ii) limited: infiltration is possible up to some amount, which is governed by the snow cover and frozen water content of the soil layer; (iii) unlimited: most of the meltwater infiltrates where the soils have a high percentage of large and air-filled pores.

Snowmelt plays a significant role for groundwater replenishment and groundwater recharge which can even exceed the monthly precipitation during the snowmelt period (Dripps 2012, Dripps and Bradbury 2010), depending on the degree of soil freezing at the timing of the spring freshet. For example, Jyrkama and Sykes (2007) have reported an increase in meltwater infiltration and groundwater recharge in the Grand river watershed in Ontario (Canada) when the soil was less frozen. In summer, a decrease in the groundwater table is expected due to the root uptake of water by growing vegetation (Ireson et al. 2013). In addition to being an important freshwater resource, groundwater discharge accounts for most of the streamflow in unregulated rivers when there is no or minimal contribution from rainfall or snowmelt such as in winter or dry seasons (Orlova and Branfireun 2014, Paznekas and Hayashi 2016).

Overland flow is formed mainly by excess of soil infiltration and excess of soil saturation. Infiltration excess runoff forms when the melt and/or rainfall rate is higher than the infiltration capacity, causing a perched water table to form near the soil surface which triggers overland flow. Alternatively, saturation excess runoff occurs when a rising water table reaches the surface, the soil becomes saturated and it triggers overland flow. Although rainfall is considered to be more effective for triggering surface flow due to rainfall rates being higher than snowmelt rates, meltwater can nonetheless contribute directly to surface runoff when the soil underneath is frozen and impermeable (DeWalle and Rango 2008). In cold regions, the common hydrological

regime encountered is the nival regime, where low flow during the cold season rises rapidly during the snowmelt spring freshet and is followed by flow recession in summer with intensified evapotranspiration rates (Woo et al. 2008). A typical example to this hydrological regime is northern Canada where the lowest flow period is late winter when rivers are covered by ice (Mortsch et al. 2000). In some cold regions such as southern Canada, on the other hand, the streamflow of rivers is driven by mixed rain and snow processes (Whitfield and Cannon 2000). Over these regions, while the lowest flow period is mostly in late summer instead of late winter, floods could occur due to either snowmelt or heavy rainfall or combination of these two. The seasonality of streamflow in cold regions, i.e. the timing, duration and magnitude of flow, is mostly governed by the distinct cold region hydrological processes related to snow and frozen soils. Climatic conditions and physiographic features specific to each catchment account for the spatial variability in streamflow seasonality.

In cold regions, the timing and volume of streamflow are significantly governed by snowmelt, and a spring flood regime prevails due to the high amount of snow and ice accumulation. Besides, evaporation rates are low to null in the spring, thus all meltwater released is available for infiltration and runoff, and the low infiltration capacity of frozen soils can result in quick and higher flood peaks. Flood magnitude can also be enhanced by ice jams caused by river ice break up in early spring (Beltaos 2003, Hicks 2009, Lindenschmidt et al. 2016). The timing of peak flow is governed by the timing of the spring freshet, which is strongly related to winter-spring temperature patterns which itself varies among the cold regions. For instance, higher latitudes in Canada have a later peak flow compared to lower latitudes due to the delayed spring freshet (Woo et al. 2008). While snowmelt induces peak flows during spring in cold regions, floods can also occur during the other seasons, depending on the rainfall regime. For instance, in the Baltic countries, the river regime is characterized by snowmelt and rainfall-generated flows, with two characteristic flood peaks in spring and autumn respectively (Krasovskaia et al. 1994, Wilson et al. 2010).

Winter flows in cold regions are generally the lowest flows of the year due to the temporary storage of precipitation as snow (Smakhtin 2001), and this low flow period mostly coincides with river ice cover (Peters et al. 2014). In fact, some rivers might not even have runoff in winter if there was no supply from the groundwater (French and Slaymaker 1993). In spring, snowmelt and rainfall events are the main sources of high spring flows. On the other hand, high infiltration rates and large evapotranspiration losses mostly result in low summer flows in cold regions, such as in the Canadian Prairies (Shook et al. 2015). Given that snowmelt in spring supplements streamflow during the warm seasons (Mote 2003), any change in the timing and/or magnitude of snowmelt due to changes in air temperature and precipitation in cold season could lead to changes in warm season streamflow levels. These changes in warm season hydrograph could even be amplified by the changes in precipitation and air temperature during the warm season. Streamflow represents the spatially integrated catchment response to water fluxes within the catchment. Therefore, streamflow provides a good proxy of the combined impact of climate change on catchment dynamics (Pradhanang et al. 2013). Any change in streamflow dynamics could result in significant impacts on water management strategies, in terms of flood mitigation and water supply.

### ***Hydrological Modelling***

Hydrological models are simplified representations of the hydrological behaviour of a catchment. They can be classified as lumped and distributed based on their representation of model parameters as a function of space, and conceptual and physically based according to the extent of physical principles applied (Devia et al. 2015, Dingman 2015).

Lumped hydrological models describe the catchment as a single entity, averaging spatial characteristics into a single parameter. On the other hand, distributed models account for an explicit representation of the spatial variability in hydrological

processes. The level of spatial representation in distributed hydrological models varies, such that while some of the models employ a full gridded distribution, some models adopt a semi distribution. Fully distributed hydrological models represent the input data and capture the outputs on a grid/finite element base. TOPKAPI (Ciarapica and Todini 2002) and SHE (Abbot et al. 1986) are some of well known fully distributed hydrological models. Semi distributed hydrological models divide the watershed into unique model elements (for example Hydrologic Response Units (HRUs)) and all hydrological processes are lumped at these elements, and because of this they have lower computational requirements compared to fully distributed models. Some of the well known semi-distributed hydrological models are SWAT (Arnold et al. 1998) and TOPMODEL (Beven 1997, Beven and Freer 2001).

Conceptual models typically represent the physical processes in a catchment with several interconnected reservoirs and model parameters are determined from both field observation and calibration. Physically based models mathematically describe the hydrologic processes operating in a catchment by employing parameters with physical interpretations, thus requiring a great number of parameters. Conceptual models are thus simpler and easier to implement compared to physically based models. These models are particularly useful to model rainfall/snowmelt-runoff relationships and have been used extensively to forecast streamflow volumes and flood within a water management context. However, conceptual models heavily rely on calibration, often streamflow alone, which is prone to climatic dependence of parameters as well as equifinality issues. This can compromise future projections. Physically based models can supply a wider amount of information including more details about the hydrologic processes operating within a basin and their interactions. While a rapid impact assessment of various climate change scenarios can be performed with the use of conceptual models, physical-based models have the capability of simulating the impacts of land use change together with climate change (Jones et al. 2006). Some well known physically based hydrological models suitable for cold regions are CRHM

(Pomeroy et al. 2007a), SUMMA (Clark et al. 2015) and Raven (Craig et al. 2020). Among these hydrological models, CRHM platform includes the most comprehensive library of cold regions hydrological processes as those presented in Section “*Cold Regions Hydrology*”.

### ***Projected Effects of Climate Change on Hydrology and Soil Erosion in Cold Regions***

The projected warming across the Northern Hemisphere is reported to be more pronounced in the cold regions of the Northern Hemisphere ( $>40^{\circ}$  N), particularly during the cold season (Liu et al. 2007, Panin et al. 2009). As a result of these higher temperatures, a shorter snow cover duration is projected for various cold regions in Northern Europe and North America (Brown and Mote 2009, Räisänen 2008). Both snow depth (SD) and snow water equivalent (SWE) are projected to decrease overall over the Northern Hemisphere for the 21st century (Shi and Wang 2015), with the most dramatic declines projected to occur along the regions which have mild cold seasons, such as coastal regions of North America (Brown and Mote 2009) and coastal and southern regions of Northern Europe (Arheimer et al. 2013, Kellomäki et al. 2010, Räisänen and Eklund 2012, Stonevičius et al. 2017). This is because these regions have already mild cold seasons, i.e. cold season temperatures closer to the freezing point, and warmer temperatures enhance the ratio of rainfall to total precipitation. Some studies, on the other hand, have reported that changes in precipitation could be the predominant control on snow accumulation in colder regions such as the coldest regions and higher altitudes of the Northern Hemisphere (Hosaka et al. 2005, Räisänen 2008, Räisänen and Eklund 2012). Considering that cold season temperatures are projected to remain below freezing level in these regions, projected increases in precipitation might result in similar or even higher snow accumulation than currently observed.

The onset of spring snowmelt is projected to shift towards earlier dates over many cold regions in North America due to warmer temperatures (Hayhoe et al. 2007, Minville et al. 2008, Shrestha et al. 2012, Stewart et al. 2004). Yet, such shifts are projected to occur faster in catchments which have relatively milder cold season temperatures (Boyer et al. 2010). Regarding the future changes in snowmelt peak runoff, the studies yield different conclusions, depending on the future climate of a given region as well as the climate change scenario considered. For example, Minville et al. (2008) showed that peak runoff in a catchment in Québec could increase or decline, depending on the selection of the climate model. Diffenbaugh et al. (2013) argued that as long as cold season temperatures remain below freezing and thus support solid precipitation, an increase in precipitation is expected to cause higher peak runoff, as is the case for northeast Eurasia. Given that precipitation projections are more spatially variable and uncertain than temperature, particularly at regional and local scales (Allen et al. 2014), this uncertainty might limit our capacity to robustly project changes to peak runoff. In this regard, sensitivity analyses, such as those performed by Wang et al. (2016) and Rasouli et al. (2019) can provide valuable assessments of how sensitive the peak runoff is to uncertain precipitation changes. Meanwhile, Molini et al. (2011) showed that while warmer cold season temperatures could lead to decreased snow accumulation, thus declined peak runoff, higher temperatures in late winter and early spring could cause higher peak runoff due to enhanced snowmelt rates. More recently, Musselman et al. (2017) reported that shallower snowpacks caused by warmer temperatures melted earlier and more slowly compared to deeper and later-lying snowpacks, which led to the development of a “slower snowmelt in a warmer world” hypothesis. As projected warming is expected to result in more frequent rainfall events and snowmelt episodes during winter, winter streamflow is projected to be higher over various cold regions such as Northern Europe (Beldring et al. 2008, Teutschbein et al. 2015), Northeastern US (Hayhoe et al. 2007), northeast Canada (Huziy et al. 2013) and southern Canada (Boyer et al. 2010, Minville et al. 2008, Mortsch et al. 2000). With respect to changes in warm season, studies have reported that higher evapotranspiration levels caused by

warmer temperatures are likely to decrease summer streamflow in some cold regions (Boyer et al. 2010, Hayhoe et al. 2007, Huntington and Niswonger 2012, Huziy et al. 2013). A similar seasonal change is projected for groundwater recharge for some cold regions, i.e. increased groundwater recharge in winter due to higher water availability associated with higher rainfall fractions and more frequent snowmelt episodes and decreased soil freezing that allows more efficient infiltration, and lower groundwater recharge in summer due to decreased water availability caused by higher evapotranspiration levels (Okkonen and Kløve 2010, Rivard et al. 2014, Sulis et al. 2011, Toews and Allen 2009). At annual scale, while some studies projected an overall increase in annual streamflow over some cold regions (Hayhoe et al. 2007, Huziy et al. 2013), others reported an overall decrease (Sulis et al. 2011, Tanzeeba and Gan 2012). This disparity in annual streamflow projections highlights the different seasonal response of streamflow to climate change, where the change in annual streamflow will depend on the compensation level between seasonal changes in streamflow.

The response of soil erosion rates to climate change have been shown to be highly variable and complex (Li and Fang 2016). Notwithstanding, higher rainfall amount, rainfall intensity and extreme rainfall events are expected to cause higher runoff and soil erosion rates over the world when other factors remain unchanged. Soil erosion and nutrient losses in winter are projected to be higher in various cold regions, such as southern Québec (Gombault et al. 2015a, Mehdi et al. 2015), Great Lakes Region (Wang et al. 2018), Northeastern US (Mukundan et al. 2013), Denmark (Andersen et al. 2006), Norway (Deelstra et al. 2015) and Sweden (Arheimer et al. 2005). These increases have been attributed to the increased winter streamflow due to the earlier onset of spring snowmelt, higher rainfall fractions and more frequent snowmelt episodes under warmer winter temperatures. At an annual scale, while the projected increase in annual streamflow is followed by an increase in soil erosion in Denmark (Andersen et al. 2006), annual soil erosion is projected to decline due to the decrease in annual streamflow in Great Lakes Region (Wang et al. 2018).

## **Research Objectives, Scope and Importance**

The purpose of this research is to explore the potential impacts of climate change on the hydrology of Acadie River and Montmorency River catchments, using a sensitivity-based approach. These catchments are representatives of two main landscape archetypes in southern Québec, namely a rugged forested landscape with cold/humid climate (Montmorency) and an agroforested landscape with warmer/less humid climate (Acadie), respectively located on the north and south shore of the St. Lawrence River. This study also aims to evaluate the potential impacts of changes in air temperature and precipitation on soil erosion in the Acadie River Catchment. Overall, the distinct biophysical and climatological settings of these two catchments make them good candidates for this study. In addition, there is an ongoing project on management of agricultural practices in the Acadie River catchment and there are several hydrological studies carried out in Forêt Montmorency experimental watershed (BEREV) and Lac Laflamme watershed, both of which are located within the Montmorency River Catchment. These studies are important references for us, and the outputs of our project will contribute to the current understanding of the hydrological processes in the study areas.

The following three objectives were defined to pursue the aforementioned purpose of this research.

**Objective 1:** Investigate the main hydrological processes over a historical period for an agroforested catchment and a forested catchment in southern Québec and examine their response to projected changes in temperature and precipitation.

The south shore of the St. Lawrence River is dominated by alternating agricultural fields and forest patches, referred to as agroforested landscapes (Jobin et al. 2014). Understanding the main hydrological processes for an agroforested environment,

therefore, is crucial in understanding the potential hydrological responses of these environments to climate change. However, there has been no application of physically based hydrological models to simulate the full set of hydrological processes and to examine their climate sensitivity in agroforested environments. Also, while several studies explored the hydrological processes and hydrological regimes for cold forest environments such as in western and northern Canada (DeBeer and Pomeroy 2017, Fang and Pomeroy 2020, Rasouli et al. 2019), northwest US (Rasouli et al. 2014, Rasouli et al. 2015) and German Alps (Weber et al. 2016), there is a lack of full physically based representation of the key hydrological processes (see Section “*Cold Regions Hydrology*”) for humid boreal forest environments of eastern Canada. In addition, the previous hydrological modelling studies performed in southern Québec (e.g. Boyer et al. 2010, Gombault et al. 2015b, Guay et al. 2015, Quilbé et al. 2008) used a top-down modeling approach in which future changes in climatic conditions are based on predetermined scenarios derived from climate models. A critical limitation of this approach is that it might ignore plausible risks by not covering all possible future conditions. This objective aims to answer the following questions:

**1-a)** What are the main hydrological processes and feedback mechanisms controlling the current hydrological regimes of the catchments?

We hypothesize that snow accumulation and its melt are the main processes controlling the current hydrological regimes of the catchments, with greater influences on the hydrology of the Montmorency River Catchment. Also, we think that while sublimation of blowing snow is the major sublimation component in the Acadie River Catchment, sublimation from canopy intercepted snow dominates the total sublimation in the Montmorency River Catchment.

**1-b)** How will the key hydrological processes respond to various climate change scenarios?

We hypothesize that a considerable amount of snow fraction to total precipitation will convert to rainfall, which would result in reduced snow cover period and advanced spring freshet in both catchments. It is hypothesized that there will be an increase in total water availability due to higher rainfall fractions, thereby an increase in infiltration ratios in both catchments. Evapotranspiration losses are presumed to be higher under a warmer and wetter climate. It is presumed that warmer temperatures will result in lower blowing snow transport in the Acadie River Catchment and declined sublimation losses in both catchments.

**Objective 2:** Examine the difference in climate sensitivity of the hydrology of two contrasted catchments.

The review study performed by Aygün et al. (2020) has revealed that the present cold season (November–March) temperature regime of a region is the main factor governing its hydrological responses to climate change. However, changes in the final hydrological output of a basin, i.e. streamflow, can represent a complex response to both climate forcing and interacting soil and snow processes. While the previous studies have analyzed the hydrological responses to climate change and/or land use change, there has been very little research about the respective roles of current climate and biophysical conditions on catchment hydrology and its responses to climate change. This objective aims to answer the following question:

**2-a)** How do different dominant biophysical features and current climate conditions influence the hydrological responses to climate change?

We hypothesize that the current climate conditions will govern the responses of the hydrological responses of the catchments to climate change, whereas the dominant biophysical characteristics will not play a significant role on the response of the catchments. In this sense, we think that snow accumulation and river discharge in the Acadie River Catchment will be more sensitive to warming due to its milder climate compared to the Montmorency River Catchment.

**Objective 3:** Assess the potential impacts of climate change on soil erosion in the Acadie River Catchment.

Responses of soil erosion to projected changes in air temperature and precipitation in cold agricultural catchments have been little explored. Yet, there is a lack of studies in implementing a hydrological model that has full physically based representation of the key cold regions hydrological process such as infiltration into frozen soils to analyze the impacts of projected changes in temperature and precipitation on the partitioning between surface and subsurface runoff, and the associated responses of the sediment amounts carried by surface and subsurface runoff. This objective aims to answer the following question:

**3-a)** How do projected changes in air temperature and precipitation influence the soil erosion in the agricultural fields?

We hypothesize that soils in the Acadie River Catchment will be more vulnerable to erosion due to a thinner snowpack, early onset of spring snowmelt, a greater number of rainfall events and more frequent snowmelt episodes caused by higher winter and spring temperatures.

## **Thesis Outline**

This dissertation consists of three main chapters related to each objective defined in section “Research Objectives, Scope and Importance”.

CHAPTER I aims to achieve the 1<sup>st</sup> objective of the dissertation by examining the impacts of changes in temperature and precipitation on the hydrology of the agroforested Acadie River Catchment. In this chapter, the main hydrological controls for the historical 1996–2019 period were first diagnosed using the physically based Cold Regions Hydrological Modelling platform (CRHM, Pomeroy et al. 2007a). Then, the model was perturbed using climate change projections and used to assess the hydrological sensitivity to climate change at the catchment and landscape (agriculture vs forest) scales.

CHAPTER II is related to the 2<sup>nd</sup> objective of the dissertation and provides a comparison of the climate sensitivity of the hydrology of Montmorency River and Acadie River catchments. The historical hydrological processes over the 2005–2019 period were first simulated using the Cold Regions Hydrological Modelling platform (CRHM). The results were compared with those from the Acadie River Catchment (CHAPTER I). The respective roles of regional climate and dominant biophysical conditions on the climate sensitivity of the hydrology of two catchments were explored and discussed.

CHAPTER III is associated with the 3<sup>rd</sup> objective of the thesis and quantifies and analyses changes to soil erosion in the Acadie River Catchment under projected changes in precipitation and temperature. The sediment yields from the Acadie River Catchment for the historical 1996–2019 period were calculated using the Modified Universal Soil Equation (MUSLE). The runoff variables of the MUSLE were obtained from the physically based hydrological model previously built and validated for the

Acadie River Catchment (CHAPTER I). Then, the hydrological model was perturbed using climate change projections and used to assess the climate sensitivity of the sediment yield. This chapter also explores impacts of different agriculture management practices on sediment yields under changing climate.

## CHAPTER I

### SHIFTING HYDROLOGICAL PROCESSES IN A CANADIAN AGROFORESTED CATCHMENT DUE TO A WARMER AND WETTER CLIMATE

Okan Aygün<sup>1</sup>, Christophe Kinnard<sup>2</sup>, Stéphane Campeau<sup>3</sup> and Sebastian A. Krogh<sup>4</sup>

<sup>1</sup> University of Québec at Trois-Rivières, Québec, Canada; Centre for Northern Studies (CEN), Québec City, Québec, Canada; Research Centre for Watershed-Aquatic Ecosystem Interactions (RIVE), University of Québec at Trois-Rivières, Canada.

<sup>2</sup> University of Québec at Trois-Rivières, Québec, Canada; Centre for Northern Studies (CEN), Québec City, Québec, Canada; Research Centre for Watershed-Aquatic Ecosystem Interactions (RIVE), University of Québec at Trois-Rivières, Canada.

<sup>3</sup> University of Québec at Trois-Rivières, Québec, Canada; Research Centre for Watershed-Aquatic Ecosystem Interactions (RIVE), University of Québec at Trois-Rivières, Canada.

<sup>4</sup> Department of Natural Resources and Environmental Science, University of Nevada, Reno, USA; Global Water Center, University of Nevada, Reno, USA.

Corresponding author: Okan Aygün ([okan.aygun@uqtr.ca](mailto:okan.aygun@uqtr.ca))

This article has been published in the Special Issue “Whither Cold Regions Hydrology under Changing Climate Conditions” of *Water* (doi:10.3390/w12030739).

**Abstract**

This study examines the hydrological sensitivity of an agroforested catchment to changes in temperature and precipitation. A physically based hydrological model was created using the Cold Regions Hydrological Modelling platform to simulate the hydrological processes over 23 years in the Acadie River Catchment in southern Québec. The observed air temperature and precipitation were perturbed linearly based on existing climate change projections, with warming of up to 8 °C and an increase in total precipitation up to 20%. The results show that warming causes a decrease in blowing snow transport and sublimation losses from blowing snow, canopy-intercepted snowfall and the snowpack. Decreasing blowing snow transport leads to reduced spatial variability in peak snow water equivalent (SWE) and a more synchronized snow cover depletion across the catchment. A 20% increase in precipitation is not sufficient to counteract the decline in annual peak SWE caused by a 1 °C warming. On the other hand, peak spring streamflow increases by 7% and occurs 20 days earlier with a 1 °C warming and a 20% increase in precipitation. However, when warming exceeds 1.5 °C, the catchment becomes more rainfall dominated and the peak flow and its timing follows the rainfall rather than snowmelt regime. Results from this study can be used for sustainable farming development and planning in regions with hydroclimatic characteristics similar to the Acadie River Catchment, where climate change may have a significant impact on the dominating hydrological processes.

**Keywords**

Cold regions hydrology; climate change; hydrological modelling; snowpack; snowmelt; river discharge; spring floods; agroforested catchment; Acadie River Catchment

## 1.1 Introduction

Ongoing and future changes in air temperature and the amount and timing of precipitation can have large impacts on the hydrological cycle, such as changes to the quantity, seasonality and timing of streamflow (Burn and Whitfield 2017, DeBeer et al. 2016, Donnelly et al. 2017, Kundzewicz et al. 2017, Wilson et al. 2010). These changes are likely to vary regionally depending on current and future regional climate conditions and catchment characteristics. In particular, climate projections at mid-latitudes in North America (40° N to 60° N) show an overall warming and increasing precipitation trend, with seasonal changes varying among regions (Allen et al. 2014). The hydrological regime of cold regions is largely controlled by snow processes that are expected to be particularly sensitive to climate change (Harder et al. 2015, Huntington and Niswonger 2012, Huziy et al. 2013, Mahmood et al. 2017, Molini et al. 2011, Rasouli et al. 2014, Rasouli et al. 2015, Stewart et al. 2005). Changes to snow accumulation and melt are expected to modify the timing, duration and magnitude of streamflow in the mid-latitudes of the Northern Hemisphere (Aygün et al. 2020), which could redefine flooding risks as well as hydrological services, such as water supply from snowmelt runoff. The interactions between snow and vegetation play a significant role in snow accumulation (Pomeroy and Gray 1995, Varhola et al. 2010), which can influence runoff volumes and timing. Snowfall intercepted by vegetation can increase sublimation losses, depending on tree species, canopy structure as well as atmospheric conditions (Ellis et al. 2010, Hedstrom and Pomeroy 1998). Once on the ground, snow can be redistributed by wind, particularly in open and wind-exposed environments, which increases sublimation losses from blowing snow (Pomeroy et al. 1993, Pomeroy and Li 2000). Snow is typically transported from sparsely vegetated and exposed terrains to densely vegetated areas and/or topographic depressions (Essery and Pomeroy 2004, Liston et al. 2007).

The traditional approach to assess climate change impact on hydrology is a “top–down” approach, where one or several hydrological models are forced by climate change scenarios from Global Circulation Models (GCMs) (Peel and Blöschl 2011). The spatially coarse outputs of GCMs (approximately 150–300 km) are downscaled to represent local climate conditions required by hydrological models, using either statistical or dynamical downscaling approaches (Salathé et al. 2007). Statistical downscaling relies on empirical relationships between GCMs and locally-observed climate variables, while dynamical downscaling uses GCM simulations to force initial and boundary conditions on a higher-resolution (approximately 1–50 km) regional climate model (Fowler et al. 2007). Although statistical downscaling is less computationally demanding, it requires long-term and high-quality observations to develop the empirical relationships (Tang et al. 2016), which may not be valid under future climate conditions. Dynamical downscaling, on the other hand, is physically based, but computationally more expensive as it involves higher-resolution climate models. Extensive reviews on the use of downscaling methods in hydrological climate change impact studies were made by Fowler et al. (2007) and Teutschbein and Seibert (2010). Meanwhile, some have advocated the use of simpler approaches to avoid the limitations of statistical and dynamical downscaling. These approaches have been used under different names, such as arbitrary/incremental scenarios (Smith and Mendelsohn 2007), sensitivity analysis (Keller et al. 2005, Rasouli et al. 2015), and scenario-neutral approaches (Prudhomme et al. 2010). The “sensitivity analysis” approach will be used in this study, where uniform and regional annual and/or seasonal climate changes are calculated and used to perturb historical time series of air temperature and precipitation. The main limitation of this method is that it does not account for changes in the variability of future climatic conditions (MacDonald et al. 2012). Nevertheless, simple sensitivity analyses of hydrological models to a wide range of plausible climate conditions can reveal how some specific hydrological characteristics (e.g. flood amplitude and timing, snow cover duration and distribution) respond to climate change (Blöschl et al. 2013, Peel and Blöschl 2011) and guide the need to conduct more

targeted scenario-based projections. The method is particularly well suited to examine the interplay of warming temperatures and increasing precipitation that are predicted for many cold regions.

There have been a large number of snow hydrology studies performed in the Canadian Prairies (Fang and Pomeroy 2009, Fang et al. 2010, Fang and Pomeroy 2007, 2008, Harder et al. 2019, Pomeroy et al. 2011, Pomeroy et al. 2013, Pomeroy et al. 2014) and in forest environments in Europe (Förster et al. 2018, Zierl and Bugmann 2005), Scandinavia (Beldring et al. 2008, Graham et al. 2007), western Canada (DeBeer and Pomeroy 2010, Ellis et al. 2010, Fang et al. 2013, MacDonald et al. 2010) and southern Québec (Brown and Tapsoba 2007, Plamondon et al. 1984, Talbot et al. 2006, Troin and Caya 2014). However, some of the main cold regions hydrological processes such as blowing snow redistribution, sublimation and infiltration into frozen soils have been ignored in previous modelling studies in southern Québec. Also, to our knowledge, there has been no application of physically based hydrological models to investigate the hydrological processes and their climate sensitivity in catchments characterized by alternating agricultural fields and forest patches, which are the dominant landscapes along the south shore of the St. Lawrence River. These mosaics of forests and agricultural fields are referred to as agroforested landscapes in southern Québec (Jobin et al. 2014). The amount and timing of available water, and the length of the growing season shape the agricultural production in this region; therefore, climate change-induced modifications of hydrological conditions could have important implications for the economic development of the region. Furthermore, southern Québec suffers from water quality problems caused by erosion from agriculture soils (Clubs-conseils en agroenvironnement 2014, Gombault et al. 2015). As soil erosion rates are enhanced during the cold season (Starkloff et al. 2017), changes in winter surface runoff processes could increase soil erosion rates and further deteriorate the water quality. Therefore, there is an urgent need to better understand cold regions hydrological processes and characterize their climate sensitivity in this region.

The main purpose of this study is to explore the impacts of changes in temperature and precipitation on the hydrology of the agroforested Acadie River Catchment (45° 11' N, 73° 26' W) at the catchment and landscape (agriculture vs. forest) scales. The main hydrological controls for the historical 1996–2019 period were first diagnosed using the physically based Cold Regions Hydrological Modelling platform (CRHM, Pomeroy et al. 2007). Then, the model was perturbed using climate change projections and used to assess the hydrological sensitivity to climate change. This study aims to answer the following questions: (1) what are the physical processes and feedback mechanisms driving the hydrological response of the catchment to warming and increasing precipitation associated with climate change? (2) how sensitive are the hydrological processes to various climate change scenarios? and (3) how do they change across different land cover types (agriculture and forest)? The climate sensitivity analysis framework used in this study provides a useful assessment of potential hydrological changes and their driving processes under a wide range of climate change scenarios.

## **1.2 Materials and Methods**

### **1.2.1 Study Area and Data**

The Acadie River begins near the Canada-United States border and flows northwards over 82 km in the Montérégie region of Québec, on the south shore of the St. Lawrence River (Figure 1.1). It is the main tributary of the Richelieu River into which it drains at the town of Carignan. The drainage area of the Acadie River Catchment is 364 km<sup>2</sup>; however, this study excludes a small (1%) part of the catchment located in US (Figure 1.1) due to the lack of data. The elevation ranges from 40 to 110 m a.s.l. with gentle slopes ranging from 0° to 2°. Approximately 77% of the catchment is covered by agricultural fields with scattered forest patches (Figure 1.1), which is representative of the intensive farming landscape of the southern St. Lawrence lowlands (Jobin et al.

2014). In total, 17% of the catchment area is covered by forest of which, 60% is deciduous, 27% is mixed forests and 13% is coniferous forests. The rest of the catchment (6%) is composed of urban areas, wetlands and lakes and shrubs (Figure 1.1).

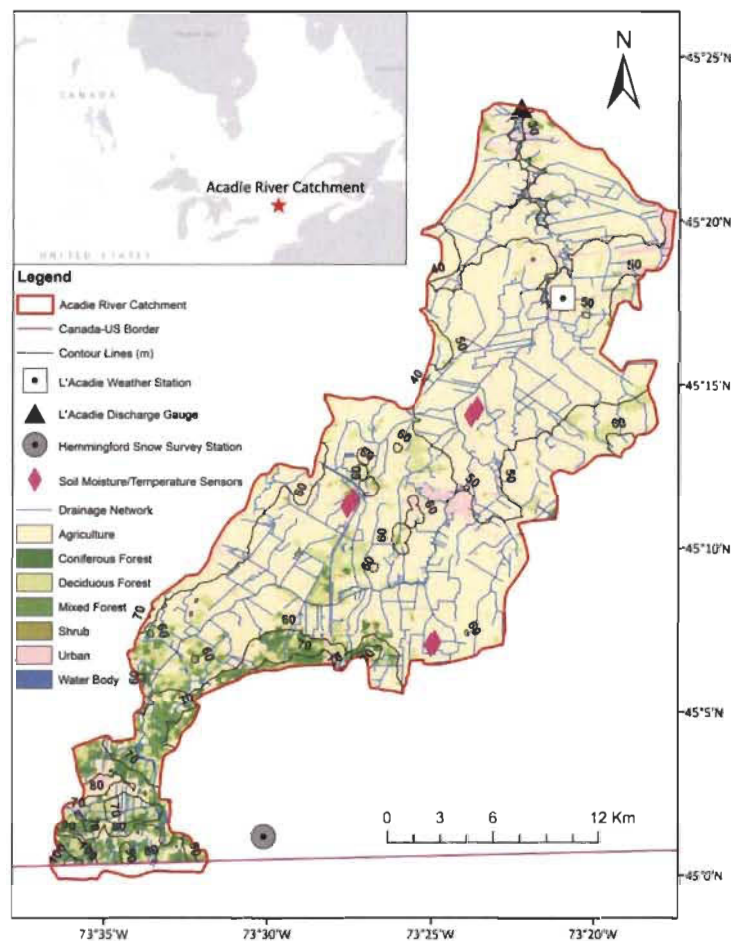


**Figure 1.1.** Acadie River Catchment drainage area, contour lines (every 10 m), land cover, discharge gauge, main meteorological station, snow survey station and soil moisture/temperature sensors.

The climate is cold and humid, with warm summers (Dfb) (Köppen climate classification, Peel et al. 2007). Based on hourly records from the L'Acadie weather station (Figure 1.1) available for the 1996–2019 period (Environment and Climate Change Canada, WMO ID 71372), the mean annual and cold season (November–April)

air temperature was 7.2 and  $-3.9$  °C, respectively, while the mean annual precipitation was 1030 mm. The hydrology of the Acadie River is driven by mixed rain and snow processes, resulting in two high flow events on a normal water year. The first high flow typically occurs in early spring following snowmelt, while the second is a rainfall-runoff event in late fall. The surficial geology of the upper catchment is mainly composed of stony tills due to the geographical proximity of the Adirondack Mountains, whereas the lower catchment is mostly composed of clayey and loamy soils formed from marine and fluvial deposits (Clubs-conseils en agroenvironnement 2014). Organic soils formed from the gradual accumulation of organic matter are present across the catchment, and discontinuous glacial till is found below the marine and fluvial sediments (Clubs-conseils en agroenvironnement 2014). Given the flat topography and poor drainage of soils (particularly clay), tile drainage is used extensively to remove excess water from the surface and rootzone. These subsurface tiles drain into a system of ditches, or surface canals, that are connected to the river network (Figure 1.1). The soil textures in the catchment are 40% clayey, 25% till deposits, 17% organic soil, 10% sandy, 4% loamy and 4% gravelly, which were acquired from Québec Research and Development Institute for the Agri-Environment (IRDA) at a 1:50,000 scale. The land use datasets were obtained from Québec Ministry of Forests, Wildlife and Parks (MFFP) and La Financière Agricole du Québec (FADQ) for both non-agricultural lands and cropping systems. While the main crop is corn (37%) followed by soybeans (33%), different crop types such as vegetables (mainly potatoes and onions), wheat, barley and other cereal grains are also cultivated in the agricultural lands. A  $1 \times 1$  m resolution LIDAR-based digital elevation model (DEM) was obtained from MFFP. The stream and open channel drainage networks were acquired from Québec Ministry of Energy and Natural Resources (MERN). Hourly air temperature, wind speed and relative humidity data within the catchment were acquired for the 1996–2019 period from the L'Acadie weather station (Figure 1.1) maintained by Environment and Climate Change Canada (ECCC). Gaps in the data were filled with data from four other ECCC weather stations (Ste-Clotilde, McTavish,

St-Anne de Bellevue and Frelighsburg) located within a radius of 50 km from the geometric center of the study area. The 1.6% gaps were filled by a principal component analysis (PCA) with the expectation-maximization algorithm (Beckers and Rixen 2003). This method uses a cross-validation procedure prior to filling the missing data to detect the number of statistically significant empirical orthogonal functions (EOFs) used for reconstructing the missing data. The temperature was spatially distributed at the catchment based on an environmental lapse rate of  $0.005\text{ }^{\circ}\text{C m}^{-1}$  (Bergeron 2016). Hourly solar radiation was extracted for the L'Acadie weather station from the database of Hydro-Québec (available at [https://www.simeb.ca:8443/index\\_fr.jsp](https://www.simeb.ca:8443/index_fr.jsp)). Daily total precipitation data were extracted from the  $0.1^{\circ} \times 0.1^{\circ}$  gridded climate data produced by the Québec Ministry of Sustainable Development, Environment, and Fight against Climate Change (MELCC). This dataset was created by spatially interpolating (kriging) quality-controlled observations of permanent weather stations from the Programme de Surveillance du Climat du Québec (PSC) and ECCC (Bergeron 2016). The main advantage of this dataset is its long coverage from 1961 to present. Bajamngigni Gbambie et al. (2017) compared the different gridded precipitation datasets and their implication for hydrological modelling in Québec and found that the MELCC data showed the best performance in catchments located on the south shore of the St. Lawrence River. Daily river discharge measured at the L'Acadie discharge gauge (Figure 1.1) were extracted from the database of Québec Center of Water Expertise (CEHQ) ([www.cehq.qc.ca](http://www.cehq.qc.ca)) for the 1996–2019 period. Observations of snow depth and density were obtained from the Hemmingford snow course station, located within a mixed forest patch a few kilometers away from the catchment (Figure 1.1). Snow surveys have been performed by the MELCC every two weeks during winter and spring since the 1980s, using 10 fixed points uniformly distributed along a 300 m transect representative of the surrounding landscape (Ministère du Développement durable de l'Environnement et des Parcs 2008). Snow depth is measured by probing with a snow tube at eight locations surrounding the fixed points and the results are averaged. Density is measured by weighting the snow tube sample taken at the center

of the fixed point and the result is multiplied by the mean snow depth to estimate SWE at the point. Finally, the mean SWE at the site is obtained by averaging the SWE measured at the 10 points along the transect. Errors on site-averaged SWE are not reported, but federal snow tubes are known to overestimate SWE, typically by 0% to 11% (Dixon and Boon 2012). Additional snow depth and density measurements were made for the winters of 2018 and 2019 along survey transects at agricultural and forest sites, where soil temperature/moisture probes were installed (Figure 1.1). SWE values were then averaged to represent landscape-scale SWE.

### **1.2.2 Hydrological Model Configuration**

The Cold Regions Hydrological Model (CRHM) (Pomeroy et al. 2007) was used to develop a hydrological model for the Acadie River Catchment. The CRHM platform has been successfully used in several catchments in Canada (Fang et al. 2013, Krogh et al. 2017, Rasouli et al. 2014), as well as other cold environments such as the Spanish Pyrenees (López-Moreno et al. 2013), Patagonia (Krogh et al. 2015), northwest US (Rasouli et al. 2015), western China (Zhou et al. 2014) and Svalbard Archipelago (López-Moreno et al. 2016). The CRHM platform has a modular structure that allows creating purpose-oriented models with great emphasis on physically based parameterizations. Modules within the CRHM platform represent hydrological processes of varying complexity that can be selected depending on available data (Harder and Pomeroy 2014). Cold regions hydrological processes included in the CRHM platform include snow accumulation and redistribution by wind, sublimation of canopy-intercepted snowfall, energy budget snowmelt, and infiltration into frozen soils. Hydrological response units (HRUs) with different biophysical attributes (e.g. vegetation cover and soil type) (Domes et al. 2008a) were used as the main spatial units for mass and energy balance calculations. Table 1.1 provides the hydrological processes and modules used to simulate the hydrology of the Acadie River Catchment.

**Table 1.1.** Modules used in the CRHM to simulate the hydrological processes in the Acadie River catchment.

<b>CRHM module</b>	<b>Description</b>
<b>Observation</b>	Meteorological data are read and extrapolated with the environmental lapse rate. The phase of precipitation is predicted with a psychometric energy balance method using air temperature and relative humidity (Harder and Pomeroy 2013).
<b>Radiation</b>	Theoretical global radiation, direct and diffuse solar radiation, and maximum sunshine hours are calculated based on latitude, elevation, slope and azimuth (Garnier and Ohmura 1970).
<b>Sunshine Hour</b>	Sunshine hours are estimated from incoming short-wave radiation (Gray and Landine 1988).
<b>Long-wave radiation</b>	Incoming long-wave radiation is estimated using observed shortwave radiation (Sicart et al. 2006).
<b>All-wave radiation</b>	The net all-wave radiation is calculated from shortwave radiation and the calculated net long-wave radiation (Brunt 1932) for snow-free conditions (Granger and Gray 1990).
<b>Albedo</b>	Snow albedo decay rate is calculated differently depending on the snow cover condition: pre-melt, melt, and post-melt. Albedo is estimated following a linear decay rate for each snow cover condition based on snow depth, new snow, and melting occurrence (Gray and Landine 1987).
<b>Canopy</b>	Estimates snowfall and rainfall intercepted by, and sublimated or evaporated from, forest canopy and unloaded or dripped from the canopy. It updates the under-canopy snowfall and rainfall, and calculates short-wave and long-wave sub-canopy radiation. This module has options for forest environments, small forest clearings, and open environments (Ellis et al. 2010).
<b>Blowing snow transport</b>	Wind redistribution of snow and sublimation (Fang and Pomeroy 2009, Pomeroy and Li 2000). Wind redistribution depends on surface roughness, wind speed and atmospheric and snowpack conditions.
<b>Snowpack energy-balance</b>	The snowpack is represented by a two-layer mass and energy balance model (SNOBAL, (Marks et al. 1998)). The energy balance includes net radiation, sensible and latent heat fluxes, ground heat, advection from rainfall, and change in internal energy.
<b>Evapotranspiration</b>	The Penman-Monteith algorithm (Monteith 1981) is used to calculate actual evapotranspiration from unsaturated surfaces and the Priestly-Taylor algorithm (Priestley and Taylor 1972) for saturated surfaces. These algorithms access water from surface depression and soil moisture.
<b>Crop Growth</b>	A linear crop development is simulated over the growing season, assuming the crops grow continuously from a prescribed Julian date to a maximum value (Pomeroy et al. 2007). Initial crop height at the beginning of the growing season, crop growth rate, crop planting date, crop maturity date and crop harvest date are used to estimate the crop height change over the growing season. These parameters are defined according to the most common crops (soya bean and corn) at the catchment using the studies performed in south Québec (Almaraz et al. 2009, Gallichand et al. 1991).

<b>CRHM module</b>	<b>Description</b>
<b>Infiltration</b>	Snowmelt infiltration into frozen soil using a parametric equation (Gray et al. 2001) and rainfall infiltration into unfrozen soil based on soil texture and ground cover (Ayers 1959) are estimated.
<b>Soil Moisture</b>	Three-layer model consisting of two soil layers (recharge layer and lower layer) and groundwater layer. It estimates soil moisture balance, depressional storage, surface/sub-surface flows within two soil layers and groundwater discharge in groundwater layer, and interactions between surface flow and groundwater (Dornes et al. 2008b, Fang et al. 2013, Leavesley et al. 1983). The recharge (top) layer receives infiltration from depressional storage, snowmelt, and rainfall. Evaporation withdraws water first from canopy interception and depressional storage and then from both soil layers via evapotranspiration, depending on the rooting depth and available soil moisture (Armstrong et al. 2010). Horizontal and vertical flows from soil layers and groundwater layer are calculated based on Darcy's law, where Brooks and Corey's relationship (Brooks and Corey 1964) is used to estimate the actual hydraulic conductivity in the unsaturated zone.
<b>Surface-subsurface runoff routing</b>	Runoff between HRUs is routed using the Muskingum method based on the geometric characteristics of the stream channel (VenTe 1964). Subsurface and groundwater flows are routed by Clark's algorithm (Clark 1945).

HRUs were delineated using a combination of six soil types (clayey, till deposits, organic soil, sandy, loamy and gravelly) and seven land use classes (agriculture, urban, deciduous forest, mixed forest, coniferous forest, shrub and wetland), resulting in 37 HRUs. The open drainage canals and river network were also defined as two separate HRUs, resulting in a total of 39 HRUs. Elevation, slope and aspect were not used for HRU delineation as they vary little over the catchment. Mean physiographic parameters for each HRU (i.e., area, altitude, slope, aspect and latitude) were extracted from the 1 m DEM and HRU maps processed in ArcGIS. Soil parameters such as soil texture, thickness of the recharge and lower soil layer, porosity and saturated hydraulic conductivity were derived from studies in neighboring catchments (Croteau 2006, Lamontagne 2005, Michaud et al. 2006, Perreault et al. 2013, Tremblay 2008), a soil survey report from the Agriculture and Agri-Food Canada (Lamontagne et al. 2002), and a groundwater study in the Montérégie region (Carrier et al. 2013). The pore size distribution indices were defined based upon soil textures (Brooks and Corey 1966). Summer leaf area index (LAI) for the agricultural and forest HRUs were transferred from the neighboring Chateauguay River basin (Croteau 2006).

An LAI value of  $3 \text{ m}^2 \text{ m}^{-2}$  was assigned to agricultural HRUs (mainly corn and soybean), while summer LAI values for forest HRUs varied between 2.2 and  $6 \text{ m}^2 \text{ m}^{-2}$  depending on forest type (deciduous, mixed and coniferous). Coniferous and mixed forests were assigned a winter LAI of 2.2 and  $0.5 \text{ m}^2 \text{ m}^{-2}$ , respectively (Croteau 2006). An LAI of  $0.4 \text{ m}^2 \text{ m}^{-2}$  was assigned to deciduous forests, which is similar to the value used for aspen forests in the Canadian Prairie during winter (Pomeroy et al. 2010). Maximum canopy snow load capacity values for the forest HRUs were assigned based on previous studies performed in western Canada (Pomeroy et al. 2010, Pomeroy et al. 1998, Pomeroy et al. 2013), using values of 6.3, 2.1,  $0.5 \text{ kg m}^{-2}$  for coniferous, mixed and deciduous forests, respectively. Based on the local measurements (Figure 1.1) from November to April in 2018 and 2019, initial average fall volumetric soil moisture content was assigned as 30%, and soil temperature was estimated at  $+2 \text{ }^\circ\text{C}$  (at 15 cm soil depth) prior to snowmelt, which controls the heat flux from the soil to the snowpack base (Marks et al. 1998). While this positive soil temperature was chosen to best represent the observed near surface (0–30 cm) temperature before snowmelt, shallow soil freezing was also observed in the agricultural fields in the winter of 2019. With this in mind, the frozen soil infiltration algorithm (Gray et al. 2001) was included in the model (Table 1.1). Blowing snow transport is simulated from the agriculture towards the forest HRUs, following the sequence from agriculture to wetland, shrub, drainage canal and finally to forest HRUs (Fang and Pomeroy 2009). The maximum value for the liquid water holding capacity of snow was set to  $0.01 \text{ mm mm}^{-1}$  as suggested by Marks et al. (1998). Saturation excess water in soils is added to the subsurface flow in the agricultural fields to emulate the effect of subsurface tile drainage. Regarding runoff routing, agricultural fields were first routed to the drainage canals, and then the outflow from the drainage canals routed to the river network, while other HRUs were routed directly to the streamflow network. Similar to the method used by Cordeiro et al. (2017), the routing length was determined as the median distances from the centroid of each HRU to the closest drainage canal

for agricultural HRUs, and as the median distances from each HRU to the streamflow network for non-agricultural HRUs.

Given that the Hemmingford snow survey station (Figure 1.1) is located a few kilometers outside of the catchment, a point-scale snowmelt model was constructed for the Hemmingford station using the CRHM platform. The point-scale model was forced with disaggregated hourly precipitation from daily precipitation extracted from the MELCC gridded climate data at the Hemmingford station (Figure 1.1), and the infilled hourly meteorological air temperature, relative humidity, wind speed and solar radiation at the L'Acadie weather station. This point-scale model was used to validate the snowpack and canopy parameters, which were assigned based on the literature, as presented in the previous section. As such, the model did not require a calibration. The SWE observations at the Hemmingford snow station were compared with the point-scale model simulations for the 1996–2019 period.

The evaluation of the hydrological model performance was carried out using statistical performance measures, including the Nash-Sutcliffe efficiency (NSE, (Nash and Sutcliffe 1970); Equation 1.1), the Kling-Gupta efficiency (KGE, (Gupta et al. 2009); Equation 1.2), the percent bias (PBIAS; Equation 1.3), the root mean square error (RMSE; Equation 1.4) and the root mean square error-observations standard deviation ratio (RSR, (Moriasi et al. 2007); Equation 1.5).

$$NSE = 1 - \frac{\sum(X_s - X_o)^2}{\sum(X_o - \mu_o)^2} \quad \text{Equation 1.1}$$

$$KGE = 1 - \sqrt{(r - 1)^2 + \left(\frac{\sigma_s}{\sigma_o} - 1\right)^2 + \left(\frac{\mu_s}{\mu_o} - 1\right)^2} \quad \text{Equation 1.2}$$

$$PBIAS = 100 \times \frac{\sum(X_s - X_o)}{\sum X_o} \quad \text{Equation 1.3}$$

$$RMSE = \sqrt{\frac{1}{n} (X_s - X_o)^2}$$
Equation 1.4

$$RSR = \frac{RMSE}{\sigma_o}$$
Equation 1.5

where  $n$  is the number of samples,  $r$  is the linear correlation between observations and simulations, and  $\mu_o$ ,  $\sigma_o$  are the mean and standard deviation of the observed values ( $X_o$ ), respectively.  $\mu_s$ ,  $\sigma_s$  are the mean and standard deviation of the simulated values ( $X_s$ ), respectively. The NSE is an often-used metric in hydrology, which determines the relative magnitude of the residual variance compared to the measured data variance (Nash and Sutcliffe 1970). While  $NSE = 1$  indicates perfect fit between the observations and simulations,  $NSE = 0$  indicates that the model simulations have the same explanatory power as the mean of the observations. KGE is based on a decomposition of NSE into its constitutive components (correlation, bias and variability) in the context of hydrological modelling (Gupta et al. 2009). While  $KGE = 1$  indicates perfect correspondence between simulations and observations, it has been argued that  $KGE < 0$  indicates that the mean of observations provides better estimates than simulations (Knoben et al. 2019). Therefore, any positive value of NSE and KGE suggests that the model has some predictive power and higher values indicate better model performance. A positive value of PBIAS indicates a model overestimation, while a negative value indicates an underestimation. The RMSE is a weighted measure of the difference between observation and simulation. The RSR standardizes RMSE using the standard deviation of the observations. The lower RSR, the lower the RMSE, and the better the model simulation performance (Moriasi et al. 2007).

### 1.2.3 Climate Sensitivity Analysis

Climate sensitivity analysis was performed at both the catchment and landscape (agriculture vs. forest) scale. The range of projected changes in temperature and precipitation was based on ensemble climate model projections available for the administrative regions of Québec (Ouranos 2015). These projections were produced from a set of 11 downscaled global climate simulations produced from the CMIP5 ensemble for two periods (2041 to 2070 and 2071 to 2100) and two greenhouse gas emission scenarios (moderate: RCP 4.5 and high: RCP 8.5) for the province of Québec (Ouranos 2015). The reference period for the projections was 1981–2010. The 1-d quantile mapping (Gennaretti et al. 2015) method was employed to downscale the raw global climate simulation outputs to a finer resolution (Chaumont 2014). Guided by the scenarios produced for the Montérégie administrative region where the Acadie River Catchment is located, temperature warming up to 8 °C (0–8 °C at 1 °C intervals) and an increase in total precipitation up to 20% (0–20%, 5% intervals) were considered in the sensitivity analysis. Thus, these scenarios encompass the most extreme end-of-the-century projection within the spread (10–90 percentile) of ensemble projections under the high emission RCP 8.5 scenario (Ouranos 2015). The different combinations of warming and precipitation changes were applied to the historical data and the hydrological run for each perturbed climate record, for a total of 45 individual climate scenarios. The baseline scenario of no change in air temperature and precipitation ( $\Delta t = 0$  °C and  $P = 100\%$ : reference run) represents the historically averaged observed data over the 1996–2019 period. The scenario of “ $\Delta t = 8$  °C and  $P = 120\%$ ” stands for a warming of 8 °C and an increase of 20% in averaged precipitation relative to the reference run.

## 1.3 Results

### 1.3.1 Historical Simulations

#### 1.3.1.1 Point-Scale Snow Simulations

Observed and simulated SWE at the Hemmingford snow survey station was compared for the 1996–2019 period (Figure 1.2). The Nash-Sutcliffe efficiency (NSE) is 0.57 over the 23-year simulation. The root mean square error (RMSE), correlation coefficient and mean percent bias (PBIAS) are 28 mm, 0.84 and  $-10\%$  for the simulation period, respectively. SWE is mostly underestimated during low snowpack years, which is likely due to uncertainties in the gridded precipitation dataset, parameters selections and limitations of the snow model (SNOBAL, Marks et al. 1998), which was originally developed to simulate deep snowpacks. Despite some discrepancies, these results are considered to be adequate for the purpose of this study.

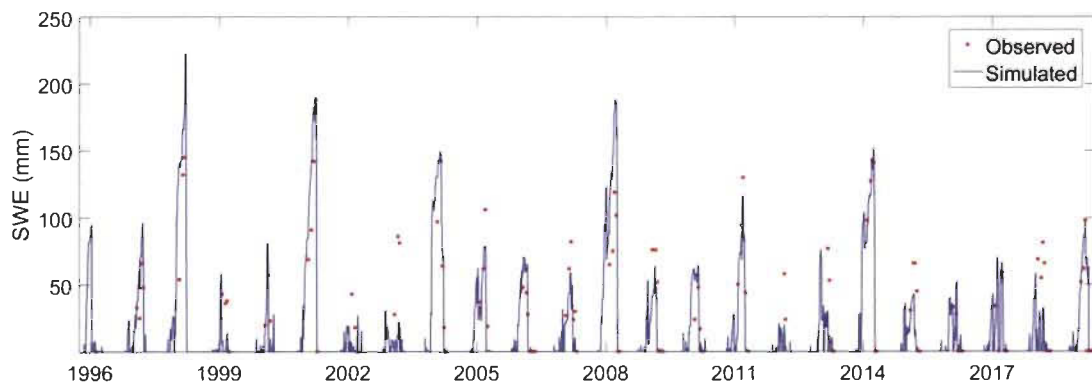


**Figure 1.2.** Observed and simulated snow water equivalent (SWE) at the Hemmingford snow survey station.

### *1.3.1.2 Simulation of Snow Mass Fluxes*

Simulated SWE was compared against snow surveys at the agriculture and forest sites for the winters of 2018 and 2019 (Figure 1.3). The observed spatial heterogeneity in snow accumulation within the agricultural sites and forest patches is represented by the error bars (Figure 1.3). The simulations show that the annual peak SWE is higher in the deciduous forest than in agricultural fields for both winters (Figure 1.3). For the forest site, the mean percent biases are 10% and -6%, and the RMSEs are 35 mm and 25 mm for the winters of 2018 and 2019, respectively. For the agriculture site, the mean percent biases are -19% and 50%, and the RMSEs are 21 mm and 41 mm for the winters of 2018 and 2019, respectively. While the overall absolute accuracy is similar between the two sites, relative errors are greater in fields where the snowpack is thinner. Hence, the model performs relatively better in forests than in fields, which could be partly explained by the fact that thinner snowpacks are more difficult to simulate by SNOBAL (Marks et al. 1998). The model could not capture the melt event leading to the complete disappearance of snow cover in agriculture fields in mid-March 2019 (Figure 1.3c), which is the main reason for the high percent bias and root mean square error. It is important to note that although there was no snow cover observed in agriculture fields in mid-March 2019, there was an ice layer with a thickness of 5 to 10 cm over the fields. Disregarding the mid-March 2019 event, the mean percent bias and RMSE becomes 23% and 11 mm, respectively, for the winter of 2019. For both agriculture and forest sites, the statistical performance measures show a better performance in the winter of 2019, which had wetter conditions and a thicker snowpack.

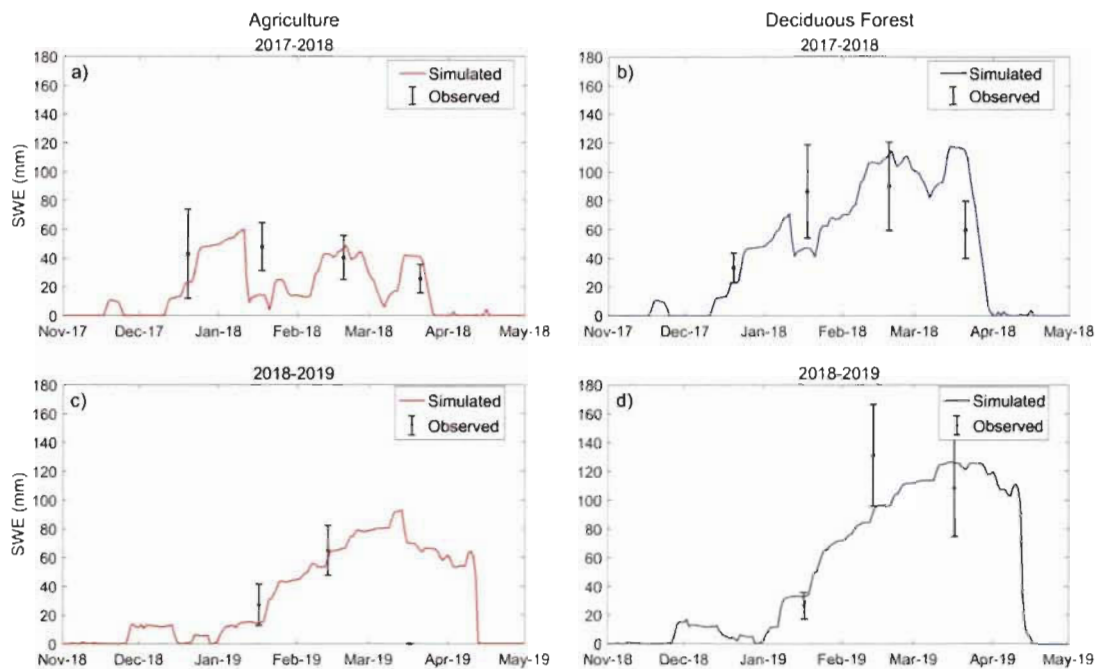


**Figure 1.3.** Comparisons of simulated and observed SWE for (a, c) agriculture and (b, d) deciduous forest for the winters of 2017–2018 and 2018–2019, respectively. Error bars represent the standard deviation of SWE.

Figure 1.4 shows simulated SWE at the catchment and landscape (i.e., agriculture, deciduous forest, mixed forest and coniferous forest) scale for the 1996–2019 period. The mean annual peak SWE at the catchment scale is 65 mm and occurs on February 25, with large inter-annual variability ranging between 21 mm and 118 mm (Figure 1.4a). Landscape scale simulated SWE shows that peak SWE is on average higher in the deciduous and mixed forest, followed by agricultural fields and coniferous forest (Figure 1.4b). The accumulated SWE in the coniferous forest is lower than in the mixed and deciduous forests because of the greater sublimation losses from canopy-intercepted snowfall, as the maximum canopy interception load capacity and LAI are significantly higher in the coniferous forests than in the deciduous and mixed forests. The bare agricultural fields suffer from sublimation losses and transport of blowing snow, resulting in lower snow accumulation than in deciduous and mixed

forests. These processes were further investigated by examining snow mass balance at the landscape scale.

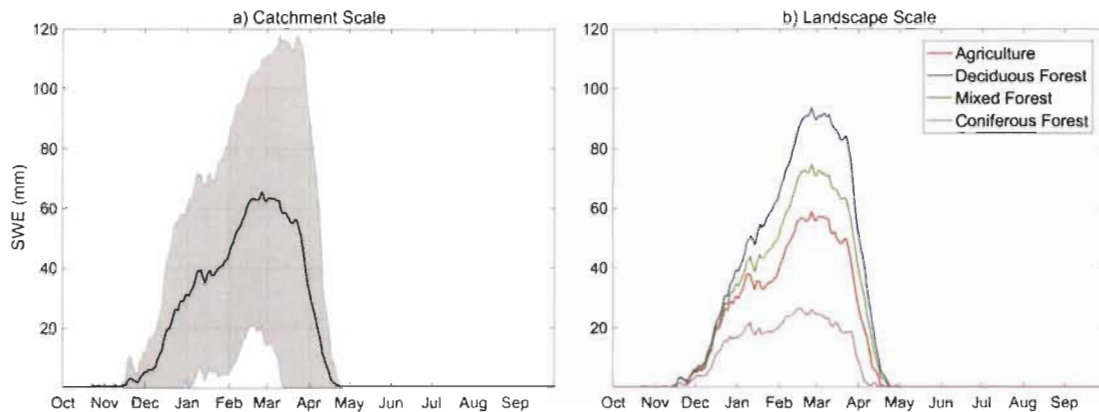


**Figure 1.4.** SWE simulations at the (a) catchment and (b) landscape scale. The grey envelope in (a) illustrates the inter-annual variability for the 1996–2019 period.

Daily average cumulative snow mass fluxes and mean daily SWE for the 1996–2019 period for agriculture and forest (i.e., deciduous, coniferous and mixed forest HRUs) landscape units are presented in Figure 1.5. Snowmelt is the largest outflux at approximately  $200 \text{ mm year}^{-1}$  for both landscape units, representing approximately 15% of the mean annual precipitation and 85% of the mean annual snowfall. Snowpack sublimation reaches an average of  $23 \text{ mm year}^{-1}$ , which is approximately 10% of the mean annual snowfall, with a negligible difference between landscape units. Overall, total sublimation losses from both snowpack and blowing snow reach  $33.7 \text{ mm year}^{-1}$  (14.3% of annual snowfall) in fields, while in forests snowpack and canopy sublimation together account for  $46.4 \text{ mm year}^{-1}$  (19.4% of annual snowfall).

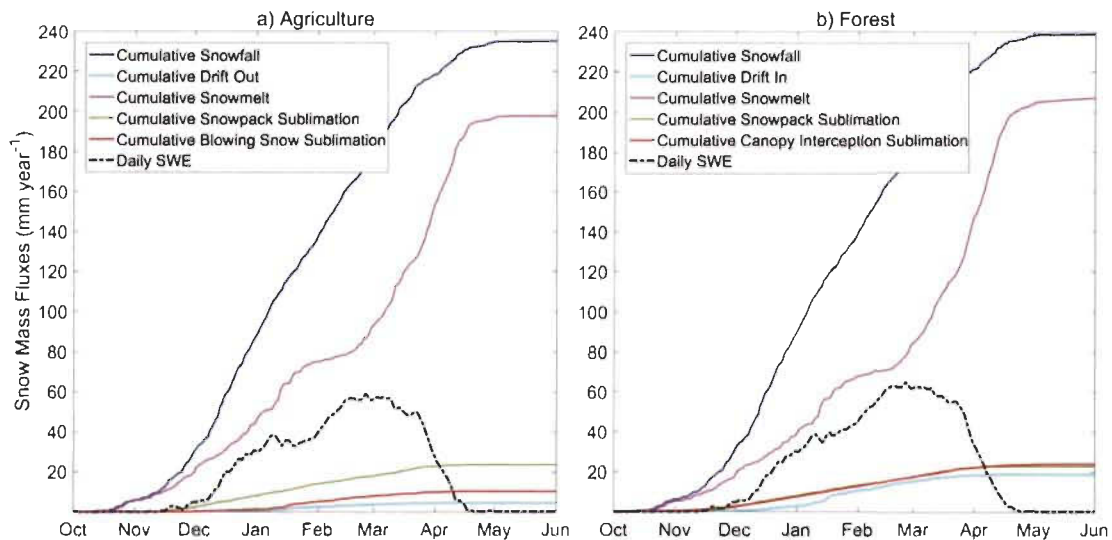


**Figure 1.5.** Average simulated cumulative snow mass fluxes and daily SWE between the years 1996 and 2019 in (a) agriculture (b) forest.

Sublimation from canopy interception exhibits large spatial variability among the forest types (Figure 1.5b). Canopy interception loss reaches approximately 40% of the mean annual snowfall in the coniferous forest, whereas it is 12% and 3% of the mean annual snowfall in the mixed and deciduous forest, respectively. Higher canopy interception losses in the coniferous canopies is attributed to the greater canopy snow interception loads and LAIs. However, the dominant deciduous (60%) and mixed (27%) forest cover in the catchment shape the average canopy interception loss in the forest, which is on average  $24 \text{ mm year}^{-1}$  (10% of the mean annual snowfall) (Figure 1.5). Simulated blowing snow transport out of agricultural fields is only  $5 \text{ mm year}^{-1}$  and the blowing snow sublimation is approximately  $10 \text{ mm year}^{-1}$ , which together represent approximately 6% of the mean annual snowfall. On the other hand, blowing snow transport into forests reaches  $19 \text{ mm year}^{-1}$  which is higher than blowing snow transport out of agricultural fields. This difference is due to the larger area of agricultural fields and also because snow is transported from other HRUs such as open drainage canals once their storage capacity is reached. Although total sublimation losses are greater in forests than in agricultural fields, the annual peak SWE is slightly

higher in forests (65 mm) than in agriculture fields (59 mm), as also observed from snow surveys (Figure 1.4). This can be explained with the redistribution of the blowing snow from the agriculture and other HRUs to the forest.

### ***1.3.1.3 Simulation of Streamflow and Water Fluxes***

Simulated daily streamflow was compared against measurements at the outlet of the catchment for the 1996–2019 period (Figure 1.6). The Nash-Sutcliffe efficiency (NSE), Kling-Gupta efficiency (KGE), percent bias (PBIAS) and the ratio of root mean square error to the standard deviation of measured discharge (RSR) for the 23 year simulation period are 0.51, 0.71, 2.4% and 0.70, respectively. Simulated streamflow properly represents flow duration curves (Figure 1.6b); however, low flows (high exceedance probability,  $>0.9$ ) are overestimated. The cumulative mean daily discharge (Figure 1.6c) shows good performance with a mean bias of 2.4% at the end of the water year. However, the model slightly overestimates winter streamflow (Figure 1.6c), which corresponds to overestimated high exceedance flows (Figure 1.6b). The peak flow timing and magnitude are generally well represented by the model (Figure 1.6a, b). The inter-annual variability of observed annual streamflow volume is approximately 30%, which is slightly higher than that of simulated streamflow (23%) (Figure 1.6c). Uncertainties in simulated streamflow may arise from uncertainties in the forcing data, parameters uncertainty and errors in the model structure. Despite these reasonable discrepancies, both the timing and volume of streamflow are overall well simulated, suggesting a good model performance.

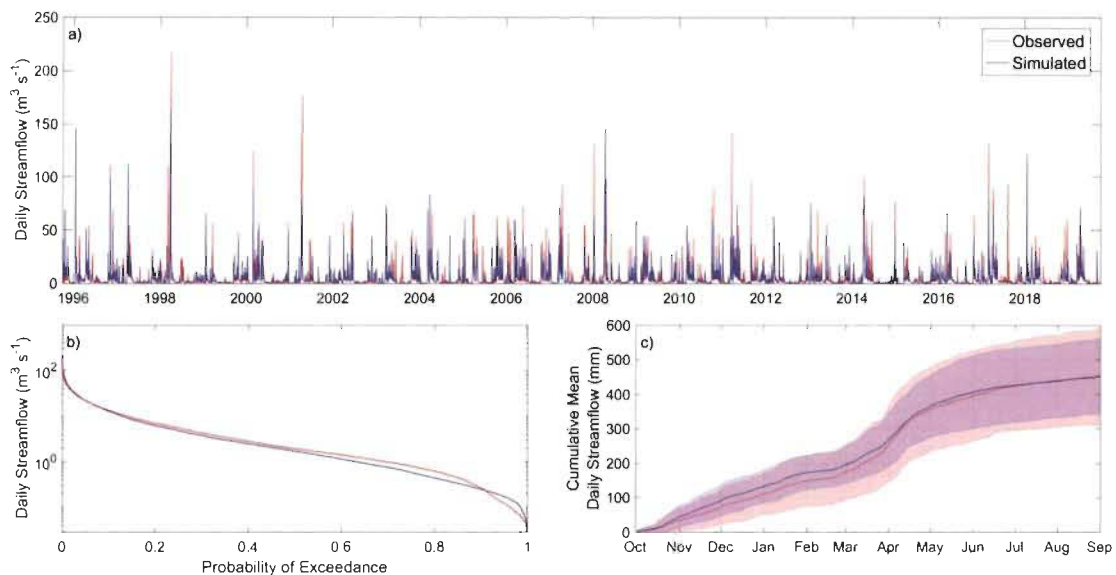


**Figure 1.6.** Assessment of the CRHM platform performance in simulating streamflow at the outlet of the Acadie River Catchment by comparing (a) daily streamflow, (b) flow duration curve, and (c) cumulative mean daily streamflow. The shades around the average values in panel (c) represent the inter-annual variability.

On average, 77% of the mean annual precipitation is rainfall and 23% is snowfall (Figure 1.7). The snowfall and rainfall ratios exhibit large inter-annual variability with the snowfall ratio varying between 17% and 34%, and the rainfall ratio between 66% and 83% (Figure 1.7). On average, 6% of the total rainfall occurs during winter months (Dec-Jan-Feb), while almost half of the total rainfall is observed from May to September. The evapotranspiration (ET) loss constitutes the largest water loss term ( $462 \text{ mm year}^{-1}$ ) (Figure 1.7), representing 45% of total annual precipitation. ET exhibits a relatively low inter-annual variability with an annual standard deviation of 28 mm (Figure 1.7). The simulated ET is very similar to the annual evapotranspiration value ( $487 \pm 42 \text{ mm}$ ) calculated for a neighboring basin (Chateauguay River basin) for the 1963–2001 period (Croteau 2006). The ratio of annual evapotranspiration to annual precipitation is also comparable to that simulated for the 1971–2001 period for the neighboring Pike River agricultural watershed using the SWAT model (47%) (Gombault et al. 2015). Annual total sublimation loss

including snowpack sublimation, canopy interception sublimation and blowing snow sublimation is 36 mm (Figure 1.7), which is approximately 3% of the annual precipitation and 15% of the mean annual snowfall. Mean annual sublimation shows an inter-annual variability of  $\pm 15$  mm (Figure 1.7). The sublimation losses are simulated between mid-November and mid-April when the snow cover is present. During the same period, ET is suppressed due to the presence of snow cover. Once the snow cover disappears, ET begins and almost 60% of the total ET occurs between mid-April and August. Mean annual streamflow is 453 mm (Figure 1.7), resulting in an average runoff ratio of 0.44. The mean annual runoff exhibits large inter-annual variability ( $\pm 110$  mm), which mostly results from the high interannual variability of rainfall ( $\pm 115$  mm) (Figure 1.7). Annual average groundwater recharge rate is 79 mm (8% of total annual precipitation) over the 23 year period, with an inter-annual variability of  $\pm 26$  mm (Figure 1.7). The historically averaged groundwater recharge rate is comparable to the simulated annual groundwater recharge of  $86 \pm 10$  mm in the neighboring Chateauguay River Basin using the physically based HELP (Hydrologic Evaluation of Landfill Performance) numerical model for the 1963–2001 period (Croteau 2006). The ratio of groundwater recharge to annual precipitation is also comparable to that (8%) simulated for the Pike River Watershed (Gombault et al. 2015). The largest increase in both cumulative streamflow and groundwater recharge is observed between April and May (Figure 1.7), which can be explained by the snowmelt contribution to both fluxes. High evapotranspiration levels in summer months decrease soil moisture levels, thereby limiting the amount of excess soil moisture available for percolation, which in turn results in very low groundwater recharge rates in summer months (Figure 1.7).

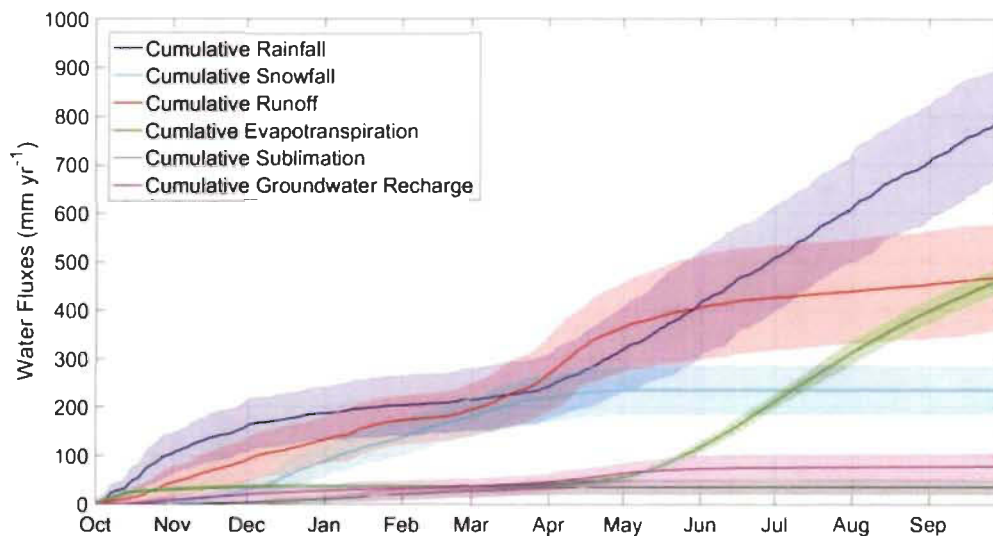


**Figure 1.7.** Average annual cumulative water fluxes at the catchment scale between the years 1996 and 2019. The shades around the average values represent the inter-annual variability ( $\pm$  standard deviation).

### 1.3.2 Climate Sensitivity

#### 1.3.2.1 Climate Sensitivity of Snow Regime and Mass Balance Components

Historically, snowfall represents 23% of the mean annual precipitation for the reference period ( $\Delta T = 0$ ;  $P = 100\%$ ) (Figure 1.7), which decreases down to 11% and 8% for a 5 and 8 °C warming scenario, respectively, regardless of changes in the mean annual precipitation (Table 1.2). With a warming of 2 °C and no change in precipitation, peak SWE decreases by 70% and occurs 8 days earlier (Table 1.2). The same scenario delays the snow onset date (SOD) by 25 days and advances the snow disappearance date (SDD) by 14 days, shortening the snow cover duration (SCD) by 39 days (Table 1.2). In case of a 5 °C warming and no change in precipitation, the peak SWE drastically shifts from late February to late December and decreases below 10 mm. Under the same scenario, SDD advances by more than a month and SCD decreases to 132 days per year (Table 1.2). With the maximum warming of 8 °C, peak SWE decreases by more than 90%. A 20% increase in precipitation would only buffer 28% of the warming

induced peak SWE decline for a +2 °C scenario, and 7% and 3% for the +5 and +8 °C scenarios, respectively. Hence increasing precipitation could only counterbalance less than a third of the SWE decline under a moderate (+2°C) warming scenario.

**Table 1.2.** Sensitivity of snow variables to selected climate change scenarios. The snow onset date (SOD) and the snow disappearance date (SDD) are the first and last days of the water year with snow on the ground (SWE > 0.1 mm), respectively. SCD, snow cover duration.

Snow Variable	$\Delta T$ (°C)	0	2	5	8	0	2	5	8
	P (%)	100	100	100	100	120	120	120	120
Snowfall Ratio (%)		23	17	11	8	23	17	11	8
Peak SWE (mm)		65	19	9	5	100	32	13	7
SOD (DOWY*)		20	45	45	58	20	26	45	58
Peak SWE Date (DOWY)		148	140	83	77	148	140	83	77
SDD (DOWY)		212	198	177	171	212	198	177	177
SCD (days)		192	153	132	113	192	172	132	119
Snowmelt (mm year <sup>-1</sup> )		201	145	99	67	251	180	121	82
Snowmelt Rate (mm day <sup>-1</sup> year <sup>-1</sup> )		1.04	0.95	0.75	0.59	1.31	1.05	0.91	0.68

DOWY\* = day of the water year (starting in October 1st).

Along with the simulated decline in SCD and snowmelt, the mean snowmelt rate also exhibits a decline under all warming scenarios. However, it is important to note that the snowmelt rate under a 2 °C warming scenario with 20% increase in precipitation slightly increases compared to the reference period. In addition, all warming scenarios lead to more frequent mid-winter snowmelt events, resulting in several snow accumulation maxima during the snow season (Figure 1.8).

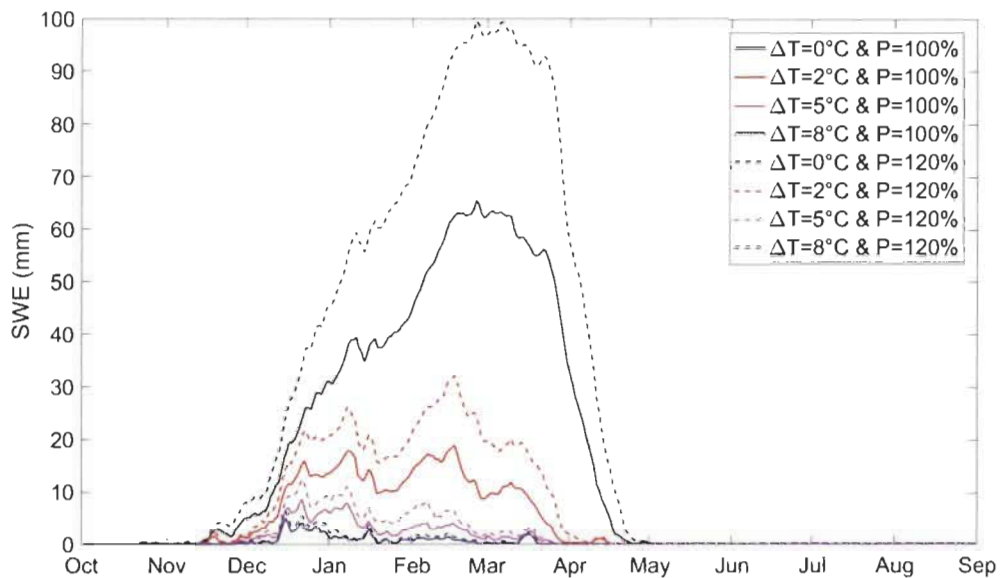


**Figure 1.8.** Sensitivity of snow accumulation to selected climate change scenarios.

The climate response surfaces demonstrate that the timing and magnitude of annual peak SWE is very sensitive to warming (Figure 1.9). Peak SWE decreases under all scenarios where warming occurs (Figure 1.9a), while peak SWE increases by 10% to 60% in response to increasing precipitation alone (Figure 1.9b). There is a positive sensitivity zone on the response surface where peak SWE increases (blue surface on Figure 1.9b) in response to increasing precipitation and limited warming ( $<1$  °C). However, once further warming occurs, peak SWE decreases regardless of simulated changes in precipitation. Considering that the catchment already has a relatively warm and wet cold season, small changes in temperature generate large changes in snowfall ratios (Table 1.2) that result in a stronger sensitivity of peak SWE as shown by the closer contours between 0 and 2 °C warming (Figure 1.9a, b). Warming causes a considerable shift in the timing of peak SWE towards earlier dates (Figure 1.9c). A more pronounced sensitivity of peak SWE timing is observed for warming between 2 and 3 °C, as shown by the closer contours in Figure 1.9c. This strong sensitivity can be explained by the occurrence of several seasonal snow accumulation maxima due to more frequent mid-winter snowmelt events in warmer winters (Figure 1.8). Although

multiple snow accumulation peaks are also simulated for warming up to 2 °C, the annual SWE peak remains towards the end of winter. However, when warming reaches 3 °C, the peak SWE simulated in early January becomes the annual peak, which explains the shift in annual peak SWE date by more than a month (Figure 1.9c).

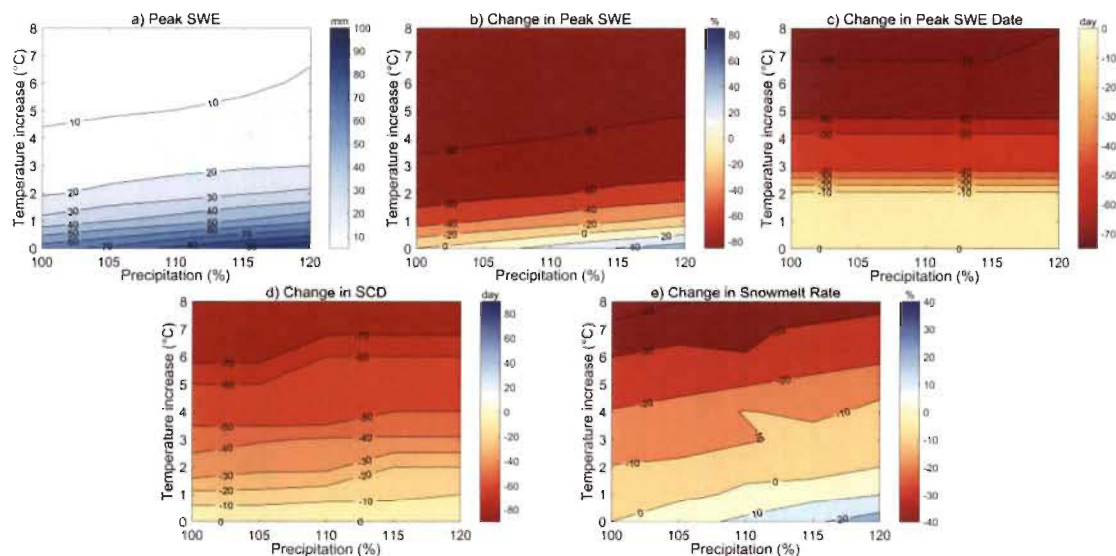


**Figure 1.9.** Climate sensitivity of snow metrics. **(a)** Annual peak SWE; **(b)** relative change in annual peak SWE; **(c)** change in annual peak SWE date—negative values represent a shift towards earlier dates; **(d)** change in snow cover duration (SCD); **(e)** relative change in the snowmelt rate.

As shown by Figure 1.9d, changes in snow cover duration (SCD) are mostly driven by warming and not by increasing precipitation. This is because the declining snowfall ratios, caused by warmer temperatures, shorten both the onset and termination of the snow season. Figure 1.9e shows that the snowmelt rate is primarily influenced by warming and to a lesser extent by increasing precipitation. If warming is not accompanied by an increase in precipitation, then snowmelt rates decrease. This occurs because with reduced snow accumulation in response to warming, snow melts earlier and at lower rates under lower available solar energy. On the other hand, the snowmelt rate could increase when low to moderate warming is accompanied by increasing precipitation. For instance, a 1 °C warming and a 20% increase in precipitation result

in a 10% increase in the snowmelt rate (Figure 1.9e). This might be explained with the increased incoming energy available for thicker snowpack. The responses of peak SWE to warming air temperatures and increasing precipitation in agriculture and forest landscapes (Figure 1.10a, b) are similar to that of the catchment average (Figure 1.9a). Here, peak SWE in forest landscape is obtained by aggregating peak SWEs in deciduous, mixed and coniferous forest HRUs. There is a considerable decline in peak SWE in response to warming temperature in both landscapes (Figure 1.10a, b). The peak SWE decreases below 10 mm in both landscapes when warming exceeds 4 °C and precipitation remains unchanged. The sensitivity of peak SWE in forests is more pronounced than in agriculture fields for warming between 0 and 2 °C, as shown by the closer contour lines in Figure 1.10c. The peak SWE in agriculture fields becomes slightly higher than in the forests when the warming reaches 2 °C (Figure 1.10c). This can be explained by changes in blowing snow transport in response to warming, such that less snow is transported into the forest under warmer temperatures, which is due to the increasing bond strength and cohesion of snow as it warms (Li and Pomeroy 1997).

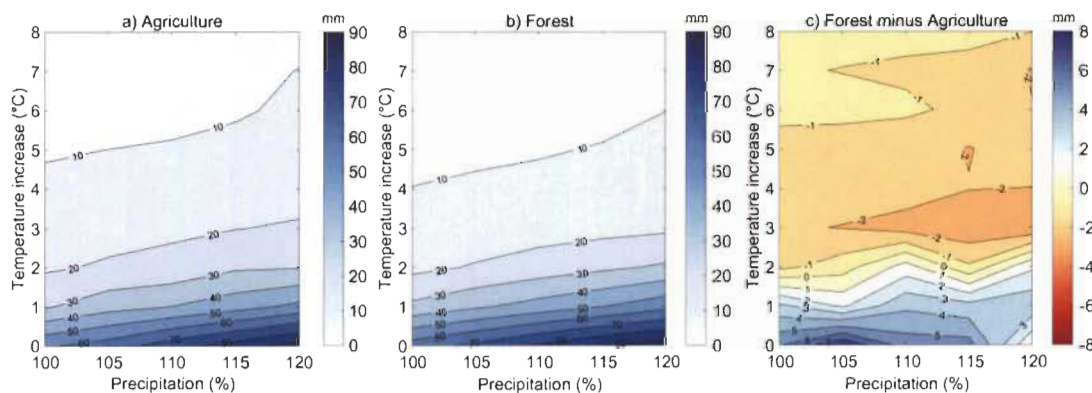


**Figure 1.10.** Peak SWE in response to temperature and precipitation changes in (a) agriculture, (b) forest, and (c) difference between forest and agriculture.

Table 1.3 summarizes the changes in key snow processes with respect to selected climate change scenarios for the agriculture fields and forests. The values in

Table 1.3b are the aggregated changes over the forest types (deciduous, mixed and coniferous). Snow erosion (drift out) from agricultural fields and snow transport to forested areas (drift in) decline by 50% in response to a 2 °C warming without changing precipitation (Table 1.3). A warming of 5 °C leads to a decline in snow transport by more than 80% even if precipitation increases by 20% (Table 1.3). Accordingly, blowing snow sublimation in agriculture fields declines considerably with warming (>85% with 5 °C warming), while snowpack sublimation is relatively less sensitivity to warming (<50% with 5 °C warming, Table 1.3a). Apart from an insignificant increase (0.3%) in the sublimation ratio in agriculture fields for a 2 °C warming, this ratio declines for the rest of the warming scenarios.

**Table 1.3.** Changes in magnitude of annual snow mass fluxes and resulting annual peak SWE in **(a)** agriculture and **(b)** forest under selected warming and increasing precipitation scenarios.

<b>a) Agriculture</b>	$\Delta T$ (°C)	0	2	5	8	0	2	5	8
	P (%)	100	100	100	100	120	120	120	120
Drift out (mm year <sup>-1</sup> )		4.5	2.2	0.6	0.2	5.0	2.7	0.8	0.3
Snowpack Sublimation (mm year <sup>-1</sup> )		23.4	19.9	13.2	7.5	19.6	19.5	14.9	8.4
Blowing Snow Sublimation (mm year <sup>-1</sup> )		10.3	5.2	1.5	0.5	11.5	6.4	2.1	0.6
Snowmelt (mm year <sup>-1</sup> )		198	145	100	68	248	179	121	83
Sublimation Ratio (%)		14.3	14.6	12.7	10.5	10.9	12.5	12.2	9.8
Drift Out Ratio (%)		1.9	1.3	0.5	0.3	1.8	1.3	0.6	0.3
Snowmelt Ratio (%)		83.8	84.2	86.7	89.2	87.3	86.2	87.2	89.9
Peak SWE (mm)		59	19	9	5	95	30	13	7
<b>b) Forest</b>	$\Delta T$ (°C)	0	2	5	8	0	2	5	8
	P (%)	100	100	100	100	120	120	120	120
Drift in (mm year <sup>-1</sup> )		18.8	8.9	2.6	1.0	20.8	11	3.4	1.1
Snowpack Sublimation (mm year <sup>-1</sup> )		22.6	18.6	12.7	6.3	18.8	18.8	13.5	7.2
Canopy Sublimation (mm year <sup>-1</sup> )		23.8	18.6	13.2	9.1	19.2	14.5	17.5	19.1
Snowmelt (mm year <sup>-1</sup> )		208	144	93	62	259	180	115	76
Sublimation Ratio (%)		18.2	20.5	21.8	19.9	12.8	15.6	21.2	25.7
Snowmelt Ratio (%)		81.8	79.5	78.2	80.1	87.2	84.4	78.8	74.3
Peak SWE (mm)		65	17	8	5	96	31	12	6

Snowpack sublimation and canopy sublimation in forests are less sensitive to a 2 °C warming (decline by <21%, Table 1.3b) than the blowing snow influx (decline by 53%, Table 1.3b). The declines in canopy sublimation are most likely due to more rapid and earlier unloading of snow with warmer temperatures. The sublimation ratio in forests increases up to 5 °C warming (with no increase in precipitation) and then declines for 8 °C warming. The sublimation ratio in forests is higher than that in agriculture fields during the reference period, and this difference accentuates under warming scenarios. Snowmelt shows a considerable decline in response to warming for both agriculture and forests (approximately 50% for 5 °C warming, Table 1.3), due to decreasing snowfall ratios. Within the 0–2 °C warming zone, the peak SWE in forests decreases faster than in agriculture fields (Figure 1.10c and Table 1.3). Eventually, a warming of 2 °C leads to a homogenization of peak SWE among the agriculture and forest landscapes (Figure 1.10c), due to reduced redistribution and sublimation of blowing snow from agriculture fields to forests, and decreased canopy sublimation in the forest.

### ***1.3.2.2 Climate Sensitivity of Streamflow Regime and Water Balance Components***

The Acadie River Catchment has a mixed snowmelt/rainfall hydrological regime and in a warmer future, it is expected to shift toward a more rainfall-dominated regime (Figure 1.11a). The ratio of snowmelt volume to mean annual streamflow volume changes from 43% in the reference period to 32% and 23% for the 2 and 5 °C warming scenarios, respectively. With a 2 °C warming and no change in precipitation, the annual peak daily flow decreases by 21% and occurs 3 months earlier (mid-January) than for the reference period (mid-April) (Figure 1.11a). In case of 2 °C warming accompanied by a 20% increase in precipitation, the annual peak daily discharge shows an insignificant increase (0.02%) (Figure 1.11a, b), but a 3 month shift in timing from mid-April to mid-January, increasing winter flows (Figure 1.11a). This effect can also be seen from the increase in flows with exceedance probability between 0.2 and 0.8 under 2 °C warming with a 20% increase in precipitation (Figure 1.11b).

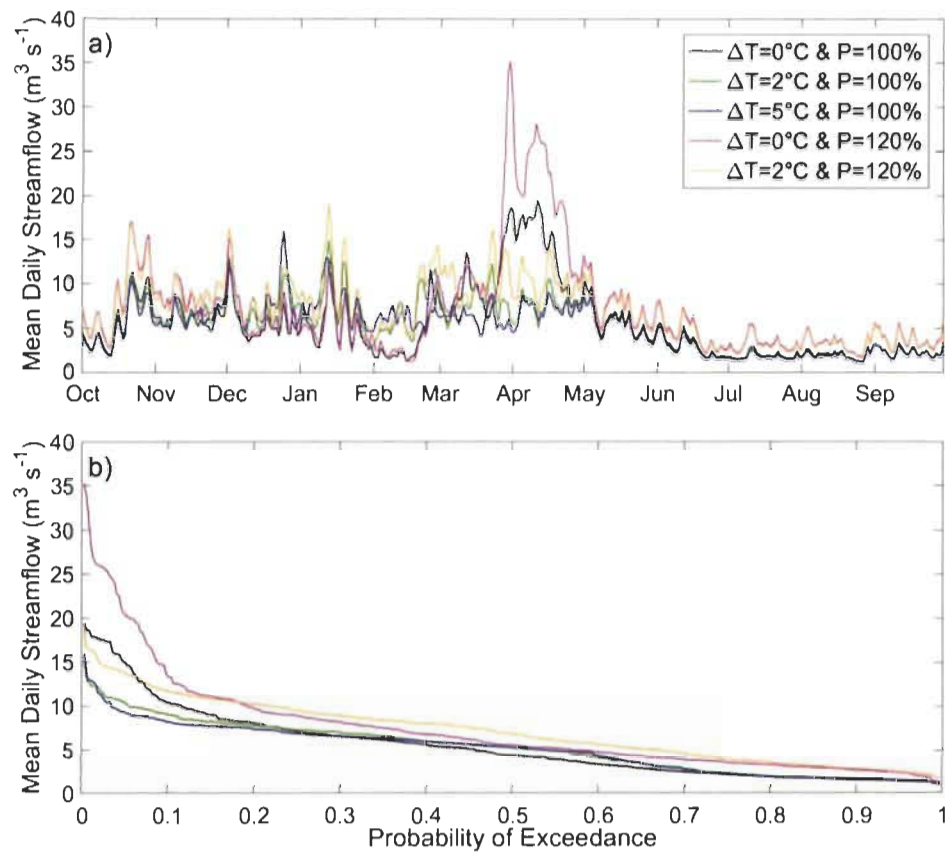


**Figure 1.11.** Changes in mean daily streamflow in response to selected warming and increasing precipitation scenarios. Changes in (a) mean daily streamflow, and (b) exceedance probability of mean daily streamflow.

In the reference period, the Acadie River mean hydrograph exhibits two peaks flow following snowmelt in spring: the first peak occurs early April, followed by a second, slightly greater peak some ten days later (Figure 1.11a). With a 20% increase in precipitation and no warming, the second peak becomes more distinct while the first peak becomes higher than the second one (Figure 1.11a). The increase in high flows (exceedance probability lower than 0.1) under a 20% increase in precipitation and no warming can also be seen in Figure 1.11b. The low flows (exceedance probability higher than 0.8), on the other hand, exhibit an increase with a 20% increase in precipitation regardless of warming (Figure 1.11b).

The response surfaces of the magnitude and timing of annual peak discharge, and total annual discharge, are presented along with projected changes in annual temperature and precipitation for the periods 2041–2070 and 2071–2100 under a moderate emission scenario (RCP 4.5) and a high emission scenario (RCP 8.5) (Ouranos 2015) (Figure 1.12). Increasing precipitation could cause an increase in annual peak daily discharge by up to 60%, depending on the warming and increase in precipitation. This zone of positive sensitivity of peak discharge is delineated by the 0% contour in Figure 1.12a, below which the peak discharge exhibits an increase. In this positive sensitivity zone, the increase in precipitation is enough to counterbalance the negative impact of warming on the peak discharge. Increasing peak daily discharge might thus represent the short-term response of peak discharge to climate change, before more significant warming (Figure 1.12d) depletes the snowpack and causes peak discharge to decline and shift from the spring to winter. This sensitivity zone is particularly interesting considering the recent flood events in southern Québec (Lin et al. 2019, Teufel et al. 2019), versus the long-term projection of reducing SWE and peak discharge. For instance, a warming of 1.2 °C increases the annual peak daily discharge by 2% if there is an increase in precipitation by 12%, whereas the same amount of warming causes peak daily discharge to decline by 15% if there is only a 1% increase in precipitation. Both of these scenarios are within the uncertainty range of projected changes in annual temperature and precipitation for the 2041–2070 period under a moderate emission scenario RCP 4.5 (Figure 1.12d). Meanwhile, when the warming exceeds 2°C, as projected under both moderate and high emission scenarios (Figure 1.12d) for the mid and end of century, the peak daily discharge declines regardless of changes in precipitation (Figure 1.12b). Warming scenarios lead to considerable shifts in the timing of annual peak discharge towards earlier dates (Figure 1.12b). With a 1.2 °C warming and a 12% increase in precipitation (Figure 1.12d), the peak discharge shifts by 20 days earlier, while a precipitation increase of less than 3% under the same warming level shifts the peak discharge 50 to 80 days earlier, i.e., before peak SWE.

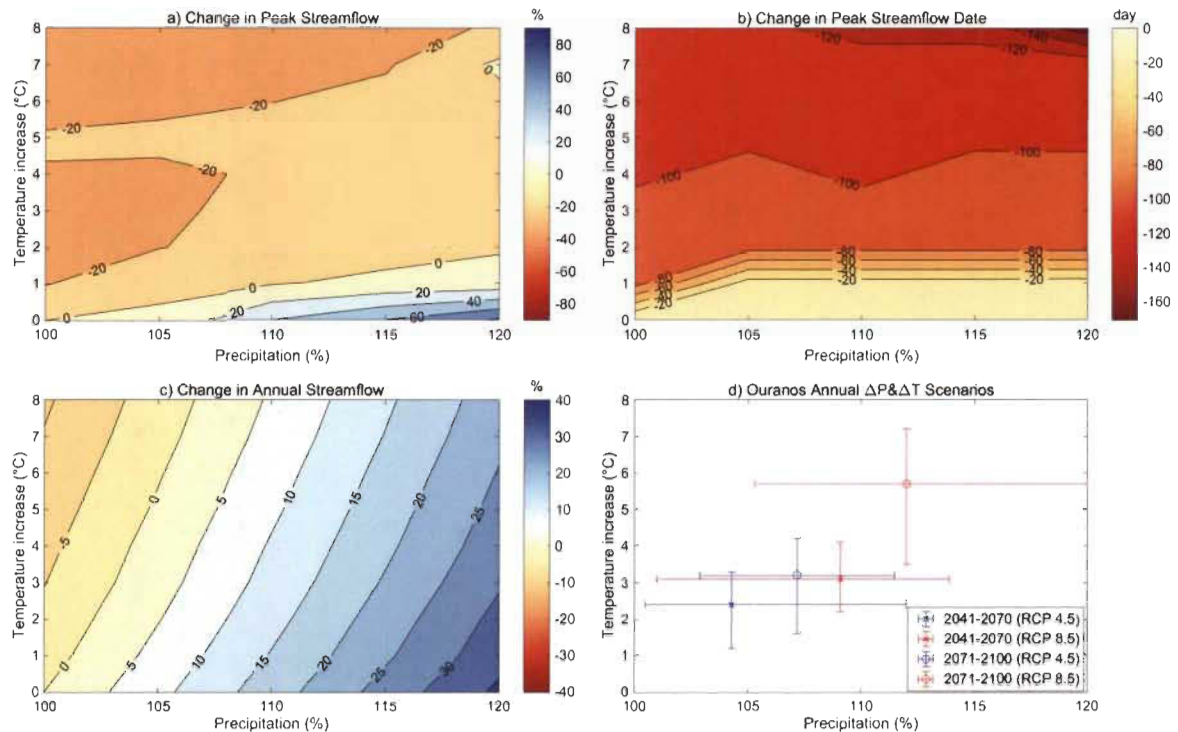


**Figure 1.12.** Climate sensitivity of streamflow in Acadie River. **(a)** Changes in annual peak daily discharge; **(b)** changes in annual peak daily discharge date; **(c)** changes in annual total discharge in response to temperature and precipitation changes; and **(d)** projected changes in annual temperature and precipitation for the periods 2041–2070 and 2071–2100 under a moderate emission scenario (RCP 4.5) and a high emission scenario (RCP 8.5) for Montérégie region of Québec (Ouranos 2015).

These results show that a higher peak daily discharge could occur earlier in response to limited warming ( $<1.5\text{ }^{\circ}\text{C}$ ) if precipitation increase sufficiently, which highlights the considerable uncertainty in future peak daily discharge caused by uncertainties in projected precipitation. Meanwhile, when warming exceeds  $1.5\text{ }^{\circ}\text{C}$ , the peak daily discharge occurs before peak SWE regardless of the precipitation increase. For instance, a  $2\text{ }^{\circ}\text{C}$  warming and 20% increase in precipitation advances the timing of peak SWE by only eight days from February 25 to February 17 (Figure 1.9c), the same warming scenario without precipitation change causes the annual peak daily discharge timing to shift from April 11 to January 13 (Figure 1.12b). This highlights that a warming beyond  $1.5\text{ }^{\circ}\text{C}$  causes a transition in the flow regime of the Acadie River

Catchment from a mixed snowmelt/rainfall to rainfall dominated regime, with the seasonality of precipitation dictating the magnitude and timing of the annual peak discharge (Figure 1.12a). Total annual discharge, on the other hand, appears much more sensitive to increasing precipitation than to warming (Figure 1.12c), which contrasts with the response of peak SWE (Figure 1.9a, b). Total annual discharge decreases by 2% with a 1 °C warming, however, an increase of 7% is simulated if this 1 °C warming occurs with an increase in precipitation of only 5%. The decrease in annual discharge volume caused by a 5 °C increase in temperature could be completely counterbalanced with an increase in precipitation of 5%.

The rainfall ratio is simulated to increase between 6% and 12%, depending on the amount of warming (Table 1.4). Increasing evapotranspiration rates occur under all warming and increasing precipitation scenarios (Table 1.4). In terms of seasonal changes in streamflow, the mean winter streamflow increases under warmer temperatures, which can be explained by the increasing rainfall ratios and more frequent snowmelt events in warmer winters. The mean winter streamflow increases by 45% and 71% under a 2 °C warming and 2 °C + 20% precipitation increase, respectively. A 20% increase in precipitation with no warming results in an unchanged rainfall ratio but an increase in total rainfall in winter, which together cause the smallest increase (9%) in winter mean runoff. The same scenario increases the mean spring streamflow by 39%, which is due to the greater amount of snow accumulation and associated snowmelt contribution as well as higher amount of rainfall. If only warming air temperatures are considered, mean streamflow declines during both spring and summer (Table 1.4). On the other hand, mean summer streamflow increases in response to increasing precipitation even under warmer temperatures which drive higher evapotranspiration rates, which means that increasing rainfall can counteract the enhanced evaporation losses in terms of streamflow volume generation.

**Table 1.4.** Mean annual catchment scale water fluxes for the selected climate change scenarios. For the reference period, the mean annual temperature is 7.2 °C and mean annual precipitation is 1030 mm.

Water Flux	$\Delta T$ (°C)	0	2	5	0	2	5
	P (%)	100	100	100	120	120	120
Rainfall Ratio (%)		77	83	89	77	83	89
Annual Peak Streamflow ( $m^3 s^{-1}$ )		19.3	14.8	15.9	35.3	19.0	18.2
Mean Winter Streamflow ( $m^3 s^{-1}$ )		4.9	7.1	7.3	5.2	8.4	9.1
Mean Spring Streamflow ( $m^3 s^{-1}$ )		9.5	6.9	6.1	13.2	9.3	8.0
Mean Summer Streamflow ( $m^3 s^{-1}$ )		2.1	2.0	1.9	3.7	3.5	3.3
Evapotranspiration ( $mm year^{-1}$ )		462	479	497	479	498	520
Winter Snowmelt Infiltration (mm) (%)		3.0 (4.2)	2.6 (2.8)	1.9 (2.5)	2.8 (4.0)	2.7 (2.4)	3.5 (3.8)
Winter Rainfall Infiltration (mm) (%)		24 (33)	39 (42)	55 (45)	24 (28)	41 (37)	60 (40)
Spring Snowmelt Infiltration (mm) (%)		4.4 (4)	1.2 (3)	0.7 (3.9)	10 (6.4)	1.0 (1.8)	0.8 (3.5)
Spring Rainfall Infiltration (mm) (%)		107 (53)	122 (55)	131 (55)	116 (47)	134 (51)	145 (51)
Summer Infiltration (mm) (%)		270 (94)	272 (94)	273 (95)	307 (88)	309 (89)	311 (90)
Groundwater Recharge ( $mm year^{-1}$ )		79	87	97	103	110	121
Winter Groundwater Recharge (mm)		17	23	30	20	26	35
Surface Runoff Ratio * (%)		43	33	24	40	32	23

Surface runoff ratio \* = The ratio of surface runoff volume to total streamflow volume.

In Table 1.4, the snowmelt infiltration ratio (%) is calculated as the ratio of snowmelt infiltration volume to total snowmelt volume, whereas the rain infiltration ratio (%) represents the ratio of rainfall infiltration volume to effective rainfall volume (total rainfall minus evaporation from canopy interception). Infiltration rates during the cold season are governed by rainfall infiltration (33% in winter and 53% in spring) rather than snowmelt infiltration (4.2% in winter and 4% in spring) (Table 1.4), due to the fact that frozen soil algorithm (Gray et al. 2001) limits the snowmelt infiltration. Warming causes a general decrease in the snowmelt infiltration ratio but an increase in the rainfall infiltration ratio. Under warming with no increase in precipitation, the winter snowmelt infiltration ratio declines by 1.4 to 3.7% (Table 1.4), which could be explained by the higher initial soil moisture saturation before snowmelt events caused by higher rainfall ratios and also more frequent mid-winter melt events. For instance, with a 2 °C warming, the rainfall ratio in winter increases from 28% to 56% and the total number of snowmelt days in January and February increases by 11 days, which in turn lead to greater soil moisture saturation. The rainfall infiltration

ratio in winter increases by 9 to 12% in response to warming (Table 1.4), which can be explained with the fact that there is an increase in rainfall fraction and rainfall infiltration is not limited by the snow cover (Gray et al. 2001). In spring, the snowmelt infiltration ratio declines by 1% (Table 1.4) with a 2 °C warming, which can be explained with declining snow accumulation and melt available for infiltration. Under warming-only scenarios, rainfall infiltration in spring increases by 2% due to higher rainfall ratios. An increase in precipitation by 20% with no warming causes an increase in the spring snowmelt infiltration ratio by 2.4% and a decrease in winter snowmelt infiltration by less than 1%, whereas rainfall infiltration ratios in both seasons exhibit a decline. Warmer temperatures cause smaller snowmelt infiltration ratios even if there is a 20% increase in precipitation, whereas rainfall infiltration ratios become higher. In summer, for the reference period, more than 90% of the effective precipitation infiltrates, which changes between -5% and 1%, depending on the climate change scenario (Table 1.4). Overall, changes in summer are lower than those in spring and winter. Therefore, changes in winter and spring conditions explain most of the decreases in surface runoff ratio in response to warming (Table 1.4). It is important to note that mimicking subsurface tile drainage plays a role in this response, since replacing snowmelt by rainfall with warming could have produced saturation excess runoff, however, this saturation excess water is added to the subsurface flow rather than surface flow. There is also an increase in both winter and annual groundwater recharge rates under all warming scenarios (Table 1.4).

A model falsification was performed to assess the impact of frozen soil infiltration process on the partitioning between surface and subsurface runoff, and on annual peak streamflow (Table 1.5). Annual streamflow declines from 468 mm to 414 mm for the reference period when the frozen soil infiltration process is removed from the model (Table 1.5). The results show that removing the frozen soil infiltration process reduces the surface runoff ratio by 40%, from 43% to 3.2% for the reference period (Table 1.4 and Table 1.5). This is due to snowmelt infiltrating rather than forming infiltration

excess surface runoff when the frozen soil infiltration parameterization is disabled (Gray et al. 2001). The small amount of surface runoff generated is thus uniquely from infiltration excess rainfall and/or snowmelt when frozen soils are not considered, since all saturation excess water is assumed to drain through the subsurface tiles. Surface runoff becomes less sensitive to warming with the falsification of frozen soil infiltration (Table 1.5) compared to when frozen soil infiltration is considered (Table 1.4). This is because the infiltration rates in winter and spring, which are driving the changes in surface runoff ratios (Table 1.4), are not primarily driven by peak snow accumulation anymore as opposed to when the frozen soil infiltration algorithm is used (Gray et al. 2001). Therefore, the declines in peak SWE caused by warming scenarios (Table 1.2) do not result in significant changes in surface runoff ratios (Table 1.5). The model falsification also indicates that annual peak streamflow would reduce by 17% for the reference period when frozen soils do not limit infiltration (Table 1.4 and Table 1.5).

**Table 1.5.** Mean annual catchment scale water fluxes (falsified model) for the selected climate change scenarios.

Water Flux	$\Delta T$ ( $^{\circ}C$ )	0	2	5
	P (%)	100	100	100
Streamflow ( $mm\ year^{-1}$ )		414	408	400
Surface Runoff ( $mm\ year^{-1}$ )		13	12	11
Surface Runoff Ratio (%)		3.2	2.9	2.8
Annual Peak Streamflow ( $m^3\ s^{-1}$ )		16	11.1	13

## 1.4 Discussion

Snow accumulation in the Acadie River Catchment has historically shown a large inter-annual variability (Figure 1.4a) due to its high sensitivity to climatic conditions. Moreover, drastic changes in snow accumulation regime are simulated under warming scenarios regardless of precipitation. This is in line with the known high temperature sensitivity of snow in the relatively mild cold regions of the warmer sectors of the Dfb

(cold climate with warm summers) climate zone (Peel et al. 2007). The decline in peak SWE caused by 1 °C warming cannot be compensated even with a 20% increase in precipitation (Figure 1.9b). Although there is a decrease in the sublimation ratio under this scenario, the decrease in snowfall ratio predominates and causes reduced snow accumulation. The peak SWE shows the highest sensitivity in the 0–2 °C warming zone, declining by 25%–35% per °C, which is higher than the 7% per °C reduction for the Svalbard Archipelago (López-Moreno et al. 2016), the 7% per °C reduction for Yukon (Rasouli et al. 2014), the 15% per °C reduction for the Swiss Alps (Beniston et al. 2003), the 11%–20% per °C reduction for the Spanish Pyrenes (López-Moreno et al. 2014, López-Moreno et al. 2013) and the 20% per °C reduction for the Washington Cascades (Casola et al. 2009). The greater sensitivity of SWE in the Acadie River Catchment is likely due to the warmer temperatures in this region than in the other study areas. Snow accumulation exhibits several peaks due to more frequent mid-winter snowmelt events within the 0–2 °C warming range (Figure 1.8), and the first peak occurring in early January becomes dominant when warming reaches 3 °C. Therefore, the peak SWE date shows its highest sensitivity in the 2–3 °C warming band (Figure 1.9c) and marks the transition from a snowmelt dominated to a rainfall dominated streamflow regime. Increasing precipitation leads to higher peak SWE only if the warming is less than 1 °C (Figure 1.9a), which may represent the transient, short-term response of the catchment to climate change for the next decades.

Under present climate conditions, annual drift out (snow erosion) from agricultural fields were low (2% of annual snowfall) compared to the prairies and steppe environments where snow erosion rates range from 30% to 75% of annual snowfall (Pomeroy et al. 1993, Tabler 1975). This is mostly due to higher bond strength and cohesion of snow resulting from relatively higher winter air temperatures in the Acadie River Catchment, which in turn leads to higher wind speed thresholds required to initiate snow saltation (Li and Pomeroy 1997). Simulated average peak SWE was slightly higher in forests than in agriculture fields under recent climate, in agreement

with field observations (Figure 1.5). However, the snow accumulation in these two landscape units become uniform when warming reaches 2 °C (Figure 1.10). This uniformization is explained by the decrease in blowing snow transport and sublimation due to increased snow cohesion under warming (Li and Pomeroy 1997) and decreasing canopy sublimation.

Snowmelt is an important contributor to groundwater recharge (Figure 1.7), in agreement with other studies (Evans et al. 2018, Jasechko et al. 2014, Mohammed et al. 2019). While the decline in snowmelt (Table 1.2) caused by warmer temperatures was expected to result in lower groundwater recharge rates, annual groundwater recharge increased instead. This is driven by significant increases in groundwater recharges during winter due to increasing mid-winter snowmelt events, as shown by previous studies (Eckhardt and Ulbrich 2003, Okkonen and Kløve 2010, Sulis et al. 2011, Toews and Allen 2009). The results show that shallower snowpacks caused by warmer temperatures melt earlier and more slowly under most of the warming scenarios considered, which is in line with the “slower snowmelt in a warmer world” hypothesis (Musselman et al. 2017). Some other studies also reported that earlier snowmelt occurring at a time of year with lower solar elevations resulted in slower snowmelt rates in different cold regions such as Spain (López-Moreno et al. 2013), the western US (Jepsen et al. 2012, Rasouli et al. 2019, Trujillo and Molotch 2014) and south western Canada (Rasouli et al. 2019). In contrast, the results also show that increasing precipitation under limited warming ( $\leq 2^{\circ}\text{C}$ ) can compensate the slower melt rates caused by warming and even accelerate snowmelt rates depending on the amount of increase in precipitation. Furthermore, some studies have also reported increasing snowmelt rates in the future such as in an Arctic headwater basin (Canada), where a 6 °C warming and a 40% increase in precipitation was projected under the RCP 8.5 scenario (Krogh and Pomeroy 2019). This suggests that there are competing mechanisms that depend on the degree of warming and projected changes in

precipitation that can either increase or decrease snowmelt rates, and that those mechanisms may vary regionally depending on historical conditions.

The peak streamflow was found to consistently shift towards earlier dates under warmer temperatures, which have also been projected for other catchments in southern Québec (Boyer et al. 2010, Gombault et al. 2015, Minville et al. 2008). The magnitude of the annual peak daily streamflow shows a non-linear response to warming and increasing precipitation. While the peak spring flow decreases under most scenarios when warming exceeds 1.5 °C, the peak flow was found to increase within a restricted climate envelope (Figure 1.12a). Hence, higher and earlier peak flows might represent the short term, transient response of peak flow to warming and increasing precipitation, increasing flooding risks on the short term. On the other hand, although greater warming causes a decline in spring peak flow, winter flows are projected to increase, in line with the higher winter streamflow projections for different catchments in Québec (Boyer et al. 2010, Gombault et al. 2015, Minville et al. 2008, Riboust and Brissette 2015) and in some other cold regions (Beldring et al. 2008, Huziy et al. 2013, Teutschbein et al. 2015). Greater winter flows can cause extreme flooding and ice jamming, resulting in significant damages (Riboust and Brissette 2015). In addition, changes in the streamflow timing and volume can have significant repercussions on reservoir operations for flood control and hydropower generation. Both the direction of change in peak spring flow under limited warming (<1.5 °C), and the amount of increasing winter flow under greater warming (>1.5 °C), will strongly depend on the projected changes in precipitation (Figure 1.12), highlighting the significant uncertainty in changes to peak discharge and flood risks, as precipitation is typically the most uncertain variable of climate projections. The falsification of frozen soil infiltration processes resulted in drastic declines in surface runoff ratios (Table 1.4 and Table 1.5), suggesting that this process is very important on the partitioning between surface and subsurface flows and overall streamflow generation in catchments with extensive subsurface tile drainage such as the Acadie River Catchment.

## 1.5 Conclusion

A physically based hydrological model was created using the CRHM platform to simulate the hydrological cycle over 23 years in an agroforested catchment in southern Québec, Canada. The model showed a reasonable performance against discontinuous SWE observations and daily streamflow measurements. A possible range of impacts of climate change on catchment hydrology was obtained by perturbing the model with warming hourly air temperatures from 1 to 8 °C and increasing daily total precipitation from 0% to 20%. The positive sensitivity zone encountered in peak streamflow response surfaces suggests a possibility for increased flood risks in the very near future (1–2 decades) given the uncertainties in precipitation projections, while longer-term warming was found to severely deplete the snowpack and reduce peak streamflow. The results of this study also have important implications for farming communities in the Acadie River Catchment. This study indicates a decreasing snow cover duration under warming temperatures, which in turn could extend the farming season. The overall agricultural production could also benefit from the increase in annual available water (annual streamflow) in response to increasing precipitation. On the other hand, higher soil moisture due to increasing rainfall ratios in warmer springs could limit the agricultural production. Considering that the catchment presents water quality issues related to soil erosion (Clubs-conseils en agroenvironnement 2014), and that in cold agricultural catchments, soil erosion rates during the snowmelt period can exceed those occurring during other seasons of the year (Costa et al. 2017, Starkloff et al. 2017), the changes in snowmelt and streamflow dynamics could alter soil erosion dynamics. Soil erosion could increase due to earlier snowmelt, increased rainfall ratios, and more frequent snowmelt events caused by higher winter and spring temperatures.

The hydrological model built in this study could be used to assess the impacts of climate change on snow accumulation and associated runoff under different tilling practices by changing the vegetation heights over the agricultural fields in the Acadie

River Catchment. Future research will aim to investigate the impact of runoff changes on soil erosion rates in response to climate change scenarios. In addition, since this model includes all the major physical processes at play in this type of environments, it would be relatively easy to apply it in similar environments or similar landscapes located in the warmer sectors of the Dfb climate class, which have been shown to be particularly sensitive to warming (Aygün et al. 2020). The model is particularly well suited to analyze the interactions between the hydrological processes at play, and to assess their sensitivity to changes in temperature and precipitation. It is important to note that the climate sensitivity framework used in this study only considers mean changes in air temperature and precipitation; therefore, changes in inter-annual variability or potential changes to other atmospheric variables such as humidity and wind speed were not considered. Future changes in precipitation frequency could have important hydrological impacts (Mailhot et al. 2007, Mareuil et al. 2007, Ouellet et al. 2012, Roy et al. 2001). Nevertheless, the climate sensitivity analysis allowed understanding how key hydrological processes could shift under a wide range of climate change scenarios, in a fast and easy way, providing useful guidance for further top-down, model-based climate impact assessments. It is worth noting that there are different sources of uncertainty in this study. For instance, the lack of long-term snow observations in agricultural fields prevents a more robust validation of the snow model. There is thus a need for additional, long-term monitoring of snow conditions in agricultural fields in the Acadie River Catchment and elsewhere in southern Québec. In addition, some of the model parameters were transferred from studies in catchments with similar hydrological conditions, which introduces uncertainties to the modelling. Future studies should perform detailed sensitivity analyses to quantify the uncertainty in simulations due to parameter uncertainty.

**Acknowledgments**

A special thanks goes to the members of GlacioLab for their help during our fieldworks. We also would like to thank Dr. John Pomeroy and Logan Fang, who provided support and resources required to learn the Cold Regions Hydrological Modelling platform.

## References

- Allen, M. R., Barros, V. R., Broome, J., Cramer, W., Christ, R., Church, J. A., et al. (2014) IPCC fifth assessment synthesis report-climate change 2014 synthesis report. Intergovernmental Panel on Climate Change, Geneva, Switzerland.
- Almaraz, J., Mabood, F., Zhou, X., Strachan, I., Ma, B. and Smith, D. (2009) Performance of Agricultural Systems under Contrasting Growing Season Conditions in South-western Quebec. *Journal of Agronomy and Crop Science*, 195(5), 319–327.
- Armstrong, R. N., Pomeroy, J. W. and Martz, L. W. (2010) Estimating evaporation in a Prairie landscape under drought conditions. *Canadian Water Resources Journal*, 35(2), 173–186.
- Ayers, H. (1959) Influence of soil profile and vegetation characteristics on net rainfall supply to runoff. Paper presented at the Proceedings of Hydrology Symposium.
- Aygün, O., Kinnard, C. and Campeau, S. (2020) Impacts of climate change on the hydrology of northern midlatitude cold regions. *Progress in Physical Geography: Earth and Environment*, 44(3), 338–375.
- Bajamgnigni Gbambie, A. S., Poulin, A., Boucher, M.-A. and Arsenault, R. (2017) Added value of alternative information in interpolated precipitation datasets for hydrology. *Journal of Hydrometeorology*, 18(1), 247–264.
- Beckers, J.-M. and Rixen, M. (2003) EOF calculations and data filling from incomplete oceanographic datasets. *Journal of Atmospheric and oceanic technology*, 20(12), 1839–1856.
- Beldring, S., Engen-Skaugen, T., Førland, E. J. and Roald, L. A. (2008) Climate change impacts on hydrological processes in Norway based on two methods for transferring regional climate model results to meteorological station sites. *Tellus A: Dynamic Meteorology and Oceanography*, 60(3), 439–450.
- Beniston, M., Keller, F., Koffi, B. and Goyette, S. (2003) Estimates of snow accumulation and volume in the Swiss Alps under changing climatic conditions. *Theoretical and Applied Climatology*, 76(3–4), 125–140.
- Bergeron, O. (2016) Guide d'utilisation 2016 – Grilles climatiques quotidiennes du Programme de surveillance du climat du Québec (1.2 ed.). Ministère du Développement Durable de l'Environnement et de la Lutte contre les Changements Climatiques du Québec.

- Blöschl, G., Viglione, A. and Montanari, A. (2013) Emerging approaches to hydrological risk management in a changing world. *Climate Vulnerability: Understanding and Addressing Threats to Essential Resources*, 3–10.
- Boyer, C., Chaumont, D., Chartier, I. and Roy, A. G. (2010) Impact of climate change on the hydrology of St. Lawrence tributaries. *Journal of Hydrology*, 384(1–2), 65–83.
- Brooks, R. and Corey, A. (1964) Hydraulic properties of porous media, hydrology papers, no. 3, colorado state university, ft. Collins, Colo.
- Brooks, R. H. and Corey, A. T. (1966) Properties of porous media affecting fluid flow. *Journal of the Irrigation and Drainage Division*, 92(2), 61–90.
- Brunt, D. (1932) Notes on radiation in the atmosphere. I. *Quarterly Journal of the Royal Meteorological Society*, 58(247), 389–420.
- Burn, D. H. and Whitfield, P. H. (2017) Changes in cold region flood regimes inferred from long-record reference gauging stations. *Water Resources Research*, 53(4), 2643–2658.
- Carrier, M.-A., Lefebvre, R., Rivard, C., Parent, M., Ballard, J.-M., Benoît, N., et al. (2013) *Portrait des ressources en eau souterraine en Montérégie Est*, Québec, Canada: INRS, Centre Eau Terre Environnement.
- Casola, J. H., Cuo, L., Livneh, B., Lettenmaier, D. P., Stoelinga, M. T., Mote, P. W. and Wallace, J. M. (2009) Assessing the impacts of global warming on snowpack in the Washington Cascades. *Journal of climate*, 22(10), 2758–2772.
- Chaumont, D. (2014) *A guidebook on climate scenarios: Using climate information to guide adaptation research and decisions*. Ouranos, Canada.
- Clark, C. (1945) Storage and the unit hydrograph. Paper presented at the Proceedings of the American Society of Civil Engineers.
- Clubs-conseils en agroenvironnement. (2014) *Rapport de caractérisation du bassin versant « amont » de la rivière L'Acadie*. Retrieved from QC, Canada.
- Cordeiro, M. R., Wilson, H. F., Vanrobaeys, J., Pomeroy, J. W. and Fang, X. (2017) Simulating cold-region hydrology in an intensively drained agricultural watershed in Manitoba, Canada, using the Cold Regions Hydrological Model. *Hydrology and Earth System Sciences*, 21(7), 3483–3506.

- Costa, D., Roste, J., Pomeroy, J., Baulch, H., Elliott, J., Wheeler, H. and Westbrook, C. (2017) A modelling framework to simulate field-scale nitrate response and transport during snowmelt: The WINTRA model. *Hydrological Processes*, 31(24), 4250–4268.
- Croteau, A. (2006) Détermination de la distribution spatiale et temporelle de la recharge à l'aquifère régional transfrontalier du bassin versant de la rivière Châteauguay, Québec et États-Unis. Université du Québec, Institut national de la recherche scientifique.
- DeBeer, C. and Pomeroy, J. (2010) Simulation of the snowmelt runoff contributing area in a small alpine basin. *Hydrology and Earth System Sciences*, 14(7), 1205.
- DeBeer, C. M., Wheeler, H. S., Carey, S. K. and Chun, K. P. (2016) Recent climatic, cryospheric, and hydrological changes over the interior of western Canada: a review and synthesis. *Hydrology and Earth System Sciences*, 20(4), 1573.
- Dixon, D. and Boon, S. (2012) Comparison of the SnowHydro snow sampler with existing snow tube designs. *Hydrological Processes*, 26(17), 2555–2562.
- Donnelly, C., Greuell, W., Andersson, J., Gerten, D., Pisacane, G., Roudier, P. and Ludwig, F. (2017) Impacts of climate change on European hydrology at 1.5, 2 and 3 degrees mean global warming above preindustrial level. *Climatic Change*, 143(1–2), 13–26.
- Dornes, P. F., Pomeroy, J. W., Pietroniro, A., Carey, S. K. and Quinton, W. L. (2008) Influence of landscape aggregation in modelling snow-cover ablation and snowmelt runoff in a sub-arctic mountainous environment. *Hydrological sciences journal*, 53(4), 725–740.
- Dornes, P. F., Tolson, B. A., Davison, B., Pietroniro, A., Pomeroy, J. W. and Marsh, P. (2008) Regionalisation of land surface hydrological model parameters in subarctic and arctic environments. *Physics and Chemistry of the Earth, Parts A/B/C*, 33(17–18), 1081–1089.
- Eckhardt, K. and Ulbrich, U. (2003) Potential impacts of climate change on groundwater recharge and streamflow in a central European low mountain range. *Journal of Hydrology*, 284(1–4), 244–252.
- Ellis, C., Pomeroy, J., Brown, T. and MacDonald, J. (2010) Simulation of snow accumulation and melt in needleleaf forest environments. *Hydrology and Earth System Sciences*, 14(6), 925–940.

- Essery, R. and Pomeroy, J. (2004) Vegetation and topographic control of wind-blown snow distributions in distributed and aggregated simulations for an Arctic tundra basin. *Journal of Hydrometeorology*, 5(5), 735–744.
- Evans, S. G., Ge, S., Voss, C. I. and Molotch, N. P. (2018) The role of frozen soil in groundwater discharge predictions for warming alpine watersheds. *Water Resources Research*, 54(3), 1599–1615.
- Fang, X. and Pomeroy, J. (2009) Modelling blowing snow redistribution to prairie wetlands. *Hydrological Processes: An International Journal*, 23(18), 2557–2569.
- Fang, X., Pomeroy, J., Ellis, C., MacDonald, M., DeBeer, C. and Brown, T. (2013) Multi-variable evaluation of hydrological model predictions for a headwater basin in the Canadian Rocky Mountains. *Hydrology and Earth System Sciences*, 17(4), 1635–1659.
- Fang, X., Pomeroy, J., Westbrook, C., Guo, X., Minke, A. and Brown, T. (2010) Prediction of snowmelt derived streamflow in a wetland dominated prairie basin. *Hydrology and Earth System Sciences*, 14(6), 991–1006.
- Fang, X. and Pomeroy, J. W. (2007) Snowmelt runoff sensitivity analysis to drought on the Canadian prairies. *Hydrological Processes: An International Journal*, 21(19), 2594–2609.
- Fang, X. and Pomeroy, J. W. (2008) Drought impacts on Canadian prairie wetland snow hydrology. *Hydrological Processes: An International Journal*, 22(15), 2858–2873.
- Förster, K., Garvelmann, J., Meißl, G. and Strasser, U. (2018) Modelling forest snow processes with a new version of WaSiM. *Hydrological sciences journal*, 63(10), 1540–1557.
- Fowler, H. J., Blenkinsop, S. and Tebaldi, C. (2007) Linking climate change modelling to impacts studies: recent advances in downscaling techniques for hydrological modelling. *International Journal of Climatology: A Journal of the Royal Meteorological Society*, 27(12), 1547–1578.
- Gallichand, J., Broughton, R., Boisvert, J. and Rochette, P. (1991) Simulation of irrigation requirements for major crops in South Western Quebec. *Canadian Agricultural Engineering*, 33(1), 1–9.
- Garnier, B. J. and Ohmura, A. (1970) The evaluation of surface variations in solar radiation income. *Solar energy*, 13(1), 21–34.

- Gennaretti, F., Sangelantoni, L. and Grenier, P. (2015) Toward daily climate scenarios for Canadian Arctic coastal zones with more realistic temperature-precipitation interdependence. *Journal of Geophysical Research: Atmospheres*, 120(23), 11862–811877.
- Gombault, C., Sottile, M.-F., Ngwa, F. F., Madramootoo, C. A., Michaud, A. R., Beaudin, I. and Chikhaoui, M. (2015) Modelling climate change impacts on the hydrology of an agricultural watershed in southern Québec. *Canadian Water Resources Journal/Revue canadienne des ressources hydriques*, 40(1), 71–86.
- Graham, L. P., Andréasson, J. and Carlsson, B. (2007) Assessing climate change impacts on hydrology from an ensemble of regional climate models, model scales and linking methods—a case study on the Lule River basin. *Climatic Change*, 81(1), 293–307.
- Granger, R. and Gray, D. (1990) A Net Radiation Model for Calculating Daily Snowmelt in Open Environments Paper presented at the 8th Northern Res. Basins Symposium/Workshop (Abisko, Sweden-March 1990) *Hydrology Research*, 21(4–5), 217–234.
- Gray, D. and Landine, P. (1987) Albedo model for shallow prairie snow covers. *Canadian Journal of Earth Sciences*, 24(9), 1760–1768.
- Gray, D. and Landine, P. (1988) An energy-budget snowmelt model for the Canadian Prairies. *Canadian Journal of Earth Sciences*, 25(8), 1292–1303.
- Gray, D., Toth, B., Zhao, L., Pomeroy, J. and Granger, R. (2001) Estimating areal snowmelt infiltration into frozen soils. *Hydrological Processes*, 15(16), 3095–3111.
- Gupta, H. V., Kling, H., Yilmaz, K. K. and Martinez, G. F. (2009) Decomposition of the mean squared error and NSE performance criteria: Implications for improving hydrological modelling. *Journal of Hydrology*, 377(1–2), 80–91. <https://doi.org/10.1016/j.jhydrol.2009.08.003>
- Harder, P. and Pomeroy, J. (2013) Estimating precipitation phase using a psychrometric energy balance method. *Hydrological Processes*, 27(13), 1901–1914.
- Harder, P. and Pomeroy, J. W. (2014) Hydrological model uncertainty due to precipitation-phase partitioning methods. *Hydrological Processes*, 28(14), 4311–4327.

- Harder, P., Pomeroy, J. W. and Helgason, W. D. (2019) Implications of stubble management on snow hydrology and meltwater partitioning. *Canadian Water Resources Journal/Revue canadienne des ressources hydriques*, 44(2), 193–204.
- Harder, P., Pomeroy, J. W. and Westbrook, C. J. (2015) Hydrological resilience of a Canadian Rockies headwaters basin subject to changing climate, extreme weather, and forest management. *Hydrological Processes*, 29(18), 3905–3924.
- Hedstrom, N. and Pomeroy, J. (1998) Measurements and modelling of snow interception in the boreal forest. *Hydrological Processes*, 12(10–11), 1611–1625.
- Huntington, J. L. and Niswonger, R. G. (2012) Role of surface-water and groundwater interactions on projected summertime streamflow in snow dominated regions: An integrated modeling approach. *Water Resources Research*, 48(11), W11524. 10.1029/2012WR012319
- Huziy, O., Sushama, L., Khaliq, M., Laprise, R., Lehner, B. and Roy, R. (2013) Analysis of streamflow characteristics over Northeastern Canada in a changing climate. *Climate Dynamics*, 40(7–8), 1879–1901.
- Jasechko, S., Birks, S. J., Gleeson, T., Wada, Y., Fawcett, P. J., Sharp, Z. D., et al. (2014) The pronounced seasonality of global groundwater recharge. *Water Resources Research*, 50(11), 8845–8867.
- Jepsen, S. M., Molotch, N. P., Williams, M. W., Rittger, K. E. and Sickman, J. O. (2012) Interannual variability of snowmelt in the Sierra Nevada and Rocky Mountains, United States: Examples from two alpine watersheds. *Water Resources Research*, 48(2).
- Jobin, B., Latendresse, C., Baril, A., Maisonneuve, C., Boutin, C. and Côté, D. (2014) A half-century analysis of landscape dynamics in southern Québec, Canada. *Environmental monitoring and assessment*, 186(4), 2215–2229.
- Keller, F., Goyette, S. and Beniston, M. (2005) Sensitivity analysis of snow cover to climate change scenarios and their impact on plant habitats in alpine terrain. *Climatic Change*, 72(3), 299–319.
- Knoben, W. J., Freer, J. E. and Woods, R. A. (2019) Inherent benchmark or not? Comparing Nash–Sutcliffe and Kling–Gupta efficiency scores. *Hydrology and Earth System Sciences*, 23(10), 4323–4331.

- Krogh, S. A. and Pomeroy, J. W. (2019) Impact of Future Climate and Vegetation on the Hydrology of an Arctic Headwater Basin at the Tundra–Taiga Transition. *Journal of Hydrometeorology*, 20(2), 197–215. <https://doi.org/10.1175/JHM-D-18-0187.1>
- Krogh, S. A., Pomeroy, J. W. and Marsh, P. (2017) Diagnosis of the hydrology of a small Arctic basin at the tundra-taiga transition using a physically based hydrological model. *Journal of Hydrology*, 550, 685–703.
- Krogh, S. A., Pomeroy, J. W. and McPhee, J. (2015) Physically based mountain hydrological modeling using reanalysis data in Patagonia. *Journal of Hydrometeorology*, 16(1), 172–193.
- Kundzewicz, Z. W., Pińskwar, I. and Brakenridge, G. R. (2017) Changes in river flood hazard in Europe: a review. *Hydrology Research*, 49(2), 294–302.
- Lamontagne, L. (2005) Base de données sur les propriétés physiques des sols du bassin versant de la rivière Châteauguay. *Pedology and Precision Agriculture Laboratories, Agriculture and Agri-Food Canada, QC, CD-Rom.*
- Lamontagne, L., Martin, A., Grenon, L. and Cossette, J.-M. (2002) Étude pédologique du comté de Saint-Jean (Québec): *Agriculture et Agroalimentaire Canada, Centre de recherche et de développement sur les sols et les grandes cultures.*
- Leavesley, G., Lichty, R., Troutman, B. and Saindon, L. (1983) *Precipitation-runoff modeling system: User's manual. Water-resources investigations report, 83, 4238.*
- Li, L. and Pomeroy, J. W. (1997) Estimates of threshold wind speeds for snow transport using meteorological data. *Journal of Applied Meteorology*, 36(3), 205–213.
- Lin, H., Mo, R., Vitart, F. and Stan, C. (2019) Eastern Canada flooding 2017 and its subseasonal predictions. *Atmosphere-Ocean*, 57(3), 195–207.
- Liston, G. E., Haehnel, R. B., Sturm, M., Hiemstra, C. A., Berezovskaya, S. and Tabler, R. D. (2007) Simulating complex snow distributions in windy environments using SnowTran-3D. *Journal of Glaciology*, 53(181), 241–256.
- López-Moreno, J., Boike, J., Sanchez-Lorenzo, A. and Pomeroy, J. (2016) Impact of climate warming on snow processes in Ny-Ålesund, a polar maritime site at Svalbard. *Global and planetary change*, 146, 10–21.

- López-Moreno, J. I., Revuelto, J., Gilaberte, M., Morán-Tejeda, E., Pons, M., Jover, E., et al. (2014) The effect of slope aspect on the response of snowpack to climate warming in the Pyrenees. *Theoretical and Applied Climatology*, 117(1–2), 207–219.
- López-Moreno, J., Pomeroy, J., Revuelto, J. and Vicente-Serrano, S. (2013) Response of snow processes to climate change: spatial variability in a small basin in the Spanish Pyrenees. *Hydrological Processes*, 27(18), 2637–2650.
- MacDonald, M., Pomeroy, J. and Pietroniro, A. (2010) On the importance of sublimation to an alpine snow mass balance in the Canadian Rocky Mountains. *Hydrology and Earth System Sciences*, 14(7), 1401–1415.
- MacDonald, R. J., Byrne, J. M., Boon, S. and Kienzle, S. W. (2012) Modelling the potential impacts of climate change on snowpack in the North Saskatchewan River Watershed, Alberta. *Water resources management*, 26(11), 3053–3076.
- Mahmood, T. H., Pomeroy, J. W., Wheeler, H. S. and Baulch, H. M. (2017) Hydrological responses to climatic variability in a cold agricultural region. *Hydrological Processes*, 31(4), 854–870.
- Mailhot, A., Duchesne, S., Caya, D. and Talbot, G. (2007) Assessment of future change in intensity–duration–frequency (IDF) curves for Southern Quebec using the Canadian Regional Climate Model (CRCM) *Journal of Hydrology*, 347(1–2), 197–210.
- Mareuil, A., Leconte, R., Brissette, F. and Minville, M. (2007) Impacts of climate change on the frequency and severity of floods in the Châteauguay River basin, Canada. *Canadian journal of civil engineering*, 34(9), 1048–1060.
- Marks, D., Kimball, J., Tingey, D. and Link, T. (1998) The sensitivity of snowmelt processes to climate conditions and forest cover during rain-on-snow: A case study of the 1996 Pacific Northwest flood. *Hydrological Processes*, 12(10–11), 1569–1587.
- Michaud, A., Deslandes, J. and Beaudin, I. (2006) Modélisation de l'hydrologie et des dynamiques de pollution diffuse dans le bassin versant de la Rivière aux Brochets à l'aide du modèle SWAT. Institut de recherche et de développement en agroenvironnement, rapport final.
- Ministère du Développement durable de l'Environnement et des Parcs. (2008) Manuel d'instructions à l'usage des observateurs en nivométrie. Québec.

- Minville, M., Brissette, F. and Leconte, R. (2008) Uncertainty of the impact of climate change on the hydrology of a nordic watershed. *Journal of Hydrology*, 358(1–2), 70–83.
- Mohammed, A. A., Pavlovskii, I., Cey, E. E. and Hayashi, M. (2019) Effects of preferential flow on snowmelt partitioning and groundwater recharge in frozen soils. *Hydrology and Earth System Sciences*, 23(12), 5017–5031.
- Molini, A., Katul, G. G. and Porporato, A. (2011) Maximum discharge from snowmelt in a changing climate. *Geophysical Research Letters*, 38(5), L05402. [10.1029/2010GL046477](https://doi.org/10.1029/2010GL046477)
- Monteith, J. (1981) Evaporation and surface temperature. *Quarterly Journal of the Royal Meteorological Society*, 107(451), 1–27.
- Moriasi, D. N., Arnold, J. G., Van Liew, M. W., Bingner, R. L., Harmel, R. D. and Veith, T. L. (2007) Model evaluation guidelines for systematic quantification of accuracy in watershed simulations. *Transactions of the ASABE*, 50(3), 885–900.
- Musselman, K. N., Clark, M. P., Liu, C., Ikeda, K. and Rasmussen, R. (2017) Slower snowmelt in a warmer world. *Nature Climate Change*, 7(3), 214–219. <https://doi.org/10.1038/nclimate3225>
- Nash, J. E. and Sutcliffe, J. V. (1970) River flow forecasting through conceptual models part I—A discussion of principles. *Journal of Hydrology*, 10(3), 282–290. [https://doi.org/10.1016/0022-1694\(70\)90255-6](https://doi.org/10.1016/0022-1694(70)90255-6)
- Okkonen, J. and Kløve, B. (2010) A conceptual and statistical approach for the analysis of climate impact on ground water table fluctuation patterns in cold conditions. *Journal of Hydrology*, 388(1–2), 1–12.
- Ouellet, C., Saint-Laurent, D. and Normand, F. (2012) Flood events and flood risk assessment in relation to climate and land-use changes: Saint-François River, southern Québec, Canada. *Hydrological sciences journal*, 57(2), 313–325.
- Ouranos. (2015) *Vers l’adaptation. Synthèse des connaissances sur les changements climatiques au Québec—Partie 1: Évolution climatique au Québec*, Ouranos, Montréal, Québec.
- P Plamondon, A., Prévost, M. and C Naud, R. (1984) Accumulation et fonte de la neige en milieux boisé et déboisé. *Géographie physique et Quaternaire*, 38(1), 27–35.

- Peel, M. C. and Blöschl, G. (2011) Hydrological modelling in a changing world. *Progress in Physical Geography*, 35(2), 249–261.
- Peel, M. C., Finlayson, B. L. and McMahon, T. A. (2007) Updated world map of the Köppen-Geiger climate classification. *Hydrology and earth system sciences discussions*, 4(2), 439–473.
- Perreault, S., Chokmani, K., Nolin, M. C. and Bourgeois, G. (2013) Validation of a soil temperature and moisture model in southern Quebec, Canada. *Soil Science Society of America Journal*, 77(2), 606–617.
- Pomeroy, J., Fang, X., Westbrook, C., Minke, A., Guo, X. and Brown, T. (2010) Prairie hydrological model study final report. University of Saskatchewan: Saskatoon, SK, Canada.
- Pomeroy, J., Fang, X. and Williams, B. (2011) Modelling snow water conservation on the Canadian Prairies. Centre for Hydrology, University of Saskatchewan, Saskatoon.
- Pomeroy, J. and Gray, D. (1995) Snowcover accumulation, relocation and management. *Bulletin of the International Society of Soil Science* no, 88(2).
- Pomeroy, J., Gray, D., Brown, T., Hedstrom, N., Quinton, W., Granger, R. and Carey, S. (2007) The cold regions hydrological model: a platform for basing process representation and model structure on physical evidence. *Hydrological Processes: An International Journal*, 21(19), 2650–2667.
- Pomeroy, J., Gray, D. and Landine, P. (1993) The prairie blowing snow model: characteristics, validation, operation. *Journal of Hydrology*, 144(1–4), 165–192.
- Pomeroy, J. and Li, L. (2000) Prairie and arctic areal snow cover mass balance using a blowing snow model. *Journal of Geophysical Research: Atmospheres*, 105(D21), 26619–26634.
- Pomeroy, J., Parviainen, J., Hedstrom, N. and Gray, D. (1998) Coupled modelling of forest snow interception and sublimation. *Hydrological Processes*, 12(15), 2317–2337.
- Pomeroy, J., Shook, K., Fang, X., Brown, T. and Marsh, C. (2013) Development of a snowmelt runoff model for the Lower Smoky River. Centre for Hydrology Report.

- Pomeroy, J., Shook, K., Fang, X., Dumanski, S., Westbrook, C. and Brown, T. (2014) Improving and testing the prairie hydrological model at Smith Creek Research Basin: Citeseer.
- Priestley, C. H. B. and Taylor, R. (1972) On the assessment of surface heat flux and evaporation using large-scale parameters. *Monthly weather review*, 100(2), 81–92.
- Prudhomme, C., Wilby, R. L., Crooks, S., Kay, A. L. and Reynard, N. S. (2010) Scenario-neutral approach to climate change impact studies: application to flood risk. *Journal of Hydrology*, 390(3–4), 198–209.
- Quilbé, R., Rousseau, A. N., Moquet, J.-S., Savary, S., Ricard, S. and Garbouj, M. S. (2008) Hydrological responses of a watershed to historical land use evolution and future land use scenarios under climate change conditions.
- Rasouli, K., Pomeroy, J. W., Janowicz, J. R., Carey, S. K. and Williams, T. J. (2014) Hydrological sensitivity of a northern mountain basin to climate change. *Hydrological Processes*, 28(14), 4191–4208.
- Rasouli, K., Pomeroy, J. W. and Marks, D. G. (2015) Snowpack sensitivity to perturbed climate in a cool mid-latitude mountain catchment. *Hydrological Processes*, 29(18), 3925–3940.
- Rasouli, K., Pomeroy, J. W. and Whitfield, P. H. (2019) Hydrological Responses of Headwater Basins to Monthly Perturbed Climate in the North American Cordillera. *Journal of Hydrometeorology*, 20(5), 863–882.
- Riboust, P. and Brissette, F. (2015) Climate change impacts and uncertainties on spring flooding of Lake Champlain and the Richelieu River. *JAWRA Journal of the American Water Resources Association*, 51(3), 776–793.
- Roy, L., Leconte, R., Brissette, F. P. and Marche, C. (2001) The impact of climate change on seasonal floods of a southern Quebec River Basin. *Hydrological Processes*, 15(16), 3167–3179.
- Salathé Jr, E. P., Mote, P. W. and Wiley, M. W. (2007) Review of scenario selection and downscaling methods for the assessment of climate change impacts on hydrology in the United States Pacific Northwest. *International Journal of Climatology: A Journal of the Royal Meteorological Society*, 27(12), 1611–1621.
- Sicart, J.-E., Pomeroy, J., Essery, R. and Bewley, D. (2006) Incoming longwave radiation to melting snow: observations, sensitivity and estimation in northern environments. *Hydrological Processes*, 20(17), 3697–3708.

- Smith, J. B. and Mendelsohn, R. O. (2007) The impact of climate change on regional systems: a comprehensive analysis of California: Edward Elgar Publishing.
- Starkloff, T., Hessel, R., Stolte, J. and Ritsema, C. (2017) Catchment hydrology during winter and spring and the link to soil erosion: A case study in Norway. *Hydrology*, 4(1), 15.
- Stewart, I. T., Cayan, D. R. and Dettinger, M. D. (2005) Changes toward earlier streamflow timing across western North America. *Journal of climate*, 18(8), 1136–1155.
- Sulis, M., Paniconi, C., Rivard, C., Harvey, R. and Chaumont, D. (2011) Assessment of climate change impacts at the catchment scale with a detailed hydrological model of surface-subsurface interactions and comparison with a land surface model. *Water Resources Research*, 47(1).
- Tabler, R. D. (1975) Estimating the transport and evaporation of blowing snow. Great Plains Agric Counc Publ.
- Talbot, J., Plamondon, A., Levesque, D., Aube, D., Prevos, M., Chazalmartin, F. and Gnocchini, M. (2006) Relating snow dynamics and balsam fir stand characteristics, Montmorency Forest, Quebec. *Hydrological Processes: An International Journal*, 20(5), 1187–1199.
- Tang, J., Niu, X., Wang, S., Gao, H., Wang, X. and Wu, J. (2016) Statistical downscaling and dynamical downscaling of regional climate in China: Present climate evaluations and future climate projections. *Journal of Geophysical Research: Atmospheres*, 121(5), 2110–2129.
- Teufel, B., Sushama, L., Huziy, O., Diro, G., Jeong, D., Winger, K., et al. (2019) Investigation of the mechanisms leading to the 2017 Montreal flood. *Climate Dynamics*, 52(7–8), 4193–4206.
- Teutschbein, C., Grabs, T., Karlsen, R. H., Laudon, H. and Bishop, K. (2015) Hydrological response to changing climate conditions: Spatial streamflow variability in the boreal region. *Water Resources Research*, 51(12), 9425–9446.
- Teutschbein, C. and Seibert, J. (2010) Regional climate models for hydrological impact studies at the catchment scale: a review of recent modeling strategies. *Geography Compass*, 4(7), 834–860.
- Toews, M. W. and Allen, D. M. (2009) Evaluating different GCMs for predicting spatial recharge in an irrigated arid region. *Journal of Hydrology*, 374(3–4), 265–281.

- Tremblay, T. (2008) Hydrostratigraphie et géologie du quaternaire dans le bassin-versant de la rivière Châteauguay, Québec.
- Trujillo, E. and Molotch, N. P. (2014) Snowpack regimes of the western United States. *Water Resources Research*, 50(7), 5611–5623.
- Varhola, A., Coops, N. C., Weiler, M. and Moore, R. D. (2010) Forest canopy effects on snow accumulation and ablation: An integrative review of empirical results. *Journal of Hydrology*, 392(3–4), 219–233.
- VenTe, C. (1964) *Handbook of applied hydrology: a compendium of water-resources technology*.
- Wilson, D., Hisdal, H. and Lawrence, D. (2010) Has streamflow changed in the Nordic countries?—Recent trends and comparisons to hydrological projections. *Journal of Hydrology*, 394(3–4), 334–346.
- Zhou, J., Pomeroy, J. W., Zhang, W., Cheng, G., Wang, G. and Chen, C. (2014) Simulating cold regions hydrological processes using a modular model in the west of China. *Journal of Hydrology*, 509, 13–24.
- Zierl, B. and Bugmann, H. (2005) Global change impacts on hydrological processes in Alpine catchments. *Water Resources Research*, 41(2).

## CHAPTER II

### CONTRASTED CLIMATE SENSITIVITIES OF TWO COLD-REGION CATCHMENTS IN EASTERN CANADA

Okan Aygün<sup>1</sup>, Christophe Kinnard<sup>2</sup>, Stéphane Campeau<sup>3</sup> and John W. Pomeroy<sup>4</sup>

<sup>1</sup> University of Québec at Trois-Rivières, Québec, Canada; Centre for Northern Studies (CEN), Québec City, Québec, Canada; Research Centre for Watershed-Aquatic Ecosystem Interactions (RIVE), University of Québec at Trois-Rivières, Canada.

<sup>2</sup> University of Québec at Trois-Rivières, Québec, Canada; Centre for Northern Studies (CEN), Québec City, Québec, Canada; Research Centre for Watershed-Aquatic Ecosystem Interactions (RIVE), University of Québec at Trois-Rivières, Canada.

<sup>3</sup> University of Québec at Trois-Rivières, Québec, Canada; Research Centre for Watershed-Aquatic Ecosystem Interactions (RIVE), University of Québec at Trois-Rivières, Canada.

<sup>4</sup> Centre for Hydrology, University of Saskatchewan, Saskatoon, Canada.

Corresponding author: Okan Aygün ([okan.aygun@uqtr.ca](mailto:okan.aygun@uqtr.ca))

This article is currently under review in *Water Resources Research*.

**Key Points**

- The climate sensitivity of peak snow water equivalent (SWE) depends on current climate and is little influenced by biophysical conditions.
- Peak SWE declines but peak discharge increases in response to combined warming and wetting in catchment with mild winter conditions.
- The forested catchment attenuates hydrological extremes under climate change compared to the agricultural catchment.

**Abstract**

This study compares the climate sensitivity of the hydrology of two catchments with contrasted biophysical and meteorological characteristics in southern Québec, Canada: a rugged and forested landscape with cold/humid climate (Montmorency) versus an agroforested and flat landscape with warmer/less humid climate (Acadie), respectively located on the north and south shore of the St. Lawrence River. A physically based hydrological model was created using the Cold Regions Hydrological Modelling platform to simulate the hydrological processes over 14 years in the Montmorency River Catchment and the results were compared to previous simulations conducted in the Acadie River Catchment. The observed air temperature and precipitation were perturbed linearly based on existing climate change projections, with a warming of up to 8 °C and increasing precipitation up to 20%. The peak snow water equivalent (SWE) was found to be more sensitive to warming under the mild climate conditions of Acadie. Under 3 °C warming, Acadie transits from mixed snowmelt/rainfall to a rainfall dominated regime, whereas Montmorency conserves snowmelt dominated regime. Permuted baseline climate experiments show that the climate sensitivity of peak SWE depends more on the regional baseline climate than on catchment biophysiology, while annual peak discharge shows more contrasted responses to a combined warming

(+3 °C) and wetting (+20%) scenario. When forced by the colder Montmorency climate, peak discharge increases in the Acadie while slightly decreasing in Montmorency. The more porous forested soils of Montmorency are found to attenuate increases in runoff amounts and extremes, promoting reduced peak flow compared to the more impervious agroforested Acadie.

**Keywords**

Cold regions hydrology; climate change; hydrological modelling; snowpack; river discharge; agroforested catchment; forested catchment

## 2.1 Introduction

Seasonal snow represents a major part of the terrestrial water storage during winter and produces significant runoff with the onset of snowmelt. It is estimated that about 2 billion people across the Northern Hemisphere depend on water supplied from snowmelt runoff (Mankin et al. 2015). Within the Northern Hemisphere, 20% of the seasonal snow cover is estimated to be located within forested areas and can account for 17% of the total terrestrial water storage during the winter season (Moeser et al. 2015). Better understanding of snow-forest interactions, therefore, is crucial for modelling relevant hydrological processes. However, the processes affecting snow cover dynamics in forests are complex and can vary at small scales. Snow accumulation patterns are predominantly altered by interception of snow on the canopy, while melting dynamics are driven by complex processes including the transfer of shortwave and longwave radiation through the canopy and the turbulent transport of heat and water (Jonas and Essery 2011, Roth and Nolin 2017). In boreal forests, up to 60% and 40% of cumulative snowfall can be intercepted and sublimated, respectively (Hedstrom and Pomeroy 1998, Pomeroy et al. 1998). Compared to open areas, snowmelt rates can be up to 70% lower in forests because of reductions in incoming shortwave radiation, and reduced sensible and latent heat fluxes resulting from dampened wind speed by canopies (Varhola et al. 2010). The interplay between accumulation and melt processes is an important control on the spatial variability of snow in forests (Clark et al. 2011). While many studies have reported that less snow accumulates in coniferous forests than that in nearby open environments (clearings) due to canopy interception losses (Gelfan et al. 2004, Jost et al. 2007, Koivusalo and Kokkonen 2002, Musselman et al. 2008, Pomeroy and Gray 1995, Pomeroy et al. 1998, Storck et al. 2002, Varhola et al. 2010, Winkler et al. 2005), in some cases it has been shown that reduced mid-winter and spring ablation rates in forest could offset the reduced accumulation (due to interception losses) and results in thicker snowpack in forest than in open areas (Gelfan et al. 2004, Veatch et al. 2009). Clearing size can also influence snow accumulation,

particularly in windy environments. While small clearings are sheltered by the nearby forest canopy, larger clearings can lose snow accumulation via blowing snow erosion, which can lead to less snow accumulation in clearings than in the adjacent coniferous forest (Pomeroy et al. 2012, Pomeroy and Gray 1995). Forest structure also affects snow accumulation. Pomeroy et al. (2002) reported that snow accumulations in forests varied with the winter effective leaf area index (LAI) and that lower and similar snow accumulation was found in open areas and deciduous forests, which have low LAI.

In the southern Québec province of Canada, agriculture dominates the landscape of the St. Lawrence Lowlands, leaving less than 25% of residual forest cover in most of southwestern Québec (Jobin et al. 2003). In this region, the climate is characterized by cold winters and warm summers with mean annual precipitation ranging between 800 and 1000 mm (Jobin et al. 2003). The typical landscapes of alternating agricultural fields and forest patches are referred to as agroforested landscapes, which are flat or undulating landscape with low to mild gradient slope (Jobin et al. 2014). Agricultural production over these landscapes highly depends on the availability of water and length of the growing season, which are partly shaped by the snow cover duration. On the other hand, forested landscapes prevail in regions with more rugged topography and soils unfavorable for agriculture. These are located mostly on the Canadian shield along the north shore of the St. Lawrence River in southern Québec (Jobin et al. 2003). These forested landscapes have a boreal ecoclimate marked by colder air temperatures and higher precipitations compared to the St. Lawrence Lowlands. The amount and timing of snowmelt are known to affect soil moisture and nutrient transport (Duchesne and Houle 2008), and can therefore play a critical role for the ecology of forests. Soil and tree carbon fluxes in winter are largely controlled by soil temperature (Zhang et al. 2008), which has been reported to be modulated by snow depth in forested environments (Campbell et al. 2010, Groffman et al. 2001, Jungqvist et al. 2014, Templer et al. 2017). Moreover, particularly on the north shore of the

St. Lawrence River, the amount and timing of snowmelt is crucial for hydropower generation since the snowmelt provides the bulk of water that fills the reservoirs.

The biophysical characteristics (physiography and land cover and land use) could also influence the hydrological responses of a catchment to climate change, which has been mostly explored through land cover/land use change studies or paired catchment studies. Most studies have shown that deforestation for agricultural or urban purposes leads to an increase in annual water yield (Brown et al. 2005, Dias et al. 2015, Savary et al. 2009), which is mainly linked to reduced evapotranspiration (Robinet et al. 2018). Furthermore, many studies reported higher peak flows when the forest cover is reduced or converted to agricultural fields or urban areas, mostly explained with the increased surface runoff due to reduced infiltration capacities resulting from compaction of the soil (Brown et al. 2005, Chandler 2006, Easton et al. 2007, Germer et al. 2010, Ziegler et al. 2004). Muma et al. (2011), on the other hand, reported lower warm season peak flows for catchments with large agricultural land use, compared to catchments with greater forest cover in southern Québec, because the water which did not infiltrate the soil was largely evaporated. This study suggests that the role of biophysical conditions on peak streamflow could vary depending on the season of the year. Indeed, another study in southern Québec found that decreasing forest cover in favor of agricultural crops caused an increase in peak flows during winter and spring, which was solely due to the reduction in infiltration capacity given that evapotranspiration is negligible during these seasons (Savary et al. 2009). Despite this vital importance of snow to the economy, ecology and society in southern Québec, relatively few studies have investigated the response of snow hydrology to anticipated climate change. The previous climate change studies performed in southern Québec (Boyer et al. 2010, Guay et al. 2015, Laforce et al. 2011, Mareuil et al. 2007, Minville et al. 2008, Quilbé et al. 2008) have ignored some of the major cold regions hydrological processes such as blowing snow redistribution, canopy snow interception, sublimation and infiltration into frozen soils. Also, all these previous studies used a top-down modeling

approach in which future changes in climatic conditions are based on predetermined scenarios derived from climate models. A critical limitation of this approach is that it might ignore plausible risks by not covering all possible future conditions (Alodah and Seidou 2019). In a previous study (Aygün et al. 2020b), a physically based model was created to simulate all the relevant cold regions hydrological processes in the Acadie River Catchment, an agroforested catchment located in southwestern Québec. The model was then used to perform a climate sensitivity analysis in order to assess the hydrological sensitivity of the catchment. The results revealed a remarkable sensitivity of hydrology of the catchment to warming. While the previous studies have analyzed the hydrological responses to climate change and/or land use change, the respective roles of current climate and biophysical conditions on catchment hydrology and its responses to climate change were little explored.

This study aims to explore the potential impacts of changes in temperature and precipitation on the hydrology of the Montmorency River Catchment (47° 19' N, 71° 08' W), a forested catchment on the north shore of the St. Lawrence River. The historical hydrological processes for the period 2005–2019 were first simulated using the physically based Cold Regions Hydrological Modelling platform (CRHM) (Pomeroy et al. 2007). The model was then perturbed using climate change projections and used to assess the hydrological sensitivity to climate change. The results are compared with those from the Acadie River Catchment (Aygün et al. 2020b), providing a comparative study of the climate sensitivity of the hydrological regimes for two contrasted catchments that are representatives of two main landscape archetypes in southern Québec, namely a rugged forested landscape (Montmorency) and an agroforested landscape (Acadie). The respective roles of regional climate and biophysical conditions on the climate sensitivity of the two catchments are explored and discussed.

## 2.2 Materials and Methods

### 2.2.1 Study Area and Data Sources

The main study area selected for this research is the Montmorency River Catchment, located in the Capitale-Nationale region of Québec, Canada (Figure 2.1b). The Montmorency River flows from Lake Montmorency in a southerly direction and drains into the St. Lawrence River. While it has a total length of 101 km and a total drainage area of 1150 km<sup>2</sup>, this study focusses on an upstream sub-basin, which has a drainage area of 267 km<sup>2</sup>. The catchment is mostly dominated by forests (85%) which are sub classified into mature coniferous forest (53%), mixed forest (6%) and regenerated forest (26%) (Figure 2.1b). Forest clearings resulting from clear cutting and regeneration practices occupy about 8% of the catchment area (Figure 2.1b). Wetlands and lakes, classified as water bodies, constitute 7% of the catchment area (Figure 2.1b). The climate is cold and humid with cool summers and cold winters (Dfc) (Peel et al. 2007). The Montmorency River displays the characteristics of a snowmelt-dominated regime (Gottschalk et al. 1979) where the highest average runoff takes place in late spring due to snowmelt and the lowest runoff is observed in late winter, caused by snow accumulation. The Montmorency River Catchment was selected for a detailed modelling study since it encloses two densely studied watersheds, namely BEREV (20 km<sup>2</sup>) and Lac Laflamme (0.7 km<sup>2</sup>) (Figure 2.1b). While earlier studies in Lac Laflamme watershed carried out modelling of snow accumulation and snow melt (Barry et al. 1990, Jones and Pomeroy 2001, Plamondon et al. 1984, Prévost et al. 1991, Roberge and Plamondon 1987), more recent studies focused on analyzing changes in soil water content and temperature (D'Orangeville et al. 2016, Houle et al. 2012) and also nutrient cycling (Duchesne and Houle 2008, Houle et al. 2016). In the BEREV watershed, previous studies explored the impacts of forest harvesting on hydrological behavior (Guillemette et al. 2005, Lavigne 2007, Plamondon and Ouellet 1980, Tremblay et al. 2008) and on water quality (Tremblay

et al. 2009), while recent studies performed plot scale studies to characterize solar radiation transmittance (Isabelle et al. 2018) and evaluate catch efficiency of different types of snowfall gauges (Pierre et al. 2019). The well-studied parameters from these watersheds could be transferred to build a physically based hydrological model, while the observations collected in these watersheds are useful to validate hydrological model outputs.

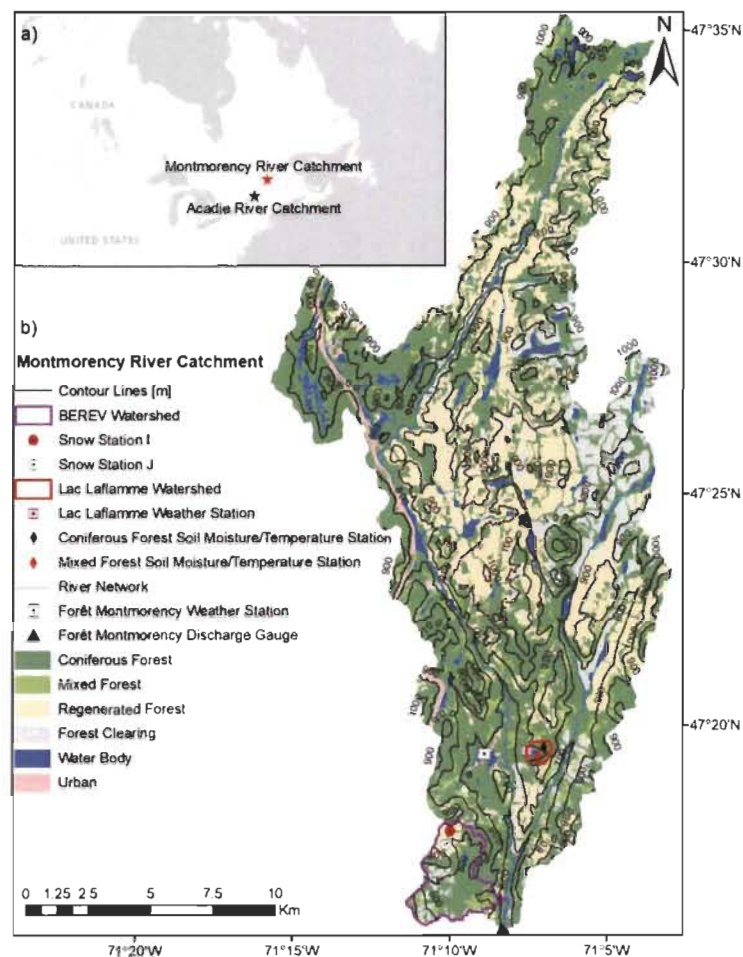


**Figure 2.1.** a) Locations of Montmorency and Acadie River catchments, b) Montmorency River Catchment drainage area, contour lines (every 100 m), land cover, discharge gauge, and main meteorological station. The Montmorency River Catchment encloses the BEREV watershed with snow stations and the Lac Laflamme watershed with soil moisture/temperature stations.

A 1x1 m resolution LIDAR-based digital elevation model (DEM), land use data sets and forest cover maps were obtained from Québec Ministry of Forests, Wildlife and Parks (MFFP). The main vegetation type is balsam fir, accompanied by white birch and white. The average canopy height ranges from 12 to 18 m in mature stands (Talbot et al. 2006). The vegetation grows on an orthic humo-ferric podzol on a sandy loam soil (D'Orangeville et al. 2016, Lavigne 2007), while the bedrock is mostly igneous and metamorphic rock (Talbot et al. 2006). The stream network was acquired from Québec Ministry of Energy and Natural Resources (MERN). Hourly temperature, wind speed, relative humidity and daily precipitation data have been acquired for the 2005–2019 period from the Forêt Montmorency weather station of Environment and Climate Change Canada (Figure 2.1b). The gaps in hourly and daily data, about 2% of the whole period, were filled with the data from the MFFP weather station (Figure 2.1b) located in the Lac Laflamme watershed, 1.7 km away from the Forêt Montmorency weather station. The temperature was spatially distributed over the catchment based on an environmental lapse rate of  $0.005\text{ }^{\circ}\text{C m}^{-1}$  (Bergeron 2016). Although shortwave radiation observations are available, they are not reliable for a large part of the simulation period. Therefore, the incoming shortwave radiation has been estimated using the method presented by Annandale et al. (2002) within the CRHM platform and validated against some of the reliable existing data. Measurements of snow depth and density at snow stations I and J (Figure 2.1b) have been collected by the Québec Ministry of Sustainable Development, Environment, and Fight against Climate Change (MDDELCC) and researchers from Laval University for the 2005–2019 period. Station I and Station J are located within regenerated forests with south-facing and north-facing slopes, respectively. Continuous measurements (since 1996) of soil temperature and moisture at the coniferous and mixed forest sites of the Lac Laflamme watershed (Figure 2.1b) were acquired from the MFFP. Daily river discharge measured at the Forêt Montmorency gauge (ID: 051005) (Figure 2.1b) were extracted from the database of Québec Center of Water Expertise (CEHQ) for the 2005–2019 period.

The Montmorency River Catchment differs from the Acadie River Catchment (Figure 2.1a) in terms of meteorological and biophysical conditions (Table 2.1). Both annual and winter mean temperatures are 6 °C lower in the Montmorency River Catchment than in the Acadie River Catchment for the 2005–2019 period (Table 2.1). Compared to the Acadie River Catchment, Montmorency River Catchment receives 30% higher precipitation and the snowfall ratio is almost twice that in Acadie (Table 2.1). While the Montmorency River Catchment is dominated by forests over hilly uplands with varying altitudes, the Acadie River Catchment is occupied by agricultural fields over flat lowlands (Table 2.1). Given these unique characteristics, these catchments are expected to demonstrate different sensitivities to warming and wetting.

**Table 2.1.** Meteorological and biophysical conditions of the Montmorency and Acadie River catchments.

Variable	Montmorency	Acadie
Annual Mean Temperature	1.3 °C	7.2 °C
Winter Mean Temperature	−12.5 °C	−6.7 °C
Annual Mean Precipitation	1460 mm	1033 mm
Snowfall Ratio	44%	23%
Catchment Area	267 km <sup>2</sup>	360 km <sup>2</sup>
Land Use	Forest (85%)	Agriculture (77%)
Slope Range	0°–60°	0°–2°
Elevation Range	550–1150 m	40–110 m

### 2.2.2 Hydrological Modelling and Parameter Estimation

In this research, the Cold Regions Hydrological Modelling platform (CRHM) (Pomeroy et al. 2007) was used to build a hydrological model for the Montmorency River Catchment. CRHM has an object-oriented and modular structure for assembling

physically based hydrological models (Fang et al. 2013). CRHM has been successfully used in several cold regions such as western and northern Canada (Fang et al. 2013, Fang and Pomeroy 2007, Krogh et al. 2017, Pomeroy et al. 2012, Pomeroy et al. 2016, Rasouli et al. 2014), northwest US (Rasouli et al. 2015, Rasouli et al. 2019), western China (Zhou et al. 2014), Spanish Pyrenees (López-Moreno et al. 2013), Patagonia (Krogh et al. 2015), German Alps (Weber et al. 2016), Svalbard Archipelago (López-Moreno et al. 2016), and more recently southern Québec (Aygün et al. 2020b).

To simulate the dominant hydrological processes in the Montmorency River Catchment, the following physically based modules were selected:

- 1) Observation module: meteorological data are read and extrapolated with the environmental lapse rate. The phase of precipitation is predicted with a psychometric energy balance method using air temperature and relative humidity (Harder and Pomeroy 2013).
- 2) Radiation module: theoretical global radiation, direct and diffuse solar radiation, maximum sunshine hours are calculated based on latitude, elevation, slope and azimuth (Garnier and Ohmura 1970).
- 3) Annandale module: estimates incoming shortwave radiation from daily minimum and maximum temperatures and adjusts the incident short-wave for slope (Annandale et al. 2002).
- 4) Long-wave radiation module: incoming long-wave radiation is calculated using air temperature, relative humidity, and shortwave transmittance (Sicart et al. 2006).
- 5) Albedo module: snow albedo decay rate is calculated differently depending on the snow cover condition: pre-melt, melt, and post-melt. Albedo is estimated

following a linear decay rate for each snow cover condition based on snow depth, new snow, and melting occurrence (Gray and Landine 1987).

- 6) Canopy module: estimates snowfall and rainfall intercepted by, and sublimated or evaporated from, forest canopy and unloaded or dripped from the canopy. It updates the under-canopy snowfall and rainfall, and calculates short-wave and long-wave sub-canopy radiation. This module has options for forest environments, small forest clearings, and open environments (Ellis et al. 2010).
- 7) Blowing snow transport module: simulates wind redistribution of snow and sublimation (Fang and Pomeroy 2009, Pomeroy and Li 2000). Wind redistribution depends on surface roughness (vegetation height), wind speed and atmospheric and snowpack conditions.
- 8) Snowpack energy balance module: snowpack is represented by a two-layer mass and energy balance model (SNOBAL; Marks et al. (1998)). The energy balance includes net radiation, sensible and latent heat fluxes, ground heat, advection from rainfall, and change in internal energy.
- 9) Evapotranspiration module: The Penman-Monteith algorithm (Monteith 1981) is used to calculate actual evapotranspiration from unsaturated surfaces and the Priestley-Taylor algorithm (Priestley and Taylor 1972) for saturated surfaces. These algorithms access water from surface depressions and soil moisture.
- 10) Infiltration module: snowmelt infiltration into frozen soil using a parametric equation (Gray et al. 2001) and rainfall infiltration into unfrozen soil based on soil texture and ground cover (Ayers 1959) are estimated.

- 11) Hillslope module: this module calculates subsurface flow and simulates groundwater–surface-water interactions using physically based parameters and principles on hillslopes (Fang et al. 2013). It calculates the soil moisture balance, groundwater storage, subsurface and groundwater discharge, depressional storage, and runoff for control volumes of two soil layers, a groundwater layer, and surface depressions. The recharge (top) layer receives infiltration from depressional storage, snowmelt, and rainfall. Evaporation withdraws water first from canopy interception and depressional storage and then from both soil layers via evapotranspiration, depending on the rooting depth and available soil moisture (Armstrong et al. 2010). Horizontal and vertical flows from soil layers and groundwater layer are calculated based on Darcy's law, where Brooks and Corey's relationship (Brooks and Corey 1964) is used to estimate the actual hydraulic conductivity in the unsaturated zone. Surface runoff occurs if snowmelt or rainfall inputs exceed subsurface withdrawals from saturated soils or if the rate of snowmelt or rainfall exceeds the infiltration rate.
  
- 12) Surface-subsurface runoff routing module: runoff between HRUs is routed using the Muskingum method based on the geometric characteristics of the stream channel (Chow 1964). Subsurface and groundwater flows are routed by Clark's routing algorithm (Clark 1945).

CRHM uses Hydrological Response Units (HRUs) to spatially disaggregate the basin. HRUs are treated as a control volume for mass and energy calculations, and are represented by one set of parameters and one set of control volumes (Pomeroy et al. 2007, Zhou et al. 2014). HRUs can be defined based on the biophysical characteristics of a basin, such as elevation, slope, aspect and land cover (Guo et al. 2012, Pomeroy et al. 2007). HRUs for the Montmorency River Catchment were developed based on land cover, aspect, slope and elevation classes. The land cover classes consisted of

coniferous forest, mixed forest, regenerated forest, forest clearing, urban and open water (rivers and lakes). Each land cover was divided into north facing, south facing and flat slopes. Then, the slopes were classified as gentle slope (0–10°), medium slope (10–30°), and steep slope (30–60°). The last classification was defined based on basin elevation: low (553–750 m), medium (750–950 m), and high (950–1150 m) elevations. This classification strategy resulted in 78 HRUs (Figure 2.2).

The physiographic parameters (i.e. area, altitude, slope and latitude) for each HRU were extracted from the DEM and HRU maps. Estimation of the parameters in the Montmorency River Catchment was based on previous studies in the BEREV and Lac Laflamme watersheds (Figure 2.1b) and also other snow-dominated basins with similar land use characteristics. The soil profile parameters were estimated from previous studies performed at Lac Laflamme (Barry et al. 1988, Jutras 2012, Ouimet and Duchesne 2005). Both soil layers in CRHM were prescribed with a sandy loam texture with a porosity of 0.56. Hydraulic conductivities of  $6.25 \times 10^{-6} \text{ m s}^{-1}$  and  $5.9 \times 10^{-6} \text{ m s}^{-1}$  were assigned to the recharge layer and lower soil layer, respectively. The pore size distribution indices, used for estimating saturated hydraulic conductivities, were defined based upon soil textures (Brooks and Corey 1966). Based on the soil temperature and soil moisture content measurements performed at the Lac Laflamme watershed (Figure 2.1b) initial average fall volumetric soil moisture content before soil freeze-up was assigned as 30%, and soil temperature was estimated at  $-0.5 \text{ }^\circ\text{C}$  (at 15 cm soil depth) prior to snowmelt, which controls the heat flux from the soil to the snowpack base (Marks et al. 1998). Vegetation height and stalk diameter were obtained from the ecoforest maps produced in southern Québec by the MFFP. Mature coniferous and mixed forest stands were assigned to have a stalk diameter of 60 cm and canopy height of 14 m, whereas regenerated forest HRUs were assigned to have a stalk diameter of 40 cm and a canopy height of 6 m. Leaf Area Index (LAI) was set to be  $2.9 \text{ m}^2 \text{ m}^{-2}$  and  $3.4 \text{ m}^2 \text{ m}^{-2}$  for regenerated and mature balsam fir forests, respectively, as reported by Isabelle (2019). The maximum snow load capacity was set

to  $3.3 \text{ kg m}^{-2}$  and  $6.3 \text{ kg m}^{-2}$  for regenerated forest and mature coniferous forest, respectively. These values are transferred from the studies performed in boreal forests of western Canada (Hedstrom and Pomeroy 1998, Pomeroy et al. 2012). All the HRUs were routed to the streamflow network, where routing lengths were calculated as median distances from each HRU to the closest tributary.

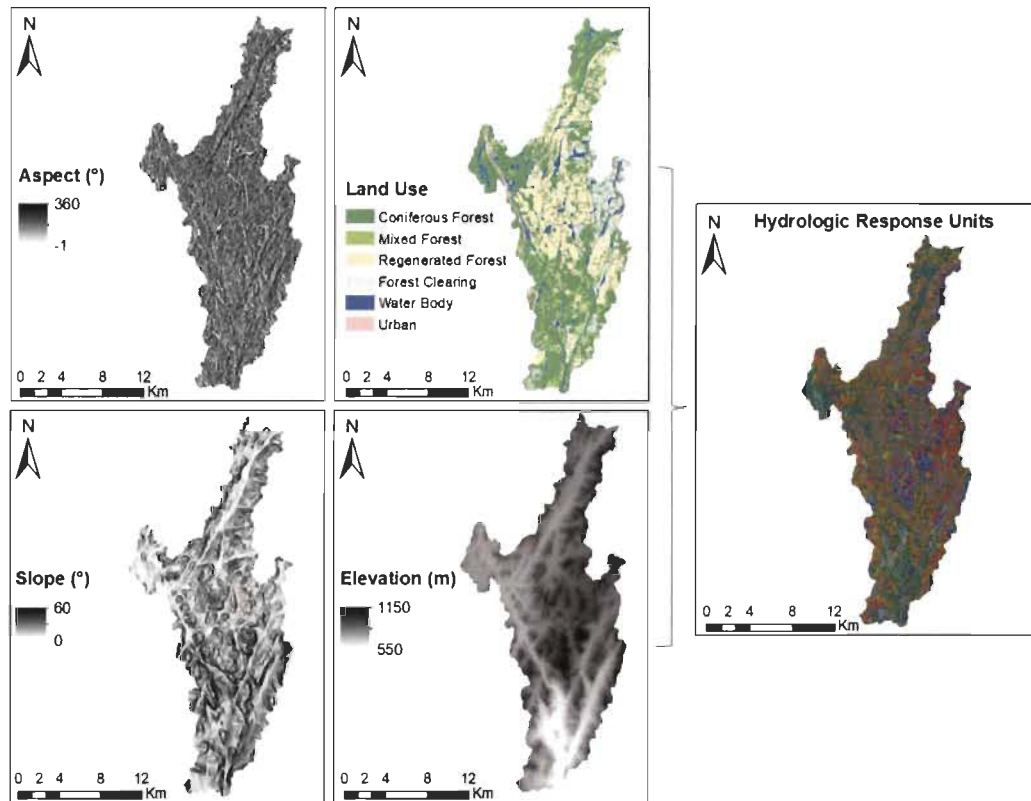


**Figure 2.2.** Pre-processing procedure showing the spatial layers used for generating Hydrologic Response Units (HRUs) in the Montmorency River Catchment.

The evaluation of the hydrological model performance was carried out using statistical performance measures, including the Nash-Sutcliffe efficiency (NSE, (Nash and Sutcliffe 1970); Equation 2.1), the Kling-Gupta efficiency (KGE, (Gupta et al. 2009); Equation 2.2), the percent bias (PBIAS; Equation 2.3), the root-mean square error (RMSE; Equation 2.4) and the normalized root-mean square error (NMRSE; Equation 2.5).

$$NSE = 1 - \frac{\sum(X_s - X_o)^2}{\sum(X_o - \mu_o)^2} \quad \text{Equation 2.1}$$

$$KGE = 1 - \sqrt{(r - 1)^2 + \left(\frac{\sigma_s}{\sigma_o} - 1\right)^2 + \left(\frac{\mu_s}{\mu_o} - 1\right)^2} \quad \text{Equation 2.2}$$

$$PBIAS = 100 \times \frac{\sum(X_s - X_o)}{\sum X_o} \quad \text{Equation 2.3}$$

$$RMSE = \sqrt{\frac{1}{n} \sum (X_s - X_o)^2} \quad \text{Equation 2.4}$$

$$NRMSE = \frac{RMSE}{X_{o_{max}} - X_{o_{min}}} \quad \text{Equation 2.5}$$

where  $n$  is the number of samples,  $r$  is the linear correlation between observations and simulations, and  $\mu_o$ ,  $X_{o_{max}}$ ,  $X_{o_{min}}$ ,  $\sigma_o$  are the mean, maximum, minimum and standard deviation of the observed values ( $X_o$ ), respectively.  $\mu_s$  and  $\sigma_s$  are the mean and standard deviation of the simulated values ( $X_s$ ), respectively. The NSE determines the relative magnitude of the residual variance compared to the measured data variance (Nash and Sutcliffe 1970) and the KGE is based on a decomposition of NSE into its constitutive components (correlation, bias and variability) in the context of hydrological modelling (Gupta et al. 2009). While  $NSE = 1$  indicates a perfect fit between the observations and simulations,  $NSE = 0$  indicates that the model simulations have the same explanatory power as the mean of the observations. Like NSE,  $KGE = 1$  indicates perfect correspondence between simulations and observations, whereas  $KGE < 0$  has been reported to indicate that the mean of observations provides better estimates than simulations (Knoben et al. 2019). Therefore, any positive value of NSE and KGE suggests that the model has some predictive power and higher values indicate better model performance. A positive value of PBIAS indicates a model overestimation, while a negative an underestimation. The absolute error metric RMSE is a weighted measure of the difference between

observation and simulation, while NRMSE is the normalization of RMSE against the range of the observed values. The lower the RMSE (NMRSE), the better the model simulation performance.

### **2.2.3 Climate Sensitivity Analysis**

In order to examine the first order impacts of climate change on hydrological state variables, the long-term temperature and precipitation observation data sets were perturbed based on ensemble climate model projections available for the administrative regions of Québec (Ouranos 2015). These projections were produced from a set of 11 downscaled global climate simulations produced from the CMIP5 ensemble for two periods (2041 to 2070 and 2071 to 2100) and two greenhouse gas emission scenarios (moderate: RCP 4.5 and high: RCP 8.5) for the province of Québec (Ouranos 2015). The reference period for the projections was 1981–2010. The 1-d quantile mapping method (Gennaretti et al. 2015) was used to downscale the raw global climate simulation output to a finer resolution (Chaumont 2014). Based on the scenarios produced for the administrative region where the Montmorency River Catchment is located (Figure 2.1a), temperature warming up to 8 °C (0–8 °C at 1 °C degree interval) and an increase in total precipitation up to 20% (0–20%, 5% interval) were considered in the sensitivity analyses. Thus, these scenarios encompass the most extreme end-of-the-century projection within the spread (10–90 percentile) of ensemble projections under the high emission RCP 8.5 scenario (Ouranos 2015). The different combinations of warming and precipitation changes were applied to the historical data and the hydrological run for each perturbed climate record, for a total of 45 individual climate scenarios. The baseline scenario of no change in air temperature and precipitation ( $\Delta t = 0$  °C &  $P = 100\%$ ; reference run) represents the historically averaged observed data over the 2005–2019 period. The scenario of “ $\Delta t = 6$  °C &  $P = 120\%$ ” stands for a warming of 6 °C and an increase of 20% in averaged precipitation relative to the reference run.

The hydrological sensitivity of the Montmorency River Catchment was compared with that of the Acadie River Catchment (Figure 2.1a; Aygün et al. 2020b) by assessing the changes in snow and water fluxes under 3 °C and 6 °C warming, and with and without a 20% increase in precipitation. While 3 °C warming represents the mean warming projection for the 2041–2070 period, a mean warming of 6 °C is projected for the 2071–2100 period under the high emission scenario for both catchments (Figure 2.3). These warming scenarios were modulated with a minimum (0%) and maximum (20%) increase in precipitation, based on existing scenarios (Figure 2.3), in order to analyze the potential compensation impact of increasing precipitation on snow and water fluxes impacted by warming. The reference run ( $\Delta t = 0\text{ °C}$  &  $P = 100\%$ ) represents the historically averaged observed data for both catchments over the 2005–2019 period.

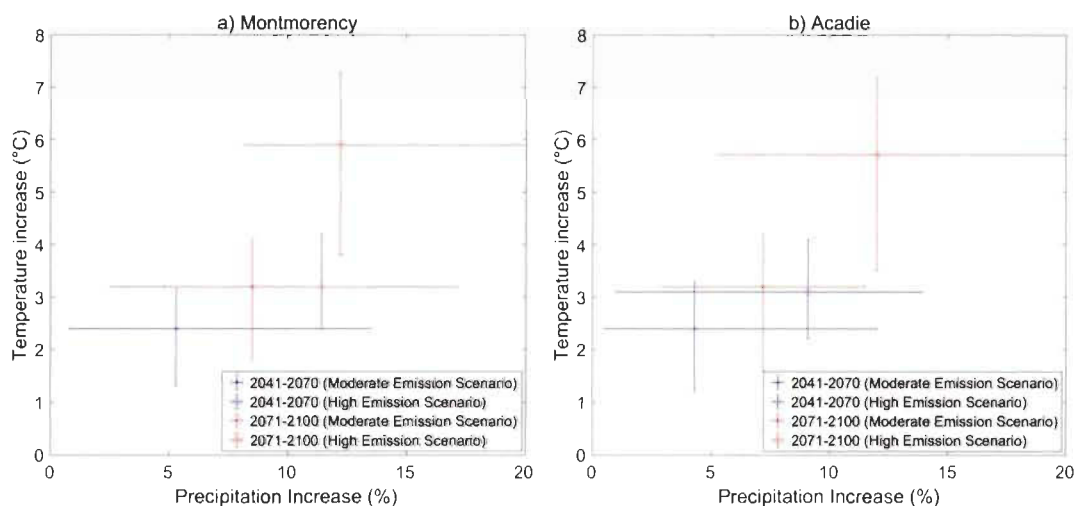


**Figure 2.3.** Projected changes in annual temperature and precipitation for the periods 2041–2070 and 2071–2100 under moderate emission scenario (RCP 4.5) and high emission scenario (RCP 8.5) for **a)** Capitale-Nationale, and **b)** Montérégie regions of Québec (Ouranos 2015).

## **2.3 Results and Discussion**

### **2.3.1 Evaluation of the Hydrological Modelling Performance**

#### ***2.3.1.1 Snow Accumulation and Snowmelt Evaluation***

Figure 2.4 compares the SWE observations at snow stations I and J (Figure 2.1b) with the simulations for the corresponding HRUs, which are regenerated forest with south-facing slope and regenerated forest with north-facing slope, respectively. The Nash-Sutcliffe efficiency (NSE), correlation coefficient, percent mean bias and normalized root mean square error varies between 54%–71%, 0.78–0.85, 1.7%–5% and 0.11–0.13, respectively, over the 14 years simulation period from 2005 to 2019. This performance is considered to be good, given that parameters were not calibrated. In some years such as 2008 the model underestimates SWE and in some other years such as 2016 SWE is overestimated, which is most probably due to the uncertainty in the station precipitation data, model parameters and also simplification of the snow processes by the model. Given these uncertainties and the complexity of the snow processes, the performance of the model at representing snow accumulation and snow melt is deemed acceptable.

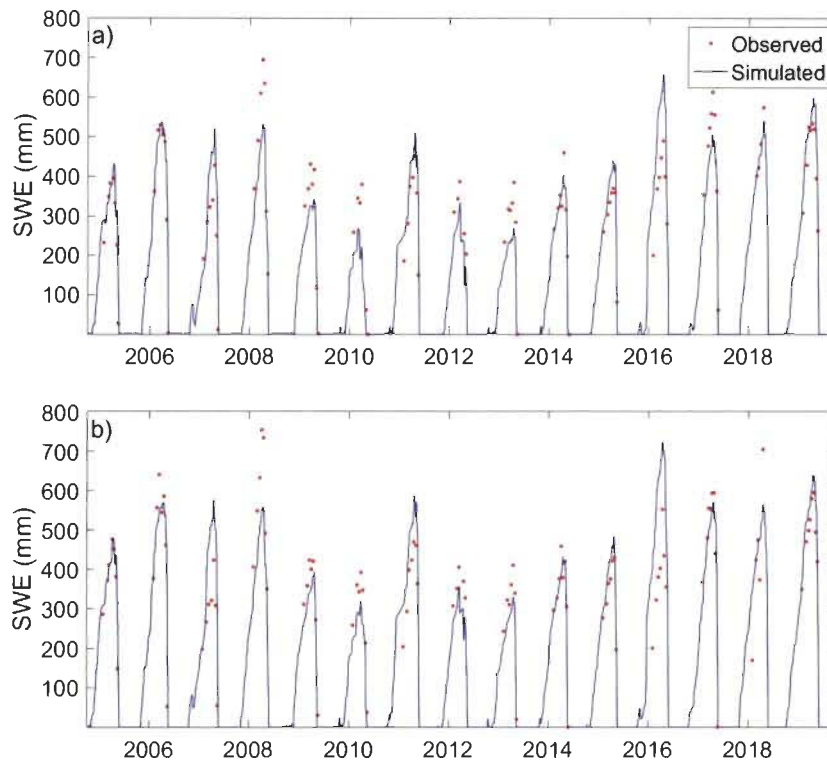


**Figure 2.4.** Observed and simulated snow water equivalent (SWE) at **a)** Station I, and **b)** Station J in the Montmorency River Catchment. The locations of the stations are given in Figure 2.1b.

### 2.3.1.2 Soil Moisture Evaluation

Simulations of soil moisture performed at the south-facing coniferous forest and the north-facing mixed forest HRUs were compared with the observations of seasonal soil moisture (i.e. non-frozen period of water year: 1 May to 1 October) during the periods 2005–2018 (Figure 2.5) and 2005–2010 (Figure 2.6), respectively. The soil temperatures are measured at 22 cm (Figure 2.5 and Figure 2.6). The simulations represent the soil moisture of the top 60 cm of soil, while the observations are the averages of soil moistures measured at depths of 22 cm and 81 cm by CS615/616 soil water content probes at the coniferous and mixed forest sites at the Lac Laflamme watershed (Figure 2.1b). Therefore, rather than soil moisture magnitudes, the patterns of change should be compared. Based on both Figure 2.5 and Figure 2.6, the temporal

patterns of the simulated soil moisture exhibit a good match with simulations, suggesting that the model fairly represents hydrological processes such as infiltration and evapotranspiration which shape the soil moisture fluctuations.

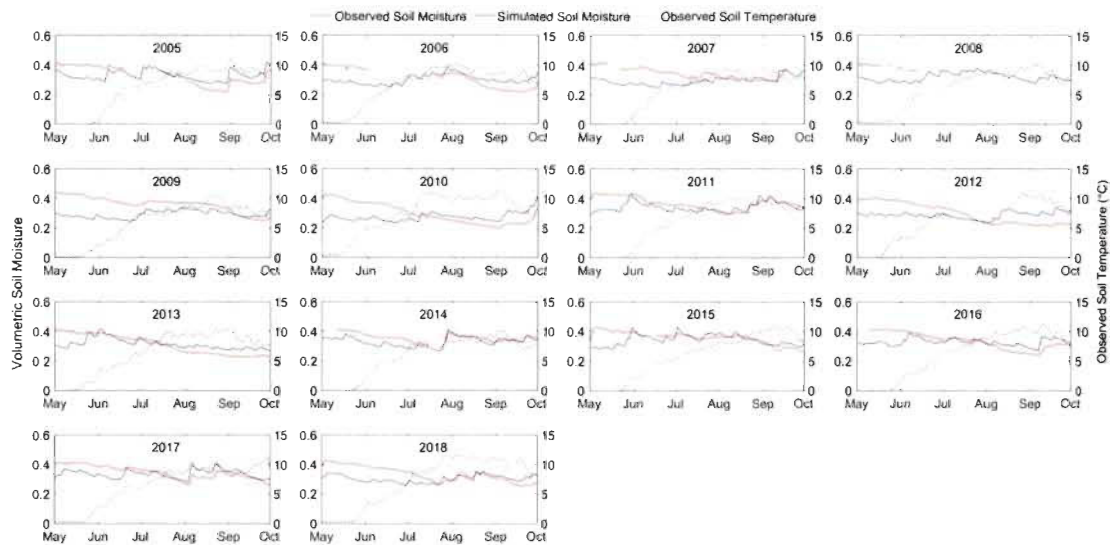


**Figure 2.5.** Comparisons of the observed and simulated seasonal daily volumetric soil moisture at the coniferous forest in the Lac Laflamme watershed from 2005 to 2018. Note that comparisons are valid only when the observed soil temperature (at 22 cm) is above 0 °C.

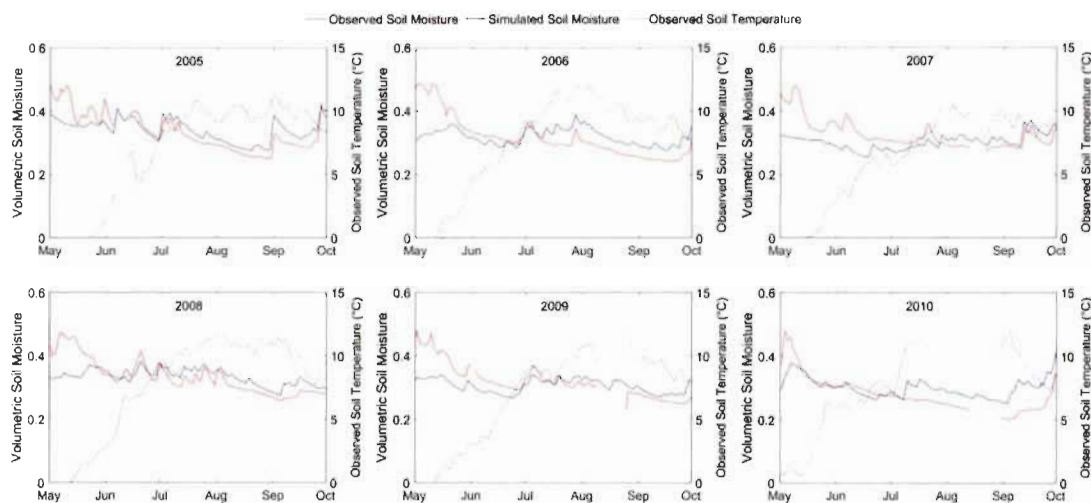


**Figure 2.6.** Comparisons of the observed and simulated seasonal daily volumetric soil moisture at the mixed forest in the Lac Laflamme watershed from 2005 to 2010. Note that comparisons are valid only when the observed soil temperature (at 22 cm) is above 0 °C.

### 2.3.1.3 Streamflow Evaluation

Simulated daily streamflow was compared against measurements at the outlet of the catchment for the period 2005–2019 (Figure 2.7). The Nash-Sutcliffe efficiency (NSE) and Kling-Gupta efficiency (KGE) for the 14-year simulation period are 0.63 and 0.82, respectively. Simulated streamflow properly represents flow duration curves (Figure 2.7b); however, low flows (high exceedance probability, >0.6) are underestimated. The cumulative mean daily discharge (Figure 2.7c) shows a good performance with a mean bias of –0.6% at the end of the water year. However, the model slightly underestimates streamflow during winter (Figure 2.7c), corresponding to the underestimated low flows in Figure 2.7b. This could be because of the uncertainties related to the discharge correction performed by CEHQ to correct the backwater effect at the Forêt Montmorency discharge gauge (Figure 2.1b) during winter months when there is ice formation. Rousseau et al. (2008) previously reported

an excessive amount of uncertainty associated with the discharge measurements at the Forêt Montmorency discharge gauge (ID: 051005), especially in winter.

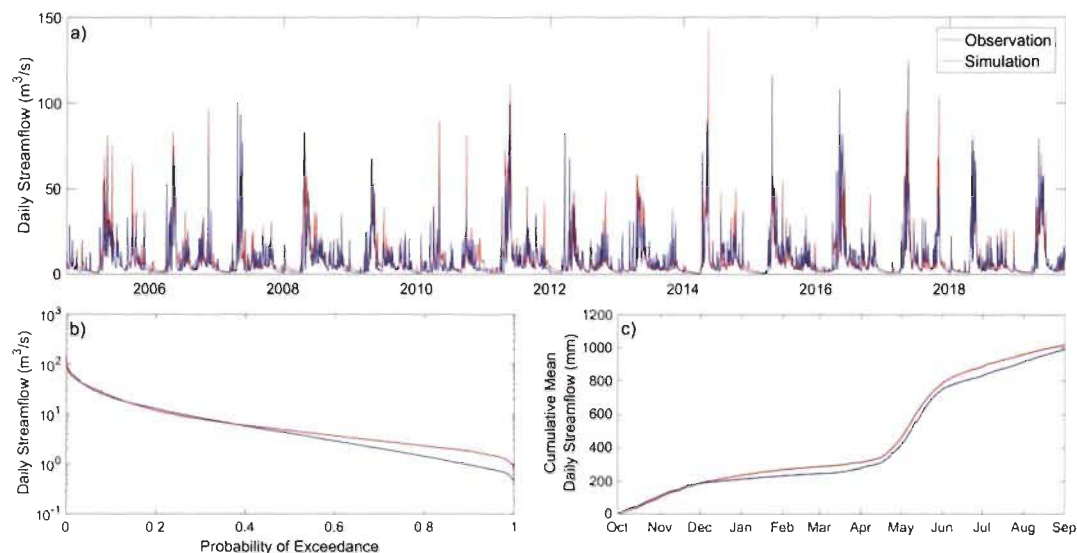


**Figure 2.7.** Assessment of the CRHM model performance in simulated streamflow at the outlet of the Montmorency River Catchment by comparing **a)** daily observed and simulated streamflow, **b)** flow duration curve of the observed and simulated streamflow, and **c)** cumulative mean daily observed and simulated streamflow.

### 2.3.2 Simulation of Water Fluxes

On average, annual precipitation is 1460 mm, of which 56% is rainfall and 44% is snowfall (Figure 2.8a). Mean annual simulated evapotranspiration (268 mm year<sup>-1</sup>), including evaporation of intercepted rain, is 18% of the annual precipitation, of which 60% occurs from June to September (Figure 2.8a). Mean annual streamflow (1067 mm) is the largest outflux of the entire water balance, representing about 73% of the total precipitation and exhibiting an inter annual variability of  $\pm 14\%$  (Figure 2.8a). Mean simulated annual sublimation is 140 mm, which represents roughly 22% of the annual mean snowfall (Figure 2.8). Sublimation losses are mainly governed by sublimation from canopy interception, which accounts for 21% of the annual snowfall, rather than snowpack sublimation (1% of the annual snowfall) (Figure 2.8b).

Mean annual snowmelt represents the remaining 78% of the annual mean snowfall. Snowmelt generates a substantial proportion (45%) of the mean annual streamflow, which can also be seen from the sharpest increase in cumulative runoff during the snowmelt period (May–June) (Figure 2.8a). The mean simulated annual peak SWE is 405 mm and occurs on April 10, with an inter-annual variability of  $\pm 130$  mm (32%) (Figure 2.8b).

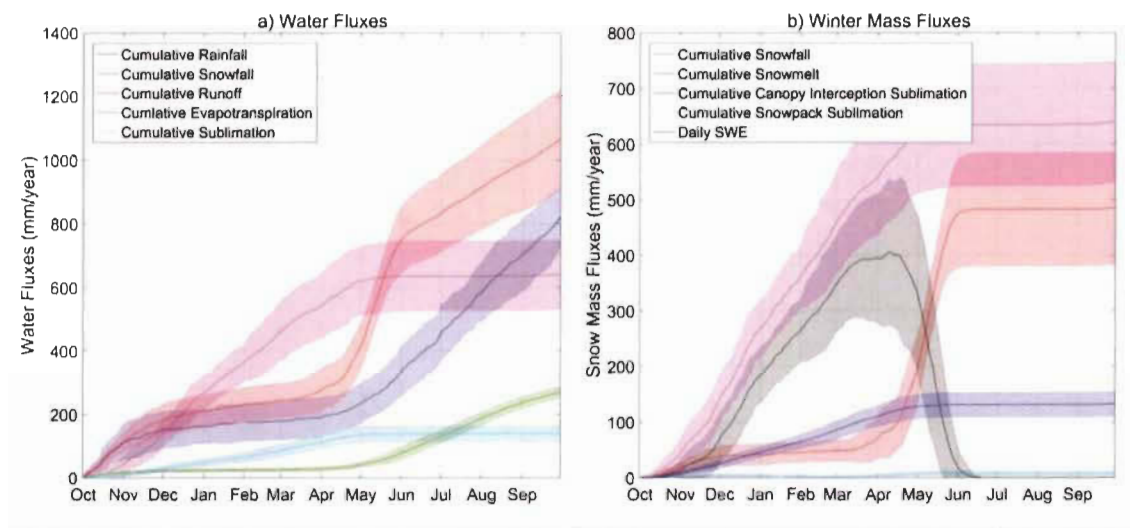


**Figure 2.8.** a) Average annual cumulative water fluxes, and b) average winter mass fluxes for the period 2005–2019. The shades around the average values represent the inter-annual variability ( $\pm$  standard deviation).

### 2.3.2.1 *Climate Sensitivity of Snow Accumulation and Snowmelt*

The sensitivity analysis shows a strong response of annual peak snow water equivalent (SWE) to warming, with declines of 10% per  $^{\circ}\text{C}$  warming (Figure 2.9a). This decline is however lower than the 11–20% per  $^{\circ}\text{C}$  reduction found in the Spanish Pyrenes (López-Moreno et al. 2014, López-Moreno et al. 2013), the 20% per  $^{\circ}\text{C}$  reduction in the Washington Cascades (Casola et al. 2009), the 20% per  $^{\circ}\text{C}$  reduction for the USA Sierra Nevada (López-Moreno et al. 2017), and the high sensitivity of 25–35% per  $^{\circ}\text{C}$  recently found for the Acadie River Catchment (Aygün et al. 2020b). The lower SWE

sensitivity in the Montmorency River Catchment is likely due to the colder temperatures in this region compared to the other study areas. Based on the contour lines in Figure 2.9a, peak SWE shows a lesser sensitivity to increasing precipitation. The impact of 1.7 °C warming on peak SWE could be fully compensated for by a 20% precipitation increase, but greater warming (>2 °C) cannot be compensated with precipitation increases of this magnitude. In the most severe climate change scenario, a warming of 8 °C with no change in precipitation causes the peak SWE to decrease by almost 90%, from 405 mm to around 55 mm.

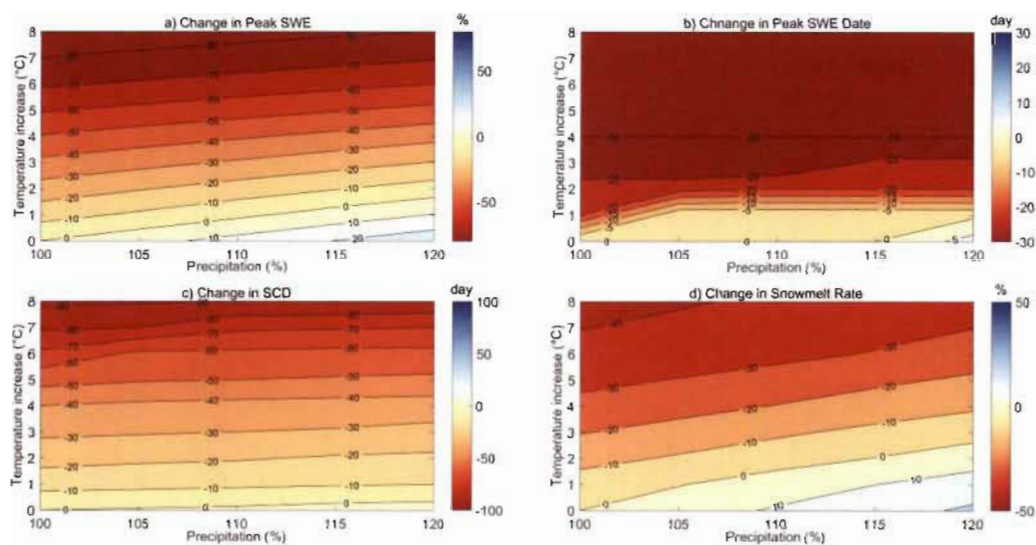


**Figure 2.9.** Sensitivity of snow accumulation to changing climate in the Montmorency River Catchment. **a)** Change in annual peak SWE; **b)** change in annual peak SWE date; **c)** change in snow cover duration (SCD); **d)** relative change in snowmelt rate.

The annual peak SWE shifts towards earlier dates under almost every warming scenario, suggesting that the timing of peak SWE is very sensitive to warming. A more pronounced sensitivity of peak SWE timing is observed when warming is between 1 °C and 2 °C, as shown by the closer contours on Figure 2.9b. This can be explained with the fact that there are two annual peak SWE events observed historically. The second peak reflects late spring snow storms under warmer conditions (Figure 2.8b). These snow storms transit to rainfall under a warming of 2 °C so that the first peak

SWE becomes more dominant. The timing of peak SWE shows a slight sensitivity to increasing precipitation under 1 °C warming. For instance, while 1 °C warming advances the timing of peak SWE by 20 days; this can be almost fully compensated for by a 20% increase in precipitation. As shown in Figure 2.9c, changes in snow cover duration (SCD), defined as the number of days with SWE>0.1 mm, are found to be completely driven by warming and not precipitation. SCD declines by roughly 10 days per degree of warming and becomes three months shorter when warming reaches its maximum (8 °C). Snowmelt rate is primarily influenced by warming and to a lesser extent by increasing precipitation (Figure 2.9d). Snowmelt rates are slower under all warming scenarios as long as there is no increase in precipitation. This is because warming leads to shallower snowpacks which melt out earlier in the year when the available energy is lower, therefore leading to overall slower melt rates, as reported by other studies performed in different snow-affected regions (López-Moreno et al. 2013, Musselman et al. 2017, Rasouli et al. 2014, Rasouli et al. 2019, Trujillo and Molotch 2014). On the other hand, snow can also melt faster when warming is accompanied by increasing precipitation. For instance, while a 1 °C warming reduces snowmelt rate by 5%, the same warming increases snowmelt rate by 15% if it is accompanied by a 20% increase in precipitation, which might be due to the fact that warming leads to higher incoming energy available for deeper snowpack (Figure 2.9a).

### ***2.3.2.2 Climate Sensitivity of Streamflow Regime***

Streamflow represents the spatially integrated basin response to snow and water fluxes within the basin, and is therefore sensitive to both warming and increasing precipitation (Figure 2.10). Peak streamflow is found to be more sensitive to increasing precipitation (Figure 2.10a) than is peak SWE (Figure 2.9a). Increasing precipitation could cause an increase in annual peak discharge by up to 20%, depending on the warming and increase in precipitation. This zone of positive sensitivity of peak discharge is delineated by the 0% contour in Figure 2.10a, below which the peak streamflow shows

an increase. In this positive sensitivity zone, the increase in precipitation is enough to counterbalance the negative impact of warming on the peak discharge. For instance, a warming of 2 °C increases the annual peak streamflow by 15% if there is an increase in precipitation by 20%, whereas the same amount of warming causes peak streamflow to decline by 1% if there is a 10% increase in precipitation. A 20% increase in precipitation could compensate peak flow declines due to warming up to 2.9 °C but beyond +3°C, warming impacts predominate and peak flow declines.

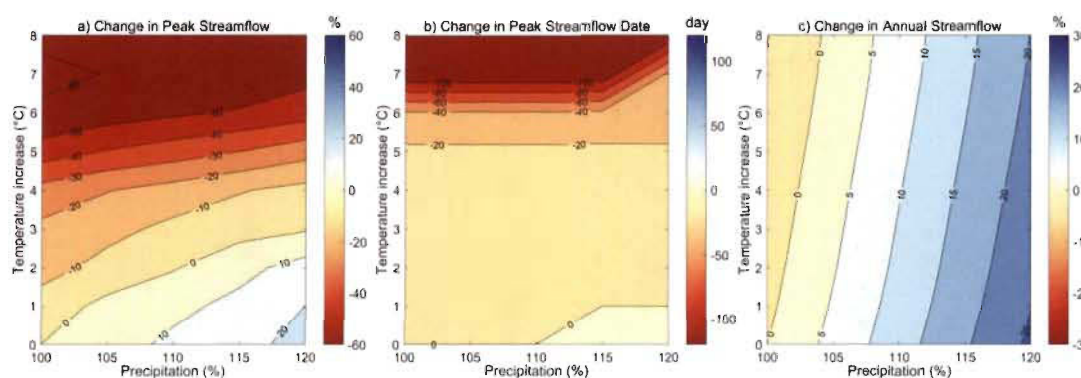


**Figure 2.10.** Sensitivity of streamflow to changing climate in the Montmorency River Catchment. Change in **a)** annual peak streamflow, **b)** annual peak streamflow timing, and **c)** total annual streamflow.

Warming causes a shift in peak streamflow timing towards earlier dates (Figure 2.10b), which is in parallel with the earlier occurrence of the peak SWE under warming scenarios (Figure 2.9b). However, the timing of peak streamflow is found to be relatively less sensitive to warming than is the timing of peak SWE (Figure 2.9b), particularly for a warming between 0 °C and 5 °C. Beyond 6 °C warming the peak streamflow timing becomes very responsive, advancing by roughly four months when warming reaches 7 °C (Figure 2.10b). Under these conditions the streamflow regime shifts towards a mixed snowmelt/rainfall regime with peak flows occurring in winter. Changes in annual streamflow contrast with those in peak SWE (Figure 2.9a) and peak streamflow (Figure 2.10a), with annual streamflow being much more sensitive to increasing precipitation than to warming. Annual streamflow increases regardless of

the warming level, as long as precipitation increases by at least 5% (Figure 2.10c). This shows the predominance of increased water inputs to the basin from increasing precipitation and reduced sublimation rates over losses from increased evapotranspiration under warming.

### **2.3.3 Comparison of the Hydrological Sensitivity of the Montmorency River Catchment to Climate Change with the Acadie River Catchment**

#### ***2.3.3.1 Comparison of Climate Sensitivity of Snow Regimes in Montmorency and Acadie River Catchments***

Under reference climate conditions, 44% of the total precipitation occurs as snowfall in Montmorency, whereas the snowfall ratio is 23% in Acadie (Table 2.2). The snowfall ratio is more sensitive to warming in the Acadie basin; with 3 °C warming in both catchments, the snowfall fraction in Acadie reduces to more than half that in Montmorency (Table 2.2). A 6 °C warming in Montmorency decreases the snowfall ratio to 23%, which is equal to the snowfall ratio in Acadie under reference climate conditions (Table 2.2). Under reference climate conditions, the annual peak SWE in Montmorency occurs on April 10, which is 40 days later than in Acadie where it presently occurs in early March (Table 2.2 and Figure 2.11). The annual peak SWE in Montmorency is presently 405 mm, which is about six times greater than that in Acadie under reference climate conditions (Table 2.2 and Figure 2.11). Under 3 °C warming, the decline in peak SWE in Acadie (80%) is twice greater than in Montmorency (38%). While a 20% increase in precipitation could compensate 48% of the decline in peak SWE in Montmorency, the same precipitation increase could only compensate 13% of the decrease in peak SWE in Acadie under 3 °C warming (Table 2.2 and Figure 2.11). A 6 °C warming reduces peak SWE in Montmorency from 405 mm to 115 mm, which is still greater than the peak SWE in Acadie under reference climate conditions. Meanwhile, the same scenario causes drastic snowpack depletion in Acadie, with peak SWE declining to 8 mm (Table 2.2 and Figure 2.11).

**Table 2.2.** Comparison of climate sensitivity of snow variables in the Montmorency River Catchment with the Acadie River Catchment.

Catchment	Warming (°C)	0	3	6	3	6
	Precipitation (%)	100	100	100	120	120
Montmorency	Snowfall ratio (%)	44	32	23	32	23
	SOD (DOWY*)	4	12	28	12	19
	Peak SWE (mm)	405	252	115	326	162
	Peak SWE date	Apr-10	Mar-11	Mar-10	Mar-17	Mar-10
	SDD (DOWY)	261	237	217	242	219
	SCD (days)	257	225	189	230	200
Acadie	Snowfall ratio (%)	23	15	10	15	10
	SOD (DOWY*)	23	49	63	40	63
	Peak SWE (mm)	65	13	8	20	10
	Peak SWE date	Mar-3	Dec-22	Dec-22	Jan-7	Dec-22
	SDD (DOWY)	210	198	172	198	173
	SCD (days)	187	149	109	158	110

DOWY\*= day of the water year (starting in October 1st).

Under warmer temperatures, peak SWE shifts towards earlier dates in both catchments, with greater shifts simulated in Acadie. For instance, peak SWE advances by about a month, from April 10 to March 11 in Montmorency with 3 °C warming. The same scenario causes the peak SWE in Acadie to shift by more than 2 months, from early March to late December. Interestingly, further warming (+6 °C) continues to deplete the snowpack in both basins but does not change the peak SWE timings further. Snow cover duration (SCD) in Montmorency is 70 days longer than in Acadie under reference climate conditions. While SCD in both catchments declines under warmer temperatures, the relative decrease in Montmorency (~12% per 3 °C warming) is lower than that in Acadie (~20% per 3 °C warming). Under 6 °C warming and no increase in precipitation, SCD in Montmorency decreases to 189 days, which is almost the same as SCD in Acadie (187 days) under reference climate conditions.

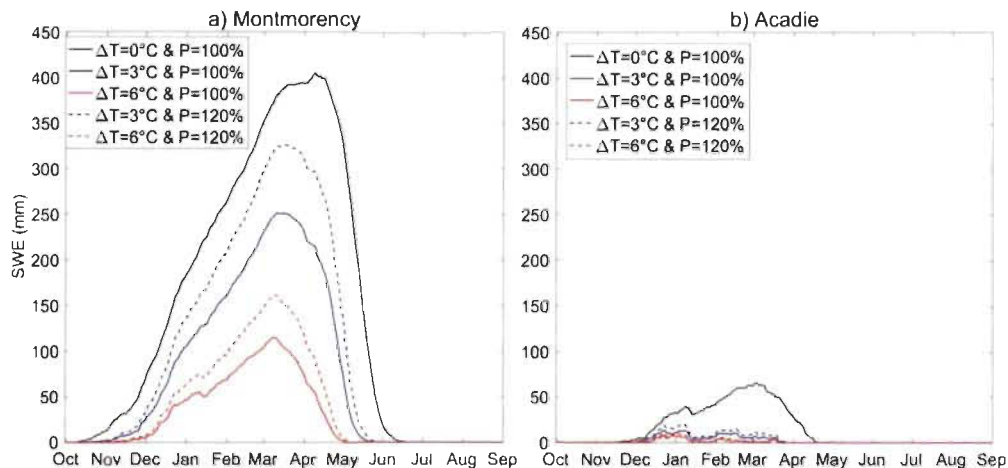


**Figure 2.11.** Snow accumulation under selected climate change scenarios in **a) Montmorency**, and **b) Acadie** River catchments.

Intercepted snow sublimation removes a considerable amount of snow ( $132 \text{ mm year}^{-1}$ : 21% of the annual snowfall) from the Montmorency River Catchment in winter under reference climate conditions (Figure 2.12). This is because Montmorency is dominated by coniferous trees that intercept a sizeable fraction of seasonal snowfall, which subsequently sublimates over the winter. The canopy interception sublimation ratio (21%) in Montmorency is however lower than the 25–45% canopy sublimation losses estimated for colder and drier boreal forest environments (Essery and Pomeroy 2001) such as the southern boreal forest in Saskatchewan (Pomeroy and Gray 1995, Pomeroy et al. 1998). This is mostly because Montmorency River Catchment has a humid climate (Dfc; Peel et al. 2007) which limits the sublimation (Essery and Pomeroy 2001). However, it is important to note that although the canopy sublimation ratio is lower for Montmorency than for the drier climate of Saskatchewan, the absolute amount is greater, which is explained by the higher amount of snowfall and hence longer duration for which intercepted snow is exposed to the atmosphere in Montmorency. On the other hand, the simulated canopy sublimation ratio in Montmorency is higher than the 10% canopy sublimation loss estimated for the Umpqua National Forest in Oregon (US) (Storck et al. 2002) where the climate is

warmer and more humid, which results in more rapid unloading and in limited sublimation (Essery and Pomeroy 2001). Warming air temperatures in Montmorency reduce the total sublimation from intercepted snowfall to 104 mm and 79 mm with 3 °C and 6 °C warming, respectively (Figure 2.12), which could be explained with the reduced snowfall ratio (Table 2.2) and also more rapid and earlier unloading of canopy snow as reported by other studies in forested environments (Ellis et al. 2010, Gelfan et al. 2004, Krogh and Pomeroy 2019, Pomeroy and Gray 1995, Rasouli et al. 2015). In comparison with the canopy sublimation, sublimation from the snowpack is small (7.8 mm year<sup>-1</sup>) and reaches only 1.2% of the annual snowfall in Montmorency under reference climate conditions (Figure 2.12). In Acadie, on the other hand, annual sublimation is mostly composed of snowpack sublimation (20.8 mm year<sup>-1</sup>; 9% of the annual snowfall), whereas the canopy sublimation loss (4 mm year<sup>-1</sup>; 1.7% of the annual snowfall) is the smallest term of the snow mass balance under the reference climate conditions (Figure 2.12). These contrasted sublimation losses can be explained with the landscape of the Acadie River Catchment, which is dominated by open agricultural fields that are subjected to high winds and relatively high surface sublimation rates, while only 17% of the catchment is covered by forest (of which 60% is deciduous), therefore resulting in relatively small canopy sublimation losses at the catchment scale. Compared to the reference climate conditions, snowpack sublimation ratios are higher in both catchments under warmer temperatures (Figure 2.12), which might be explained by the greater available energy for sublimation with warming temperatures. However, it is important to note that the snowpack sublimation ratio in Acadie River Catchment is lower under 6 °C warming than that under 3 °C warming, which might be explained with the reduction in SCD (Table 2.2) becoming a limiting factor for the snowpack sublimation losses. Canopy sublimation ratios are also greater particularly in Montmorency under warmer temperatures (Figure 2.12). These higher sublimation ratios suggest that sublimation is a more efficient snow removal process under warmer temperatures. While there is no blowing snow sublimation component in the forested Montmorency as blowing snow transport is suppressed, blowing snow

sublimation reaches 2% of the annual snowfall under reference climate conditions in Acadie. In comparison with the other sublimation components in Acadie, blowing snow sublimation shows the greatest sensitivity to warming, declining by 74% and 90% with 3 °C and 6 °C warming, respectively. This is due to the increasing inter-crystal bond strength and cohesion of snow as it warms, which raises the threshold wind speed required to initiate saltation (Li and Pomeroy 1997).

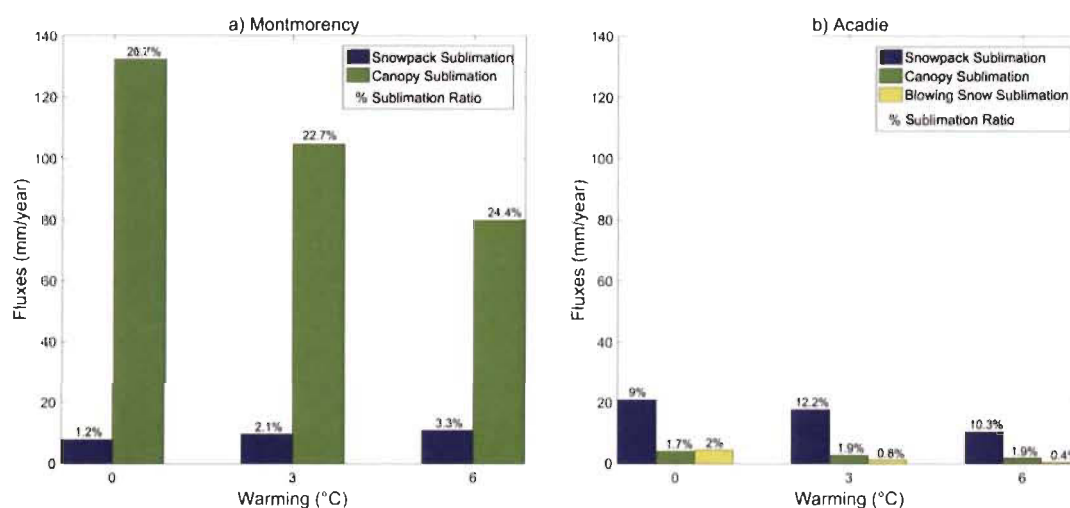


**Figure 2.12.** Sublimation losses under selected climate change scenarios in **a) Montmorency River Catchment**, and **b) Acadie River Catchment**. The ratio of sublimation to annual snowfall is given above each bar.

### 2.3.3.2 Comparison of Climate Sensitivity of Water Fluxes in Montmorency and Acadie River Catchments

With a 6 °C warming, the rainfall ratio in Montmorency increases from 56% to 77%, which is equal to the rainfall fraction in Acadie under reference climate conditions (Table 2.3). Under the same warming, 90% of the precipitation occurs as rainfall in Acadie (Table 2.3). While a considerable amount of annual precipitation (73%) translates into river discharge in Montmorency, the runoff ratio in Acadie is less than 50% under reference climate conditions, due to the high amount of evapotranspiration losses (Table 2.3). The annual peak streamflow in Montmorency is more than twice

that of Acadie and it occurs roughly a month later under reference climate conditions (Table 2.3 and Figure 2.13). Although the annual peak streamflow declines and shifts towards earlier dates in both catchments under warming temperatures, the shifts are more considerable in Acadie such that the timing of peak streamflow desynchronizes from the date of peak snow accumulation (Table 2.3 and Figure 2.13). For both Montmorency and Acadie River catchments, warmer temperatures lead to increased annual evapotranspiration, with the greatest increases occurring in spring due to increasing number of snow-free days during which evapotranspiration can take place.

**Table 2.3.** Comparison of climate sensitivity of water fluxes in the Montmorency River Catchment with the Acadie River Catchment.

Catchment	Warming (°C)	0		3		6	
		Precipitation (%)	100	100	100	120	120
Montmorency	Rainfall ratio (%)		56	68	77	68	77
	Runoff ratio (%)		73	72	71	76	75
	Annual peak streamflow (m <sup>3</sup> s <sup>-1</sup> )		43.8	36.1	18.0	43.4	24.2
	Annual peak streamflow date		May-9	Apr-23	Apr-2	Apr-23	Apr-2
	Evapotranspiration (mm year <sup>-1</sup> )		268	311	347	316	354
Acadie	Rainfall ratio (%)		77	85	90	85	90
	Runoff ratio (%)		45	43	41	49	47
	Annual peak streamflow (m <sup>3</sup> s <sup>-1</sup> )		21.3	19.6	16.2	26.5	18.2
	Annual peak streamflow date		Apr-12	Jan-13	Dec-25	Jan-13	Jan-13
	Evapotranspiration (mm year <sup>-1</sup> )		462	485	502	506	523

Under a warming of 3 °C and more, the Acadie River mean hydrograph becomes very flashy and the seasonality of precipitation dictates the magnitude and timing of the annual peak streamflow (Figure 2.13c); in other words, the flow regime of the Acadie River Catchment transits to a rainfall dominated regime. Hence the increase in annual peak flow observed in the Acadie River Catchment under 3 °C warming and 20% increasing precipitation results from increasing rainfall amounts rather than snowmelt.

In contrast, the Montmorency River conserves a distinct snowmelt-dominated peak streamflow under 3 °C warming. Moreover, a 20% increase in precipitation almost completely (94%) counterbalances the decline in peak streamflow caused by 3 °C warming; however, the peak flow occurs on April 23 rather than May 9 (Table 2.3). This highlights the considerable uncertainty in future peak streamflow magnitude and timing and flood risks caused by uncertainties in projected precipitations. Meanwhile, a 6 °C warming causes the flow regime of Montmorency River to transit from a snowmelt to a mixed snowmelt/rainfall regime (Figure 2.13a).

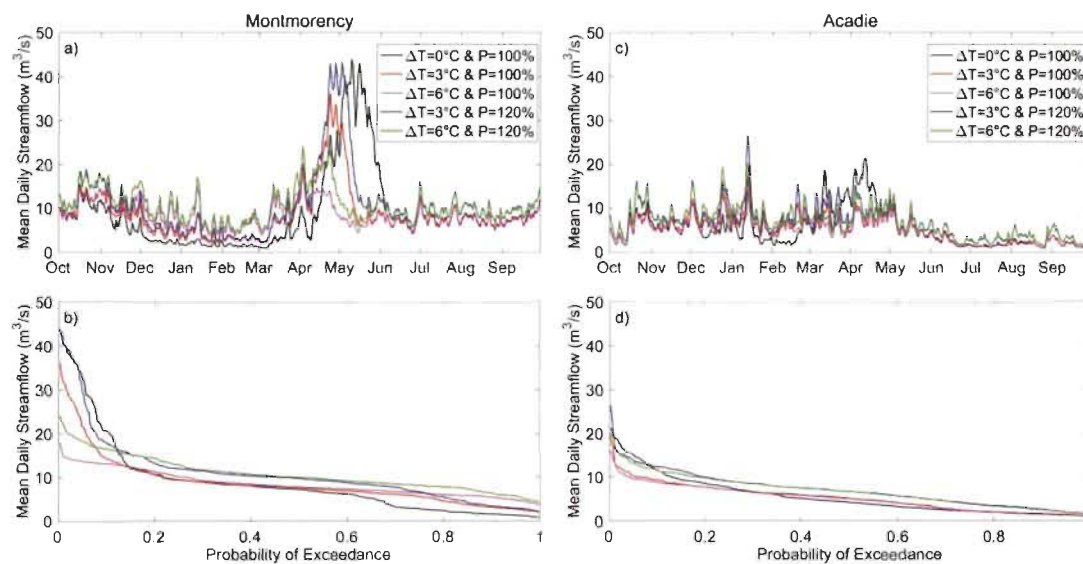


**Figure 2.13.** Changes in mean daily streamflow and exceedance probability of mean daily streamflow to selected warming and increasing precipitation scenarios in (a-b) Montmorency River Catchment and (c-d) Acadie River Catchment.

Warmer temperatures cause an increase in streamflow in both catchments during winter (Figure 2.13a, c), which can be explained with the increase in available water in winter due to higher winter rainfall and more frequent mid-winter snowmelt events. Increasing precipitation leads to even higher streamflow in winter. This is also evident in the increase in flows with exceedance probabilities between 0.3 and 0.8, and 0.5 and 1, respectively for Acadie and Montmorency River catchments (Figure 2.13b, d). This is

in parallel with the increasing winter streamflow previously projected for several tributaries of the St. Lawrence River in the future (Boyer et al. 2010). Greater winter flows are of concerns, as they can trigger river ice breakup and jamming, resulting in extreme flooding and high damages (Riboust and Brissette 2015).

### ***2.3.3.3 Influences of Current Climate Conditions and Biophysical Characteristics on Climate Sensitivity of Catchment Hydrology***

In order to explore the respective roles of the dominant biophysical conditions and current climates on the climate sensitivity of hydrological responses, a set of climate sensitivity analyses were performed in which the historical climates of both basins were permuted. Historical (2005–2019) time series of air temperature and precipitation of the Acadie River Catchment were thus used as meteorological inputs for the Montmorency River Catchment and vice-versa (Figure 2.14). While the solid arrows indicate the effect of regional climate, the dashed arrows indicate the influence of the biophysical conditions of the catchment on the climate sensitivity of annual peak SWE (Figure 2.14a, b and c) and annual peak specific discharge (Figure 2.14d, e and f). When both catchments are forced by the colder and snowier historical climate of Montmorency, the simulated peak SWE in Montmorency (405 mm) is smaller than in Acadie (431 mm) (Figure 2.14a), which could be explained with the higher (canopy) sublimation losses in the forested landscape of Montmorency. When forced by the warmer and rainier climate of Acadie, canopy sublimation losses in Montmorency decrease but the total sublimation ratio in Montmorency (36%) is still greater than that in Acadie (13%), showing again how coniferous forests increase total sublimation losses. However, the amount of snowmelt simulated in mid-winter in Montmorency is about 22% less than that in Acadie, mostly due to the reduced amount of energy available for melting in Montmorency due to shading by the forest canopy cover. This compensates the sublimation losses and as a result, the peak snow accumulations are almost equal in both catchments when forced by the Acadie climate (Figure 2.14a).

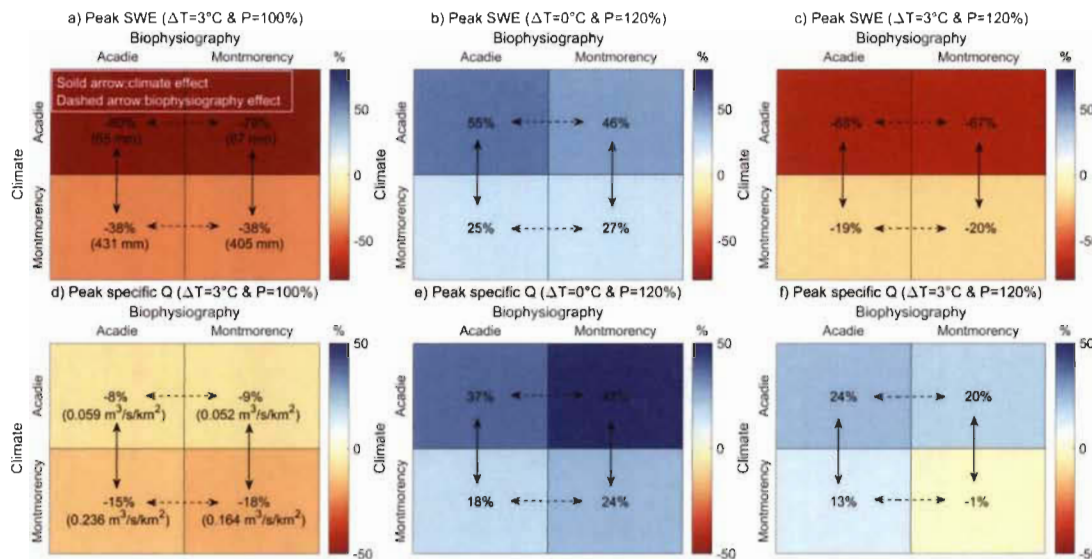


**Figure 2.14.** The influences of biophysical and climatological characteristics of the catchments on the climate sensitivity of the annual peak snow water equivalent (SWE) and annual peak specific discharge (Q). **(a-b-c)** The response of peak SWE and **(d-e-f)** peak specific Q to 3 °C and/or 20% increasing precipitation under permuted baseline climate conditions. The values in parentheses below the sensitivities (panel a and d) present the current (historically averaged) baseline values of the variables under a given regional climate and biophysiology combination.

Notwithstanding, the peak SWE shows rather similar sensitivities to warming and increasing precipitation in both catchments when forced by the same climate (Figure 2.14a, b and c). In other words, the climate sensitivity of the peak SWE appears to be little influenced by the biophysical conditions but is rather shaped by the current regional climate conditions. The peak SWE sensitivity to warming and precipitation changes is much more pronounced when both catchments are forced by the warmer and drier Acadie baseline climate, than by the colder and more humid Montmorency climate (Figure 2.14a, b and c). This highlights the stronger sensitivity of snow conditions to current climate conditions. Under Acadie-type climate conditions, a small to moderate warming leads to significant declines in snow accumulation due to already mild winter temperatures (Table 2.1). This finding is in parallel with previous studies which reported that precipitation phase is much more sensitive to warming in basins

with warmer winter temperatures in western North America (Knowles et al. 2006, Rasouli et al. 2019).

Under the same historical climates, the Acadie-type biophysiology produces higher peak specific discharges than the Montmorency-type biophysiology (Figure 2.14d). This can be explained with the higher runoff efficiency in Acadie due to lower infiltration and storage capacities of the compacted agricultural soils compared to the forested porous soils in Montmorency. For 3 °C warming, the peak Q under Montmorency climate shows a stronger sensitivity (–15% to –18%) than under the climate conditions of Acadie (–8% to –9%) (Figure 2.14d), unlike the much greater sensitivity of peak SWE under Acadie climate (–78% to –80%) than under Montmorency climate (–38%) (Figure 2.14a). This occurs because when the climate of Acadie is warmed by 3 °C the peak Q decouples from the snow cycle (Table 2.2 and Table 2.3), so that the large declines in peak SWE (Figure 2.14a) do not translate in large changes in peak Q (Figure 2.14d). In contrast, when forced with the Montmorency baseline climate, the peak Q remains synchronized with the snow cycle under 3 °C warming (Table 2.2 and Table 2.3), and the peak Q of both catchments responds more strongly to changes in peak SWE (Figure 2.14d) even though the declines in peak SWE are smaller (Figure 2.14a). These results show that the peak SWE and peak Q can show contrasted responses to warming, depending on the current climate conditions. Under a 20% increase in precipitation, the increase in peak Q under Acadie climate (37% to 47%) is higher than under Montmorency climate (18% to 24%) (Figure 2.14e), which could be explained with the higher increases in peak SWE under Acadie climate for the same scenario (Figure 2.14b). Under combined warming (+3 °C) and wetting (+20%), the peak Q rises by 24% and 20% in Acadie-type and Montmorency-type biophysiology, respectively, when forced by Acadie baseline climate conditions. This is unlike the significant declines in peak SWE for the same scenario (Figure 2.14c). Considering that the peak Q under Acadie climate decouples from the snow cycle under 3 °C warming, these increases in peak Q are mostly

explained by increased annual peak runoff (net rainfall + snowmelt – infiltration) (Figure S2.1a, b in the supporting material) which result from simultaneous increases in winter rainfall and snowmelt amounts in response to 3 °C warming and 20% increasing precipitation. Under baseline Montmorency climate conditions, on the other hand, the response of peak Q to 3 °C warming and 20% increasing precipitation is quite different between the two catchments (Figure 2.14f). Annual peak runoff decreases in both catchments under this scenario (see Figure S2.1c, d). Despite an increase in available mean water flux in response to combined 3 °C warming and 20% increasing precipitation in Montmorency under its own climate (see Figure S.2.2d), the mean runoff (net rainfall + snowmelt – infiltration) declines (Figure S2.3d), which in turn leads to decline in peak Q by 1% (Figure 2.14f). This is mostly because the forested soils have higher infiltration and storage capacities in Montmorency, which buffer the increased mean water fluxes and lead to decreased mean runoff (see Figure S2.3d) and peak Q (Figure 2.14f). On the other hand, for the same amount of warming and wetting, the increase in mean water flux (net rainfall + snowmelt) simulated for Acadie under Montmorency baseline climate (Figure S.2.2c) translates into an increase in mean runoff (net rainfall + snowmelt – infiltration) (Figure S2.3c), which then leads to an increase in peak Q by 13% (Figure 2.14f). Hence the reduced infiltration and storage capacity of the agricultural soils are less apt to buffer the increased runoff and leading to increased peak flow.

This study clearly shows that the hydrology of both the Montmorency and Acadie River catchments is sensitive to climate change, particularly to warming which causes less winter precipitation to fall as snow. However, warming impacts on snow accumulation and associated changes in streamflow regime are more evident in the Acadie River Catchment, which has winter temperatures that are currently milder and closer to the freezing level. In contrast, the colder Montmorency River Catchment shows some resilience to warming and the simulated changes in snow and streamflow conditions are less dramatic. This finding is in parallel with the study of Boyer et al. (2010) which

projected that the southern tributaries of the St. Lawrence River Basin would transit more quickly towards a new rain-fed hydrological regime given that mean air temperatures are already relatively high for these watersheds compared to more northerly basins. Many other cold regions have also been reported to exhibit different sensitivities to warming and precipitation change, depending on the cold season temperature regime governed by latitude and/or elevation: more drastic changes were found to be occurring over regions with near-freezing air temperatures, whereas colder regions, on the other hand, were found to be comparatively less sensitive to climate change (Aygün et al. 2020a). This is because precipitation phase is more resilient to warming in the colder regions and increasing precipitation could compensate the hydrological impacts of warming as long as cold season temperatures remain below freezing and thus support solid precipitation.

In this study, both the current climate conditions and biophysical characteristics have been shown to influence annual peak snow accumulation and annual peak specific discharge. While the biophysical conditions of the catchments did not significantly influence the climate sensitivity of peak SWE, a large effect is found for the peak streamflow sensitivities. This impact is particularly manifest for the response of annual peak streamflow to combined warming and increasing precipitation under the climate conditions of Montmorency. The biophysical conditions of Acadie, i.e. lower infiltration and storage capacities of the compacted agricultural soils, have been found to be favoring increasing peak streamflow in response to increasing mean water fluxes, as more precipitation occurs in the form of rainfall under this scenario. The same climate scenario, on the other hand, leads to a slight decline in the peak streamflow in Montmorency due to the higher infiltration and storage capacities of forested soils that buffer a portion of the increase in mean water flux.

## 2.4 Conclusions

The Montmorency and Acadie River catchments represent two end members of the contrasting landscapes which characterize the opposite shores of the St. Lawrence River: temperate, flat and agriculture dominated Acadie on the south shore and the rugged, boreal forested Montmorency with colder and more humid climate on the north shore. The results of this study are illustrative of the unique hydrological changes that could be observed in the future in southern Québec. The main implication of the results is that despite the apparent proximity of these two catchments (Figure 2.1a), their hydrological processes and responses to climate change differ substantially because of the different temperature regimes. The warming induced shift in winter precipitation from snow to rain and its impact on snow accumulation and river regime will have implications for the water management in both catchments, with faster and more drastic changes projected to occur in Acadie. The decline in snow cover duration under warming temperatures could extend the farming season, which in turn could benefit the agricultural production in the Acadie River Catchment (Aygün et al. 2020b). Soil erosion rates over the Acadie River Catchment could increase due to earlier snowmelt, increased rainfall ratios, and more frequent snowmelt events caused by higher winter and spring temperatures (Aygün et al. 2020b). On the other hand, managers may have to adopt new operation strategies for the dams and reservoirs located along the Montmorency River. Furthermore, changes in snow accumulation and snowmelt would alter the soil moisture and temperature which might cause significant impacts on forest growth and biochemical cycles in the forests of the Montmorency River Catchment (Houle et al. 2012). The results of this study regarding the vulnerability of the Montmorency River Catchment to first order climate change can also inform the water resources stakeholders of several other catchments in southern Québec, two third of which is covered by boreal forests.

The physically based nature of the model used, which includes a full set of representations of cold regions hydrological processes such as intercepted snow, sublimation, infiltration to frozen soils, enabled the diagnosis of interactions between processes and variables within the cold regions hydrological cycle, an advantage that could not be achieved with the previous hydrological model studies in southern Québec. For example, catchment-scale sublimation fluxes have not been estimated before in southern Québec (but see Aygün et al., 2020b). Our results show that under both reference and future climate conditions, sublimation from intercepted snow is the major sublimation component in the forested Montmorency River Catchment, whereas snowpack sublimation dominates the total sublimation in the agricultural Acadie River Catchment. When both catchments are forced with a cold baseline climate (Montmorency), the historical peak SWE is found to be lower in Montmorency than in Acadie, due to high canopy sublimation losses in forested Montmorency.

The climate sensitivity analysis used in this study allowed understanding how key hydrological processes could shift under a wide range of climate change scenarios in different biophysical conditions, providing useful guidance for further top-down, model-based climate impact assessments. The positive sensitivity zone encountered in the peak streamflow response surface (Figure 2.10a) of the Montmorency River Catchment suggests a possibility for increased flood risks in spring in the near future (2020–2070) given limited warming ( $<3\text{ }^{\circ}\text{C}$ ) and uncertainties in precipitation projections, while longer-term warming was found to deplete the snowpack and reduce peak streamflow. On the other hand, the previous study by Aygün et al. (2020b) reported that increasing precipitation could lead to higher peak spring streamflow in the Acadie River Catchment only when warming is below  $1.5\text{ }^{\circ}\text{C}$ , and that the peak streamflow occurs before peak SWE regardless of the precipitation increase when the warming is greater ( $>1.5\text{ }^{\circ}\text{C}$ ). This suggests that the transition in the hydrological regime of the Acadie River Catchment towards a more rainfall-dominated regime will occur sooner than that of the Montmorency River Catchment.

Biophysical conditions were also shown to play a significant role on the response of hydrological variables, particularly streamflow, to climate change, which has not been addressed in previous studies. When both catchments are forced by common climate conditions, the annual peak specific flow is higher in Acadie River Catchment, which shows that the reduced infiltration and storage capacity of agricultural soils favor runoff, despite the lower slopes compared to Montmorency. Our results show that peak discharge in catchments with a mild, Acadie-type winter climate could increase in response to a combination of +3 °C warming and 20% increasing precipitation due the large conversion of snowfall to rainfall and enhanced winter snowmelt, which together lead to higher surface runoff extremes in winter. The Acadie-type biophysiology, with limited infiltration and storage capacity, is more sensitive to this scenario than the Montmorency-type forested environment, whose increased storage and infiltration capacities attenuate extremes rainfall-snowmelt events. Conversely, under a colder/humid Montmorency-type climate and for the same climate change scenario, the streamflow remains largely synchronized with the snow cycle. The bulk of snowmelt continues to occur in the spring with more limited conversion of snowfall to rainfall, which attenuates extreme runoff events. However catchments respond differently to the increased water inputs: in the more impervious Acadie catchment, the amount of runoff (but not its intensity) increases and leads to higher peak discharge in the spring, while the porous soils of the Montmorency largely buffer the increased flux, resulting in decreased runoff amount and peak discharge. Hence, while the regional climatological characteristics were found to dominate the hydrological response of the catchments to climate change, biophysical conditions can modulate the response of peak discharge to a common climate change signal, especially when increasing precipitation are involved. The concept of “uniqueness of place” (Beven 2000), in which the unique combination of topography, soil, geology, vegetation and anthropogenic modifications give rise to catchment specific behaviour, thus also applies to the climate sensitivity of peak discharge in snow-fed catchments.

## Acknowledgments

We would like to thank Sylvain Jutras and Maxime Beaudoin-Galais from Laval University and Louis Duchesne from Québec Ministry of Forests, Wildlife and Parks (MFFP) for providing us hydrological and meteorological data for the BEREV and Lac Laflamme watersheds. Requests for hydrological and meteorological data should be made through BEREV watershed platform (at <http://www.cef-cfr.ca/index.php?n=Membres.SylvainJutrasBEREV?userlang=en>) and MFFP (at <https://mffp.gouv.qc.ca/>) for BEREV and Lac Laflamme watersheds, respectively. The historical climate data from Forêt Montmorency weather station is available at the website of Environment and Climate Change Canada (at <https://climate.weather.gc.ca/>). The daily river discharge data used in this study could be obtained from the database of Québec Center of Water Expertise (CEHQ) (at <https://www.cehq.gouv.qc.ca/>). LIDAR-based digital elevation model (DEM) and forest cover maps used in this study are available at the Forêt Ouverte web portal of MFFP (at <https://www.foretouverte.gouv.qc.ca/>). The climate change projections used in this study could be found at the Climate Portal of Ouranos (at <https://www.ouranos.ca/climate-portraits/#/>).

## Supporting Information

This supplementary document includes three figures, namely sensitivity of annual peak runoff to changing climate (Figure S2.1), sensitivity of annual mean water flux to changing climate (Figure S.2.2) and sensitivity of annual mean runoff to changing climate (Figure S2.3). These figures are used to help interpreting the Figure 2.14 in the article.

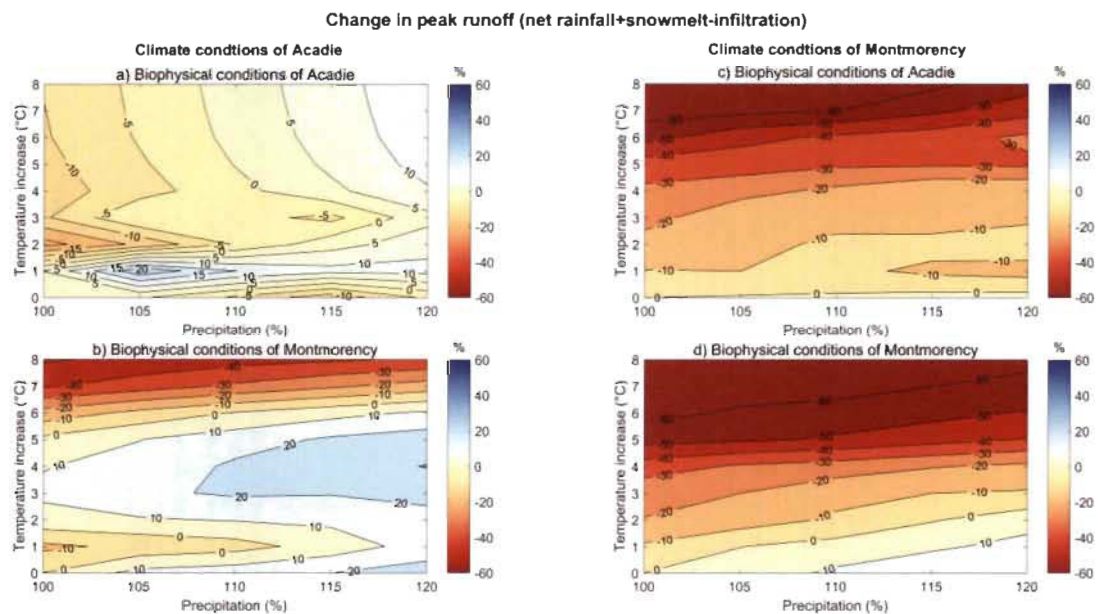


**Figure S2.1.** Sensitivity of annual peak runoff to changing climate in: **a)** biophysical conditions of Acadie under the climate conditions of Acadie, **b)** biophysical conditions of Montmorency under the climate conditions of Acadie, **c)** biophysical conditions of Acadie under the climate conditions of Montmorency, and **d)** biophysical conditions of Montmorency under the climate conditions of Montmorency.

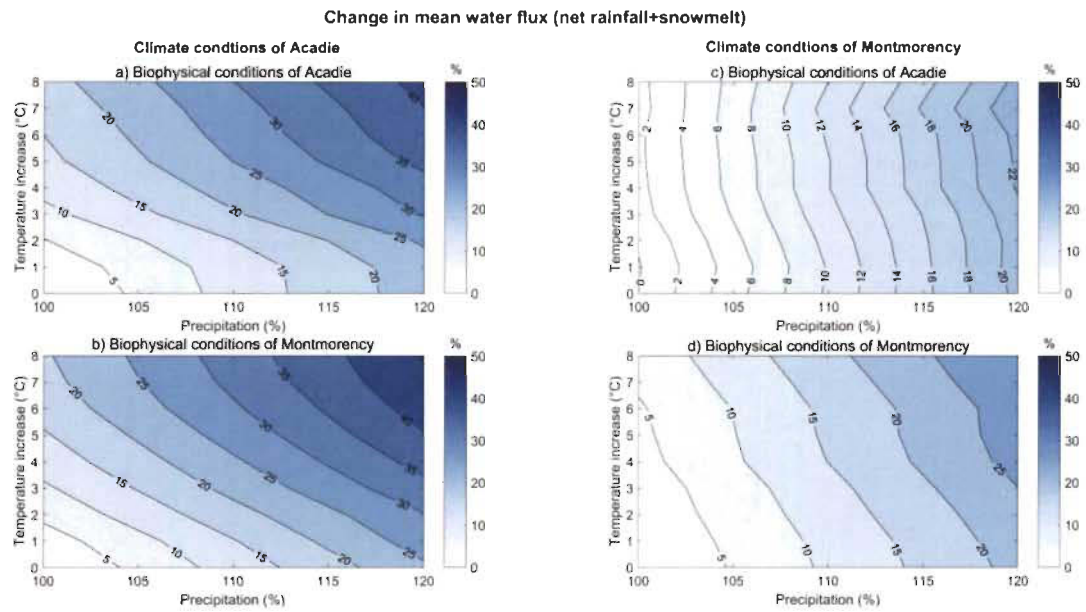


**Figure S.2.2.** Sensitivity of annual mean water flux to changing climate in: **a)** biophysical conditions of Acadie under the climate conditions of Acadie, **b)** biophysical conditions of Montmorency under the climate conditions of Acadie, **c)** biophysical conditions of Acadie under the climate conditions of Montmorency, and **d)** biophysical conditions of Montmorency under the climate conditions of Montmorency.

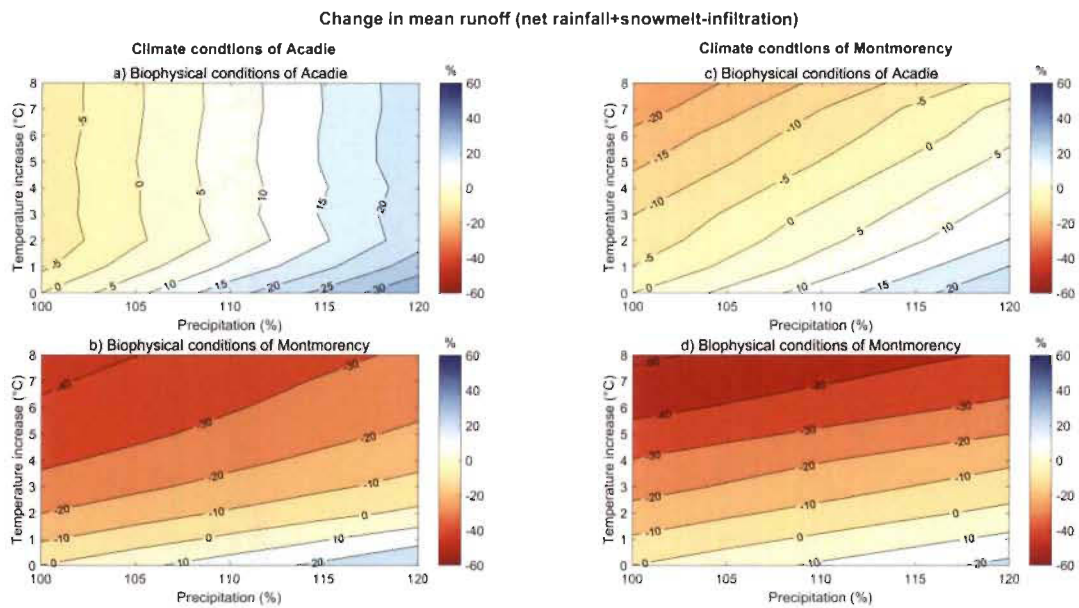


**Figure S2.3.** Sensitivity of annual mean runoff to changing climate in **a)** biophysical conditions of Acadie under the climate conditions of Acadie, **b)** biophysical conditions of Montmorency under the climate conditions of Acadie, **c)** biophysical conditions of Acadie under the climate conditions of Montmorency, and **d)** biophysical conditions of Montmorency under the climate conditions of Montmorency.

## References

- Alodah, A. and Seidou, O. (2019) Assessment of Climate Change Impacts on Extreme High and Low Flows: An Improved Bottom-Up Approach. *Water*, 11(6), 1236. <https://doi.org/10.3390/w11061236>
- Annandale, J., Jovanovic, N., Benade, N. and Allen, R. (2002) Software for missing data error analysis of Penman-Monteith reference evapotranspiration. *Irrigation Science*, 21(2), 57–67. <https://doi.org/10.1007/s002710100047>
- Armstrong, R. N., Pomeroy, J. W. and Martz, L. W. (2010) Estimating evaporation in a Prairie landscape under drought conditions. *Canadian Water Resources Journal*, 35(2), 173–186. <https://doi.org/10.4296/cwrj3502173>
- Ayers, H. D. (1959) Influence of soil profile and vegetation characteristics on net rainfall supply to runoff. Paper presented at the Proceedings of Hydrology Symposium
- Aygün, O., Kinnard, C. and Campeau, S. (2020a) Impacts of climate change on the hydrology of northern midlatitude cold regions. *Progress in Physical Geography: Earth and Environment*, 44(3), 338–375.
- Aygün, O., Kinnard, C., Campeau, S. and Krogh, S. A. (2020b) Shifting Hydrological Processes in a Canadian Agroforested Catchment due to a Warmer and Wetter Climate. *Water*, 12(3), 739. <https://doi.org/10.3390/w12030739>
- Barry, R., Plamondon, A. P. and Stein, J. (1988) Hydrologic soil properties and application of a soil moisture model in a balsam fir forest. *Canadian Journal of Forest Research*, 18(4), 427–434.
- Barry, R., Prévost, M., Stein, J. and Plamondon, A. P. (1990). Simulation of snowmelt runoff pathways on the Lac Laflamme watershed. *Journal of Hydrology*, 113(1–4), 103–121. [https://doi.org/10.1016/0022-1694\(90\)90169-X](https://doi.org/10.1016/0022-1694(90)90169-X)
- Bergeron, O. (2016). Guide d'utilisation 2016 – Grilles climatiques quotidiennes du Programme de surveillance du climat du Québec (1.2 ed.). Ministère du Développement Durable de l'Environnement et de la Lutte contre les Changements Climatiques du Québec.
- Beven, K. J. (2000) Uniqueness of place and process representations in hydrological modelling. *Hydrol. Earth Syst. Sci.*, 4(2), 203–213.

- Boyer, C., Chaumont, D., Chartier, I. and Roy, A. G. (2010) Impact of climate change on the hydrology of St. Lawrence tributaries. *Journal of Hydrology*, 384(1–2), 65–83. <https://doi.org/10.1016/j.jhydrol.2010.01.011>
- Brooks, R. and Corey, A. (1964) Hydraulic properties of porous media, hydrology papers, no. 3, colorado state university, ft. Hydrology papers (Colorado State University)(3), 37.
- Brooks, R. H. and Corey, A. T. (1966) Properties of porous media affecting fluid flow. *Journal of the Irrigation and Drainage Division*, 92(2), 61–90.
- Brown, A. E., Zhang, L., McMahon, T. A., Western, A. W. and Vertessy, R. A. (2005) A review of paired catchment studies for determining changes in water yield resulting from alterations in vegetation. *Journal of Hydrology*, 310(1–4), 28–61. <https://doi.org/10.1016/j.jhydrol.2004.12.010>
- Campbell, J. L., Ollinger, S. V., Flerchinger, G. N., Wicklein, H., Hayhoe, K. and Bailey, A. S. (2010) Past and projected future changes in snowpack and soil frost at the Hubbard Brook Experimental Forest, New Hampshire, USA. *Hydrological Processes*, 24(17), 2465–2480. <https://doi.org/10.1002/hyp.7666>
- Casola, J. H., Cuo, L., Livneh, B., Lettenmaier, D. P., Stoelinga, M. T., Mote, P. W. and Wallace, J. M. (2009) Assessing the impacts of global warming on snowpack in the Washington Cascades. *Journal of Climate*, 22(10), 2758–2772. <https://doi.org/10.1175/2008JCLI2612.1>
- Chandler, D. G. (2006) Reversibility of forest conversion impacts on water budgets in tropical karst terrain. *Forest Ecology and Management*, 224(1–2), 95–103. <https://doi.org/10.1016/j.foreco.2005.12.010>
- Chaumont, D. (2014) A guidebook on climate scenarios: Using climate information to guide adaptation research and decisions. Montreal, Canada: Ouranos.
- Chow, V. T. (1964) Handbook of applied hydrology: a compendium of water-resources technology (Vol. 1) New York, USA: McGraw-Hill Companies.
- Clark, C. (1945) Storage and the unit hydrograph. Paper presented at the Proceedings of the American Society of Civil Engineers.
- Clark, M. P., Hendrikx, J., Slater, A. G., Kavetski, D., Anderson, B., Cullen, N. J., et al. (2011) Representing spatial variability of snow water equivalent in hydrologic and land-surface models: A review. *Water Resources Research*, 47(7) <https://doi.org/10.1029/2011WR010745>

- D'Orangeville, L., Houle, D., Duchesne, L. and Côté, B. (2016) Can the Canadian drought code predict low soil moisture anomalies in the mineral soil? An analysis of 15 years of soil moisture data from three forest ecosystems in Eastern Canada. *Ecohydrology*, 9(2), 238–247.
- Dias, L. C. P., Macedo, M. N., Costa, M. H., Coe, M. T. and Neill, C. (2015) Effects of land cover change on evapotranspiration and streamflow of small catchments in the Upper Xingu River Basin, Central Brazil. *Journal of Hydrology: Regional Studies*, 4, 108–122. <https://doi.org/10.1016/j.ejrh.2015.05.010>
- Duchesne, L. and Houle, D. (2008) Impact of nutrient removal through harvesting on the sustainability of the boreal forest. *Ecological Applications*, 18(7), 1642–1651. <https://doi.org/10.1890/07-1035.1>
- Easton, Z. M., Gérard-Marchant, P., Walter, M. T., Petrovic, A. M. and Steenhuis, T. S. (2007) Hydrologic assessment of an urban variable source watershed in the northeast United States. *Water Resources Research*, 43(3).
- Ellis, C., Pomeroy, J., Brown, T. and MacDonald, J. (2010) Simulation of snow accumulation and melt in needleleaf forest environments. *Hydrol. Earth Syst. Sci.*, 14(6), 925–940. <https://doi.org/10.5194/hess-14-925-2010>
- Essery, R. and Pomeroy, J. (2001) Sublimation of snow intercepted by coniferous forest canopies in a climate model. Paper presented at the 6th IAHS Scientific Assembly Maastricht, Netherlands.
- Fang, X. and Pomeroy, J. (2009) Modelling blowing snow redistribution to prairie wetlands. *Hydrological Processes*, 23(18), 2557–2569.
- Fang, X., Pomeroy, J., Ellis, C., MacDonald, M., DeBeer, C. and Brown, T. (2013) Multi-variable evaluation of hydrological model predictions for a headwater basin in the Canadian Rocky Mountains. *Hydrol. Earth Syst. Sci.*, 17(4), 1635–1659. <https://doi.org/10.5194/hess-17-1635-2013>
- Fang, X. and Pomeroy, J. W. (2007) Snowmelt runoff sensitivity analysis to drought on the Canadian prairies. *Hydrological Processes*, 21(19), 2594–2609. <https://doi.org/10.1002/hyp.6796>
- Garnier, B. J. and Ohmura, A. (1970) The evaluation of surface variations in solar radiation income. *Solar energy*, 13(1), 21–34. [https://doi.org/10.1016/0038-092X\(70\)90004-6](https://doi.org/10.1016/0038-092X(70)90004-6)
- Gelfan, A., Pomeroy, J. and Kuchment, L. (2004) Modeling forest cover influences on snow accumulation, sublimation, and melt. *Journal of Hydrometeorology*, 5(5), 785–803.

- Gennaretti, F., Sangelantoni, L. and Grenier, P. (2015) Toward daily climate scenarios for Canadian Arctic coastal zones with more realistic temperature-precipitation interdependence. *Journal of Geophysical Research: Atmospheres*, 120(23), 11862–811877. <https://doi.org/10.1002/2015JD023890>
- Germer, S., Neill, C., Krusche, A. V. and Elsenbeer, H. (2010) Influence of land-use change on near-surface hydrological processes: undisturbed forest to pasture. *Journal of Hydrology*, 380(3–4), 473–480.
- Gottschalk, L., Jensen, J. L., Lundquist, D., Solantie, R. and Tollan, A. (1979) Hydrologic regions in the Nordic countries. *Hydrology Research*, 10(5), 273–286. <https://doi.org/10.2166/nh.1979.0010>
- Gray, D. and Landine, P. (1987) Albedo model for shallow prairie snow covers. *Canadian Journal of Earth Sciences*, 24(9), 1760–1768.
- Gray, D., Toth, B., Zhao, L., Pomeroy, J. and Granger, R. (2001) Estimating areal snowmelt infiltration into frozen soils. *Hydrological Processes*, 15(16), 3095–3111. <https://doi.org/10.1002/hyp.320>
- Groffman, P. M., Driscoll, C. T., Fahey, T. J., Hardy, J. P., Fitzhugh, R. D. and Tierney, G. L. (2001) Colder soils in a warmer world: a snow manipulation study in a northern hardwood forest ecosystem. *Biogeochemistry*, 56(2), 135–150. <https://doi.org/10.1023/A:1013039830323>
- Guay, C., Minville, M. and Braun, M. (2015) A global portrait of hydrological changes at the 2050 horizon for the province of Québec. *Canadian Water Resources Journal/Revue canadienne des ressources hydriques*, 40(3), 285–302. <https://doi.org/10.1080/07011784.2015.1043583>
- Guillemette, F., Plamondon, A. P., Prévost, M. and Lévesque, D. (2005) Rainfall generated stormflow response to clearcutting a boreal forest: peak flow comparison with 50 world-wide basin studies. *Journal of Hydrology*, 302(1–4), 137–153. <https://doi.org/10.1016/j.jhydrol.2004.06.043>
- Guo, X., Pomeroy, J. W., Fang, X., Lowe, S., Li, Z., Westbrook, C. and Minke, A. (2012) Effects of classification approaches on CRHM model performance. *Remote sensing letters*, 3(1), 39–47.
- Gupta, H. V., Kling, H., Yilmaz, K. K. and Martinez, G. F. (2009) Decomposition of the mean squared error and NSE performance criteria: Implications for improving hydrological modelling. *Journal of Hydrology*, 377(1–2), 80–91. <https://doi.org/10.1016/j.jhydrol.2009.08.003>

- Harder, P. and Pomeroy, J. (2013) Estimating precipitation phase using a psychrometric energy balance method. *Hydrological Processes*, 27(13), 1901–1914. <https://doi.org/10.1002/hyp.9799>
- Hedstrom, N. and Pomeroy, J. (1998) Measurements and modelling of snow interception in the boreal forest. *Hydrological Processes*, 12(10–11), 1611–1625.
- Houle, D., Bouffard, A., Duchesne, L., Logan, T. and Harvey, R. (2012) Projections of future soil temperature and water content for three southern Quebec forested sites. *Journal of Climate*, 25(21), 7690–7701. <https://doi.org/10.1175/JCLI-D-11-00440.1>
- Houle, D., Lajoie, G. and Duchesne, L. (2016) Major losses of nutrients following a severe drought in a boreal forest. *Nature plants*, 2(12), 1–5.
- Isabelle, P.-E. (2019) Analyse de l'évapotranspiration et du bilan d'énergie de surface d'une forêt boréale humide aux échelles locales et régionales. (PhD), Université Laval, Québec, Canada.
- Isabelle, P.-E., Nadeau, D. F., Asselin, M.-H., Harvey, R., Musselman, K. N., Rousseau, A. N. and Anctil, F. (2018) Solar radiation transmittance of a boreal balsam fir canopy: Spatiotemporal variability and impacts on growing season hydrology. *Agricultural and forest meteorology*, 263, 1–14.
- Jobin, B., Beaulieu, J., Grenier, M., Bélanger, L., Maisonneuve, C., Bordage, D. and Fillion, B. (2003) Landscape changes and ecological studies in agricultural regions, Québec, Canada. *Landscape Ecology*, 18(6), 575–590. <https://doi.org/10.1023/A:1026047625427>
- Jobin, B., Latendresse, C., Baril, A., Maisonneuve, C., Boutin, C. and Côté, D. (2014) A half-century analysis of landscape dynamics in southern Québec, Canada. *Environmental monitoring and assessment*, 186(4), 2215–2229. <https://doi.org/10.1007/s10661-013-3531-6>
- Jonas, T. and Essery, R. (2011) Snow Cover and Snowmelt in Forest Regions. In V. P. Singh, P. Singh and U. K. Haritashya (Eds.), *Encyclopedia of Snow, Ice and Glaciers* (pp. 1033–1036). Dordrecht: Springer Netherlands. doi:[https://doi.org/10.1007/978-90-481-2642-2\\_499](https://doi.org/10.1007/978-90-481-2642-2_499)
- Jones, H. and Pomeroy, J. (2001) Early spring snowmelt in a small boreal forest watershed: influence of concrete frost on the hydrology and chemical composition of streamwaters during rain-on-snow events. Paper presented at the 58th Eastern Snow Conference, Ottawa, Ontario, Canada.

- Jost, G., Weiler, M., Gluns, D. R. and Alila, Y. (2007) The influence of forest and topography on snow accumulation and melt at the watershed-scale. *Journal of Hydrology*, 347(1–2), 101–115. <https://doi.org/10.1016/j.jhydrol.2007.09.006>
- Jungqvist, G., Oni, S. K., Teutschbein, C. and Futter, M. N. (2014) Effect of climate change on soil temperature in Swedish boreal forests. *PloS one*, 9(4) <https://doi.org/10.1371/journal.pone.0093957>
- Jutras, M.-F. (2012) Modeling Stream Discharge in Forest Catchments across Canada: Hydraulic Conductivity Calibrations. (PhD), University of New Brunswick, New Brunswick, Canada.
- Knoben, W. J., Freer, J. E. and Woods, R. A. (2019) Inherent benchmark or not? Comparing Nash–Sutcliffe and Kling–Gupta efficiency scores. *Hydrol. Earth Syst. Sci.*, 23(10), 4323–4331. <https://doi.org/10.5194/hess-23-4323-2019>
- Knowles, N., Dettinger, M. D. and Cayan, D. R. (2006) Trends in snowfall versus rainfall in the western United States. *Journal of Climate*, 19(18), 4545–4559. <https://doi.org/10.1175/JCLI3850.1>
- Koivusalo, H. and Kokkonen, T. (2002) Snow processes in a forest clearing and in a coniferous forest. *Journal of Hydrology*, 262(1–4), 145–164.
- Krogh, S. A. and Pomeroy, J. W. (2019) Impact of Future Climate and Vegetation on the Hydrology of an Arctic Headwater Basin at the Tundra–Taiga Transition. *Journal of Hydrometeorology*, 20(2), 197–215. <https://doi.org/10.1175/JHM-D-18-0187.1>
- Krogh, S. A., Pomeroy, J. W. and Marsh, P. (2017) Diagnosis of the hydrology of a small Arctic basin at the tundra-taiga transition using a physically based hydrological model. *Journal of Hydrology*, 550, 685–703.
- Krogh, S. A., Pomeroy, J. W. and McPhee, J. (2015) Physically based mountain hydrological modeling using reanalysis data in Patagonia. *Journal of Hydrometeorology*, 16(1), 172–193. <https://doi.org/10.1175/JHM-D-13-0178.1>
- Laforce, S., Simard, M. C., Leconte, R. and Brissette, F. (2011) Climate Change and Floodplain Delineation in Two Southern Quebec River Basins 1. *JAWRA Journal of the American Water Resources Association*, 47(4), 785–799. <https://doi.org/10.1111/j.1752-1688.2011.00560.x>
- Lavigne, M.-P. (2007) Modélisation du régime hydrologique et de l'impact des coupes forestières sur l'écoulement du ruisseau des Eaux-Volées à l'aide d'Hydrotel. (MSc), Université du Québec, Institut national de la recherche scientifique, Québec City, Québec, Canada.

- Li, L. and Pomeroy, J. W. (1997) Estimates of threshold wind speeds for snow transport using meteorological data. *Journal of Applied Meteorology*, 36(3), 205–213.
- López-Moreno, J., Boike, J., Sanchez-Lorenzo, A. and Pomeroy, J. (2016) Impact of climate warming on snow processes in Ny-Ålesund, a polar maritime site at Svalbard. *Global and planetary change*, 146, 10–21.
- López-Moreno, J. I., Gascoin, S., Herrero, J., Sproles, E., Pons, M., Alonso-González, E., et al. (2017) Different sensitivities of snowpacks to warming in Mediterranean climate mountain areas. *Environmental Research Letters*, 12(7), 074006. <https://doi.org/10.1088/1748-9326/aa70cb>
- López-Moreno, J. I., Revuelto, J., Gilaberte, M., Morán-Tejeda, E., Pons, M., Jover, E., et al. (2014) The effect of slope aspect on the response of snowpack to climate warming in the Pyrenees. *Theoretical and applied climatology*, 117(1–2), 207–219. <https://doi.org/10.1007/s00704-013-0991-0>
- López-Moreno, J., Pomeroy, J., Revuelto, J. and Vicente-Serrano, S. (2013) Response of snow processes to climate change: spatial variability in a small basin in the Spanish Pyrenees. *Hydrological Processes*, 27(18), 2637–2650. <https://doi.org/10.1002/hyp.9408>
- Mankin, J. S., Viviroli, D., Singh, D., Hoekstra, A. Y. and Diffenbaugh, N. S. (2015) The potential for snow to supply human water demand in the present and future. *Environmental Research Letters*, 10(11), 114016.
- Mareuil, A., Leconte, R., Brissette, F. and Minville, M. (2007) Impacts of climate change on the frequency and severity of floods in the Châteauguay River basin, Canada. *Canadian journal of civil engineering*, 34(9), 1048–1060. <https://doi.org/10.1139/107-022>
- Marks, D., Kimball, J., Tingey, D. and Link, T. (1998) The sensitivity of snowmelt processes to climate conditions and forest cover during rain-on-snow: A case study of the 1996 Pacific Northwest flood. *Hydrological Processes*, 12(10–11), 1569–1587.
- Minville, M., Brissette, F. and Leconte, R. (2008) Uncertainty of the impact of climate change on the hydrology of a nordic watershed. *Journal of Hydrology*, 358(1–2), 70–83. <https://doi.org/10.1016/j.jhydrol.2008.05.033>
- Moeser, D., Stähli, M. and Jonas, T. (2015) Improved snow interception modeling using canopy parameters derived from airborne LiDAR data. *Water Resources Research*, 51(7), 5041–5059. <https://doi.org/10.1002/2014WR016724>

- Monteith, J. (1981) Evaporation and surface temperature. *Quarterly Journal of the Royal Meteorological Society*, 107(451), 1–27.
- Muma, M., Assani, A. A., Landry, R., Quessy, J.-F. and Mesfioui, M. (2011) Effects of the change from forest to agriculture land use on the spatial variability of summer extreme daily flow characteristics in southern Quebec (Canada). *Journal of Hydrology*, 407(1–4), 153–163.
- Musselman, K., Molotch, N. P. and Brooks, P. D. (2008) Effects of vegetation on snow accumulation and ablation in a mid-latitude sub-alpine forest. *Hydrological Processes*, 22(15), 2767–2776. <https://doi.org/10.1002/hyp.7050>
- Musselman, K. N., Clark, M. P., Liu, C., Ikeda, K. and Rasmussen, R. (2017) Slower snowmelt in a warmer world. *Nature Climate Change*, 7(3), 214–219. <https://doi.org/10.1038/nclimate3225>
- Nash, J. E. and Sutcliffe, J. V. (1970) River flow forecasting through conceptual models part I—A discussion of principles. *Journal of Hydrology*, 10(3), 282–290. [https://doi.org/10.1016/0022-1694\(70\)90255-6](https://doi.org/10.1016/0022-1694(70)90255-6)
- Ouimet, R. and Duchesne, L. (2005) Base cation mineral weathering and total release rates from soils in three calibrated forest watersheds on the Canadian Boreal Shield. *Canadian Journal of Soil Science*, 85(2), 245–260. <https://doi.org/10.4141/S04-061>
- Ouranos. (2015) *Vers l'adaptation. Synthèse des connaissances sur les changements climatiques au Québec—Partie 1: Évolution climatique au Québec*, Ouranos, Montréal, Québec.
- Peel, M. C., Finlayson, B. L. and McMahon, T. A. (2007) Updated world map of the Köppen-Geiger climate classification. *Hydrol. Earth Syst. Sci*, 11, 1633–1644. <https://doi.org/10.5194/hess-11-1633-2007>
- Pierre, A., Jutras, S., Smith, C., Kochendorfer, J., Fortin, V. and Anctil, F. (2019) Evaluation of Catch Efficiency Transfer Functions for Unshielded and Single-Alter-Shielded Solid Precipitation Measurements. *Journal of Atmospheric and Oceanic Technology*, 36(5), 865–881. <https://doi.org/10.1175/JTECH-D-18-0112.1>
- Plamondon, A. and Ouellet, D. (1980) Partial clearcutting and streamflow regime of ruisseau des Eaux-Volées experimental basin. Paper presented at the The influence of man on the hydrological regime with special reference to representative and experimental basins, Helsinki, Finland. Edited by IAHS. *Proceedings of the Helsinki Symposium*.

- Plamondon, A., Prévost, M. and C Naud, R. (1984) Accumulation et fonte de la neige en milieux boisé et déboisé. *Géographie physique et Quaternaire*, 38(1), 27–35.
- Pomeroy, J., Fang, X. and Ellis, C. (2012) Sensitivity of snowmelt hydrology in Marmot Creek, Alberta, to forest cover disturbance. *Hydrological Processes*, 26(12), 1891–1904. <https://doi.org/10.1002/hyp.9248>
- Pomeroy, J. and Gray, D. (1995) Snowcover accumulation, relocation and management. *Bulletin of the International Society of Soil Science*, 88(2).
- Pomeroy, J., Gray, D., Brown, T., Hedstrom, N., Quinton, W., Granger, R. and Carey, S. (2007) The cold regions hydrological model: a platform for basing process representation and model structure on physical evidence. *Hydrological Processes*, 21(19), 2650–2667. <https://doi.org/10.1002/hyp.6787>
- Pomeroy, J., Gray, D., Hedstrom, N. and Janowicz, J. (2002) Prediction of seasonal snow accumulation in cold climate forests. *Hydrological Processes*, 16(18), 3543–3558. <https://doi.org/10.1002/hyp.1228>
- Pomeroy, J. and Li, L. (2000) Prairie and arctic areal snow cover mass balance using a blowing snow model. *Journal of Geophysical Research: Atmospheres*, 105(D21), 26619–26634. <https://doi.org/10.1029/2000JD900149>
- Pomeroy, J., Parviainen, J., Hedstrom, N. and Gray, D. (1998) Coupled modelling of forest snow interception and sublimation. *Hydrological Processes*, 12(15), 2317–2337.
- Pomeroy, J. W., Fang, X. and Marks, D. G. (2016) The cold rain-on-snow event of June 2013 in the Canadian Rockies—Characteristics and diagnosis. *Hydrological Processes*, 30(17), 2899–2914. <https://doi.org/10.1002/hyp.10905>
- Prévost, M., Barry, R., Stein, J. and Plamondon, A. P. (1991) Snowmelt modeling in a balsam fir forest: comparison between an energy balance model and other simplified models. *Canadian Journal of Forest Research*, 21(1), 1–10.
- Priestley, C. H. B. and Taylor, R. (1972) On the assessment of surface heat flux and evaporation using large-scale parameters. *Monthly weather review*, 100(2), 81–92.
- Quilbé, R., Rousseau, A. N., Moquet, J.-S., Trinh, N. B., Dibike, Y., Gachon, P. and Chaumont, D. (2008) Assessing the effect of climate change on river flow using general circulation models and hydrological modelling—Application to the Chaudière River, Quebec, Canada. *Canadian Water Resources Journal*, 33(1), 73–94. <https://doi.org/10.4296/cwrj3301073>

- Rasouli, K., Pomeroy, J. W., Janowicz, J. R., Carey, S. K. and Williams, T. J. (2014) Hydrological sensitivity of a northern mountain basin to climate change. *Hydrological Processes*, 28(14), 4191-4208. <https://doi.org/10.1002/hyp.10244>
- Rasouli, K., Pomeroy, J. W. and Marks, D. G. (2015) Snowpack sensitivity to perturbed climate in a cool mid-latitude mountain catchment. *Hydrological Processes*, 29(18), 3925–3940. <https://doi.org/10.1002/hyp.10587>
- Rasouli, K., Pomeroy, J. W. and Whitfield, P. H. (2019) Hydrological Responses of Headwater Basins to Monthly Perturbed Climate in the North American Cordillera. *Journal of Hydrometeorology*, 20(5), 863–882. <https://doi.org/10.1175/JHM-D-18-0166.1>
- Riboust, P. and Brissette, F. (2015) Climate change impacts and uncertainties on spring flooding of Lake Champlain and the Richelieu River. *JAWRA Journal of the American Water Resources Association*, 51(3), 776–793.
- Roberge, J. and Plamondon, A. P. (1987) Snowmelt runoff pathways in a boreal forest hillslope, the role of pipe throughflow. *Journal of Hydrology*, 95(1–2), 39–54. [https://doi.org/10.1016/0022-1694\(87\)90114-4](https://doi.org/10.1016/0022-1694(87)90114-4)
- Robinet, J., Minella, J. P., de Barros, C. A., Schlesner, A., Lücke, A., Ameijeiras-Mariño, Y., et al. (2018) Impacts of forest conversion and agriculture practices on water pathways in Southern Brazil. *Hydrological Processes*, 32(15), 2304–2317. <https://doi.org/10.1002/hyp.13155>
- Roth, T. R. and Nolin, A. W. (2017) Forest impacts on snow accumulation and ablation across an elevation gradient in a temperate montane environment. *Hydrol. Earth Syst. Sci.*, 21(11). <https://doi.org/10.5194/hess-21-5427-2017>
- Rousseau, A. N., Savary, S. and Konan, B. (2008) Implantation du modèle HYDROTEL sur le bassin de la rivière Montmorency afin de simuler les débits observés et de produire des scénarios de crues du printemps pour l'année 2008. Quebec City, Quebec, Canada: Centre Eau Terre et Environnement, Institut national de la recherche scientifique (INRS-ETE).
- Savary, S., Rousseau, A. N. and Quilbé, R. (2009) Assessing the effects of historical land cover changes on runoff and low flows using remote sensing and hydrological modeling. *Journal of Hydrologic Engineering*, 14(6), 575–587. [https://doi.org/10.1061/\(ASCE\)HE.1943-5584.0000024](https://doi.org/10.1061/(ASCE)HE.1943-5584.0000024)
- Sicart, J.-E., Pomeroy, J., Essery, R. and Bewley, D. (2006) Incoming longwave radiation to melting snow: observations, sensitivity and estimation in northern environments. *Hydrological Processes*, 20(17), 3697–3708.

- Storck, P., Lettenmaier, D. P. and Bolton, S. M. (2002) Measurement of snow interception and canopy effects on snow accumulation and melt in a mountainous maritime climate, Oregon, United States. *Water Resources Research*, 38(11), 5-1-5-16. <https://doi.org/10.1029/2002WR001281>
- Talbot, J., Plamondon, A., Levesque, D., Aube, D., Prevos, M., Chazalmartin, F. and Gnocchini, M. (2006) Relating snow dynamics and balsam fir stand characteristics, Montmorency Forest, Quebec. *Hydrological Processes*, 20(5), 1187–1199. <https://doi.org/10.1002/hyp.5938>
- Templer, P. H., Reinmann, A. B., Sanders-DeMott, R., Sorensen, P. O., Juice, S. M., Bowles, F., et al. (2017) Climate Change Across Seasons Experiment (CCASE): A new method for simulating future climate in seasonally snow-covered ecosystems. *PloS one*, 12(2).
- Tremblay, Y., Rousseau, A. N., Plamondon, A. P., Lévesque, D. and Jutras, S. (2008) Rainfall peak flow response to clearcutting 50% of three small watersheds in a boreal forest, Montmorency Forest, Québec. *Journal of Hydrology*, 352(1–2), 67–76. <https://doi.org/10.1016/j.jhydrol.2007.12.028>
- Tremblay, Y., Rousseau, A. N., Plamondon, A. P., Lévesque, D. and Prévost, M. (2009) Changes in stream water quality due to logging of the boreal forest in the Montmorency Forest, Québec. *Hydrological Processes*, 23(5), 764–776. <https://doi.org/10.1002/hyp.7175>
- Trujillo, E. and Molotch, N. P. (2014) Snowpack regimes of the western United States. *Water Resources Research*, 50(7), 5611–5623.
- Varhola, A., Coops, N. C., Weiler, M. and Moore, R. D. (2010) Forest canopy effects on snow accumulation and ablation: An integrative review of empirical results. *Journal of Hydrology*, 392(3–4), 219–233.
- Veatch, W., Brooks, P., Gustafson, J. and Molotch, N. (2009) Quantifying the effects of forest canopy cover on net snow accumulation at a continental, mid-latitude site. *Ecohydrology: Ecosystems, Land and Water Process Interactions, Ecohydrogeomorphology*, 2(2), 115–128. <https://doi.org/10.1002/eco.45>
- Weber, M., Bernhardt, M., Pomeroy, J., Fang, X., Härer, S. and Schulz, K. (2016) Description of current and future snow processes in a small basin in the Bavarian Alps. *Environmental Earth Sciences*, 75(17), 1223. <https://doi.org/10.1007/s12665-016-6027-1>

- Winkler, R., Spittlehouse, D. and Golding, D. (2005) Measured differences in snow accumulation and melt among clearcut, juvenile, and mature forests in southern British Columbia. *Hydrological Processes*, 19(1), 51–62.
- Zhang, Y., Wang, S., Barr, A. G. and Black, T. (2008) Impact of snow cover on soil temperature and its simulation in a boreal aspen forest. *Cold Regions Science and Technology*, 52(3), 355–370.
- Zhou, J., Pomeroy, J. W., Zhang, W., Cheng, G., Wang, G. and Chen, C. (2014) Simulating cold regions hydrological processes using a modular model in the west of China. *Journal of Hydrology*, 509, 13–24.
- Ziegler, A. D., Giambelluca, T. W., Tran, L. T., Vana, T. T., Nullet, M. A., Fox, J., et al. (2004) Hydrological consequences of landscape fragmentation in mountainous northern Vietnam: evidence of accelerated overland flow generation. *Journal of Hydrology*, 287(1–4), 124–146.

## CHAPTER III

### RESPONSES OF SOIL EROSION TO WARMING AND WETTING IN A COLD CANADIAN AGRICULTURAL CATCHMENT

Okan Aygün<sup>1</sup>, Christophe Kinnard<sup>2</sup> and Stéphane Campeau<sup>3</sup>

<sup>1</sup> University of Québec at Trois-Rivières, Québec, Canada; Centre for Northern Studies (CEN), Québec City, Québec, Canada; Research Centre for Watershed-Aquatic Ecosystem Interactions (RIVE), University of Québec at Trois-Rivières, Canada.

<sup>2</sup> University of Québec at Trois-Rivières, Québec, Canada; Centre for Northern Studies (CEN), Québec City, Québec, Canada; Research Centre for Watershed-Aquatic Ecosystem Interactions (RIVE), University of Québec at Trois-Rivières, Canada.

<sup>3</sup> University of Québec at Trois-Rivières, Québec, Canada; Research Centre for Watershed-Aquatic Ecosystem Interactions (RIVE), University of Québec at Trois-Rivières, Canada.

Corresponding author: Okan Aygün ([okan.aygun@uqtr.ca](mailto:okan.aygun@uqtr.ca))

This article is currently under review in *CATENA*.

## Highlights

- Tile drain contribution to the sediment yield is seasonally variable
- Tile drains account for 39% of the total annual sediment yield
- The highest soil losses occur during winter in a warmer and wetter climate
- Annual sediment could decline or increase, depending on the precipitation projections

## Abstract

This study explores the potential impacts of climate change on soil erosion in an agricultural catchment in eastern Canada. The Modified Universal Soil Loss Equation (MUSLE) was used to calculate the sediment yields from the Acadie River Catchment for the historical 1996–2019 period. The runoff variables of the MUSLE were obtained from a physically based hydrological model previously built and validated for the catchment. Then, the hydrological model was perturbed using climate change projections and used to assess the climate sensitivity of the sediment yield. Two runoff scenarios representing possible pathways of sediment export were considered. While scenario a represents a baseline scenario in which soil erosion occurs due to surface runoff only, scenario b is more realistic since it assumed that tile drains also contribute to sediment export, but with a varying efficiency throughout the year. The calibration and validation of the tile efficiency factors against measurements in 2009–2015 for scenario b suggest that tile drains export the sediments with an efficiency of 20% and 50% in freezing and non-freezing conditions, respectively. Results indicate that tile drains account for 39% of the total annual sediment yield in the present climate. The timing of highest soil erosion shifts from spring to winter in response to warming and wetting, which can be explained by increasing winter runoff

caused by shifting snowmelt timing towards winter, a greater number of mid-winter melt events as well as increasing rainfall fractions. The large uncertainties in precipitation projections cascade down to the erosion uncertainties in the more realistic scenario b, with annual sediment yield increasing or decreasing according to the precipitation uncertainty in a given climate change scenario. This study demonstrates the benefit of conservation and no-till practices, which could reduce the annual sediment yields by 20% and 60%, respectively, under any given climate change scenario.

**Keywords**

Soil erosion; sediment yield; climate change; agricultural catchment; surface runoff; subsurface tile drainage

### 3.1 Introduction

Soil erosion is a major threat to agricultural productivity as it causes losses of nutrient rich topsoil, therefore reducing soil fertility and crop yield (Sartori et al., 2019). Each year about 10 million ha of cropland worldwide have been reported to be abandoned because of lack of productivity caused by soil erosion, resulting in declines in food production (Pimentel, 2006). Furthermore, sediments and attached pollutants such as nutrients, pesticides and toxic metals eroded from fertilized agricultural lands are also transported to lakes and rivers, which in turn lead to deterioration of water quality and disturbance of delicate aquatic systems (Issaka and Ashraf, 2017; Zhang et al., 2009). The eutrophication caused by nutrient enrichment has been particularly associated with the formation of harmful algal substances that kill fish and cause diseases in animals and humans (Heisler et al., 2008; Schoumans et al., 2014).

Soil erosion dynamics reflect a complex interaction of soil type, agricultural practices and climate. Regarding the soil texture, fine sand and silt soil particles have been reported to be most susceptible to detachment and transport (Wischmeier and Mannering, 1969). Also, the lower weight of soil particles with a high amount of light organic matter increases the probability of transport compared with soil particles with a higher portion of heavy mineral particles (Kuhn, 2007). Intensive tillage practices have been reported to cause a significant loss of soil, whereas conservation tillage, i.e. any form of reduced tillage that intends to reduce soil disturbance during seedbed preparation has been shown to be an effective tool to decrease soil erosion (Montgomery, 2007). Multiple studies argue that a reduction in tillage results in a decline in surface runoff as it improves water infiltration in soils, which in turn decreases soil erosion (Huggins and Reganold, 2008; Klik and Rosner, 2020; Williams et al., 2009). Reduced tillage has been shown to decrease average annual sediment yields by 20 to 50% in corn and soybean fields in the Mississippi River Basin (Parajuli et al., 2016). Garbrecht et al. (2015) have reported that a switch from conventional to

conservation tillage would be sufficient to offset the average increase in soil erosion projected under future climates for croplands in the Southern Great Plains of the US. Meanwhile, a global literature on tillage impact on soil erosion by water (Mhazo et al., 2016) has indicated that reduced tillage has greater potential to reduce runoff and soil losses in cooler temperate regions where the soils are moderately weathered and have a weaker structure compared to the heavily weathered and well aggregated soils in tropical regions.

In cold regions, while a significant fraction of annual runoff occurs in spring as a result of melting snow and ice (Su et al., 2011), seasonally frozen soils also influence the partition ratios between surface and subsurface flows (Aygün et al., 2020a). Soil freezing has also been reported to modify the erodibility of the soil (Ollesch et al., 2005). Ice layers developed at different depths in the soil during winter conditions can push soil particles apart and decrease the soil density, declining the stability of soil upon thawing (Gatto, 2000). During the snowmelt period, the soil surface thaws first and infiltration into the upper thawed layer results in a weakened density and saturated surface which is highly unstable (Wall et al., 2002). Ollesch et al. (2006) reported that the total modelled soil erosion for snowmelt events with unfrozen soil and low amount of surface runoff were 40 times smaller than those with a partly frozen soil in a German agricultural catchment. Some other studies also have argued that soil sediments and associated nutrients transferred from agricultural fields to water bodies by snowmelt represent the major parts of the annual exports. Vliet and Hall (1991) found that 80% of the total annual soil loss is generated during the snowmelt period in the Peace River watershed in western Canada. In the Pike River watershed in Québec, more than 90% of the annual sediment and total phosphorous yield occurred during snowmelt (Jamieson et al., 2003).

Surface runoff was traditionally considered to be the major pathway for sediment and nutrient transport because of its ability to erode, whereas sediment transfer via

subsurface runoff was assumed to be small or negligible (Eastman et al., 2010; Van Esbroeck et al., 2016). Meanwhile, some studies have shown that subsurface drainage systems could also be an important pathway for sediment export. However, the proportion of the total sediment and associated nutrients carried by subsurface tile drains was found to vary amongst regions and within neighbouring catchments. For instance, Van Esbroeck et al. (2016) found that tile drains export 40% to 77% of the annual total phosphorus load and 19% to 67% of annual total dissolved phosphorous load across three agricultural fields in Ontario. The sediment budget established for two lowland agricultural catchments in the UK showed that subsurface tile drains accounted for 30% to 60% of the sediment output (Walling et al., 2002).

The review study performed by Li and Fang (2016) on the impacts of climate change on soil erosion has shown that the response of soil erosion rates to climate change is highly variable. Notwithstanding, changes in rainfall have been reported to be the major factor influencing soil erosion rates over the world, and increased rainfall amount is likely to cause higher runoff and soil erosion when other factors remain unchanged. However, the response of soil erosion to climate change in cold regions, where snowmelt is a major component of runoff, have been little explored. A warmer and wetter climate projected over the cold regions of the northern midlatitudes (Pachauri et al., 2014) is projected to shift snowmelt floods towards earlier dates and increase streamflow during winter (Aygün et al., 2020a). A few studies have shown that these climatic and hydrological changes in cold regions would induce greater winter soil erosion and nutrient losses by the end of the century. Mukundan et al. (2013) projected an increase in soil erosion and sediment yield in winter and early spring in a New York State watershed. In the Pike River watershed of Québec, sediment and nutrient loading in winter could increase three to four times over current levels in response to increasing air temperatures (Gombault et al., 2015).

In southern Québec, agriculture dominates the landscape of the St Lawrence Lowlands leaving less than 25% of the residual forest cover in most of southwestern Québec (Bélanger et al., 2002; Jobin et al., 2014). The low vegetation cover on cultivated lands, frequent soil compaction and poorly vegetated riverbanks all make agricultural landscape highly susceptible to erosion. Also, the presence of organic soils, formed by the accumulation of plant and animal residues after the retreat of the postglacial Champlain Sea (Millette et al., 1982), makes the agricultural fields even more susceptible to erosion. For instance, on average 2 cm of thickness of organic soil has been reported to be lost every year due to erosion in the Montérégie region in southern Québec (Prévost, 2006). The average depth of organic soil in agriculture fields in this region has been reported to be about 120 cm (Prévost, 2006), meaning that current erosion rate could eliminate the organic soil within 60 years. Although there is a number of soil erosion and sediment loss studies in southern Québec, they were all conducted in the same catchment, i.e. the Pike River watershed (Eastman et al., 2010; Gollamudi et al., 2007; Gombault et al., 2015; Jamieson et al., 2003; Mehdi et al., 2015; Michaud et al., 2007). Therefore, this study has undertaken to further improve the knowledge about soil erosion rates from agriculture intensive catchments in southern Québec such as the Acadie River Catchment. This river is known to suffer from water quality issues because of the fine sediments transported from the agricultural fields (Clubs-conseils en agroenvironnement, 2014; Simoneau and Thibault, 2009), deteriorating not only the natural environments of the Acadie River itself, but also that of its confluence, the Richelieu River, where several municipalities draw their drinking water (Tremblay and Gareau, 2020). Climate change could induce considerable changes to the amount and seasonality of the sediment yield from the catchment considering that the hydrology of the Acadie River Catchment has been shown to be very sensitive to climate change (Aygün et al., 2020b).

The main purpose of this study is to explore the impacts of the changes in temperature and precipitation on the amount of sediment yields from the agricultural fields in the

Acadie River Catchment (45° 11' N, 73° 26' W). The sediment yields from the Acadie River Catchment for the historical 1996–2019 period were first calculated using the Modified Universal Soil Equation (MUSLE). The runoff variables of the MUSLE equation were obtained from a physically based hydrological model previously built and validated for the Acadie River Catchment (Aygün et al., 2020b). Then, the hydrological model was perturbed using climate change projections and used to assess the climate sensitivity of the sediment yield. The impacts that different agriculture management practices have on sediment yield under changing climate were further investigated. The climate sensitivity analysis framework used in this study provides a useful assessment of potential changes in sediment yield under a wide range of climate change scenarios.

### **3.2 Materials and Methods**

The Acadie River is one of the main tributaries of the Richelieu River that flows northwards through the southwestern region of Montérégie in the Canadian province of Québec. The Acadie River starts near the Canada-United States border and drains into the Richelieu River near the town of Carignan after flowing 82 km. The drainage area of the Acadie River Catchment is 364 km<sup>2</sup>; however, this study excludes a small (1%) part of the catchment located in the US due to the lack of data. The elevation varies between 40 and 110 m a.s.l. with gentle slopes (<2°). More than 70% of the catchment is occupied by agricultural fields with scattered forest patches, which is representative of the intensive farming landscape of the southern St. Lawrence lowlands (Jobin et al., 2014). The catchment includes 7490 agricultural fields, where the main crop types are corn (37%) and soybeans (33%) followed by vegetables (24%), hay (3%), and cereal grains (3%) including wheat, barley and oat (Figure 3.1).

Daily river discharge is measured at the l'Acadie discharge gauge (Figure 3.1) by the Center of Water Expertise (CEHQ), while the Québec Ministry of Sustainable

Development, Environment, and Fight against Climate Change (MELCC) measures the main water quality parameters including suspended sediment concentration (SSC) at the l'Acadie water quality station which is located about 4 km downstream from the discharge gauge (Figure 3.1). The water quality sampling has been carried out at a monthly frequency between 2009 and 2015.

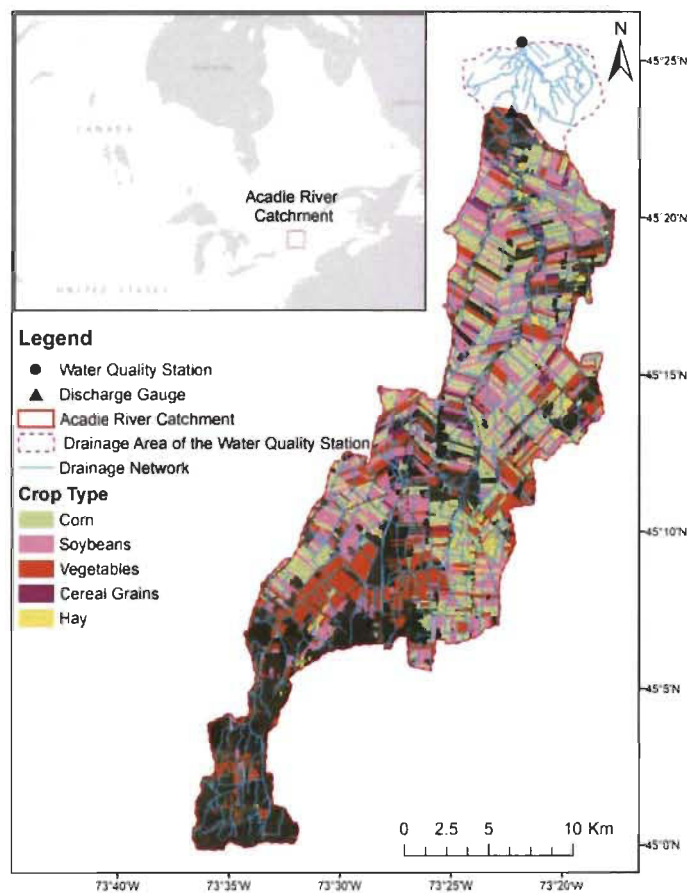


**Figure 3.1.** Acadie River Catchment drainage area, crop type, the location of the discharge gauge and water quality station, and the drainage area of the water quality station.

In this study, the Flux32 software (Walker, 1996) was used to estimate the actual sediment yields from daily streamflow measurements and discrete measurements of SSC over the 2009–2015 period. The monthly, seasonal and annual loads of sediments

were calculated using the log-log regression method that has been previously applied by Quilbé et al. (2006) to calculate the yearly sediment and nutrient loads in the Beaurivage River in Québec. The sediment loads were then divided by the total area of the agricultural fields included in the drainage area of the water quality station (Figure 3.1) in order to calculate the average specific sediment yield.

The universal soil equation (USLE) (Wischmeier and Smith, 1965; Wischmeier and Smith, 1978) has been reported to be the most widely accepted and utilized soil loss equation in the world (Kinnell, 2010). USLE estimates the long term annual average soil loss for a given combination of rainfall pattern, soil type, topography, crop system and management practices. While the USLE was originally developed at the plot scale to predict soil losses from agricultural fields in the USA (Wischmeier and Smith, 1978), it has been extended to use at different scales in numerous countries. The revised USLE (RUSLE) (Renard, 1997) was later developed to provide several improvements in determining the USLE factors whereby the formula remained the same. Interesting reads on global applications of USLE and RUSLE can be found in the review studies performed by Kinnell (2010) and Benavidez et al. (2018). A modified version of USLE (MUSLE) proposed by Williams (1975) differs from both USLE and RUSLE in that it uses the runoff hydrograph rather than the rainfall energy to estimate sediment yield. Using the runoff characteristics instead of rainfall patterns, the MUSLE offers the potential to account for the eroding power of snowmelt runoff (McConkey et al., 1997), which is especially important in cold regions such as Québec. The MUSLE estimates the sediment yield rates as a product of the transport efficiency of runoff and soil loss rates (Jackson et al., 1986). While the soil loss rates are calculated by soil erosion factors, the transport efficiency of runoff is indexed by the product of total runoff volume and peak runoff rate (Equation 3.1).

$$Y = a * (Q * qp)^b * K * LS * C * P \quad \text{Equation 3.1}$$

where  $Y$  is the sediment yield (t),  $Q$  is the total runoff volume ( $\text{m}^3$ ),  $q_p$  is the peak flow rate ( $\text{m}^3 \text{ s}^{-1}$ ),  $K$  is the soil erodibility factor ( $\text{t ha h ha}^{-1} \text{ MJ}^{-1} \text{ mm}^{-1}$ ),  $LS$  is the slope factor (dimensionless),  $C$  is the crop management factor (dimensionless), and  $P$  is the soil conservation practice factor (dimensionless). As the MUSLE is an empirical model, there is an inconsistency between the dimensions on both sides of equation 3.1. The disagreement of the MUSLE equation with the principles of dimensional analysis has been explained by Cardei (2010). Among the MUSLE factors, the soil erodibility factor ( $K$ ) is a measure of the soil's inherent susceptibility/resistance to erosion and the soil's influence on runoff amount and rate.  $K$  is controlled by soil texture and structure, organic matter content and permeability. The slope factor ( $LS$ ) reflects the impacts of slope angle and length on erosion. The crop-management factor ( $C$ ) measures the relative effectiveness of soil and crop management systems in reducing soil erosion. The support practice factor ( $P$ ) is defined to account for the impacts of support measures taken to reduce the amount of erosion such as contour farming, terracing etc. Although the MUSLE is originally intended to estimate the sediment yield on a single storm basis, it has also been applied to estimate annual sediment yield (Sadeghi et al., 2014). In this study, daily sediment yields from the agricultural fields of the Acadie River Catchment were calculated using MUSLE, then averaged at the monthly, seasonal and annual scale.

Soil survey report maps (1:50,000) and soil erodibility factors for Québec soils, both of which are produced by the Québec Research and Development Institute for the Agri-Environment (IRDA), were used to assign the soil erodibility factor ( $K$ ) for the agricultural fields in the Acadie River Catchment (Figure 3.2a). The  $K$  factors vary from 0.013 for gravelly sandy loam soil to 0.073 for the organic soil (Figure 3.2a). It is important to note that there was no  $K$  factor given for the organic soil by IRDA. Therefore, the organic soil was assumed to have the highest  $K$  factor among all soil types defined by IRDA, due to its greatest susceptibility to erosion (Clubs-conseils en agroenvironnement 2014). A high resolution (1x1 m) LIDAR based DEM of the

Acadie River Catchment was used to calculate the average LS factor for each agricultural field, following the methodology proposed by Desmet and Govers (1996) implemented in the SAGA-GIS platform (Conrad et al. 2015). The LS factors of the fields vary from 0.03 to 1.605 (Figure 3.2b). Generalized crop management factors for Québec (Wall et al. 2002) were used to assign the crop management factor (C) for conventional till, conservation till and no-till practices over different crop types that were acquired from La Financière Agricole du Québec (FADQ).

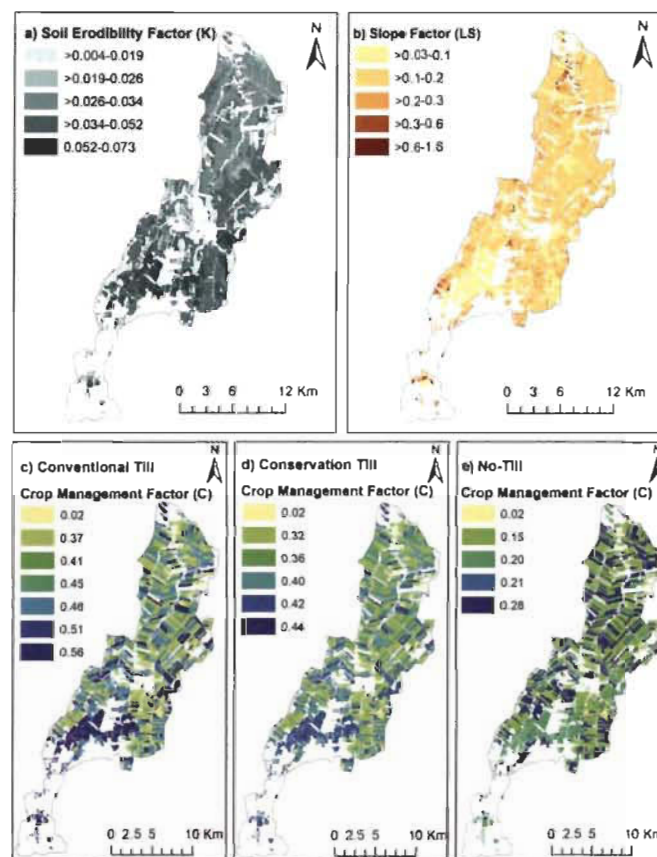


**Figure 3.2.** MUSLE soil erosion factors. **a)** Soil erodibility factor (K); **b)** Slope factor (LS); **c)** Conventional till crop management factor (C); **d)** Conservation till crop management factor (C); **e)** No-till crop management factor (C).

Given that conventional till is the dominant practice in the Acadie River Catchment (Clubs-conseils en agroenvironnement 2014), historical sediment yield calculations

were performed using the conventional till crop management (C) factors (Figure 3.2c). In order to explore the impact of tillage practices on sediment yield, conservation till crop management (C) factors (Figure 3.2d) and no-till crop management (C) factors (Figure 3.2e) were also used along with the conventional crop management factors under different climate change scenarios. Under conventional till, the C factor is the highest for the vegetables (0.56) followed by silage corn (0.51), soybeans (0.46), potatoes (0.45), cereal grains (0.41) and corn grain (0.37), while the lowest C factor (0.02) is assigned to hay (Figure 3.2c). While the C factor stays the same for hay, all other crops were assigned to have lower C factors for the conservation till (Figure 3.2d) and no-till (Figure 3.2e) compared to the conventional till (Figure 3.2c).

In this study, the runoff components of the MUSLE equation were transferred from our previous study (Aygün et al. 2020b) in which a physically based hydrological model has been built to simulate the hydrological processes in the Acadie River Catchment over an historical period (1996–2019) and under various climate change scenarios. They used the Cold Regions Hydrological Model (CRHM, Pomeroy et al. 2007), a physically based, modular hydrological model which represents all specific processes relevant for cold regions, such as snowpack accumulation, sublimation and melting, blowing snow transport and sublimation, canopy snow interception and unloading, and frozen soil infiltration. They validated the hydrological model against discontinuous snow water equivalent (SWE) observations and daily streamflow measurements taken at the discharge gauge of the Acadie River Catchment (Figure 3.1) over the 1996–2019 period. The timing and volume of streamflow has been successfully simulated with a Nash-Sutcliffe efficiency of 0.51, Kling-Gupta efficiency of 0.71 and percent bias of 2.4% for the 23-year simulation period (Aygün et al., 2020b). Given the physically based structure of the hydrological model and its successful performance on simulating streamflow over a historical period, it is expected to accurately simulate changes in sediment yield caused by altered runoff processes under changing climate conditions.

A combination of six soil types (clayey, till deposits, organic soil, sandy, loamy and gravelly) and seven land use classes (agriculture, urban, deciduous, mixed, coniferous forest, shrub and wetland) were used to classify the Acadie River Catchment into hydrological response units (HRUs) which are the main spatial units for mass and energy balance calculations. Since this study aims to calculate the sediment yields from the agriculture fields, the runoff components were transferred only from the agriculture HRUs (Figure 3.3).

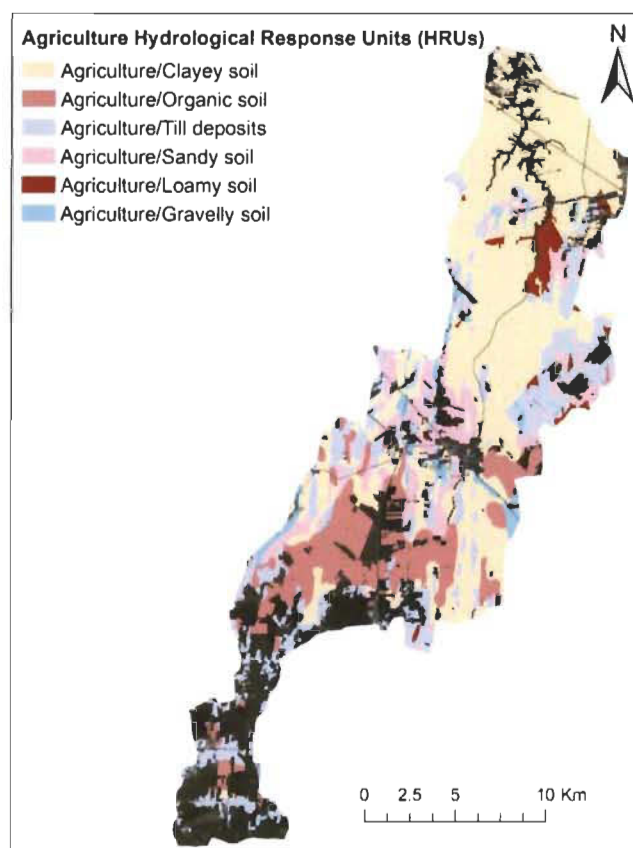


**Figure 3.3.** Agriculture hydrological response units (HRUs) of the Acadie River Catchment.

The daily specific runoff volume (mm) and specific peak runoff ( $\text{mm s}^{-1}$ ) for each agriculture HRU (Figure 3.3) were calculated using the hourly outputs of the hydrological model. Since the sediment calculations were aimed to perform at field

scale (Figure 3.1) rather than HRU scale (Figure 3.3), the specific runoff components of the agriculture HRUs were converted into daily runoff volume ( $\text{m}^3$ ) and daily peak runoff ( $\text{m}^3 \text{ s}^{-1}$ ) using the areas of the corresponding agricultural fields. Daily sediment yields were then summed over the periods of interest, i.e. months, seasons and whole year.

Given the flat topography and poor drainage of the soils in the Acadie River Catchment, tile drainage is used extensively to remove excess water from agricultural soils below their surface (Aygün et al., 2020b). Therefore, any water in excess of soil saturation is expected to be removed by subsurface tile drains. Surface runoff, on the other hand, typically occurs during high-intensity rainfall or snowmelt events that result in infiltration excess overland flow, similar to the other tile drained agricultural catchments in cold regions (Klaiber et al., 2020). Based on this, we set our first scenario (scenario a) in which soil erosion occurs due to surface runoff only. Hence in scenario a, it is hypothesized that the surface runoff formed by infiltration excess is the only pathway for sediment transport, assuming that soil saturation excess water drained through tiles carry no sediment. The second scenario (scenario b) assumes that both surface runoff and tile drainage contribute to the sediment yield. However, the tiles might not have the same transport efficiency as surface runoff and the tile efficiency is likely to change throughout the year, in part due to soil freezing that blocks the tiles in winter. Therefore, for scenario b, we explored a range of tile efficiency scenarios from 0% to 100% (at 10% interval) for freezing and non-freezing conditions, resulting in 121 (11x11) scenarios in total, and chose the best seasonal partition on a monthly basis based on model fit over the 2009–2015 period. Considering that a calendar-based definition of seasons would change under climate change, a dynamic hydroclimate-based season classification was used in this study. As snow cover provides a perfect insulation between the ground surface and the atmosphere (Pomeroy and Brun, 2001) with maximum insulation efficiency when the snow depth reaches about 40 cm (Sutinen et al., 2008; Zhang, 2005), the days were classified as freezing days when the

daily minimum air temperature was below 0 °C and the simulated daily snow depth was less than 40 cm. Conversely, the day was assumed to be non-freezing when both conditions were unmet. This dynamic classification allows identifying periods of the year when tiles are likely to be less effective due to soil freezing. The sediment yields in freezing and non-freezing days were multiplied with the freezing day tile efficiency and non-freezing day tile efficiency, respectively. The simulated daily sediment yields were then aggregated to monthly yields and compared with the monthly observations over the 2009–2015 period. The tile efficiency factors for freezing and non-freezing conditions were calibrated on odd years (2009, 2011, 2013 and 2015), using the root mean square error (RMSE) and Nash-Sutcliffe efficiency (NSE) (Nash and Sutcliffe, 1970) to assess the goodness of fit between monthly observations and simulations. Odd years (2010, 2012 and 2014) were used for independent validation. Taken together, while scenario a presents a base-line scenario for the amount of sediment eroded from the agricultural fields, scenario b presents a more realistic scenario involving a seasonally variable tile drain contribution to the sediment yield.

In order to explore the potential impacts of climate change on soil erosion in the Acadie River Catchment, climate sensitivity analyses were performed according to the range of air temperature and precipitation changes for the mid (2041–2070) and end (2071–2100) of century under two greenhouse gas emissions scenarios (RCP 4.5: moderate and RCP 8.5: high) (Ouranos, 2015). These projections are used for adaptation support in the province of Québec and are available for each administrative region of Québec at the climate portal of Ouranos (<https://www.ouranos.ca/climate-portraits/#/>). According to the climate projections for the Montérégie region of Québec which includes the Acadie River Catchment, a warming of mean air temperature up to 8 °C at 1 °C intervals and an increase in mean precipitation up to 20% at 5% intervals in climate were used in the sensitivity analyses.

### 3.3 Results

Among all the possible combinations of tile efficiency factors (0% to 100% in both freezing and non-freezing days, at 10% interval) in scenario b, the observed monthly sediment yields were best simulated with a tile efficiency of 20% during freezing days and 50% during non-freezing days, with a RMSE of  $0.018 \text{ t ha}^{-1}$  and a NSE of 0.68 for the calibration period (2009, 2011, 2013 and 2015) (Figure 3.4a). The RMSE and NSE for the validation period (2010, 2012 and 2014) are  $0.049 \text{ t ha}^{-1}$  and 0.56, respectively (Figure 3.4b). The inter-annual variability of the observed monthly sediment yield is larger in the validation period than in the calibration period, due in part to the shorter record used for validation. Both observations and simulations by scenario b suggest that the sediment yield in March and April are the largest compared to the rest of the year over both calibration and validation periods, respectively (Figure 3.4). This can be explained with the snowmelt contribution to streamflow which peaks in March and April. Meanwhile, scenario a simulates the highest monthly sediment yield in March over both calibration and validation periods.

The sediment yields observed in summer months (June to September) are lower than the other months, which is on par with the simulated yields by scenario b. The monthly sediment yield is often underestimated by scenario a during both calibration and validation periods. In fact, there is almost no sediment yield simulated by scenario a from May to July and from May to August in both calibration and validation period, respectively. This can be explained by the low amount of surface runoff as the effective precipitation mostly infiltrates during summer months (Aygün et al., 2020b). Regarding the annual budget, while the average annual sediment yield (sum of monthly average yields in Figure 3.4a and b) over the 2009–2015 period was  $0.39 \text{ t ha}^{-1}$ , it is simulated as  $0.19 \text{ t ha}^{-1}$  and  $0.34 \text{ t ha}^{-1}$  by scenario a and scenario b, respectively. This suggests that 44% of the simulated annual average sediment yield ((scenario b - scenario a)/scenario b) was carried by the tile drains over the 2009–2015 period.

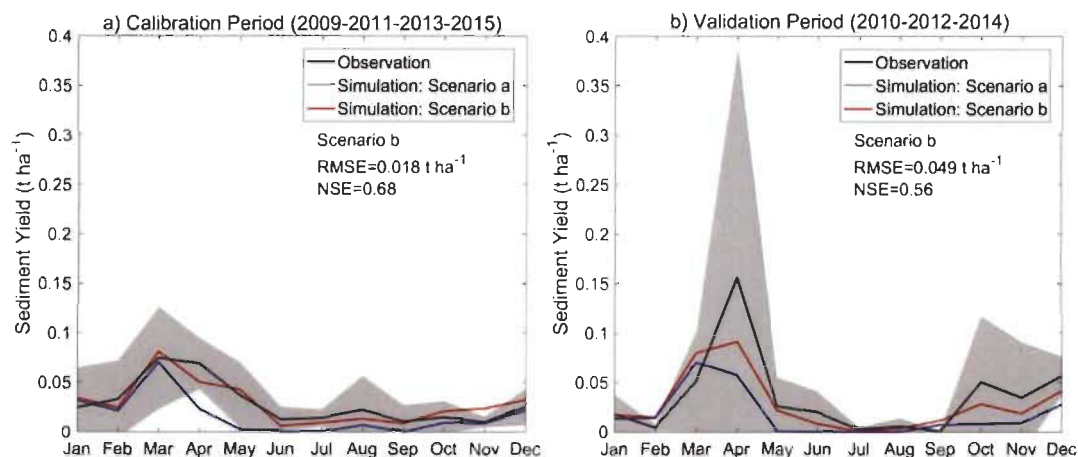


**Figure 3.4.** Comparison of observed and simulated monthly average sediment yields for scenario a and b in **a)** calibration and **b)** validation periods. While the non-calibrated scenario a considers the surface runoff as the only pathway for sediment transport, scenario b represents a more realistic simulation in which the sediments are carried by surface runoff and subsurface tile drains with an efficiency of 20% in freezing days and 50% in non-freezing days. RMSE and NSE for scenario b are presented for calibration and validation periods. The grey envelope around the mean monthly observation represents the inter-annual variability ( $\pm$  standard deviation) of monthly sediment yields for the calibration period (a) and validation period (b).

Over the full 1996–2019 simulation period, the simulated average annual sediment yield from the agricultural fields varied from  $0.0013$  to  $4.3\ t\ ha^{-1}\ year^{-1}$  with an average of  $0.22\ t\ ha^{-1}\ year^{-1}$  and from  $0.0022$  to  $7.2\ t\ ha^{-1}\ year^{-1}$  with an average of  $0.36\ t\ ha^{-1}\ year^{-1}$ , for scenario a and scenario b, respectively (Figure 3.5). This implies that sediments carried by tiles constitute 39% of the mean annual sediment yield over the 1996–2019 period, which is only slightly lower than the 2009–2015 calibration/validation period. These yields are of similar magnitudes than the  $0.1$  to  $12.9\ t\ ha^{-1}\ year^{-1}$  yield reported for the twenty-four individual agricultural fields in the Boyer River watershed in southern Québec (Mabit et al., 2007). The average sediment yields in Acadie were found to be relatively high in the central/southeastern part of the catchment (Figure 3.5) which is dominated by vegetable fields underlain by erodible organic soil, with the larger yields occurring over fields with higher slope factors (Figure 3.2b). Also, the agriculture fields located along the riverbank were simulated

to have higher sediment yields, mostly due to the high slope factors (Figure 3.2b). On the other hand, the smallest sediment yields were found over the hay fields due to low C factor (Figure 3.2c).

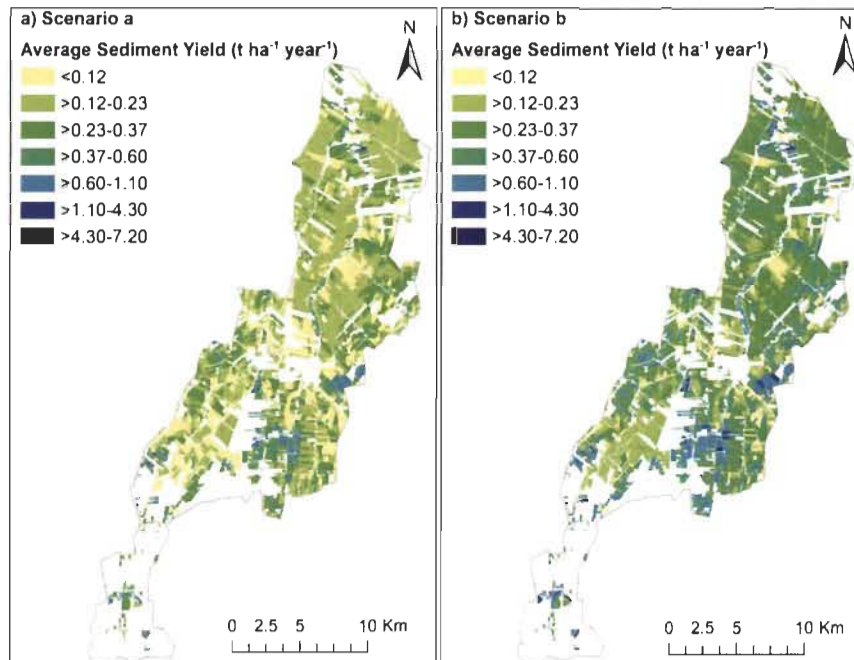


**Figure 3.5.** Average annual sediment yields (1996–2019) from the agricultural fields in the Acadie River Catchment simulated by **a)** Scenario a and **b)** Scenario b.

All the annual sediment yields are below the suggested tolerable soil loss rates (i.e. the maximum rate that could occur indefinitely without adversely affecting soil productivity) for most Canadian soils ( $6 \text{ t ha}^{-1} \text{ year}^{-1}$ ) (Wall et al., 2002), except one vegetable field from which the sediment yield is simulated to be  $7.2 \text{ t ha}^{-1} \text{ year}^{-1}$  by scenario b (Figure 3.5b). This would suggest at first sight that the agricultural fields in the Acadie River Catchment have very slight to no erosion issues. However, it is important to note that the tolerable rate of erosion varies depending on the type, depth and condition of soil as well as past erosion (Wall et al., 2002). Although the soil erodibility (K) factor for the organic soils were assumed to be highest among the K factors provided by IRDA for Québec soils, our computations could still have

underestimated erosion from these soils. Organic soils are already shallower than the other soils in the catchment and their light weight combined with friable texture make them more sensitive to soil erosion, leading to even thinner soil layers. Also, fields with organic soils were reported to be more prone to flooding by the nearby Acadie River, and hence to soil erosion, than the rest of the catchment due to their lower elevations and the natural phenomenon of organic soil subsidence (Clubs-conseils en agroenvironnement, 2014).

The responses of the average annual sediment yield to warming air temperatures and increasing precipitation are presented for scenario a (Figure 3.6a) and scenario b (Figure 3.6b). The average sediment yield simulated by scenario a is primarily influenced by warming and to a lesser extent by increasing precipitation (Figure 3.6a). Decreased snowmelt and a reduced influence of frozen soil on infiltration in response to warming both favor reduced surface runoff (Aygün et al., 2020b), which leads to reduced soil erosion under scenario a (by ~10% per °C) (Figure 3.6a). On the other hand, increasing precipitation could cause an increase in annual average sediment yield by up to 30% under limited warming (<2 °C), depending on the combined levels of warming and wetting (Figure 3.6a). This zone of positive sensitivity of sediment yield is delineated by the 0% contour in Figure 3.6a, below which the annual sediment yield exhibits an increase. Meanwhile, the annual average sediment yield declines regardless of changes in precipitation, when the warming exceeds 2 °C for scenario a (Figure 3.6a). The annual sediment yield simulated by scenario b, on the contrary, appears more sensitive to increasing precipitation than to warming (Figure 3.6b). The annual sediment yield mostly increases in response to increasing precipitation (Figure 3.6b), which is governed by an increase in annual water availability in response to wetting in the Acadie River Catchment (Aygün et al., 2020b). Meanwhile, if warming occurs without any change in precipitation, the annual sediment yield could decline by up to 30% for scenario b, depending on the amount of warming (Figure 3.6b).

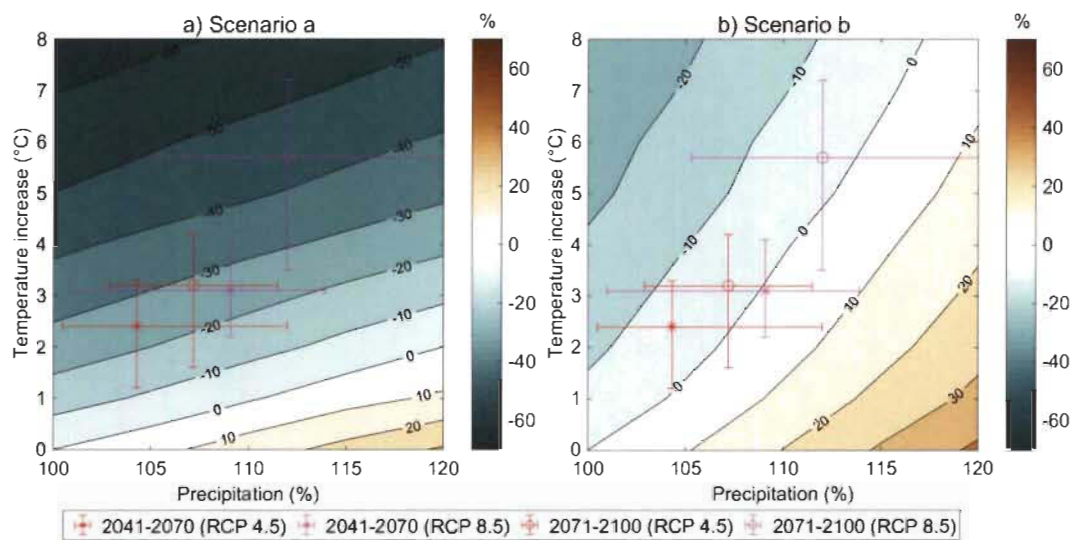


**Figure 3.6.** Change in average annual sediment yields under climate change scenarios for **a)** Scenario a (surface runoff only), and **b)** Scenario b (surface runoff plus tile drainage with an efficiency of 20% in freezing days and 50% in non-freezing days). The crosses overlain on the panels represent the mean and spread (90% confidence) of ensemble projected changes in mean annual temperature and precipitation for the periods 2041–2070 and 2071–2100 under a moderate (RCP 4.5) and high (RCP 8.5) emission scenario for the Montérégie region of Québec (Ouranos, 2015).

Comparing both scenarios in the light of ensemble climate projections shows that while the annual average sediment yield could decrease by 10% to 50% for scenario a, it could either decrease by 15% or increase by up to 15% for the more realistic scenario b, depending on the projection period and RCP scenario considered (Figure 3.6). The results suggest that the tiles in scenario a buffer the agricultural fields against increasing precipitation as the infiltrated water does not contribute to soil erosion. In contrast to scenario a, increasing precipitations under scenario b are only partially buffered by the tiles and as such can lead to increased erosion rates (Figure 3.6b). When excess soil water draining through tiles has an efficiency of 20% in freezing days and 50% in non-freezing days (scenario b), the decline in erosion in response to warming alone is much less pronounced compared to scenario a (Figure 3.6) and is mainly due to decreased peak snowmelt runoff rates alone.

The historically averaged annual and seasonal sediment yields over the 1996–2019 reference period ( $\Delta t = 0\text{ }^{\circ}\text{C}$  &  $P = 100\%$ ) were compared to the projected sediment yields under selected climate change scenarios representing the mean of ensemble projections for the 2041–2070 and 2071–2100 periods, i.e.  $2\text{ }^{\circ}\text{C}$  warming and 5% increasing precipitation ( $\Delta t = 2\text{ }^{\circ}\text{C}$  &  $P = 105\%$ ) and  $5\text{ }^{\circ}\text{C}$  warming and 10% increasing precipitation ( $\Delta t = 5\text{ }^{\circ}\text{C}$  &  $P = 110\%$ ), respectively (Figure 3.7a and b).

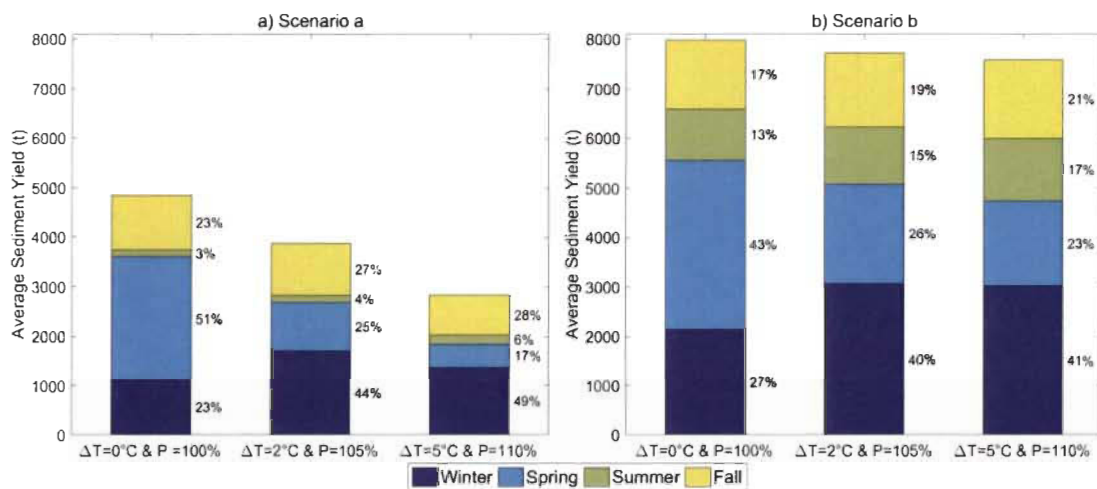


**Figure 3.7.** Average annual and seasonal sediment yields under selected climate change scenarios for **a)** Scenario a (surface runoff) and **b)** Scenario b (surface runoff + tile drainage).

Depending on the climate change scenario, while the annual average sediment yield declines by 20 to 40% in scenario a, it decreases by 3 to 5% in scenario b (Figure 3.7a and b). With  $2\text{ }^{\circ}\text{C}$  warming and a 5% increase in precipitation, the winter sediment yield becomes dominant during the year for scenario a, increasing by 21% (Figure 3.7a), which can be explained with the significant increase (51%) in surface runoff in winter resulting from the conversion of snowfall to rainfall, the shift in snowmelt timing from spring to winter and more frequent mid-winter melt events in the Acadie River Catchment under  $2\text{ }^{\circ}\text{C}$  warming (Aygün et al., 2020b). Under the same climate scenario, subsurface runoff also becomes higher due to increased infiltration ratios. However, the increase in winter subsurface runoff (25%) represents

only half the increase in surface runoff. Therefore, a 2 °C warming with 5% precipitation increase causes a smaller increase in sediment yield in winter relative to baseline conditions, under scenario b. Under the same climate change scenario, the sediment yield in spring decreases from 51% to 25% in scenario a (Figure 3.7a), which can be attributed to declined snow storage and reduced spring snowmelt, causing a decline in spring surface runoff by 56%. Meanwhile, the same climate change scenario in scenario b leads to a smaller decline (17%) in spring sediment yield (Figure 3.7b). This is because subsurface runoff slightly increases (10%) due to higher rainfall infiltration caused by increasing rainfall amounts, which then leads to a smaller decline in total runoff (surface plus subsurface) in spring compared to the spring surface runoff-only scenario a. The sensitivity of sediment yields in winter and spring is greater in the 0–2 °C warming zone compared to the 2–5 °C warming zone in both scenarios (Figure 3.7). This is explained by the large sensitivity of the snow regime of the Acadie River Catchment to warming in the 0–2 °C warming zone, with most of the snowpack disappearing beyond 2 °C warming (Aygün et al., 2020b).

Under the climate change scenarios, the annual contribution of fall and summer sediment yield gradually increases under both scenarios a and b (Figure 3.7). Meanwhile, the summer contribution continues to be the smallest during the year for both scenarios (Figure 3.7). While there is a decline in annual average sediment yield simulated by scenario b in response to the selected climate change scenarios (Figure 3.7b), the relative contribution of tile drains to the annual sediment yield increases from 40% to 50% in response to 2 °C warming and 5% increasing precipitation, and to 60% under 5 °C warming and 10% increasing precipitation. This can be explained by the increased subsurface runoff as well as greater tile efficiency as the number of warm (non-freezing) days increases in response to decreased snow depth and warming air temperatures.

With regards to the impact of conservation practices, the average annual sediment yield declines by 20% and 60%, with conservation till and no-till management practices, respectively, under any given climate scenario (Figure 3.8). Yet, the combination of replacing conventional till crop management practice under changing climate could cause a considerable reduction in average sediment yield compared to the historical conditions. For instance, under 2 °C warming and 5% increasing precipitation, the annual average sediment yield could decrease by 34 to 64% and by 23 to 57% for scenario a and b, respectively, depending on the selected crop management practice.

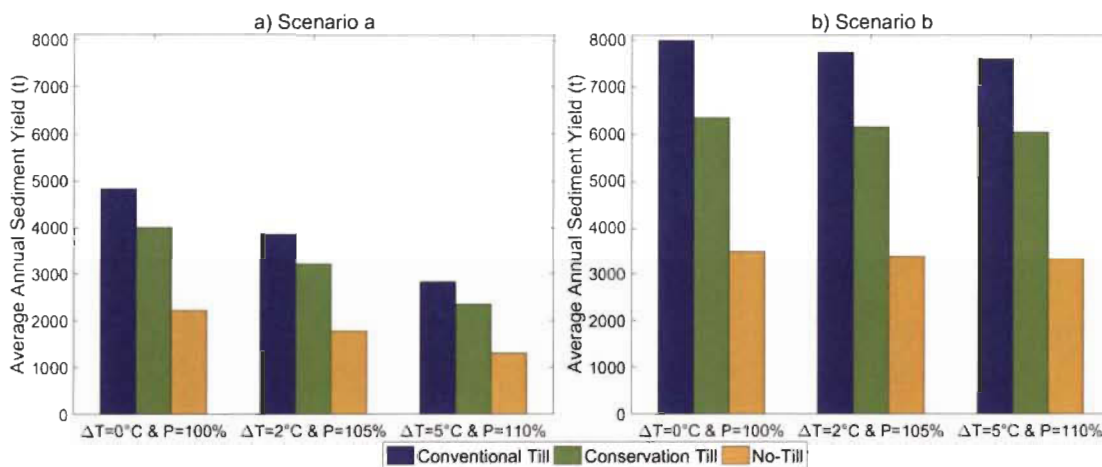


**Figure 3.8.** Average annual sediment yields under selected climate change and crop management scenarios for **a)** Scenario a (surface runoff) and **b)** Scenario b (surface runoff + tile drainage).

If no-till practices are implemented under the end-of-century climate scenario (5 °C warming and 10% increasing precipitation), the annual average sediment yields become one fourth (scenario a) and half (scenario b) of those under baseline climate conditions with conventional till practices. In a transition period where precipitation would increase faster than temperatures, it is noteworthy that the adoption of conservation practices could partly compensate the increased erosion associated with greater runoff.

### 3.4 Discussion and Conclusions

Over the 1996–2019 period, the simulated average annual sediment yield from the agricultural fields of the Acadie River catchment was 0.22 and 0.36 t ha<sup>-1</sup> year<sup>-1</sup>, for the scenario a (surface runoff) and b (surface runoff and subsurface tile drainage), respectively. These yields are of similar magnitudes with a median of 0.147 t ha<sup>-1</sup> year<sup>-1</sup> calculated for nine agricultural watersheds in Québec using the flux ratio estimator method for the 1991–1995 period (Gangbazo and Babin, 2000), 0.23 t ha<sup>-1</sup> year<sup>-1</sup> estimated for the Beaurivage River watershed in southern Québec for the 1989–1995 period using the ratio estimator method (Quilbé et al., 2006), and 0.49 t ha<sup>-1</sup> year<sup>-1</sup> simulated for the Pike River watershed for 2000–2003 using the SWAT model (Michaud et al., 2007). The measured monthly sediment yields are found to be closer to the sediment yields estimated by scenario b than to those estimated by scenario a for the 2009–2015 period, highlighting the importance of subsurface tile drains as a pathway for sediment transfer. The comparison of scenario b with scenario a showed that the tile drains accounted for 39% of the annual total sediment yield over the 1996–2019 period, which agrees with the previous studies performed in similar agroclimatic environments. For instance, the tile drains were reported to export 43% of the annual total phosphorus in an agricultural catchment in Waterloo, Ontario (Macrae et al., 2007). Jamieson et al. (2003) reported that subsurface total phosphorous load accounted for 37% of the total loads in an agricultural field in southern Québec. Our results show that the contribution of tile drains to the total erosion in the Acadie River Catchment increases as the climate warms and infiltration increases in response to reducing snowpacks and soil freezing. There is therefore an urgent need to better understand sediment export through tile drainage, particularly in cold humid regions where agricultural fields are often drained to allow agricultural activities (Michaud et al., 2019).

The methodology used in this study does not account for stream bank erosion and channel deposition and re-suspension of sediments. Very little data is available on the contribution of streambank net erosion to the sediment load at the catchment outlet. Bernard and Laverdière (2000) used the radioactive isotope of caesium (Cs) as a tracer and estimated that about 25% of the total sediment load originated from stream banks in an agricultural catchment in Québec. In a subbasin of the Pike River watershed, Michaud et al. (2006) simulated that the net erosion in the river network adds an additional sediment load corresponding to 15% of the yields out of the agricultural fields. Although the proportion of the sediment load originating from the banks would vary from one catchment to another, these reported values are currently the best estimates for the agricultural catchments in southern Québec. If 15% is assumed for net erosion (deposition-erosion) in the river network of the Acadie River Catchment and added to the simulated yields from the fields, the sediment yield simulated by scenario b ( $0.34 \text{ t ha}^{-1} \text{ year}^{-1}$ ) becomes almost equal to the historically averaged observed sediment yield ( $0.39 \text{ t ha}^{-1} \text{ year}^{-1}$ ).

Previous application of RUSLE to estimate potential soil loss rates in the Acadie River Catchment reported that while soil erosion is less than the tolerable soil loss rate of  $6 \text{ t ha}^{-1} \text{ year}^{-1}$  (Wall et al., 2002) over more than half of the cultivated fields, values between 6 and  $11 \text{ t ha}^{-1} \text{ year}^{-1}$  were reported over a quarter of the fields and exceeding  $11 \text{ t ha}^{-1} \text{ year}^{-1}$  over some fields (Clubs-conseils en agroenvironnement, 2014). These values are drastically larger than the annual average sediment yields calculated for the 1996–2019 period in this study using MUSLE. Since MUSLE considers runoff factors as representing the energy used in transporting as well as in detaching sediment, the sediment yield estimations in this study are expected to be closer to real values than the RUSLE predictions that depend strictly upon rainfall as the source of erosive energy to provide potential erosion estimates. In this sense, using runoff from a physically based hydrological model that has been successfully validated for the Acadie River Catchment (Aygün et al., 2020b), increases the realism of MUSLE-based sediment

yield estimations. Despite these low sediment yields calculated, it is important to note that the tolerable loss may vary in terms of agricultural and environmental significance (Verheijen et al., 2009). Organic soils of the Acadie River Catchment are thin (<150 cm in some agricultural fields (Hallema et al., 2015)) so that even a small amount of soil loss may threaten the sustainability of these soils. These would have important implications for the farming community as vegetable farms are mostly located over the fertile organic soils and constitute an important economic activity in the catchment. Suspended soil particles can increase the water temperature, as these particles absorb and scatter sunlight more efficiently than water (Paaijmans et al., 2008). Suspended sediments can also reduce the light transmission through water and decrease photosynthesis by aquatic plants, influencing dissolved oxygen levels (Kjelland et al., 2015). Furthermore, fine sediments, particularly clay, transported from the agricultural fields of the Acadie River Catchment to downstream water bodies can have a high nutrient content due to the use of fertilizers in fields which adhere to soil particles. The water samples taken at the l'Acadie water quality station in 2013 revealed the presence of 25 pesticides some of which had high amount of toxic compounds for aquatic organisms (COVABAR, 2015). Considering that the Acadie River and its tributaries are home to at least 19 species of fish, some of which being endangered such as the copper redhorse (Tremblay and Gareau, 2020), soil erosion from agricultural fields of the Acadie River Catchment can threaten the integrity of the habitat and the survival of these species, despite erosion rates being lower than the recommended tolerable soil loss for most Canadian soils (Wall et al., 2002), which is based on soil productivity alone and does not consider offsite environmental impacts such as water quality issues.

The annual sediment yield responds differently to warming and increasing precipitation for scenario a and scenario b. In scenario a, the annual sediment yield declines under most climate change scenarios due to the declining surface runoff. On the other hand, increasing total water availability under a warmer and wetter climate could lead to

higher annual sediment yield under scenario b, i.e. when tiles are assumed to have a sediment carrying efficiency of 20% in freezing days and 50% in non-freezing days. This suggests that the large uncertainties in precipitation projections cascade down to the erosion uncertainties in scenario b, with annual sediment yield increasing or decreasing according to the precipitation uncertainty in a given scenario. Historically, almost half of the annual sediment yield from the agriculture fields of the Acadie River Catchment has occurred during the spring season due to the high amounts of surface runoff resulting from snowmelt. Warming temperatures, on the other hand, increases winter snowmelt and rain events, causing an increase in winter sediment yield under both scenario a and b (Figure 3.7), which is in agreement with previous studies performed in southern Québec (Gombault et al., 2015; Mehdi et al., 2015) as well as other cold regions such as Great Lakes Region (Wang et al., 2018), Norway (Deelstra et al., 2015), Sweden (Arheimer et al., 2005) and Denmark (Andersen et al., 2006). This finding has important implications for crop management strategies in the Acadie River Catchment. Our results suggest that the implementation of conservation-till and no-till practices, which both ensure a soil residue cover in winter, would be beneficial for soil protection in the context of climate change where significant soil erosion could occur during winter months. This would in turn improve the crop yields and address the problem of non-point source eutrophication. Future studies should extend the simulation of the effects of management practices on soil erosion by evaluating other practices such as riparian buffer strips, which have been reported to be an efficient way of reducing sediment and nutrient loads at watershed outlet (Rousseau et al., 2013).

It is worth noting that there are different sources of uncertainties in this study. For example, the assumption that the soil erodibility factor of the organic soil in the Acadie River Catchment is the highest among all Québec soils results in an uncertainty in the erosion estimate for this soil type. The climate sensitivity framework used in this study only considers annual mean changes in air temperature and precipitation; therefore, considering changes in climate variability and extremes could further alter

the seasonal estimates of soil erosion, especially given the sensitivity of erosion projections to precipitation under scenario b. For example, it has been projected that the extent, frequency and magnitude of soil erosion would increase in response to changes in rainfall intensity caused by climate change (Deelstra et al., 2015; Pruski and Nearing, 2002; Starkloff and Stolte, 2014). While the sensitivity analysis here represents a useful assessment of the first order response of soil erosion to a wide range of changes in mean climate, future studies should extend this analysis to changes in the intensity, duration and frequency of precipitation as well as its seasonality. In this study, while the impacts of different crop management strategies on soil erosion were analyzed, the crop types were kept constant for both historical and future climate conditions. However, the projected changes in air temperature and precipitation can influence the decisions about the most suitable crop types to grow in the Acadie River Catchment. Further studies, therefore, could extend the climate sensitivity analyses to include the impacts of expected changes in crop types on soil erosion by modifying the crop management factor (C). Meanwhile, the results of this study offer useful guidance to decision makers and farming communities about the first-order climate sensitivity of soil erosion and the potential mitigation of crop management strategies in the context of climate change.

### **Acknowledgments**

This research was funded by the Natural Sciences and Engineering Council of Canada, grant number RGPIN-2015-03844 (Christophe Kinnard) and RGPIN-2017-06571 (Stéphane Campeau) and the Canada Research Chair program, grant number 231380 (Christophe Kinnard).

## References

- Andersen, H.E. et al., 2006. Climate-change impacts on hydrology and nutrients in a Danish lowland river basin. *Science of the Total Environment*, 365, 223–237.
- Arheimer, B. et al., 2005. Climate change impact on water quality: model results from southern Sweden. *AMBIO: A Journal of the Human Environment*, 34, 559–566.
- Aygün, O., Kinnard, C., Campeau, S., 2020a. Impacts of climate change on the hydrology of northern midlatitude cold regions. *Progress in Physical Geography: Earth and Environment*, 44, 338–375.
- Aygün, O., Kinnard, C., Campeau, S., Krogh, S.A., 2020b. Shifting Hydrological Processes in a Canadian Agroforested Catchment due to a Warmer and Wetter Climate. *Water*, 12, 739.
- Bélanger, L., Grenier, M., Deslandes, S., 2002. Report on habitat and land use in southern Québec, Environment Canada, Canadian Wildlife Service, Québec Region.
- Benavidez, R., Jackson, B., Maxwell, D., Norton, K., 2018. A review of the (Revised) Universal Soil Loss Equation ((R) USLE): with a view to increasing its global applicability and improving soil loss estimates. *Hydrology and Earth System Sciences*, 22, 6059–6086.
- Bernard, C., Laverdière, M., 2000. Using <sup>137</sup>Cs as a tool for the assessment and the management of erosion/sedimentation risks in view of the restoration of the Rainbow Smelt (*Osmerus mordax*) fish population in the Boyer River basin (Québec, Canada). *Acta geológica hispánica*, 321–327.
- Cardei, P., 2010. The dimensional analysis of the USLE-MUSLE soil erosion model, *Proc. Rom. Acad. Ser. B*, pp. 249–253.
- Clubs-conseils en agroenvironnement, 2014. Rapport de caractérisation du bassin versant « amont » de la rivière L'Acadie, Club Techno-Champ 2000, QC, Canada.
- Conrad, O. et al., 2015. System for automated geoscientific analyses (SAGA) v. 2.1. 4. *Geoscientific Model Development Discussions*, 8.
- COVABAR, 2015. Plan directeur de l'eau – Portrait du bassin versant de la Rivière Richelieu et de la zone Saint-Laurent, Beloeil, Quebec, Canada.

- Deelstra, J., Øygarden, L., Blankenberg, A.-G.B., Eggestad, H.O., 2015. Climate change and runoff from agricultural catchments in Norway. *New Perspectives in Climate Change*, 1.
- Desmet, P., Govers, G., 1996. A GIS procedure for automatically calculating the USLE LS factor on topographically complex landscape units. *Journal of soil and water conservation*, 51, 427–433.
- Eastman, M., Gollamudi, A., Stämpfli, N., Madramootoo, C., Sarangi, A., 2010. Comparative evaluation of phosphorus losses from subsurface and naturally drained agricultural fields in the Pike River watershed of Quebec, Canada. *Agricultural Water Management*, 97, 596–604.
- Gangbazo, G., Babin, F., 2000. Pollution de l'eau des rivières dans les bassins versants. *Vecteur Environnement*, 33, 47–57.
- Garbrecht, J.D., Nearing, M.A., Steiner, J.L., Zhang, X.J., Nichols, M.H., 2015. Can conservation trump impacts of climate change on soil erosion? An assessment from winter wheat cropland in the Southern Great Plains of the United States. *Weather and Climate Extremes*, 10, 32–39.
- Gatto, L.W., 2000. Soil freeze–thaw-induced changes to a simulated rill: potential impacts on soil erosion. *Geomorphology*, 32, 147–160.
- Gollamudi, A., Madramootoo, C., Enright, P., 2007. Water quality modeling of two agricultural fields in southern Quebec using SWAT. *Transactions of the ASABE*, 50, 1973–1980.
- Gombault, C. et al., 2015. Impacts of climate change on nutrient losses from the Pike River watershed of southern Québec. *Canadian Journal of Soil Science*, 95, 337–358.
- Hallema, D.W., Périard, Y., Lafond, J.A., Gumiere, S.J., Caron, J., 2015. Characterization of water retention curves for a series of cultivated Histosols. *Vadose Zone Journal*, 14, 1–8.
- Heisler, J. et al., 2008. Eutrophication and harmful algal blooms: a scientific consensus. *Harmful algae*, 8, 3–13.
- Huggins, D.R., Reganold, J.P., 2008. No-till: the quiet revolution. *Scientific American*, 299, 70–77.
- Issaka, S., Ashraf, M.A., 2017. Impact of soil erosion and degradation on water quality: a review. *Geology, Ecology, and Landscapes*, 1, 1–11.

- Jackson, W.L., Gebhardt, K., Van Haveren, B.P., 1986. Use of the modified universal soil loss equation for average annual sediment yield estimates on small rangeland drainage basins. IAHS-AISH publication, 413–423.
- Jamieson, A., Madramootoo, C., Enright, P., 2003. Phosphorus losses in surface and subsurface runoff from a snowmelt event on an agricultural field in Quebec. *Canadian Biosystems Engineering*, 45, 1.1–1.1.
- Jobin, B. et al., 2014. A half-century analysis of landscape dynamics in southern Québec, Canada. *Environmental monitoring and assessment*, 186, 2215–2229.
- Kinnell, P., 2010. Event soil loss, runoff and the Universal Soil Loss Equation family of models: A review. *Journal of hydrology*, 385, 384–397.
- Kjelland, M.E., Woodley, C.M., Swannack, T.M., Smith, D.L., 2015. A review of the potential effects of suspended sediment on fishes: potential dredging-related physiological, behavioral, and transgenerational implications. *Environment Systems and Decisions*, 35, 334–350.
- Klaiber, L.B., Kramer, S.R., Young, E.O., 2020. Impacts of Tile Drainage on Phosphorus Losses from Edge-of-Field Plots in the Lake Champlain Basin of New York. *Water*, 12, 328.
- Klik, A., Rosner, J., 2020. Long-term experience with conservation tillage practices in Austria: Impacts on soil erosion processes. *Soil and Tillage Research*, 203, 104669.
- Kuhn, N.J., 2007. Erodibility of soil and organic matter: independence of organic matter resistance to interrill erosion. *Earth Surface Processes and Landforms*, 32, 794–802.
- Li, Z., Fang, H., 2016. Impacts of climate change on water erosion: A review. *Earth-Science Reviews*, 163, 94–117.
- Mabit, L., Bernard, C., Laverdière, M.R., 2007. Assessment of erosion in the Boyer River watershed (Canada) using a GIS oriented sampling strategy and <sup>137</sup>Cs measurements. *Catena*, 71, 242–249.
- Macrae, M., English, M., Schiff, S., Stone, M., 2007. Intra-annual variability in the contribution of tile drains to basin discharge and phosphorus export in a first-order agricultural catchment. *Agricultural Water Management*, 92, 171–182.
- McConkey, B., Nicholaichuk, W., Steppuhn, H., Reimer, C., 1997. Sediment yield and seasonal soil erodibility for semiarid cropland in western Canada. *Canadian Journal of Soil Science*, 77, 33–40.

- Mehdi, B. et al., 2015. Simulated impacts of climate change and agricultural land use change on surface water quality with and without adaptation management strategies. *Agriculture, Ecosystems & Environment*, 213, 47–60.
- Mhazo, N., Chivenge, P., Chaplot, V., 2016. Tillage impact on soil erosion by water: discrepancies due to climate and soil characteristics. *Agriculture, Ecosystems & Environment*, 230, 231–241.
- Michaud, A., Beaudin, I., Deslandes, J., Bonn, F., Madramootoo, C., 2007. SWAT-predicted influence of different landscape and cropping system alterations on phosphorus mobility within the Pike River watershed of south-western Québec. *Canadian journal of soil science*, 87, 329–344.
- Michaud, A., Deslandes, J., Beaudin, I., 2006. Modélisation de l'hydrologie et des dynamiques de pollution diffuse dans le bassin versant de la Rivière aux Brochets à l'aide du modèle SWAT. Institut de recherche et de développement en agroenvironnement, rapport final.
- Michaud, A.R., Poirier, S.C., Whalen, J.K., 2019. Tile drainage as a hydrologic pathway for phosphorus export from an agricultural subwatershed. *Journal of Environmental Quality*, 48, 64–72.
- Millette, J., Vigier, B., Broughton, R., 1982. An evaluation of the drainage and subsidence of some organic soils in Quebec. *Can. Agric. Eng.*, 24, 5–10.
- Montgomery, D.R., 2007. Soil erosion and agricultural sustainability. *Proceedings of the National Academy of Sciences*, 104, 13268–13272.
- Mukundan, R. et al., 2013. Suspended sediment source areas and future climate impact on soil erosion and sediment yield in a New York City water supply watershed, USA. *Geomorphology*, 183, 110–119.
- Nash, J.E., Sutcliffe, J.V., 1970. River flow forecasting through conceptual models part I—A discussion of principles. *Journal of hydrology*, 10, 282–290.
- Ollesch, G., Kistner, I., Meissner, R., Lindenschmidt, K.-E., 2006. Modelling of snowmelt erosion and sediment yield in a small low-mountain catchment in Germany. *Catena*, 68, 161–176.
- Ollesch, G., Sukhanovski, Y., Kistner, I., Rode, M., Meissner, R., 2005. Characterization and modelling of the spatial heterogeneity of snowmelt erosion. *Earth Surface Processes and Landforms: The Journal of the British Geomorphological Research Group*, 30, 197–211.

- Ouranos, 2015. Vers l'adaptation. Synthèse des connaissances sur les changements climatiques au Québec—Partie 1: Évolution climatique au Québec. Édition 2015 ed. Ouranos, Montréal, Québec.
- Paaijmans, K., Takken, W., Githeko, A., Jacobs, A., 2008. The effect of water turbidity on the near-surface water temperature of larval habitats of the malaria mosquito *Anopheles gambiae*. *International journal of biometeorology*, 52, 747–753.
- Pachauri, R.K. et al., 2014. Climate change 2014: synthesis report. Contribution of Working Groups I, II and III to the fifth assessment report of the Intergovernmental Panel on Climate Change. *Ipcc*.
- Parajuli, P., Jayakody, P., Sassenrath, G., Ouyang, Y., 2016. Assessing the impacts of climate change and tillage practices on stream flow, crop and sediment yields from the Mississippi River Basin. *Agricultural Water Management*, 168, 112–124.
- Pimentel, D., 2006. Soil erosion: a food and environmental threat. *Environment, development and sustainability*, 8, 119–137.
- Pomeroy, J., Brun, E., 2001. Physical properties of snow. *Snow ecology: An interdisciplinary examination of snow-covered ecosystems*, 45–126.
- Pomeroy, J. et al., 2007. The cold regions hydrological model: a platform for basing process representation and model structure on physical evidence. *Hydrological Processes: An International Journal*, 21, 2650–2667.
- Prévost, R., Trady, L., Douville, Y., 2006. Inventaire des problématiques environnementales spécifiques au secteur maraîcher québécois Agriculture et Agroalimentaire Canada, Longueuil, QC, Canada.
- Pruski, F., Nearing, M., 2002. Climate-induced changes in erosion during the 21st century for eight US locations. *Water Resources Research*, 38, 34-1–34-11.
- Quilbé, R. et al., 2006. Selecting a calculation method to estimate sediment and nutrient loads in streams: application to the Beaurivage River (Québec, Canada). *Journal of hydrology*, 326, 295–310.
- Renard, K.G., 1997. Predicting soil erosion by water: a guide to conservation planning with the Revised Universal Soil Loss Equation (RUSLE). United States Government Printing.

- Rousseau, A.N., Savary, S., Hallema, D.W., Gumiere, S.J., Foulon, É., 2013. Modeling the effects of agricultural BMPs on sediments, nutrients, and water quality of the Beaurivage River watershed (Quebec, Canada). *Canadian Water Resources Journal*, 38, 99–120.
- Sadeghi, S., Gholami, L., Khaledi Darvishan, A., Saeidi, P., 2014. A review of the application of the MUSLE model worldwide. *Hydrological Sciences Journal*, 59, 365–375.
- Sartori, M. et al., 2019. A linkage between the biophysical and the economic: Assessing the global market impacts of soil erosion. *Land Use Policy*, 86, 299–312.
- Schoumans, O. et al., 2014. Mitigation options to reduce phosphorus losses from the agricultural sector and improve surface water quality: a review. *Science of the Total Environment*, 468, 1255–1266.
- Simoneau, M., Thibault, G., 2009. État de l'écosystème aquatique du bassin versant de la rivière Richelieu : faits saillants 2005-2007. Ministère du Développement durable, de l'Environnement et des Parcs, Direction du suivi de l'état de l'environnement. Québec. 23 p.
- Starkloff, T., Stolte, J., 2014. Applied comparison of the erosion risk models EROSION 3D and LISEM for a small catchment in Norway. *Catena*, 118, 154–167.
- Su, J. et al., 2011. Effects of snowmelt on phosphorus and sediment losses from agricultural watersheds in Eastern Canada. *Agricultural water management*, 98, 867–876.
- Sutinen, R., Hänninen, P., Venäläinen, A., 2008. Effect of mild winter events on soil water content beneath snowpack. *Cold Regions Science and Technology*, 51, 56–67.
- Tremblay, J., Gareau, P., 2020. Plan de protection de la zone amont de la rivière L'Acadie, Groupe Ambioterra, Saint-Chrysostome, Québec, Canada.
- Van Esbroeck, C.J., Macrae, M.L., Brunke, R.I., McKague, K., 2016. Annual and seasonal phosphorus export in surface runoff and tile drainage from agricultural fields with cold temperate climates. *Journal of Great Lakes Research*, 42, 1271–1280.
- Verheijen, F.G., Jones, R.J., Rickson, R., Smith, C., 2009. Tolerable versus actual soil erosion rates in Europe. *Earth-Science Reviews*, 94, 23–38.

- Vliet, L.V., Hall, J., 1991. Effects of two crop rotations on seasonal runoff and soil loss in the Peace River region. *Canadian journal of soil science*, 71, 533–543.
- Walker, W.W., 1996. Simplified procedures for eutrophication assessment and prediction: User manual, U.S. Army Engineer Waterways Experiment Station, Vicksburg, MS.
- Wall, G., Coote, D., Pringle, E., Shelton, I., 2002. RUSLEFAC—Revised universal soil loss equation for application in Canada: A handbook for estimating soil loss from water erosion in Canada. Research Branch, Agriculture and Agri-Food Canada. Ottawa. Contribution No. AAFC/AAC2244E, 117.
- Walling, D., Russell, M., Hodgkinson, R., Zhang, Y., 2002. Establishing sediment budgets for two small lowland agricultural catchments in the UK. *Catena*, 47, 323–353.
- Wang, L., Cherkauer, K.A., Flanagan, D.C., 2018. Impacts of climate change on soil erosion in the Great Lakes region. *Water*, 10, 715.
- Williams, J.D., Gollany, H.T., Siemens, M.C., Wuest, S.B., Long, D.S., 2009. Comparison of runoff, soil erosion, and winter wheat yields from no-till and inversion tillage production systems in northeastern Oregon. *journal of soil and water conservation*, 64, 43–52.
- Williams, J.R., 1975. Sediment-yield prediction with universal equation using runoff energy factor. *ARS-S.*, 40, 244.
- Wischmeier, W.H., Mannering, J., 1969. Relation of soil properties to its erodibility. *Soil Science Society of America Journal*, 33, 131–137.
- Wischmeier, W.H., Smith, D.D., 1965. Predicting rainfall-erosion losses from cropland east of the Rocky Mountains: Guide for selection of practices for soil and water conservation. US Department of Agriculture.
- Wischmeier, W.H., Smith, D.D., 1978. Predicting rainfall erosion losses: a guide to conservation planning. Department of Agriculture, Science and Education Administration.
- Zhang, T., 2005. Influence of the seasonal snow cover on the ground thermal regime: An overview. *Reviews of Geophysics*, 43.
- Zhang, Y., Degroote, J., Wolter, C., Sugumaran, R., 2009. Integration of Modified Universal Soil Loss Equation (MUSLE) into a GIS framework to assess soil erosion risk. *Land Degradation & Development*, 20, 84–91.

## CONCLUSIONS

### **Synthesis and Concluding Discussions**

This thesis provides the synthesis of our work and research contribution to cold regions hydrology. Our research diagnosed and assessed the climate sensitivity of the hydrological cycle of two cold region catchments with distinct biophysical and climate conditions in eastern Canada. This dissertation also provides key estimations of the current soil erosion and its response to climate change scenarios in the agriculture dominated catchment. Key aspects of the methodology implemented in this thesis include: 1) the inclusion of the major hydrological processes found in cold agroforested landscapes for the first time in a single modelling framework, such as blowing snow redistribution, sublimation, and infiltration into frozen soils; 2) the simulation of the key hydrological processes found in a humid boreal forest environment, such as snow interception by canopy and sublimation, which was ignored in previous studies performed in eastern Canada; 3) the coupling of the runoff outputs from a physically based hydrological model with an empirical soil loss equation to assess the sediment yield; 4) the application of a climate sensitivity framework for assessment of potential hydrological changes and their driving processes under a wide range of climate change scenarios.

The main conclusions regarding the specific objectives proposed in Introduction are presented below.

**Objective 1:** Investigate the main hydrological processes over a historical period for an agroforested catchment and a forested catchment in southern Québec and examine their response to projected changes in temperature and precipitation.

The first step to accomplish this objective was to build a physically based hydrological model using Cold Regions Hydrological Modelling platform (CRHM) to simulate the key hydrological processes for the agroforested Acadie River Catchment over the 1996–2019 period (Chapter I) and forested Montmorency River Catchment over the 2005–2019 period (Chapter II). The novelty of the hydrological models built in Chapter I and Chapter II lies in the fact that they are the first physically based hydrological model that couples all the key hydrological processes specific to agroforested environments (Chapter I) and eastern Canadian boreal forests (Chapter II). The hydrological models properly represented snow accumulation and melt processes from snow survey records and daily stream streamflow over the historical periods (Chapter I and Chapter II). In order to examine the first order impacts of climate change on hydrological state variables, the long-term temperature and precipitation observation data sets were perturbed based on ensemble climate model projections (Chapter I and Chapter II).

Chapter I has revealed that snow erosion from agricultural fields of the Acadie River Catchment (2% of historical annual snowfall) is considerably lower than those in the prairies and steppe environments where snow erosion rates range from 30 to 75% of annual snowfall (Pomeroy et al. 1993, Tabler 1975), due to higher bond strength and cohesion of snow resulting from relatively higher winter air temperatures in the Acadie River Catchment, which in turn leads to higher wind speed thresholds required to initiate snow saltation. The simulated average peak SWE was found to be slightly lower in agricultural fields than in forests in the Acadie River Catchment (Chapter I). However, the snow accumulation in these two landscape units become uniform when warming reaches 2 °C (Chapter I), explained by the change in blowing snow transport in response to warming: less snow is eroded from agriculture fields and deposited in forests under warmer temperatures. Under reference climate conditions, snowpack sublimation (9% of the annual snowfall) dominates the total sublimation in the Acadie River Catchment (Chapter I). On the other hand, sublimation from intercepted

snow (21% of the annual snowfall) is the major sublimation component in the forested Montmorency River Catchment (Chapter II). This canopy interception sublimation, however, is below the canopy sublimation losses (25–45%) simulated for the boreal forests in western Canada (Essery and Pomeroy 2001, MacDonald et al. 2010, Pomeroy and Gray 1995, Pomeroy et al. 1998). This is mostly because of the humid climate of the Montmorency River Catchment, which limits the sublimation losses (Essery and Pomeroy 2001). Compared to the reference climate conditions, the total sublimation ratios are higher in both catchments under warmer temperatures (Chapter II), suggesting that sublimation is a more efficient snow removal process under warmer temperatures. It is important to highlight that these are the first modelled estimates of snow sublimation in Québec.

Chapter I discussed in detail the response of infiltration to changing climate in the Acadie River Catchment. The falsification of frozen soil infiltration processes resulted in drastic declines in surface runoff ratios (Chapter I), suggesting that this process is very influential on the partitioning between surface and subsurface flows and overall streamflow generation in catchments with extensive subsurface tile drainage such as the Acadie River. Under reference climate conditions, infiltration rates during the cold season are found to be governed by rainfall infiltration rather than snowmelt infiltration in Acadie River Catchment (Chapter I), since frozen soil algorithm limits the snowmelt infiltration (Gray et al. 2001). Warming air temperature causes higher rainfall ratios and more frequent mid-winter melt events, leading the higher initial soil moisture saturation before snowmelt events (Chapter I). As a result, winter snowmelt infiltration ratio decreases in response to warming air temperatures in Acadie River Catchment. Snowmelt infiltration in spring also declines with warming, explained with declining snow accumulation and melt available for infiltration (Chapter I). On the other hand, warming causes an increase in the rainfall infiltration ratio particularly in winter, due the increase in rainfall fraction and the fact that rainfall infiltration is not limited by the snow cover (Gray et al. 2001). The annual surface runoff ratio decreases in

response to warming in Acadie River Catchment, which is mostly explained with changes in winter and spring conditions rather than the changes in warm season (Chapter I).

**Objective 2:** Examine the difference in climate sensitivity of the hydrology of two contrasted catchments.

Chapter II explored the difference in climate sensitivity between a rugged and forested landscape with cold/humid climate (Montmorency) and an agroforested and flat landscape with warmer/less humid climate (Acadie). In order to explore the respective roles of the dominant biophysical conditions and current climates on the climate sensitivity of hydrological responses, a set of climate sensitivity analyses were performed in which the historical climates of both basins were permuted. Historical (2005–2019) time series of air temperature and precipitation of the Acadie River Catchment were thus used as meteorological inputs for the Montmorency River Catchment and vice-versa.

Chapter II has shown that warming impacts on snow accumulation and associated changes in streamflow regime are more evident in the Acadie River Catchment, which has currently milder cold season temperatures. The results suggest that the transition in the hydrological regime of the Acadie River Catchment towards a more rainfall-dominated regime will occur sooner than that of the Montmorency River Catchment. Permuted baseline climate experiments showed that the climate sensitivity of peak SWE depends on the regional baseline climate and is little influenced by catchment biophysiology. The peak SWE sensitivity to warming and wetting is much more pronounced when both catchments are forced by the warmer and drier Acadie baseline climate, than by the colder and more humid Montmorency climate. Next, this research has shown that biophysical conditions could also play a significant role on the response of hydrological variables, particularly streamflow, to climate

change, which has not been addressed in previous studies. When forced by the colder Montmorency climate, peak discharge increases in the Acadie while slightly decreasing in Montmorency. The more porous forested soils of Montmorency are found to attenuate increases in runoff amounts and extremes, promoting reduced peak flow compared to the more impervious agroforested Acadie. When both catchments are forced by common climate conditions, the annual peak specific flow is higher in Acadie River Catchment, which shows that the reduced infiltration and storage capacity of agricultural soils favor runoff, despite the lower slopes compared to Montmorency.

**Objective 3:** Assess the potential impacts of climate change on soil erosion in the Acadie River Catchment.

Chapter III first diagnosed the monthly, seasonal and annual sediment yields eroded from the agricultural fields for the historical period and then assessed their sensitivity to climate change. We used the Modified Universal Soil Loss Equation (MUSLE) for which the runoff variables were transferred from a physically based hydrological model previously built and validated for the catchment, providing an increased realism of MUSLE-based sediment yield estimations. Two runoff scenarios (scenario a and scenario b) were considered in order to represent possible pathways of sediment export. While scenario a represents a baseline scenario in which soil erosion occurs due to surface runoff only, scenario b is more realistic since it assumed that tile drains also contribute to sediment export, but with a varying efficiency throughout the year. The calibration and validation of the tile efficiency factors against measurements in 2009–2015 for scenario b suggested that tile drains export the sediments with an efficiency of 20% and 50% in freezing and non-freezing conditions, respectively. Results indicated that tile drains account for 39% of the total annual sediment yield in the present climate.

The timing of highest soil erosion is projected to shift from spring to winter in response to warming and wetting, which can be explained by increasing winter runoff caused by shifting snowmelt timing towards winter, a greater number of mid-winter melt events as well as increasing rainfall fractions. The large uncertainties in precipitation projections cascade down to the erosion uncertainties in the more realistic scenario b, with annual sediment yield increasing or decreasing according to the precipitation uncertainty in a given climate change scenario. This study demonstrates the benefit of conservation and no-till practices, which could reduce the annual sediment yields by 20% and 60%, respectively, under any given climate change scenario.

### **Concluding Remarks**

In this research, two spatially distributed and physically based hydrological models suitable for two unique landscapes of southern Québec were developed using the Cold Regions Hydrological Model platform (CRHM, Pomeroy et al. 2007a). These hydrological models provide a comprehensive understanding of the hydrological processes controlling the water cycling in different biophysical conditions of southern Québec as they include all the major hydrological processes found in an agroforested and a forested catchment, such as blowing snow redistribution and sublimation, sublimation from canopy intercepted snowfall, snowpack sublimation, snowmelt, infiltration into frozen and unfrozen soils, evapotranspiration and streamflow routing. This study represents a step forward for a comprehensive understanding of the interactions between these processes and their impact on hydrological regime under historical and future climate conditions as previous studies in Québec lack the representation of some of these processes, such as blowing snow redistribution and sublimation, snowfall interception by canopy and infiltration to frozen soils, or/and simple parametric approaches such as the degree day method for simulating snowmelt. Despite a few studies (e.g. Gombault et al. 2015b, Novotná et al. 2014, Ricard and Ancil 2019), most hydrological model applications in Québec have been more

conceptual, resting on multiple parameters calibrated at once on streamflow. This increases the risk that process sensitivity may be ill-represented. The climate sensitivity framework used in this study enabled us to understand how key hydrological processes could shift under a wide range of climate change scenarios in different biophysical conditions in southern Québec and how these shifts can modulate hydrological regimes, which is one of the main strengths of the study as no previous study in Québec performed climate sensitivity analyses.

The results of this study have shown that despite the apparent proximity (<400 km) of Acadie River Catchment and Montmorency River Catchment, their hydrological processes and regimes show remarkably different sensitivities to climate change. The hydrology of the Acadie River Catchment characterized by a milder climate has been found to be very sensitive to warming, whereas the hydrology of the Montmorency River Catchment shows some resilience to changing climate. This finding is in agreement with the previous studies which project more drastic changes to occur over relatively mild cold regions compared to the colder regions (Aygün et al. 2020). Permuted baseline climate experiments in Chapter II have demonstrated that while the regional climate conditions are primary drivers of the hydrological responses of the catchments to climate change, biophysical characteristics can alter the response of peak discharge to a common external climate change forcing. This suggests that analyzing the hydrological responses of one catchment to climate change to generalize over a larger region can lead to overly simplistic conclusions (Teutschbein et al. 2015) and turn hydrological sensitivity studies into gambling “just throwing a dice” (Blöschl and Montanari 2010). Given this “uniqueness of place” (Beven 2000), we suggest research and modelling efforts to be tailored to each particular catchment in order for the results to be useful for water managers.

There is a possibility for increased flood risks in spring in the near future (2020–2070) given limited warming and uncertainties in precipitation projections, while longer-term

warming was found to deplete the snowpack and reduce peak streamflow in both catchments. These results are particularly interesting considering the recent flood events in southern Québec (Lin et al. 2019, Rondeau-Genesse 2020, Teufel et al. 2019), versus the long-term projection of reducing SWE and peak discharge. Yet, our study suggests that the transition in the hydrological regime of the Acadie River Catchment towards a more rainfall-dominated regime will occur sooner than that of the Montmorency River Catchment. Greater winter flows simulated for both catchments can increase the potential for ice-jam floods, which can generate more damage compared to open water floods (Beltaos and Prowse 2009, Morse and Turcotte 2018). These results suggest for renewed assessments of flood risk management strategies. Due to the changes in streamflow regime and volume, managers may have to adopt new operation strategies for the dams and reservoirs located along the Montmorency River. On the other hand, agricultural production in the Acadie River Catchment could increase as warmer temperatures can extend the farming season by declining snow cover duration. The overall agricultural production could also benefit from the increase in annual available water in response to increasing precipitation.

Future changes in sediment yield in Acadie River Catchment appear more significant in the winter due to increased winter runoff caused by earlier snowmelt, a greater number of mid-winter melt events as well as increased rainfall fractions. The implementation of soil conservation practices, which ensure a soil residue cover in winter, is found to be an effective strategy for soil protection in the context of climate change (Chapter III). The results obtained in Chapter III indicate that the warmer and wetter climate could lead to increased or decreased annual sediment yield, depending on the contribution of the tile drains to total sediment load. This uncertainty highlights the need for better understanding and quantifying the relative importance of subsurface drainage as a pathway for movement of sediment in cold humid agricultural catchments. Notwithstanding, the future annual sediment yields are found to be lower than the suggested tolerable soil loss rates for most Canadian soils (i.e.  $6 \text{ t ha}^{-1} \text{ year}^{-1}$ ) (Wall

et al. 2002)). Anyhow, the recommended erosion tolerability value is only an approximation and can vary regionally depending on many factors such as the rate of soil formation from parent material, reduction of crop yield by erosion, soil profile thickness etc. (Li et al. 2009). For example, the productivity and sustainability of shallow organic soils in the Acadie River Catchment (<1.5 m locally (Hallema et al. 2015)) could be threatened even with small amount of losses. This can hinder the economy of the region as these fertile organic soils are devoted for horticultural crop production. Next, the concept of tolerable soil does not reach a comprehensive environmental approach as it neglects the off-site effects (Bazzoffi 2009). Therefore, we argue that eroded sediments from the agricultural fields of the Acadie River Catchment can still threaten the survival of the aquatic life even if erosion rates are below the suggested values.

## **Outlook**

Many of the subjective choices made in hydrological and soil erosion modelling in this thesis can have a significant impact on the magnitude of the output uncertainty. The separation of precipitation into rainfall or snowfall is one of the most sensitive parameterizations in simulating cold regions hydrological processes Harder and Pomeroy (2013). Underestimation (overestimation) of rainfall can advect less (more) energy to snowpack, decrease (increase) snowpack liquid content, lead to earlier (later) warming and ripening and in turn impact the magnitude and timing of snowmelt streamflow peak flow. In this thesis, the total precipitation was partitioned between liquid and solid precipitation using a psychometric energy balance method proposed by Harder and Pomeroy (2013). Rainfall fraction was calculated as a function of the temperature of falling precipitation estimated using the air temperature and relative humidity. There are in situ record of precipitation phase in BEREV watershed within the Montmorency River Catchment (Pierre et al. 2019), therefore, future studies can use locally derived or calibrated air temperature-precipitation phase relationships to

reduce the error in phase partitioning. Next, due to the lack of data, some of the model parameters in the hydrological models built in Chapter I and Chapter II were transferred from studies in catchments with similar biophysical and hydrological conditions, which introduces uncertainties to the hydrological models. Also, soil erodibility factor of the organic soil is assumed to be the highest among all Québec soils as no factor has been provided for this soil type by IRDA. This assumption leads to an uncertainty in the erosion estimate for this soil type. Future studies therefore should perform detailed sensitivity analyses to quantify the uncertainty in hydrological simulations and soil erosion estimates due to parameter uncertainty.

While this study had an important focus on the representation of hydrological processes found in cold environments of southern Québec by implementing the physically based algorithms within the Cold Regions Hydrological Model platform (CRHM), future applications should explore further improvements to existing algorithms used for representing certain hydrological processes such as infiltration into froze soils. The frozen soil infiltration parametrization used in our hydrological models (Gray et al. 2001) is a simplified representation of this process. The algorithm of Gray et al. (2001) calculates the amount of infiltration to frozen soil assuming a fixed soil temperature at the start of each snowmelt period throughout the simulation period, therefore the interactions between the snow cover and soil temperature are not taken into account. This is considered to be an important aspect in the context of climate change as the climate change related declines in snow depth might result in (more) soil freezing depending on the air temperature (Aygün et al. 2020). Therefore, there is a need for a more elaborate frozen soil treatment in future studies. This could be done by coupling the hydrological models built in this study with a physically based soil model, such as SHAW (Flerchinger 2000) or SNTHERM (Frankenstein et al. 2008) which can account for mass and energy exchanges between the soil and snowpack. While the CRHM platform allows defining any river and surface runoff drainage network, it does not account for the subsurface drainage systems. Therefore, in the hydrological model built

for the Acadie River Catchment, the effect of subsurface drainage was emulated by adding the saturation excess water in soils to subsurface flow in the agricultural fields. Future studies are needed to extend to the hydrological model developed in this study to include an explicit representation of the tile drainage networks in the agricultural fields, similar to SWAT (Soil and Water Assessment Tool) model (Du et al. 2005). However, then the challenge would be mapping of the locations and geometrical properties of all the tile drains beneath the agricultural fields. Also, a representation of the whole drainage network in the model might result in long model simulation times. Alternatively, the drainage network can be simplified by considering only the main collecting pipes of the network (De Schepper et al. 2015). Inclusion of the tile drains in the modelling would help better understanding the subsurface water dynamics as well as better quantifying the subsurface runoff as a pathway for sediment transport.

Modified universal soil loss equation (MUSLE) replaces the rainfall energy factor (in USLE/RUSLE) with a runoff factor. Therefore, coupling of the MUSLE equation with the runoff outputs from a physically based hydrological model is considered to be an improvement to the previous application of RUSLE to estimate potential soil loss rates in the Acadie River Catchment (Clubs-conseils en agroenvironnement 2014) as runoff is an integrated output of hydrological meteorological processes including rainfall energy at a catchment or hydrological response unit (HRU) scale. However, neither MUSLE nor RUSLE accounts for the effects of gully and streambank erosion. Future research is therefore required to extend the hydrological model built for the Acadie River Catchment to include physically based channel erosion and sediment transport modules within the CRHM platform along with the internally coupled MUSLE equation.

The climate sensitivity framework used in this study only considers mean changes in air temperature and precipitation; therefore, any future changes in precipitation intensity, frequency, duration, number and length of wet and dry spells are not

represented. All precipitation amounts were changed by the same amount. However, research indicates that global warming will modify the occurrence of extreme precipitation events. For instance, return periods of extreme rainfall events in southern Québec are projected to be halved in future climate (2041–2070) compared to the reference climate (1961–1990) (Mailhot et al. 2007). Therefore, our results might rather underestimate the future flood events resulting from more powerful rain and snowstorms. Projected increases in soil erosion rates might also be rather conservative since the increases in rainfall intensity were not incorporated in this thesis. Next, a shift in rainfall season, or a lengthening of the dry season could have important implications for the seasonal distribution of the soil moisture, and in turn, on the capacity of a catchment to absorb rainfall or alternatively, to be saturated and generate larger floods (Prudhomme et al. 2010). Future investigation is therefore required to incorporate future modifications in rainfall patterns in the climate sensitivity framework developed in this study. This can be done by using a series of climate projections derived from regional scale climate models by Ouranos (Rondeau-Genesse and Braun 2020) as inputs for the hydrological models developed in this study in order to assess the changes in catchment hydrology and soil erosion.

## REFERENCES

- Abbot, M., Bathurst, J., Cunge, J., O'Connell, P. and Rasmussen, J. (1986) An introduction to the European hydrological system "SHE", 2. Structure of a physically based, distributed modelling system. *Journal of Hydrology* 87, 61–77.
- Allen, M.R., Barros, V.R., Broome, J., Cramer, W., Christ, R., Church, J.A., Clarke, L., Dahe, Q., Dasgupta, P. and Dubash, N.K. (2014) IPCC fifth assessment synthesis report-climate change 2014 synthesis report.
- Andersen, H.E., Kronvang, B., Larsen, S.E., Hoffmann, C.C., Jensen, T.S. and Rasmussen, E.K. (2006) Climate-change impacts on hydrology and nutrients in a Danish lowland river basin. *Science of the Total Environment* 365(1–3), 223–237.
- Andersland, O.B. and Ladanyi, B. (2004) *Frozen ground engineering*, John Wiley & Sons.
- Arheimer, B., Andréasson, J., Fogelberg, S., Johnsson, H., Pers, C.B. and Persson, K. (2005) Climate change impact on water quality: model results from southern Sweden. *AMBIO: A Journal of the Human Environment* 34(7), 559–566.
- Arheimer, B., Donnelly, C. and Strömqvist, J. (2013) Large-scale effects of climate change on water resources in Sweden and Europe. *VATTEN: Journal of Water Management and Research* 69, 201–207.
- Armstrong, R.L. and Brun, E. (2008) *Snow and climate. Physical Processes, Surface Energy Exchange and Modeling*. Cambridge University Press, Cambridge, UK.
- Arnold, J.G., Srinivasan, R., Mutiah, R.S. and Williams, J.R. (1998) Large area hydrologic modeling and assessment part I: model development I. *JAWRA Journal of the American Water Resources Association* 34(1), 73–89.
- Asare, S., Rudra, R., Dickinson, W. and Wall, G. (1999) Effect of freeze–thaw cycle on the parameters of the Green and Ampt infiltration equation. *Journal of agricultural engineering research* 73(3), 265–274.

- Aygün, O., Kinnard, C. and Campeau, S. (2020) Impacts of climate change on the hydrology of northern midlatitude cold regions. *Progress in Physical Geography: Earth and Environment* 44(3), 338–375.
- Barnett, T.P., Adam, J.C. and Lettenmaier, D.P. (2005) Potential impacts of a warming climate on water availability in snow-dominated regions. *Nature* 438(7066), 303–309.
- Bates, R.E. and Bilello, M.A. (1966) Defining the cold regions of the northern hemisphere USA Cold Regions Research and Engineering Laboratory.
- Bazzoffi, P. (2009) Soil erosion tolerance and water runoff control: minimum environmental standards. *Regional Environmental Change* 9(3), 169–179.
- Beldring, S., Engen-Skaugen, T., Førland, E.J. and Roald, L.A. (2008) Climate change impacts on hydrological processes in Norway based on two methods for transferring regional climate model results to meteorological station sites. *Tellus A: Dynamic Meteorology and Oceanography* 60(3), 439–450.
- Beltaos, S. (2003) Threshold between mechanical and thermal breakup of river ice cover. *Cold Regions Science and Technology* 37(1), 1–13.
- Beltaos, S. and Prowse, T. (2009) River-ice hydrology in a shrinking cryosphere. *Hydrological Processes: An International Journal* 23(1), 122–144.
- Benson, C., Abichou, T., Olson, M. and Bosscher, P. (1995) Winter effects on hydraulic conductivity of compacted clay. *Journal of Geotechnical Engineering* 121(1), 69–79.
- Beven, K. (1997) *Distributed modelling in hydrology: applications of TOPMODEL*. Chichester: Wiley.
- Beven, K. and Freer, J. (2001) A dynamic topmodel. *Hydrological Processes* 15(10), 1993–2011.
- Beven, K.J. (2000) Uniqueness of place and process representations in hydrological modelling. *Hydrol. Earth Syst. Sci.* 4(2), 203–213.
- Blöschl, G. and Montanari, A. (2010) Climate change impacts—throwing the dice? *Hydrological Processes: An International Journal* 24(3), 374–381.
- Blöschl, G., Viglione, A. and Montanari, A. (2013) Emerging approaches to hydrological risk management in a changing world. *Climate Vulnerability: Understanding and Addressing Threats to Essential Resources*, 3–10.

- Boyer, C., Chaumont, D., Chartier, I. and Roy, A.G. (2010) Impact of climate change on the hydrology of St. Lawrence tributaries. *Journal of Hydrology* 384(1–2), 65–83.
- Brown, R.D. and Mote, P.W. (2009) The response of Northern Hemisphere snow cover to a changing climate. *Journal of Climate* 22(8), 2124–2145.
- Ciarapica, L. and Todini, E. (2002) TOPKAPI: A model for the representation of the rainfall-runoff process at different scales. *Hydrological Processes* 16(2), 207–229.
- Clark, M.P., Nijssen, B., Lundquist, J.D., Kavetski, D., Rupp, D.E., Woods, R.A., Freer, J.E., Gutmann, E.D., Wood, A.W. and Brekke, L.D. (2015) A unified approach for process-based hydrologic modeling: 1. Modeling concept. *Water Resources Research* 51(4), 2498–2514.
- Clubs-conseils en agroenvironnement (2014) Rapport de caractérisation du bassin versant « amont » de la rivière L'Acadie, pp. 1–127, Club Techno-Champ 2000, QC, Canada.
- Craig, J.R., Brown, G., Chlumsky, R., Jenkinson, W., Jost, G., Lee, K., Mai, J., Serrer, M., Snowdon, A.P. and Sgro, N. (2020) Flexible watershed simulation with the Raven hydrological modelling framework. *Environmental Modelling & Software*, 104728.
- Dayyani, S., Prasher, S., Madani, A. and Madramootoo, C. (2012) Impact of climate change on the hydrology and nitrogen pollution in a tile-drained agricultural watershed in Eastern Canada. *Transactions of the ASABE* 55(2), 389–401.
- De Schepper, G., Therrien, R., Refsgaard, J.C. and Hansen, A.L. (2015) Simulating coupled surface and subsurface water flow in a tile-drained agricultural catchment. *Journal of Hydrology* 521, 374–388.
- DeBeer, C.M. and Pomeroy, J.W. (2017) Influence of snowpack and melt energy heterogeneity on snow cover depletion and snowmelt runoff simulation in a cold mountain environment. *Journal of Hydrology* 553, 199–213.
- Deelstra, J., Øygarden, L., Blankenberg, A.-G.B. and Eggestad, H.O. (2015) Climate change and runoff from agricultural catchments in Norway. *New Perspectives in Climate Change*, 1.
- Devia, G.K., Ganasri, B. and Dwarakish, G. (2015) A review on hydrological models. *Aquatic Procedia* 4, 1001–1007.

- DeWalle, D.R. and Rango, A. (2008) Principles of snow hydrology, Cambridge University Press, Cambridge, UK.
- Diffenbaugh, N.S., Scherer, M. and Ashfaq, M. (2013) Response of snow-dependent hydrologic extremes to continued global warming. *Nature climate change* 3(4), 379–384.
- Dingman, S.L. (2015) Physical hydrology, Waveland press.
- Dripps, W. (2012) An integrated field assessment of groundwater recharge. *Open Hydrology Journal* 6, 15–22.
- Dripps, W. and Bradbury, K. (2010) The spatial and temporal variability of groundwater recharge in a forested basin in northern Wisconsin. *Hydrological Processes* 24(4), 383–392.
- Du, B., Arnold, J., Saleh, A. and Jaynes, D. (2005) Development and application of SWAT to landscapes with tiles and potholes. *Transactions of the ASAE* 48(3), 1121–1133.
- Essery, R., Li, L. and Pomeroy, J. (1999) A distributed model of blowing snow over complex terrain. *Hydrological Processes* 13(1415), 2423–2438.
- Essery, R. and Pomeroy, J. (2001) Sublimation of snow intercepted by coniferous forest canopies in a climate model, pp. 343–348, IAHS PUBLICATION, Maastricht, Netherlands.
- Essery, R. and Pomeroy, J. (2004) Vegetation and topographic control of wind-blown snow distributions in distributed and aggregated simulations for an Arctic tundra basin. *Journal of Hydrometeorology* 5(5), 735–744.
- Fang, X. and Pomeroy, J.W. (2020) Diagnosis of future changes in hydrology for a Canadian Rockies headwater basin. *Hydrology and Earth System Sciences* 24(5), 2731–2754.
- Feng, S. and Hu, Q. (2007) Changes in winter snowfall/precipitation ratio in the contiguous United States. *Journal of Geophysical Research: Atmospheres* 112(D15).
- Ferrick, M. and Gatto, L.W. (2005) Quantifying the effect of a freeze–thaw cycle on soil erosion: laboratory experiments. *Earth Surface Processes and Landforms* 30(10), 1305–1326.

- Flerchinger, G.N. (2000) The simultaneous heat and water (SHAW) model: Technical documentation. Northwest Watershed Research Center USDA Agricultural Research Service, Boise, Idaho.
- Fouli, Y., Cade-Menun, B.J. and Cutforth, H.W. (2013) Freeze—thaw cycles and soil water content effects on infiltration rate of three Saskatchewan soils. *Canadian Journal of Soil Science* 93(4), 485–496.
- Frankenstein, S., Sawyer, A. and Koeberle, J. (2008) Comparison of FASST and SNTherm in three snow accumulation regimes. *Journal of Hydrometeorology* 9(6), 1443–1463.
- French, H.M. and Slaymaker, O. (1993) *Canada's cold environments*, McGill-Queen's Press-MQUP.
- Gariépy, S., Ruiz, J., Comtois, S. and Zingraff, V. (2016) Multiscale modelling as a tool for sharing the perspectives of researchers practitioners and farmers on beneficial management practices to be adopted in an intensive agricultural watershed, pp. 12–15.
- Gelfan, A., Pomeroy, J. and Kuchment, L. (2004) Modeling forest cover influences on snow accumulation, sublimation, and melt. *Journal of Hydrometeorology* 5(5), 785–803.
- Gelfan, A.N. and Motovilov, Y.G. (2009) Long-term Hydrological Forecasting in Cold Regions: Retrospect, Current Status and Prospect. *Geography Compass* 3(5), 1841–1864.
- Gollamudi, A., Madramootoo, C. and Enright, P. (2007) Water quality modeling of two agricultural fields in southern Quebec using SWAT. *Transactions of the ASABE* 50(6), 1973–1980.
- Gombault, C., Madramootoo, C., Michaud, A., Beaudin, I., Sottile, M., Chikhaoui, M. and Ngwa, F. (2015a) Impacts of climate change on nutrient losses from the Pike River watershed of southern Québec. *Canadian Journal of Soil Science* 95(4), 337–358.
- Gombault, C., Sottile, M.-F., Ngwa, F.F., Madramootoo, C.A., Michaud, A.R., Beaudin, I. and Chikhaoui, M. (2015b) Modelling climate change impacts on the hydrology of an agricultural watershed in southern Québec. *Canadian Water Resources Journal/Revue canadienne des ressources hydriques* 40(1), 71–86.
- Gray, D. and Landine, P. (1988) An energy-budget snowmelt model for the Canadian Prairies. *Canadian Journal of Earth Sciences* 25(8), 1292–1303.

- Gray, D., Toth, B., Zhao, L., Pomeroy, J. and Granger, R. (2001) Estimating areal snowmelt infiltration into frozen soils. *Hydrological Processes* 15(16), 3095–3111.
- Gray, D.M. and Granger, R.J. (1987) Frozen soil: the problem of snowmelt infiltration. *Infiltration Development and Application*. Water Resources Research Center, University of Hawaii at Manoa, Honolulu, Hawaii, 179–188.
- Groffman, P.M., Driscoll, C.T., Fahey, T.J., Hardy, J.P., Fitzhugh, R.D. and Tierney, G.L. (2001) Colder soils in a warmer world: a snow manipulation study in a northern hardwood forest ecosystem. *Biogeochemistry* 56(2), 135–150.
- Guay, C., Minville, M. and Braun, M. (2015) A global portrait of hydrological changes at the 2050 horizon for the province of Québec. *Canadian Water Resources Journal/Revue canadienne des ressources hydriques* 40(3), 285–302.
- Hallema, D.W., Périard, Y., Lafond, J.A., Gumiere, S.J. and Caron, J. (2015) Characterization of water retention curves for a series of cultivated Histosols. *Vadose Zone Journal* 14(6), 1–8.
- Harder, P. and Pomeroy, J. (2013) Estimating precipitation phase using a psychrometric energy balance method. *Hydrological Processes* 27(13), 1901–1914.
- Harder, P., Pomeroy, J.W. and Westbrook, C.J. (2015) Hydrological resilience of a Canadian Rockies headwaters basin subject to changing climate, extreme weather, and forest management. *Hydrological Processes* 29(18), 3905–3924.
- Hayhoe, H., Coote, D. and Pelletier, R. (1992) Soil erodibility and the frequency of freeze-thaw cycles, rainfall and snowmelt on frozen soil in Canada. *Climatological Bulletin* 26(1), 3–15.
- Hayhoe, K., Wake, C.P., Huntington, T.G., Luo, L., Schwartz, M.D., Sheffield, J., Wood, E., Anderson, B., Bradbury, J. and DeGaetano, A. (2007) Past and future changes in climate and hydrological indicators in the US Northeast. *Climate Dynamics* 28(4), 381–407.
- Henry, H.A. (2008) Climate change and soil freezing dynamics: historical trends and projected changes. *Climatic Change* 87(3), 421–434.
- Hicks, F. (2009) An overview of river ice problems. *Cold Regions Science and Technology* 55, 175–185.

- Hosaka, M., Nohara, D. and Kitoh, A. (2005) Changes in snow cover and snow water equivalent due to global warming simulated by a 20km-mesh global atmospheric model. *Sola* 1, 93–96.
- Hu, Z., Kuenzer, C., Dietz, A.J. and Dech, S. (2017) The Potential of Earth Observation for the Analysis of Cold Region Land Surface Dynamics in Europe—A Review. *Remote Sensing* 9(10), 1067.
- Huntington, J.L. and Niswonger, R.G. (2012) Role of surface-water and groundwater interactions on projected summertime streamflow in snow dominated regions: An integrated modeling approach. *Water Resources Research* 48(11).
- Huziy, O., Sushama, L., Khaliq, M., Laprise, R., Lehner, B. and Roy, R. (2013) Analysis of streamflow characteristics over Northeastern Canada in a changing climate. *Climate Dynamics* 40(7–8), 1879–1901.
- Ireson, A., Van Der Kamp, G., Ferguson, G., Nachshon, U. and Wheeler, H. (2013) Hydrogeological processes in seasonally frozen northern latitudes: understanding, gaps and challenges. *Hydrogeology Journal* 21(1), 53–66.
- Jobin, B., Latendresse, C., Baril, A., Maisonneuve, C., Boutin, C. and Côté, D. (2014) A half-century analysis of landscape dynamics in southern Québec, Canada. *Environmental monitoring and assessment* 186(4), 2215–2229.
- Jones, R.N., Chiew, F.H., Boughton, W.C. and Zhang, L. (2006) Estimating the sensitivity of mean annual runoff to climate change using selected hydrological models. *Advances in Water Resources* 29(10), 1419–1429.
- Jyrkama, M.I. and Sykes, J.F. (2007) The impact of climate change on spatially varying groundwater recharge in the grand river watershed (Ontario). *Journal of Hydrology* 338(3), 237–250.
- Keller, F., Goyette, S. and Beniston, M. (2005) Sensitivity analysis of snow cover to climate change scenarios and their impact on plant habitats in alpine terrain. *Climatic Change* 72(3), 299–319.
- Kellomäki, S., Maajärvi, M., Strandman, H., Kilpeläinen, A. and Peltola, H. (2010) Model computations on the climate change effects on snow cover, soil moisture and soil frost in the boreal conditions over Finland. *Silva Fennica* 44(2), 213–233.
- Krasovskaia, I., Arnell, N. and Gottschalk, L. (1994) Flow regimes in northern and western Europe: development and application of procedures for classifying flow regimes. *IAHS Publications-Series of Proceedings and Reports-Intern Assoc Hydrological Sciences* 221, 185–192.

- Krogh, S.A., Pomeroy, J.W. and Marsh, P. (2017) Diagnosis of the hydrology of a small Arctic basin at the tundra-taiga transition using a physically based hydrological model. *Journal of Hydrology* 550, 685–703.
- Li, L., Du, S., Wu, L. and Liu, G. (2009) An overview of soil loss tolerance. *Catena* 78(2), 93–99.
- Li, Z. and Fang, H. (2016) Impacts of climate change on water erosion: A review. *Earth-Science Reviews* 163, 94–117.
- Lin, H., Mo, R., Vitart, F. and Stan, C. (2019) Eastern Canada flooding 2017 and its subseasonal predictions. *Atmosphere-Ocean* 57(3), 195–207.
- Lindenschmidt, K.E., Das, A., Rokaya, P. and Chu, T. (2016) Ice-jam flood risk assessment and mapping. *Hydrological Processes* 30(21), 3754–3769.
- Liston, G.E., Haehnel, R.B., Sturm, M., Hiemstra, C.A., Berezovskaya, S. and Tabler, R.D. (2007) Simulating complex snow distributions in windy environments using SnowTran-3D. *Journal of Glaciology* 53(181), 241–256.
- Liu, J., Curry, J.A., Dai, Y. and Horton, R. (2007) Causes of the northern high-latitude land surface winter climate change. *Geophysical Research Letters* 34(14).
- Lundberg, A., Ala-Aho, P., Eklo, O., Klöve, B., Kværner, J. and Stumpp, C. (2016) Snow and frost: implications for spatiotemporal infiltration patterns—a review. *Hydrological Processes* 30(8), 1230–1250.
- Lundberg, A., Nakai, Y., Thunehed, H. and Halldin, S. (2004) Snow accumulation in forests from ground and remote-sensing data. *Hydrological Processes* 18(10), 1941–1955.
- MacDonald, M., Pomeroy, J. and Pietroniro, A. (2010) On the importance of sublimation to an alpine snow mass balance in the Canadian Rocky Mountains. *Hydrology and Earth System Sciences* 14(7), 1401.
- Mahmood, T.H., Pomeroy, J.W., Wheeler, H.S. and Baulch, H.M. (2017) Hydrological responses to climatic variability in a cold agricultural region. *Hydrological Processes* 31(4), 854–870.
- Mailhot, A., Duchesne, S., Caya, D. and Talbot, G. (2007) Assessment of future change in intensity–duration–frequency (IDF) curves for Southern Quebec using the Canadian Regional Climate Model (CRCM). *Journal of Hydrology* 347(1–2), 197–210.

- Mankin, J.S., Viviroli, D., Singh, D., Hoekstra, A.Y. and Diffenbaugh, N.S. (2015) The potential for snow to supply human water demand in the present and future. *Environmental Research Letters* 10(11), 114016.
- Mazurkiewicz, A.B., Callery, D.G. and McDonnell, J.J. (2008) Assessing the controls of the snow energy balance and water available for runoff in a rain-on-snow environment. *Journal of Hydrology* 354(1), 1–14.
- Mehdi, B., Lehner, B., Gombault, C., Michaud, A., Beaudin, I., Sottile, M.-F. and Blondlot, A. (2015) Simulated impacts of climate change and agricultural land use change on surface water quality with and without adaptation management strategies. *Agriculture, Ecosystems & Environment* 213, 47–60.
- Meiers, G.P., Barbour, S.L., Qualizza, C.V. and Dobchuk, B.S. (2011) Evolution of the hydraulic conductivity of reclamation covers over sodic/saline mining overburden. *Journal of Geotechnical and Geoenvironmental Engineering* 137(10), 968–976.
- Minville, M., Brisette, F. and Leconte, R. (2008) Uncertainty of the impact of climate change on the hydrology of a nordic watershed. *Journal of Hydrology* 358(1–2), 70–83.
- Molini, A., Katul, G.G. and Porporato, A. (2011) Maximum discharge from snowmelt in a changing climate. *Geophysical Research Letters* 38(5).
- Morse, B. and Turcotte, R. (2018) Risque d'inondations par embâcles de glaces et estimation des débits hivernaux dans un contexte de changements climatiques, p. 79, Ouranos, Montreal.
- Mortsch, L., Hengeveld, H., Lister, M., Wenger, L., Lofgren, B., Quinn, F. and Slivitzky, M. (2000) Climate change impacts on the hydrology of the Great Lakes-St. Lawrence system. *Canadian Water Resources Journal* 25(2), 153–179.
- Mote, P.W. (2003) Trends in snow water equivalent in the Pacific Northwest and their climatic causes. *Geophysical Research Letters* 30(12).
- Mukundan, R., Pradhanang, S.M., Schneiderman, E.M., Pierson, D.C., Anandhi, A., Zion, M.S., Matonse, A.H., Lounsbury, D.G. and Steenhuis, T.S. (2013) Suspended sediment source areas and future climate impact on soil erosion and sediment yield in a New York City water supply watershed, USA. *Geomorphology* 183, 110–119.
- Musselman, K.N., Clark, M.P., Liu, C., Ikeda, K. and Rasmussen, R. (2017) Slower snowmelt in a warmer world. *Nature climate change* 7(3), 214–219.

- Novotná, B., van Bochove, E. and Thériault, G. (2014) Potential ecological impact of climate change on the water quality of an intensively managed agricultural watershed in Quebec, Canada. *Journal of Water and Climate Change* 5(1), 81–99.
- Okkonen, J. and Kløve, B. (2010) A conceptual and statistical approach for the analysis of climate impact on ground water table fluctuation patterns in cold conditions. *Journal of Hydrology* 388(1–2), 1–12.
- Orlova, J. and Branfireun, B.A. (2014) Surface water and groundwater contributions to streamflow in the James Bay Lowland, Canada. *Arctic, antarctic, and alpine research* 46(1), 236–250.
- Ouranos (2015) *Vers l'adaptation. Synthèse des connaissances sur les changements climatiques au Québec*, p. 115, Ouranos Montréal, Québec.
- Panin, G., Solomonova, I. and Vyruchalkina, T.Y. (2009) Climatic trends in the middle and high latitudes of the Northern Hemisphere. *Water resources* 36(6), 718.
- Paznekas, A. and Hayashi, M. (2016) Groundwater contribution to winter streamflow in the Canadian Rockies. *Canadian Water Resources Journal/Revue canadienne des ressources hydriques* 41(4), 484–499.
- Peel, M.C. and Blöschl, G. (2011) Hydrological modelling in a changing world. *Progress in Physical Geography* 35(2), 249–261.
- Peters, D.L., Monk, W.A. and Baird, D.J. (2014) Cold-regions Hydrological Indicators of Change (CHIC) for ecological flow needs assessment. *Hydrological Sciences Journal* 59(3–4), 502–516.
- Pierre, A., Jutras, S., Smith, C., Kochendorfer, J., Fortin, V. and Anctil, F. (2019) Evaluation of catch efficiency transfer functions for unshielded and single-alter-shielded solid precipitation measurements. *Journal of Atmospheric and Oceanic Technology* 36(5), 865–881.
- Pomeroy, J. and Brun, E. (2001) Physical properties of snow. *Snow ecology: An interdisciplinary examination of snow-covered ecosystems*, 45–126.
- Pomeroy, J. and Gray, D. (1995) Snowcover accumulation, relocation and management. *Bulletin of the International Society of Soil Science* no 88(2).
- Pomeroy, J., Gray, D., Brown, T., Hedstrom, N., Quinton, W., Granger, R. and Carey, S. (2007a) The cold regions hydrological model: a platform for basing process representation and model structure on physical evidence. *Hydrological Processes: An International Journal* 21(19), 2650–2667.

- Pomeroy, J., Gray, D., Hedstrom, N. and Janowicz, J. (2002) Physically based estimation of seasonal snow accumulation in the boreal forest, pp. 93–108.
- Pomeroy, J., Gray, D. and Landine, P. (1993) The prairie blowing snow model: characteristics, validation, operation. *Journal of Hydrology* 144(1–4), 165–192.
- Pomeroy, J., Parviainen, J., Hedstrom, N. and Gray, D. (1998) Coupled modelling of forest snow interception and sublimation. *Hydrological Processes* 12(15), 2317–2337.
- Pomeroy, J. and Schmidt, R. (1993) The use of fractal geometry in modeling intercepted snow accumulation and sublimation, pp. 1–10.
- Pomeroy, J.W., de Boer, D. and Martz, L.W. (2007b) *Hydrology and water resources. Saskatchewan: geographic perspectives*, 63–80.
- Pradhanang, S.M., Mukundan, R., Schneiderman, E.M., Zion, M.S., Anandhi, A., Pierson, D.C., Frei, A., Easton, Z.M., Fuka, D. and Steenhuis, T.S. (2013) Streamflow responses to climate change: Analysis of hydrologic indicators in a New York City water supply watershed. *JAWRA Journal of the American Water Resources Association* 49(6), 1308–1326.
- Quilbé, R., Rousseau, A.N., Moquet, J.-S., Trinh, N.B., Dibike, Y., Gachon, P. and Chaumont, D. (2008) Assessing the effect of climate change on river flow using general circulation models and hydrological modelling—Application to the Chaudière River, Quebec, Canada. *Canadian Water Resources Journal* 33(1), 73–94.
- Räisänen, J. (2008) Warmer climate: less or more snow? *Climate Dynamics* 30(2–3), 307–319.
- Räisänen, J. and Eklund, J. (2012) 21st century changes in snow climate in Northern Europe: a high-resolution view from ENSEMBLES regional climate models. *Climate Dynamics* 38(11–12), 2575–2591.
- Rasouli, K., Pomeroy, J.W., Janowicz, J.R., Carey, S.K. and Williams, T.J. (2014) Hydrological sensitivity of a northern mountain basin to climate change. *Hydrological Processes* 28(14), 4191–4208.
- Rasouli, K., Pomeroy, J.W. and Marks, D.G. (2015) Snowpack sensitivity to perturbed climate in a cool mid-latitude mountain catchment. *Hydrological Processes* 29(18), 3925–3940.

- Rasouli, K., Pomeroy, J.W. and Whitfield, P.H. (2019) Hydrological responses of headwater basins to monthly perturbed climate in the North American cordillera. *Journal of Hydrometeorology* 20(5), 863–882.
- Ricard, S. and Anctil, F. (2019) Forcing the Penman-Montheith Formulation with Humidity, Radiation, and Wind Speed Taken from Reanalyses, for Hydrologic Modeling. *Water* 11(6), 1214.
- Rivard, C., Paniconi, C., Vigneault, H. and Chaumont, D. (2014) A watershed-scale study of climate change impacts on groundwater recharge (Annapolis Valley, Nova Scotia, Canada). *Hydrological Sciences Journal* 59(8), 1437–1456.
- Rondeau-Genesse, G. (2020) Réduire la vulnérabilité aux inondations et à l'érosion associées aux changements climatiques pour des communautés riveraines du tronçon fluvial du Saint-Laurent, p. 47, Ouranos, Montréal.
- Rondeau-Genesse, G. and Braun, M. (2020) Production des scénarios climatiques pour les projets : Impact des changements climatiques sur les débits au Québec (cQ2) et la thématique Évolution du climat du projet de Soutien à INFO-Crue, p. 55, Ouranos, Montreal.
- Rousseau, A.N., Savary, S., Hallema, D.W., Gumiere, S.J. and Foulon, É. (2013) Modeling the effects of agricultural BMPs on sediments, nutrients, and water quality of the Beaurivage River watershed (Quebec, Canada). *Canadian Water Resources Journal* 38(2), 99–120.
- Shi, H. and Wang, C. (2015) Projected 21st century changes in snow water equivalent over Northern Hemisphere landmasses from the CMIP5 model ensemble. *The Cryosphere* 9(5), 1943–1953.
- Shook, K., Pomeroy, J. and van der Kamp, G. (2015) The transformation of frequency distributions of winter precipitation to spring streamflow probabilities in cold regions; case studies from the Canadian Prairies. *Journal of Hydrology* 521, 395–409.
- Shrestha, R.R., Dibike, Y.B. and Prowse, T.D. (2012) Modelling of climate-induced hydrologic changes in the Lake Winnipeg watershed. *Journal of Great Lakes Research* 38, 83–94.
- Sicart, J.-E., Pomeroy, J., Essery, R. and Bewley, D. (2006) Incoming longwave radiation to melting snow: observations, sensitivity and estimation in northern environments. *Hydrological Processes* 20(17), 3697–3708.
- Smakhtin, V.U. (2001) Low flow hydrology: a review. *Journal of Hydrology* 240(3), 147–186.

- Smith, J.B. and Mendelsohn, R.O. (2007) *The impact of climate change on regional systems: a comprehensive analysis of California*, Edward Elgar Publishing.
- Smith, J.B. and Pitts, G.J. (1997) Regional climate change scenarios for vulnerability and adaptation assessments. *Climatic Change* 36(1–2), 3–21.
- Sproles, E., Nolin, A., Rittger, K. and Painter, T. (2013) Climate change impacts on maritime mountain snowpack in the Oregon Cascades.
- Stewart, I.T., Cayan, D.R. and Dettinger, M.D. (2004) Changes in snowmelt runoff timing in western North America under a business as usual climate change scenario. *Climatic Change* 62(1–3), 217–232.
- Stonevičius, E., Rimkus, E., Štaras, A., Kažys, J. and Valiuškevičius, G. (2017) Climate change impact on the Nemunas River basin hydrology in the 21st century. *Boreal Environment Research* 22(1), 49–65.
- Sulis, M., Paniconi, C., Rivard, C., Harvey, R. and Chaumont, D. (2011) Assessment of climate change impacts at the catchment scale with a detailed hydrological model of surface-subsurface interactions and comparison with a land surface model. *Water Resources Research* 47(1).
- Sutinen, R., Hänninen, P. and Venäläinen, A. (2008) Effect of mild winter events on soil water content beneath snowpack. *Cold Regions Science and Technology* 51(1), 56–67.
- Tabler, R.D. (1975) Estimating the transport and evaporation of blowing snow. *Great Plains Agric Counc Publ.*
- Tanzeeba, S. and Gan, T.Y. (2012) Potential impact of climate change on the water availability of South Saskatchewan River Basin. *Climatic Change* 112(2), 355–386.
- Teufel, B., Sushama, L., Huziy, O., Diro, G., Jeong, D., Winger, K., Garnaud, C., de Elia, R., Zwiers, F. and Matthews, H. (2019) Investigation of the mechanisms leading to the 2017 Montreal flood. *Climate Dynamics* 52(7–8), 4193–4206.
- Teutschbein, C., Grabs, T., Karlsen, R.H., Laudon, H. and Bishop, K. (2015) Hydrological response to changing climate conditions: Spatial streamflow variability in the boreal region. *Water Resources Research* 51(12), 9425–9446.
- Toews, M.W. and Allen, D.M. (2009) Evaluating different GCMs for predicting spatial recharge in an irrigated arid region. *Journal of Hydrology* 374(3–4), 265–281.

- Wall, G., Coote, D., Pringle, E. and Shelton, I. (2002) RUSLEFAC—Revised universal soil loss equation for application in Canada: A handbook for estimating soil loss from water erosion in Canada. Research Branch, Agriculture and Agri-Food Canada. Ottawa. Contribution No. AAFC/AAC2244E 117.
- Wang, L., Cherkauer, K.A. and Flanagan, D.C. (2018) Impacts of climate change on soil erosion in the Great Lakes region. *Water* 10(6), 715.
- Wang, R., Kumar, M. and Link, T.E. (2016) Potential trends in snowmelt-generated peak streamflows in a warming climate. *Geophysical Research Letters* 43(10), 5052–5059.
- Weber, M., Bernhardt, M., Pomeroy, J., Fang, X., Härer, S. and Schulz, K. (2016) Description of current and future snow processes in a small basin in the Bavarian Alps. *Environmental Earth Sciences* 75(17), 1223.
- Whitehead, P.G., Wilby, R.L., Battarbee, R.W., Kernan, M. and Wade, A.J. (2009) A review of the potential impacts of climate change on surface water quality. *Hydrological Sciences Journal* 54(1), 101–123.
- Whitfield, P.H. and Cannon, A.J. (2000) Recent variations in climate and hydrology in Canada. *Canadian Water Resources Journal* 25(1), 19–65.
- Wilson, D., Hisdal, H. and Lawrence, D. (2010) Has streamflow changed in the Nordic countries?—Recent trends and comparisons to hydrological projections. *Journal of Hydrology* 394(3), 334–346.
- Winkler, R., Spittlehouse, D. and Golding, D. (2005) Measured differences in snow accumulation and melt among clearcut, juvenile, and mature forests in southern British Columbia. *Hydrological Processes* 19(1), 51–62.
- Woo, M.-k., Thorne, R., Szeto, K. and Yang, D. (2008) Streamflow hydrology in the boreal region under the influences of climate and human interference. *Philosophical Transactions of the Royal Society B: Biological Sciences* 363(1501), 2249–2258.
- Xie, S.B., Jianjun, Q., Yuanming, L., Zhiwei, Z. and Xiangtian, X. (2015) Effects of freeze-thaw cycles on soil mechanical and physical properties in the Qinghai-Tibet Plateau. *Journal of Mountain Science* 12(4), 999–1009.
- Zhang, T. (2005) Influence of the seasonal snow cover on the ground thermal regime: An overview. *Reviews of Geophysics* 43(4).
- Zuzel, J.F. and Pikul, J. (1987) Infiltration into a seasonally frozen agricultural soil. *Journal of Soil and Water Conservation* 42(6), 447–450.